# Investigation of NAI-107 immunity in the lantibiotic producer *Microbispora* ATCC PTA-5024

**Dissertation**

der Mathematisch-Naturwissenschaftlichen Fakultät

der Eberhard Karls Universität Tübingen

zur Erlangung des Grades eines

Doktors der Naturwissenschaften

(Dr. rer. nat.)

vorgelegt von

Roberta Pozzi

aus Merate (Italien)

Tübingen

2015

Gedruckt mit Genehmigung der Mathematisch-Naturwissenschaftlichen Fakultät der Eberhard Karls Universität Tübingen.

Tag der mündlichen Qualifikation: 29.06.2015

| | |
|---|---|
| Dekan: | Prof. Dr. Wolfgang Rosenstiel |
| 1. Berichterstatter: | Prof. Dr. Wolfgang Wohlleben |
| 2. Berichterstatter: | Prof. Dr. Heike Brötz-Oesterhelt |
| 3. Berichterstatter: | Prof. Dr. Andreas Bechthold |

*Alla mia famiglia e a Buzzo*

## Declaration

I declare that this dissertation, entitled 'Investigation of NAI-107 immunity in the lantibiotic producer *Microbispora* ATCC PTA-5024' is my own work and that all the sources I have used had been indicated or noted in the list of references.

Tübingen, 02.04.2015

# TABLE OF CONTENTS

# ABSTRACT

The actinomycete *Microbispora* ATCC PTA-5024 produces the lantibiotic NAI-107, currently in pre-clinical development for the treatment of multi-drug resistant Gram-positive bacteria. NAI-107 displays its antibacterial activity by binding bactoprenol-pyrophosphate-coupled peptidoglycan precursors, thereby interfering with peptidoglycan biosynthesis. In the present study, a comprehensive analysis of the immunity of this lantibiotic-producing actinomycete was carried out.

In order to understand how *Microbispora* counteracts the action of its own antibiotic, its peptidoglycan composition was analysed in detail. *Microbispora* peptidoglycan consists of muropeptides with Ala, Gly and Ser in the fourth or fifth position of peptide stems. Muropeptides with alternative 3-3 cross-links besides the classical 4-3 cross-links were detected. The non-producing *Microbispora* RP0 and *Microbispora* spp. JCM 10266 and JCM 10267 possess the same muropeptides found in *Microbispora* ATCC PTA-5024, thus the diversity of the muropeptides is not correlated with NAI-107 production.

In addition, the NAI-107 biosynthetic gene cluster (*mlb*) was analysed for the expression of immunity proteins. Distinct immunity determinants are encoded in the *mlb* cluster: the ABC transporter MlbYZ acting cooperatively with the transmembrane protein MlbJ and the lipoprotein MlbQ. MlbJ was hypothesized to act as substrate-binding protein for MlbYZ, while MlbQ to have an independent mode of action. MlbQ was further investigated by genetic and biochemical analyses. Deletion analysis showed that MlbQ is required for normal growth under NAI-107 production. NMR structural analysis of MlbQ revealed a hydrophobic surface patch, which was proposed to bind the cognate lantibiotic. Moreover, localization studies by fluorescence microscopy showed a spore localization of the chimeric protein MlbQ-mCherry.

This study demonstrates that immunity in *Microbispora* is not only based on one determinant but on the action of the distinct immunity proteins MlbYZ, MlbJ and MlbQ.

# ZUSAMMENFASSUNG

Der Actinomyzet *Microbispora* ATCC PTA-5024 produziert das Lantibiotikum NAI-107, das sich derzeit in der späten präklinischen Testphase für die Behandlung von multi-resistenten gram-positiven Bakterien befindet. Der antibakterielle Wirkmechanismus von NAI-107 beruht auf seiner Bindung an Bactoprenol-Pyrophosphat-gebundene Peptidoglykanvorstufen und der damit verbundenen Hemmung der Zellwandbiosynthese. Ziel dieser Arbeit war es, die Immunität des NAI-107 Produzenten gegen sein eigenes Lantibiotikum aufzuklären.

Um zu untersuchen, wie *Microbispora* der antimikrobiellen Wirkung von NAI-107 entgegenwirkt, wurde das Peptidoglykan isoliert und detailliert analysiert. Das Peptidoglykan von *Microbispora* besteht aus Muropeptiden, die sich durch den variablen Einbau von Alanin, Glycin oder Serin an den Positionen vier oder fünf der Oligopeptidkette auszeichnen. Diese Oligopeptidgruppen werden durch Transpeptidierungsreaktionen miteinander quervernetzt. Neben den klassischen 4-3 Quervernetzungen wurden im Peptidoglykan von *Microbispora* auch alternative 3-3 Quervernetzungen identifiziert. Da sowohl die NAI-107-Nullmutante RP0 sowie weitere *Microbispora* Stämme (JCM10266 und JCM10267), die alle kein NAI-107 produzieren, dennoch Peptidoglykan mit denselben Modifikationen wie *Microbispora* ATCC PTA-5024 besitzen, gibt es keine Korrelation zwischen der Muropeptiddiversität und der Resistenz gegen NAI-107.

Allerdings konnten in *Microbispora* ATCC PTA-5024 Immunitätsproteine identifiziert werden, die im NAI-107 Biosynthese Gencluster (*mlb*) kodiert sind. Diese Immunitätsdeterminanten sind der ABC Transporter MlbYZ, das Transmembranprotein MlbJ und das Lipoprotein MlbQ. Heterologe Expressionion von *mlbYZ* und *mlbJ* In *Streptomyces coelicolor* zeigten, dass der ABC-Transporter MlbYZ ausschließlich in Abhängigkeit von MlbJ Immunität vermittelt, wobei dieses Transmemembranprotein wahrscheinlich Substratbindefunktion hat. Die Expression des Lipoproteins MlbQ in *S. coelicolor* alleine verleiht dem heterologen Wirt ebenfalls Resistenz gegen NAI-107. Des Weiteren ist MlbQ für *Microbispora* ATCC PTA-5024 essentiell, um in NAI-107 Anwesenheit normal wachsen zu können. Die Strukturanalyse von MlbQ mittels NMR

wies eine hydrophobe Furche auf der Oberfläche des Proteins auf, in die das Lantibiotikum binden könnte.

Lokalisationsstudien mittels Fluoreszenz-Mikroskopie zeigten eine überwiegende Einlagerung des Fusionsproteins MlbQ-mCherry in der Sporenmembran.

Diese Arbeit belegt, dass die Immunität von *Microbispora* gegen sein hoch potentes Lantibiotikum nicht nur auf einer Determinante beruht, sondern durch die Wirkungsweisen verschiedener, unabhängiger Immunitätsproteinen (MlbYZ, MlbJ und MlbQ) gewährleistet wird.

# 1. INTRODUCTION

## 1.1 The peptidoglycan

### 1.1.1 Overview of peptidoglycan biosynthesis

The peptidoglycan (PG) is a polymer that surrounds the cytoplasmic membrane preserving the cell integrity from the turgor and maintaining the cell shape. As an essential component of the bacterial cell envelope, PG is involved in cell growth and cell division. Since the inhibition of PG biosynthesis during cell growth causes ultimately cell lysis, PG biosynthesis is intimately regulated with bacterial growth (Typas *et al.*, 2011). PG is also essential for other components of the cell envelope such as proteins (Dramsi *et al.*, 2008) and teichoic acids (Brown *et al.*, 2013) that use PG as an anchor. PG was discovered by Weidel and co-workers, who firstly described the PG composition of *Escherichia coli* (Weidel *et al.*, 1960). Since then, several studies on PG composition (Schleifer and Kandler, 1972; Vollmer *et al.*, 2008a), PG recycling (Johnson *et al.*, 2013) and regulation of PG biosynthesis (Typas *et al.*, 2011) were conducted.

PG is formed by linear glycan chains of repeated N-acetylglucosamine-N-acetylmuramic acid disaccharide units (GlcNAc-MurNAc) that are interconnected by peptide cross-links. The key component of PG biosynthesis is lipid II that consists of the disaccharide GlcNAc-MurNAc loaded onto the lipid carrier undecaprenyl pyrophosphate and linked to a pentapeptide through the D-lactoyl group of MurNAc. The pentapeptide is typically L-Ala-γ-D-Glu-X-D-Ala-D-Ala, where X is *meso*-$A_2$pm (2,6-diaminopimelic acid) or L-Lys (Vollmer *et al.*, 2008a). The presence of D-amino acids, non-proteinogenic amino acids and the unusual amino sugar MurNAc confers a peculiar chemical structure to PG, which varies between species and in relation to the growth conditions. Variations in the PG composition occur in the glycan strands, peptide stems and cross-links. Several modifications of PG glycan strands were described: N-deacetylation at MurNAc and GluNAc, N-glycolylation at MurNAc, O-acetylation at MurNAc and the formation of a δ-lactam or 1-6 anhydro ring at MurNAc (Vollmer, 2008). Moreover, teichoic acids are linked to PG via a phosphodiester bond to the C6 oxydril group of MurNAc (Brown *et al.*,

2013). High diversity in PG structure is also found in the composition and sequence of PG peptides. The greatest variability is in the third position of the stem peptide that can be occupied by L,L- or *meso*-$A_2$pm, L-Lys, L-Orn, L-Homoserine, L-2,4-Diaminobutyrate, L-Ala or L-Glu. Besides incorporation of different amino acids, variability in the peptide stem is also introduced by reactions that occur at later steps of PG biosynthesis. These reactions comprise amidation, hydroxylation, acetylation and attachment of amino acids or proteins. Variations in the cross-links reflect the cross-link type, according to the amino acids that act as donors and acceptors and the composition of the interpeptide bridge (Vollmer *et al.,* 2008a).

PG biosynthesis can be divided in three main stages (Fig. 1).

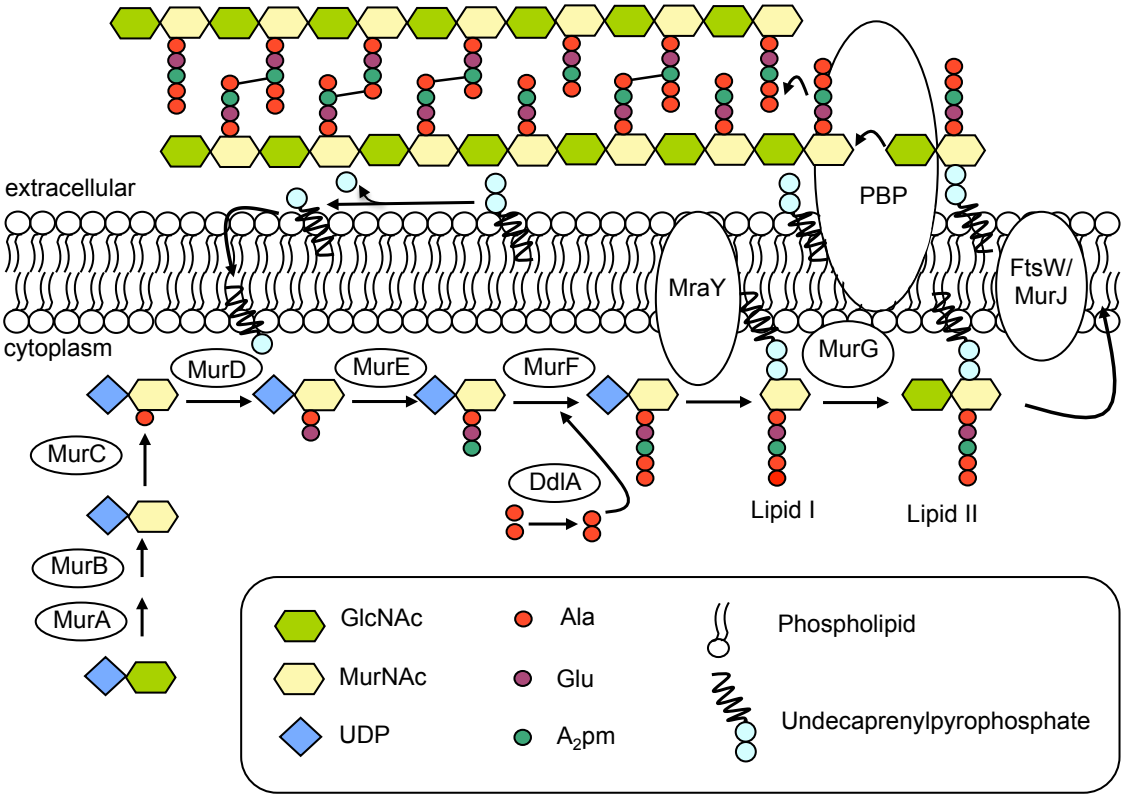


**Fig. 1. Representation of the peptidoglycan biosynthesis.** PG biosynthesis takes place in three different locations in the cell (cytoplasm, cytoplasmic membrane and extracellular space). The nucleotide-linked PG precursor is synthesized in the cytoplasm by successive reactions catalyzed by MurA-MurF. MraY and MurG synthesize lipid II, which is translocated across the membrane and successively incorporated in the PG by penicillin-binding proteins (PBP). Figure adapted from Pinho *et al.*, 2013.

First, soluble, nucleotide-linked PG precursors (UDP-MurNAc pentapeptides) are synthesised in the cytoplasm (cytoplasmic steps). Second, these PG precursors are linked to the lipid carrier undecaprenyl phosphate to form the lipid-anchored disaccharide pentapeptide subunit called lipid II (membrane steps). Finally, lipid II is translocated and exposed to the outer leaflet of the cytoplasmic membrane where it is incorporated in the nascent glycan chains by transglycosylases and processed by transpeptidases which cross-link the peptide side chains of adjacent glycan strands (PG polymerization and remodelling).

#### 1.1.1.1 Cytoplasmic steps of PG biosynthesis

The first steps of PG biosynthesis occur in the cytoplasm and culminate with the formation of UDP-MurNAc pentapeptides through a pathway that was established by characterization of isolated nucleotide precursors and enzymes involved in each step. The cytoplasmic steps of PG biosynthesis can be divided in three groups of reactions: formation of UDP-GlcNAc, UDP-MurNAc and UDP-MurNAc pentapeptide (Barreteau *et al.*, 2008).

MurNAc and GlcNAc differ by the D-lactoyl group at C3. UDP-GlcNAc derives from fructose-6-P through the intermediate glucosamine-1-P. UDP-MurNAc is formed from UDP-GlcNAc by two successive reactions: transfer of enoylpyruvate to C3 of UDP-GlcNAc and reduction of the enoylpyruvate moiety to D-lactoyl. The enzymes involved in this process are MurA and MurB, a transferase and a reductase, respectively (van Heijenoort, 2001).

In the final step, a pentapeptide is linked to the D-lactoyl group of UDP-MurNAc. The assembly of the peptide proceeds by the stepwise addition of L-Ala, D-Glu, $A_2$pm or L-Lys and the dipeptide D-Ala-D-Ala. Each step is catalysed by a highly specific cytoplasmic enzyme, designed as Mur synthase (MurC, MurD, MurE and MurF). These enzymes, which were studied in a great detail in *E. coli*, catalyse the formation of an amide bond with cleavage of ATP to ADP and inorganic phosphate (van Heijenoort, 2001). The substrate specificity of these enzymes exhibits some variations between bacterial species. As an example, MurC can efficiently ligate Gly and L-Ser instead of L-Ala, but it preferentially binds L-Ala due to its higher intracellular concentration. However, Gly is found in the first position of the PG peptide in *Corynebacterium poinsettiae* (Wyke and

Perkins, 1975) and *Mycobacterium leprae* (Mahapatra *et al.*, 2000). In the first case, MurC is highly specific to Gly, whereas in *Mycobacterium leprae* the incorporation of Gly instead of L-Ala seems to be due to the intracellular environment.

In the last reaction catalysed by MurF, a dipeptide is linked to the growing peptide instead of a single amino acid. The dipeptide D-Ala-D-Ala is synthesised by Ddl ligase. The specificity of Ddl to the N-terminal amino acid and of MurF to the C-terminal amino acid of the dipeptide ensures the synthesis of a pentapeptide ending in D-Ala-D-Ala, the so-called 'double sieving' mechanism. The presence of Gly at position 4 and 5 of UDP-linked PG precursors in culture media containing increasing concentration of Gly (Hammes *et al.*, 1973), showed that the 'double sieving' mechanism can be circumvent.

### 1.1.1.2 Membrane steps of PG biosynthesis

Lipid II represents the central building block of PG biosynthesis. It consists of MurNAc-(pentapeptide)-GlcNAc loaded onto the lipid carrier undecaprenyl pyrophosphate (Fig. 2).

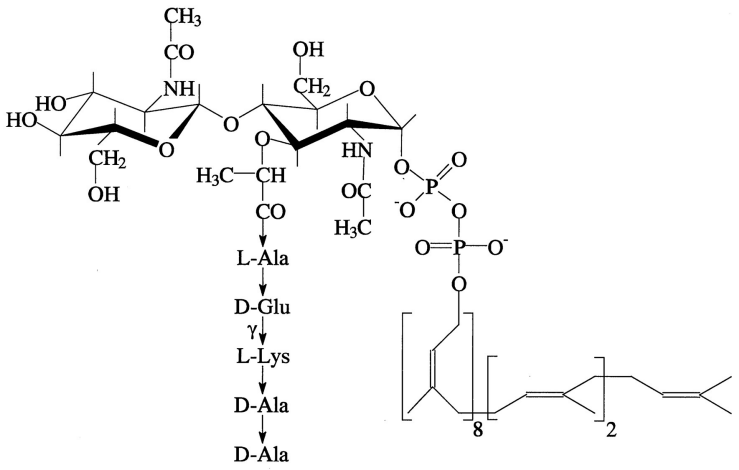


**Fig. 2. Structure of lipid II.** Pentapeptide L-Ala-D-Glu-L-Lys-D-Ala-D-Ala linked to the disaccharide GlcNAc-MurNAc through the D-lactoyl group of MurNAc. The lipid carrier undecaprenyl phosphate is linked *via* a phosphodiester bond to the C1 of MurNAc. Figure reproduced from Brötz *et al.*, 1998b.

Lipid II is obtained by two successive reactions that occur at the cytoplasmic membrane. First, the phospho-MurNAc-pentapeptide moiety from UDP-MurNAc-pentapeptide is transferred to the membrane acceptor undecaprenyl phosphate ($C_{55}$-P) to yield lipid I.

Second, GlcNAc from UDP-GlcNAc is added to lipid I resulting in lipid II (Bouhss *et al.*, 2008). The fact that these steps are membrane associated is reflected also by the enzymes that catalyse the two reactions: MraY and MurG, respectively. These enzymes are membrane proteins, the first one being an integral protein and the second one a peripheral protein.

Lipid II is modified in several bacterial species. Amidation of the α-carboxyl of Glu and the ε-carboxyl of $A_2$pm of the stem peptide were described in different bacteria (Vollmer *et al.*, 2008a) and the enzymes involved in these modifications were characterized in *Staphylococcus aureus* (Münch *et al.*, 2012) and *Lactobacillus plantarum* (Bernard *et al.*, 2011). Moreover, hydroxylation of the amino acids at position 2 and 3 and acetylation at position 3 were reported (Vollmer *et al.*, 2008a). In some bacterial species, the stem peptides of different glycan strands are connected by an interbridge that is usually added at the lipid II stage. *S. aureus* possesses a penta-glycine bridge that is linked to lipid II by the action of FemX, FemA and FemB, which use glycyl-tRNA as substrate. FemX is responsible for the addition of the first Gly, FemA of the next two Gly and FemB of the last two Gly (Rohrer and Berger-Bächi, 2003). The actinomycete *Streptomyces coelicolor* possesses a single Gly as interbrigde, but differently to *S. aureus*, Gly is linked to the UDP-activated PG precursors and not at the lipid II stage (Ruzin *et al.*, 2002; Hong *et al.*, 2005).

The fully modified lipid II is then translocated across the cytoplasmic membrane to become the substrate of the polymerization reactions that form the glycan strands. Mohammadi *et al.*, 2011 firstly described a flippase involved in the translocation of lipid II. In a FRET-based study they showed that FtsW, an essential protein in the bacterial division machinery, transports lipid II across the membrane. Recently, MurJ was indicated to be the lipid II flippase in *E. coli.* Using a strategy to rapidly block flippase function, it was demonstrated that MurJ transports lipid II *in vivo* (Sham *et al*., 2014). Thus, it is probable that both proteins are involved in the translocation of lipid II. MurJ could be the main lipid II flippase and FtsW could act at the septum, where a high concentration of lipid II is required.

### 1.1.1.3 PG polymerization and remodelling

PG synthesis requires glycosyltransferase activity to incorporate lipid II in the glycan chains and transpeptidase activity to cross-link the peptides of adjacent glycan strands, thereby forming a three-dimensional network. Such enzymatic activities are carried out by penicillin-binding proteins (PBPs), which were initially identified because of their ability to covalently bind penicillin.

PBPs are classified in bifunctional glycosyltransferase-transpeptidases (TPase-GTases) and monofunctional TPases (Sauvage *et al.*, 2008). The bifunctional TPase-GTases possess a N-terminal domain that is responsible for the glycosyltransferase activity and a C-terminal domain that catalyses the formation of cross-links. These activities were reconstituted *in vitro* using the bifunctional syntheses PBP1A and PBP1B from *E. coli* and lipid II as substrate (Bertsche *et al.*, 2005; Born *et al.*, 2006). The GTase domain catalyses the elongation of the uncross-linked glycan strands of PG using lipid II as acceptor and the growing glycan chain as donor. For bifunctional synthases, the transglycosylation activity is essential for PG polymerization. Inactivation of the glycosyltransferase domain by mutation or treatment with moenomycin blocks PG synthesis, since TPase activity requires GTase activity to occur.

Transpeptidation is responsible for the formation of an amide bond between the carboxylic group of D-Ala$^4$ (donor) and the free amino group of the diamino acid in position 3 ($A_2$pm or L-Lys, acceptor), forming a 4-3 cross-link. The cross-link can be direct or through an interpeptide bridge (Vollmer *et al.*, 2008a). Transpeptidase reaction occurs *via* an acyl-enzyme intermediate, successive release of the C-terminal D-Ala and cross-link formation (Sauvage *et al.*, 2008). Alternatively, PBPs can function as D,D-carboxypeptidases, by forming a tetrapeptide upon hydrolysis of the acyl-enzyme intermediate (carboxypeptidase activity *versus* transpeptidase activity). Because of the ability to cleave the D,D-bond between D-Ala$^4$ and D-Ala$^5$, PBPs are also called D,D-transpeptidases (Sauvage *et al.*, 2008).

A novel cross-link type, named 3-3 cross-link, was discovered firstly in Mycobacteria and successively in *E. coli* (Wietzerbin *et al.*, 1974; Glauner *et al.*, 1988). A 3-3 cross-link consists of a peptide bond between the carboxylic group of $A_2$pm in the donor muropeptide and the amino group of $A_2$pm in the acceptor muropeptide. 3-3 cross-links

were detected also in other bacterial species like *Mycobacterium tuberculosis* (Lavollay *et al.,* 2008) and *S. coelicolor* (Hugonnet *et al.*, 2014). The enzyme catalysing the formation of 3-3 cross-links was identified by Mainardi and co-workers about 30 years after the discovery of this cross-link type (Mainardi *et al.*, 2005). The enzyme is structurally unrelated to PBPs and differs from PBPs in the catalytic site (Ser *versus* Cys). It was designed L,D-transpeptidase (LDT) because the formation of 3-3 cross-links involves the cleavage of the L,D bond between $A_2pm^3$ and D-$Ala^4$. Indeed, LDTs use tetrapeptides as acyl donors, in contrast to PBPs, which act on pentapeptides (Mainardi *et al*., 2008).

The diamino acid in position 3 is not the only possible acceptor of cross-link reactions. $Glu^2$ acts as acceptor in the 4-2 cross-link in *Corynebacterium pointsettiae*, which possesses an interbridge containing the diamino acid D-Orn (Schleifer and Kandler, 1972). Besides the diversity in the nature of the cross-link, a considerable variation in the degree of the cross-link can be found in different bacterial species. For example, the cross-link varies from 20% in *E. coli* to 90% in *S. aureus* (Vollmer *et al*., 2008a).

After biosynthesis, PG is continuously subjected to remodelling to maintain the cell shape during growth and cell division. To insert new material into the PG layer, hydrolases like amidases, lytic transglycosylases and endopeptidases are required to cleave covalent bonds (Vollmer *et al*., 2008b). Moreover, carboxypeptidases cleave the C-terminal amino acid of the stem peptides resulting in shorter peptide stems. The material that is removed by PG hydrolases as soluble fragments is then reused via an efficient PG-recycling pathway (Johnson *et al.*, 2013).

A wide variety of bacteria incorporate non-canonical D-amino acids (D-Met, D-Leu) into their cell wall to alter PG density, PG strength and to control PG abundance (Cava *et al.*, 2011; Horcajo *et al.*, 2012). These non-canonical D-amino acids do not only influence PG characteristics but also act as paracrine-like regulators. A study in *Bacillus subtilis* demonstrated that their environmental release could induce biofilm disruption (Kolodkin-Gal *et al.*, 2010). LDTs contribute as well to PG remodelling by exchanging D-$Ala^4$ of the stem peptide with D-amino acids or Gly. This process is considered a side reaction of LDTs (Magnet *et al.*, 2008).

### 1.1.2 PG targeting antibiotics

PG is a unique and essential polymer in the bacterial world, thus it constitutes a good target for antibiotics. Most steps involved in PG biosynthesis are target of well-known antibiotics or are explored for designing novel drugs. Penicillin, the first discovered antibiotic, inhibits the transpeptidase activity catalysed by PBPs by forming a covalent complex with the active serine of the catalytic domain. In this way, cross-link of the stem peptides is prevented (Tipper and Strominger, 1965; Blumberg, 1974; Sauvage *et al.*, 2008).

Transglycosylation is inhibited by moenomycin, a phosphoglycolipid antibiotic that binds to monofunctional transglycosylases (MGTs) or to the transglycosylase domain of PBPs (van Heijenoort *et al.*, 1978; Ostash and Walker, 2010). Moenomycin was for long time the only known antibiotic that directly inhibits PG transglycosylases but in the last two decades new glycopeptide derivatives were described to act in the same way (Sinha Roy *et al.*, 2001; Leimkuhler *et al.*, 2005).

Besides these compounds that directly inhibit transglycosylases, several classes of antibiotics are able to interfere with the transglycosylase reaction indirectly by binding the substrate lipid II. Among these antibiotics, glycopeptides and lantibiotics are the most prominent examples. The glycopeptide vancomycin binds the D-Ala-D-Ala terminus of lipid II and of uncross-linked PG. In this way the glycopeptide inhibits the formation of glycan chains, probably by steric hindrance (Reynolds, 1989). Lantibiotics are ribosomally synthesized peptide antibiotics containing lanthionine residues (1.2.1). The most studied lantibiotic nisin was shown to bind lipid II at the pyrophosphate moiety (1.2.4).

In addition to glycopeptides and lantibiotics, other antibiotics target lipid II. Mannopeptymicins are cyclic glycopeptide antibiotics discovered about a decade ago (Singh *et al.*, 2003) that bind lipid II to a different site than the D-Ala-D-Ala terminus (Ruzin *et al.*, 2004). The lipodepsipeptide empedopeptin form a complex with lipid II in the region comprising the pyrophosphate group, the MurNAc and the proximal parts of the pentapeptide and undecaprenyl chain. Empedopeptin binds lipid II in a 1:2 ratio and calcium ions promote this interaction (Müller *et al.*, 2012a). Ramoplanin, a glycolipodepsipeptide antibiotic, binds lipid II at the pyrophosphate moiety and MurNAc (Cudic *et al.*, 2002). For long time it was thought that ramoplanin inhibits MurG, the

glycosyltransferase that catalyses the conversion of lipid I to lipid II. However, since ramoplanin is unable to penetrate the cytoplasmic membrane, lipid II is considered the primary physiological target because of its accessibility from the outer leaflet of the cytoplasmic membrane (Walker *et al.*, 2005).

Although some lipid II binding antibiotics were widely exploited for clinical uses, lipid II remains an attractive target for antibacterial chemotherapy because of the diversity of compounds that bind to it and their effectiveness. The low pool level of lipid II in a single cell, estimated to be about 2000 molecules/cell (van Heijenoort *et al.*, 1992), allows an efficient inhibition of polymerization reactions by lipid II-targeting antibiotics.

Besides inhibitors of the final steps of PG biosynthesis, several antibacterial molecules that inhibit the cytoplasmic steps of PG biosynthesis or interfere with the undecaprenyl phosphate cycle were described. D-cycloserine impairs the formation of the dipeptide D-Ala-D-Ala by inhibiting both D-alanine racemase and D-alanine ligase (Lambert and Neuhaus, 1972). MurA, the first enzyme of PG biosynthesis, is targeted by phosphomycin (Skarzynski *et al.*, 1996). The uridylpeptides mureidomycin, tunicamycin and liposidomycin inhibit MraY, which acts on UDP-activated MurNAc-pentapeptides (Kimura and Bugg, 2003).

The undecaprenyl phosphate cycle is target mainly of two antibiotics: bacitracin and friulimicin. Bacitracin sequesters the lipid carrier $C_{55}$-PP preventing its dephosphorilation (Siewert and Strominger, 1967), whereas the lipopeptide friulimicin binds to the mono-phosphorylated lipid carrier $C_{55}$-P (Schneider *et al.*, 2009). The block of the undecaprenyl phosphate cycle does not exclusively impair the synthesis of PG but also of various cell wall polymers, since $C_{55}$-PP is also involved in the synthesis of teichoic acids, lipopolysaccharides and capsule polysaccharides.

### 1.1.3 Antibiotic resistance mechanisms based on PG modifications

Resistance to antibiotics represents the major challenge for antibacterial chemotherapy and for the development of novel effective drugs. Bacteria develop resistance in several ways: enzyme modification, expression of antibiotic-inactivating enzymes, increased efflux, changes in permeability and surface properties, target overproduction and target modification.

Regarding PG targeting antibiotics, several examples fulfil the mechanisms reported above. In Gram-positive bacteria, β-lactam resistance commonly results from the expression of intrinsic low-affinity PBPs, whereas in Gram-negative bacteria the production of β-lactamases, β-lactam-inactivating enzymes, represents a common way to degrade the antibiotic before it reaches the target (Rice, 2012). *E. coli* is resistant to the uridylpeptide mureidomycin due to the expression of the multidrug efflux system AcrAB-TolC (Gotoh *et al.*, 2003). However, since PG targeting antibiotics often do not penetrate the cell, many resistance mechanisms are based on the action of ABC transporters instead of efflux pumps. In the case of lantibiotics and bacitracin, ABC transporters act as immunity proteins by decreasing the concentration of the antibiotic in proximity of the target (Gebhard, 2012). Decrease of the negative charge of the cell surface due to D-alanylation of teichoic acids confers nisin resistance to *S. aureus* (Peschel *et al.*, 1999). In the case of bacitracin, different resistance mechanisms were described and one implies the amplification of the *bacA* gene encoding the undecaprenol phosphokinase that leads to an increase of the undecaprenyl phosphate pool (Cain *et al.*, 1993).

Given one example for each of the resistance mechanisms listed above, the following part is focused on resistance mechanisms based on target modifications. Diversification of the PG assembly pathway leading to glycopeptide resistance by modification of lipid II had been widely described in literature. The first mechanism was discovered in a clinical isolate of *Enterococcus faecium* that has acquired resistance to vancomycin by production of lipid II ending in D-Lac instead of D-Ala. The modified target is drastically less affine to vancomycin than lipid II ending in D-Ala. The synthesis of the D-Ala-D-Lac terminus is achieved by expression of the *vanHAX* operon present on the acquired transposon Tn*1546*. D-Lac is synthesized from pyruvate by VanH, a D-lactate dehydrogenase. D-Lac is then ligated to D-Ala by the ligase VanA yielding the depsipeptide D-Ala-D-Lac, which is successively incorporated in the peptide stem of PG precursors. Efficient incorporation of the depsipeptide instead of the dipeptide D-Ala-D-Ala is achieved by hydrolysis of D-Ala-D-Ala by the D,D-peptidase VanX. A second backup mechanism is provided by the accessory protein VanY, a D,D-carboxypeptidase that cleaves the C-terminal D-Ala residue of PG precursors.

Close homologs of VanH, VanA and VanX were identified in glycopeptide-producing actinomycetes like *Actinoplanes teichomyceticus*, *Amycolatopsis orientalis* and *Amycolatopsis balhimycina,* producing teicoplanin, vancomycin and balhimycin, respectively (Yim *et al.*, 2014). *vanHAX* homologs were also found in *S. coelicolor*, a non-producing-glycopeptide actinomycete that shares the same ecosystem with actinomycetes producing glycopeptides (Hong *et al.*, 2004). The presence of resistance genes in environmental bacteria led to the introduction of the concept of 'resistome' to indicate the reservoirs of potential resistant determinants in nature (Wright, 2007). In contrast to other glycopeptide-producers, *Nonomurea* ATCC 39727 does not possess *vanHAX* homologs but a VanY-like protein, ($VanY_n$) which confers the resistant phenotype to the strain (Binda *et al.*, 2012). $VanY_n$ forms UDP-MurNAc-tetrapeptides that are processed to lipid II and incorporated into the growing glycan chain. The modification of lipid II in not lethal for the cell because transpeptidation of tetrapeptide substrates is carried out by LDTs (Mainardi *et al.*, 2005). This target modification confers resistance also to β-lactams by bypassing the β-lactam sensitive D,D-transpeptidase activity of PBPs (Mainardi *et al*., 2008).

Another resistance mechanism based on target modification is the amidation of $Glu^2$ of the stem peptide of cytoplasmic PG precursors. Münch *et al.*, 2012 showed that amidation of the α-carboxylic group of $Glu^2$ renders *S. aureus* less susceptible towards the defensin plectasin.

## 1.2 Lantibiotics

### 1.2.1 Structure and biosynthesis of lantibiotics

Lantibiotics are ribosomally-synthesized and post-translationally modified peptides (RiPPs) which display antimicrobial activity (Arnison *et al.*, 2013). They are characterised by the thioether-cross-linked amino acids *meso*-lanthionine (Lan) and (2*S*,3*S*,6*R*)-3-methyllanthionine (MeLan) (Fig. 3), thus the name lantibiotic was introduced to refer to 'lanthionine-containing antibiotics' (Kellner *et al.*, 1988). Lantibiotics are synthesized as a longer precursor peptide encoded by the structural gene *lanA*. The precursor peptide

contains a N-terminal leader sequence, which is cleaved to give the mature product after post-translational modifications (Arnison *et al.*, 2013).

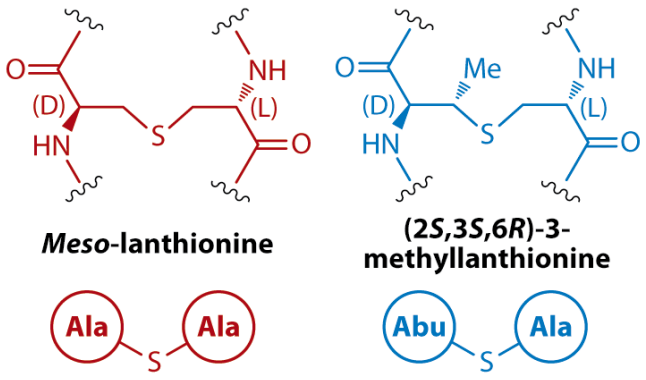


**Fig. 3. Structure of lanthionines.** Characteristic residues of lanthipeptides: *meso*-lanthionine and (2*S*,3*S*,6*R*)-3-methyllanthionine (shorthand notation at the bottom). Figure reproduced from Knerr and van der Donk, 2012.

The characteristic Lan and MeLan residues are formed by dehydration of serine or threonine residues to the corresponding dehydroamino acids 2,3-didehydro-alanine (Dha) and (*Z*)-2,3-didehydro-butyrine (Dhb) and successive intramolecular addition of a cysteinyl thiol to the resulting dehydroamino acids (Knerr and van der Donk, 2012). Besides Lan and MeLan residues, which are critical for activity and confer protease resistance, lantibiotics possess several other post-translational modifications. For example, oxidative decarboxylation of the C-terminal Cys residue yields to *S*-aminovinyl-D-cysteine (AviCys), L-Ser may be converted in D-Ala and the N-terminal Dha and Dhb residues can spontaneously hydrolyse to form 2-oxopropionyl (OPr) and 2-oxobutyryl (OBu) groups (Willey and van der Donk, 2007). The N-terminal leader peptide is required to introduce the lanthionine residues but not to install the other post-translational modifications.

Lantibiotics were initially grouped into type-A and type-B peptides, according to their structure and functionality (Sahl and Bierbaum, 1998). However, the discovery of new lanthionine-containing molecules that possess intermediate features or that do not have

an antibacterial activity led to the introduction of a new classification for this class of compounds. According to the new nomenclature, lantibiotics are classified into the lanthipeptide family, which comprises lanthionine-containing peptides regardless their biological activities (Arnison *et al.*, 2013). Lanthipeptides are divided into four classes (I-IV) on the basis of the enzymatic machinery that introduces the Lan and MeLan motifs (Knerr and van der Donk, 2012). At present, the known lantibiotics belong to class I and II, whereas class III and IV comprise compounds with morphogenetic activity (Kodani *et al.*, 2004) or molecules whose natural function is still unknown (Goto *et al.*, 2010).

The *loci* of lanthipeptides biosynthetic genes, which are organized in clusters, have been generally designed with the symbol *lan*. For instance*, lanA* is the gene encoding the precursor peptide that undergoes post-translational modifications and cleavage of the leader peptide to result in the mature product.

Class I lanthipeptides are modified by the two distinct enzymes LanB (dehydratase) and LanC (cyclase), which form a multi-enzyme complex with the exporter LanT. Recently, the exact mechanism of LanB proteins has been described. Unexpectedly, aminoacyl-tRNAs are involved in the formation of dehydroamino acids by activation of Ser and Thr residues by glutamylation (Ortega *et al.*, 2014).

For class II lanthipeptides, dehydratation and cyclization are carried out by bifunctional lanthionine synthetases (LanM). LanM lanthionine synthetases have N-terminal dehydratation domains that do not have homology neither with LanB proteins nor with other known enzymes. The C-terminal cyclization domains, however, display homology with LanC cyclases (Knerr and van der Donk, 2012). Besides the precursor peptide and the enzymes involved in lanthionine formation, lanthipeptide biosynthetic gene clusters encode transporters, proteases, modifying enzymes, regulators and immunity proteins (Willey and van der Donk, 2007).

### 1.2.2 Lantibiotics from low-GC Gram-positive bacteria

The first lantibiotic activity was described in 1928 during a study on lactic bacteria that showed an inhibiting effect of *Lactococcus lactis*, formerly *Streptococcus lactis*, on *Lactobacillus bulgaricus* (Rogers, 1928). The antibacterial molecule responsible for this effect was named nisin (Mattick and Hirsch, 1947) and the structure was elucidated in

1971 (Gross and Morell, 1971). Nisin possesses 5 lanthionine residues (one Lan and four MeLan) that form the rings A, B, C, D and E. Nisin is a flexible molecule with two amphiphilic domains consisting of the three N-terminal rings (A, B, and C) and the C-terminal D and E rings, which are joined by a flexible hinge region (Fig. 4a). A decade later, the structure of epidermin, isolated from *Staphylococcus epidermidis*, was elucidated (Allgaier *et al.*, 1985). Epidermin is shorter than nisin and possesses an AviCys residue instead of the C-terminal tail of nisin (Fig. 4b).

The ribosomal origin of lanthionine-containing peptides was verified in 1988, when the gene encoding the precursor peptide of epidermin (*epiA*) was identified (Schnell *et al.*, 1988). After few years, the biosynthetic gene clusters of epidermin and nisin were described and characterized (Schnell *et al*., 1992; Kuipers *et al.*, 1993). The genes were designed *epi* and *nis*, according to the name of the produced lantibiotics. The nisin biosynthetic gene cluster encodes the precursor peptide NisA, the modification enzymes NisB and NisC, the ABC transporter NisT, involved in the transport of the lantibiotic in the extracellular space (Qiao and Saris, 1996), and NisP, a serine protease that is responsible for the cleavage of the leader peptide (van der Meer *et al.*, 1993). Furthermore, the *nis* cluster encodes the immunity proteins NisI and NisEFG (1.2.5), NisR and NisK, a response regulator and a sensor histidine kinase involved in the regulation of lantibiotic synthesis. The autoregulatory process of nisin production described by Kuipers and co-workers was considered a form of quorum sensing. Sub-inhibitory concentrations of extracellular nisin trigger the activity of the two-component regulatory system NisK and NisR, resulting in the transcription of the target genes (Kuipers *et al.*, 1995).

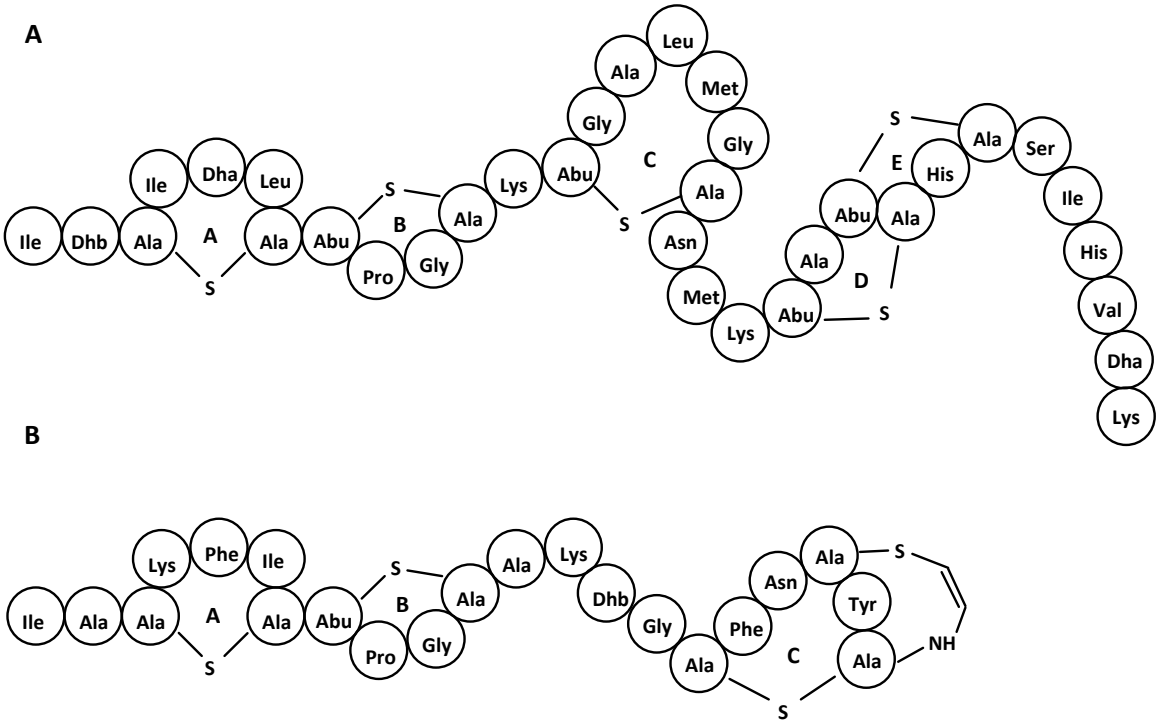


**Fig. 4. Representation of (A) nisin and (B) epidermin.** Letters (A-E) indicate Lan and MeLan rings.

Lactococci and staphylococci species were described to produce also other lantibiotics like gallidermin (Kellner *et al.*, 1988), Pep5 (Kaletta *et al.*, 1989) and epilancin 15X (van de Kamp *et al.*, 1995). The genus *Bacillus* was reported to produce lantibiotics as well. The most prominent example is subtilin produced by *B. subtilis*, one of the most studied lantibiotics. Subtilin possesses the same thioether-ring arrangement of nisin and a biosynthetic gene cluster (*spa*) that contains Nis homologs, except NisP. Regulation and immunity of subtilin were widely investigated as for nisin (Klein *et al.*, 1993; Klein and Entian, 1994; Stein *et al.*, 2005).

Besides class I lantibiotics, low-GC Gram-positive bacteria are known to produce also lantibiotics belonging to class II lanthipeptides. Two of the most prominent examples are lacticin 481 and mersacidin, produced by *L. lactis* and *Bacillus* sp., respectively (Willey and van der Donk, 2007). Lacticin 481 has a linear N-terminus and three overlapping thioether bridges that render the C-terminal globular. Mersacidin is also characterised by a globular structure, with a N-terminal thioether bridge between two adjacent residues and two methyllanthionine bridges, the C-terminal one overlapping with an AviCys residue.

The characterisation of the lacticin 481 and the mersacidin gene clusters led to the identification of the respective bifunctional enzymes, LctM and MrsM, responsible for the formation of the thioether bridges (Rincé *et al.*, 1997; Altena *et al.*, 2000; Uguen *et al.*, 2000). Besides *lanA* and *lanM*, both clusters contain two ABC transporters: one involved in the export of the lantibiotic (LanT) and one in the immunity (LanFEG). LctT and MrsT possess an N-terminal protease domain and homology with bacteriocin ABC transporters that process the precursor peptide during export (Håvarstein *et al.*, 1995). Maturation of lacticin 481 by LctT was verified by Uguen *et al.*, 2005 and an alternative cleavage of lacticin 481 was observed in absence of LctT. In addition to the ABC transporters LanT and LanFEG, the mersacidin gene cluster encode a two-component regulatory system (MrsR2, MrsK2), a response regulator (Mrs1) and the decarboxylase MrsD that catalyses the oxidative decarboxylation of the C-terminal Cys to yield AviCys.

Class II lanthipeptides also comprises two-component lantibiotics that consist of two modified peptides (Lanα, Lanβ) which possess antimicrobial synergistic activity. Each precursor peptide (LanA1, LanA2) is modified by a separate bifunctional LanM enzyme (LanM1, LanM2). The most studied two-component lantibiotics are lacticin 3147 from a *L. lactis* strain and haloduracin from *Bacillus halodurans*, an alkaliphilic bacterium (Ryan *et al.*, 1996; McClerren *et al.*, 2006).

### 1.2.3 Lantibiotics from actinomycetes

Actinomycetes are prolific producers of natural products and of about two-thirds of the naturally occurring antibiotics (Newman and Cragg, 2007). With the discovery of the first lantibiotics produced by low-GC Gram-positive bacteria, lanthionine-containing peptides with antibacterial activities have been identified also in actinomycete cultures. The first described lantibiotics produced by actinomycetes were cinnamycin and actagardine, formely gardimycin, from *Streptomyces cinnamoneus* and *Actinoplanes garbadinensis*, respectively (Benedict *et al.*, 1952; Parenti *et al.*, 1976). However, the presence of lanthionine-rings was verified only few decades later (Fredenhagen *et al*., 1990; Zimmermann *et al.,* 1995).

Cinnamycin is a globular lantibiotic containing one Lan, two MeLan, an unusual lysinoalanine ring and a hydroxylated Asp. Actagardine resembles the structure of

mersacidin with the C-terminal lanthionine ring oxidized to a sulphoxide and no AviCys residue. Few compounds related to these two lantibiotics were described in literature: duramycin A, B, and C and deoxyactagardine (Fredenhagen *et al.*, 1990; Boakes *et al.*, 2010).

Although these few examples, lantibiotics were thought to be predominantly produced by low-GC Gram-positive bacteria. However, in the last decade, genome mining and screening programs revealed the high potential of actinomycetes as lantibiotic producers. During a screening aimed to identify new cell wall-targeting antibiotics from actinomycetes extracts, the lantibiotics 97518 from *Planomonospora* sp. and NAI-107 from *Microbispora* ATCC PTA-5024 were identified (Castiglione *et al.*, 2007; Castiglione *et al.*, 2008). The revised structure of 97518 showed that these two compounds are related (Maffioli *et al.*, 2009). Both 97518 (planosporicin) and NAI-107 (microbisporicin) possess the same ring organization, with three Lan and one MeLan. Recently, new 97518-related lantibiotics were described and NAI-107 was indicated as the most divergent lantibiotic of this family (Maffioli, *et al.*, 2015). In the same screening program the actagardine derivative NAI-802 from *Actinoplanes* sp. was identified (Simone *et al.*, 2013).

In the last decade, the gene clusters involved in the biosynthesis of lantibiotics from actinomycetes were described. Sequence analysis of the genes encoding the modifying enzymes allowed to classify cinnamycin and actagardine into class II lanthipeptides (Widdick *et al.*, 2003; Boakes *et al.*, 2009), whereas the 97518-like lantibiotics into class I (Foulston and Bibb, 2010; Sherwood *et al.*, 2013).

The actagardine gene cluster (*gar*) contains the genes encoding the precursor peptide GarA, the bifunctional modifying enzyme GarM, an ABC transporter (GarTH), a two-component regulatory system (GarKR) and GarR1, a *Streptomyces* antibiotic regulatory protein (SARP). The cluster lacks a LanT-type transporter and a LanP-type protease. The cinnamycin cluster (*cin*) encodes homologs to Gar proteins and several proteins with unknown functions.

The similarity of the biosynthetic gene clusters of planosporicin (*psp*) and microbisporicin (*mib*) reflects the similar structure of the two lantibiotics. The *mib* cluster contains the additional genes *mibO*, *mibD*, *mibH*, *mibS*, which are responsible for

the introduction of the post-translational modifications found in microbisporicin but not in planosporicin (Foulston and Bibb, 2010). In addition, the *mib* cluster encodes the sodium/proton antiporter MibN, whose function in microbisporicin production is still unknown.

Few lantibiotics from actinomycetes are in pre-clinical or clinical test. NVB302 is an actagardine derivative developed by Novacta for the treatment of hospital acquired *Clostriudium difficile* infections and Moli1901 is a structure analogue of cinnamycin that completed phase II clinical trials for the treatment of cystic fibrosis.

### 1.2.4 Mode of action of lantibiotics

Most of the known lantibiotics are lipid II-targeting antibiotics (Bauer and Dicks, 2005; Islam *et al*., 2012). The binding of the prototype lantibiotic nisin to lipid-bound PG precursors was firstly demonstrated by Reisinger *et al*, 1980 and successively widely studied (Breukink *et al.*, 1999). Elucidation of lipid II binding was achieved by solving the solution structure of nisin-lipid II complex in DMSO using a lipid II variant, consisting of a shortened prenyl tail (3 isoprene units instead of 11) (Hsu *et al.*, 2004). Nisin recognizes the pyrophosphate, MurNAc and the first isoprene unit of lipid II. The N-terminal A and B rings of nisin form five hydrogen bonds with the pyrophosphate group through their backbone amides. The N-terminal rings of nisin form a cage-like structure, which was suggested to be a unique lipid II-binding motif (Hsu *et al.*, 2004). The N-terminal A and B rings are conserved in the class I lantibiotics epidermin, subtilin, mutacin 1140 and NAI-107 in position 3 and 7-11. Moreover, the hydrophobic character of the amino acid at position 6 is preserved (Ile or Leu). Because lantibiotics bind to lipid II at a site different from that affected by vancomycin and related glycopeptides, they are active against drug resistance Gram-positive pathogens and have attracted attention as potential drug candidates.

Nisin possesses a dual activity mediated by lipid II-binding: pore formation and inhibition of PG biosynthesis (Wiedemann *et al.*, 2001). The pore-forming activity of nisin is unique in that the lipid II is used as a docking molecule. Upon lipid II binding, the C-terminus of nisin inserts into the membrane in a perpendicular orientation with respect to the phospholipid bilayer. Pores consist of eight nisin and four lipid II molecules and have a

diameter of 2-2.5 nm (Wiedemann *et al.*, 2004). By forming pores in the membrane, nisin leads to cell depolarization and efflux of cytoplasmic solutes and ions. The flexible hinge region between ring C and D is essential for pore formation. Peptides mutated in this region are completely inactive in the pore formation assay and their *in vivo* activity is reduced (Wiedemann *et al.*, 2001).

The retained *in vivo* activity of these mutated peptides is the result of the second mechanism of action of nisin. Nisin is able to inhibit PG polymerization in a concentration manner by binding the PG precursor lipid II (Wiedemann *et al.*, 2001). Whereas mutations in the hinge region affect the pore-forming activity of nisin, lipid II binding is not compromised. Hence, the dual mechanism of action of nisin combined with a high affinity for the target lipid II may explain the high potency of this lantibiotic (nM range). In addition, nisin was demonstrated to remove lipid II from the site of PG biosynthesis by sequestering it in patches on the cytoplasmic membrane (Hasper *et al.*, 2006).

Epidermin and gallidermin possess a lipid II binding motif similar to nisin but they miss the C-terminal tail. The fact that epidermin and gallidermin are considerable shorter than nisin explains why lipid II-mediated pore formation depends on the membrane-thickness of the target strain (Bonelli *et al.*, 2006). Recently, binding of gallidermin and nisin to the wall teichoic acid (WTA) precursors lipid III and lipid IV was demonstrated (Müller *et al.*, 2012b). However, since these cell wall precursors are exclusively found in the cytoplasm, their function as *in vivo* target could only be hypothesized with an internalization of the lantibiotics.

The pore-forming lantibiotic Pep5 does not possess a nisin-like lipid II binding motif and experiments conducted with lipid II-depleted strains showed that Pep5 does not use lipid II as a docking molecule (Brötz *et al.*, 1998a). The fact that Pep5 is active in nM concentration against some bacteria indicates a target-mediated Pep5 activity, though a target has not been identified yet.

The class II lantibiotic mersacidin blocks PG biosynthesis by binding to lipid II but it does not form pores in the cytoplasmic membrane (Brötz *et al.*, 1998b). Lipid II binding involves a motif different to the one described for nisin. The C ring of mersacidin, conserved in other class II lantibiotics, is considered to be essential for lipid II recognition

(Hsu *et al.*, 2003). A stimulating effect of $Ca^{2+}$ on the mersacidin antibacterial activity was reported. $Ca^{2+}$ was suggested to facilitate the interaction with lipid II and the cytoplasmic membrane, rather than being part of the lipid II complex (Böttiger *et al.*, 2009).

A mersacidin-like lipid II binding motif is also found in Ltnα, the alpha peptide of the two-component lantibiotic lacticin 3147. Ltnα was demonstrated to interact with lipid II forming a complex that recruits Ltnβ. The synergistic effect of Ltnα and Ltnβ leads to bacterial death due to inhibition of PG biosynthesis combined with pore formation (Wiedemann *et al.*, 2006). A synergistic mode of action mediated by lipid II binding was also reported for the two-component lantibiotic haloduracin (Oman *et al.*, 2011).

Cinnamycin is a lantibiotic that possesses a different target than most of the known lantibiotics, exhibiting a peculiar mode of action. Cinnamycin induces transbilayer lipid movement, the so-called 'flip-flop' of phospholipids. Its antibacterial and haemolytic activity is due to the binding of phosphatydilethanolamine (PE), a phospholipid found in the inner leaflet of the cytoplasmic membranes that is exposed to the outer leaflet of the cytoplasmic membrane by lipid movement (Choung *et al.*, 1988). The PE-dependent binding of cinnamycin to the cell surface promotes changes in membrane permeability, membrane reorganization and membrane fusion (Makino *et al.*, 2003).

### 1.2.5 Immunity in lantibiotic-producing bacteria

Antibiotic synthesis requires that the producer organisms have mechanisms conferring protection to their antibacterial product. The targets of lantibiotics are molecules conserved across the bacterial word (e.g. lipid II), therefore lantibiotic-producing strains have evolved several mechanisms to escape from the antibacterial activity of their own produced lantibiotic. The leader peptide, which is cleaved only during or after secretion of the lantibiotic to the extracellular space, maintains the lantibiotic in an inactive form (Willey and van der Donk, 2007). In this way, the binding of the lantibiotic to the targets in the cytoplasm (e.g. lipid II) is avoided.

Once outside the cell, the lantibiotic can attack the producer strain. For this reason, lantibiotic producers express immunity proteins to counteract the action of their product (Draper *et al.*, 2008; Alkhatib *et al.*, 2012). The protection mechanism of

lantibiotic-producing strains was called ‘immunity’ instead of ‘self-resistance’, according to the term employed for the related antibacterials bacteriocins. The first proteins involved in lantibiotic protection were designed ‘immunity proteins’ (Klein and Entian, 1994; Siegers and Entian, 1995), due to their homology with the immunity proteins of microcin B17 from *E. coli* (Garrido *et al.*, 1988).

The immunity proteins expressed by lantibiotic producers are widely diverse both in structure and function and comprise ABC transporters, lipoproteins, transmembrane proteins and membrane-associated peptides (Okuda and Sonomoto, 2011).

ABC transporters are membrane proteins that use ATP hydrolysis to translocate many substrates across the membrane. They consist of an ATPase subunit or nucleotide-binding domain (NBD) and a permease, also designed as transmembrane domain (TMD), which are encoded by one or multiple ORFs (Rees *et al.*, 2009). The first described ABC transporters involved in lantibiotic immunity were the ones encoded by the genes *spaFEG* and *nisFEG* from the subtilin and nisin cluster, respectively (Klein and Entian, 1994; Siegers and Entian, 1995). These genes, designed with the general term *lanFEG*, encode an ATPase (LanF) and two permeases (LanE and LanG). It was deduced that the ABC transporters assemble as a complex $F_2EG$, consisting of two homodimeric NDBs and two heterodimeric TMDs, like the maltose transporter $MalFGK_2$ (Garrido *et al.*, 1988). *lanFEG* genes were also identified in the epidermin cluster (*epiFEG*). The overexpression of *epiFEG* in the heterologous host *Staphylococcus carnosus* led to a fivefold increase of epidermin production, suggesting a mechanism based on the extrusion of the lantibiotic from the membrane to the extracellular space instead of internalization and degradation (Peschel and Götz, 1996). This theory was demonstrated two years later by Otto *et al.*, 1998 by a cell-based transport assay that showed that EpiFEG is able to transport lantibiotic molecules inserted into the membrane back to the culture supernatant. The same mode of action was proved for NisFEG and SpaFEG (Stein *et al.*, 2003; Stein *et al.*, 2005). Recently, the activity of NisFEG was demonstrated to be dependent on the C-terminal rings of nisin, the part of the lantibiotic that inserts into the membrane (Alkhatib *et al.*, 2014).

Whereas EpiFEG is the only determinant conferring epidermin immunity, full immunity to nisin and subtilin is achieved by expression of LanI proteins in addition to the ABC

transporters NisFEG and SpaFEG. NisI and SpaI are two proteins possessing the characteristic signatures of lipoproteins: a N-terminal signal peptide and a lipobox. *In vivo* labelling with [$^3$H]-palmitic acid was used to demonstrate that NisI is attached to the outer leaflet of the cytoplasmic membrane by a lipid anchor (Qiao *et al.*, 1995). However, it was shown that about half of the produced NisI escapes lipid modification and it is secreted into the medium, forming the lipid-free pool of NisI (LF-Nis) (Koponen *et al.*, 2004). Although the lantibiotics nisin and subtilin have similar structures, the corresponding immunity lipoproteins NisI and SpaI do not show any homology and they do not confer cross-resistance. A SpaI'-'NisI fusion protein obtained by replacing 21 C-terminal amino acids from SpaI by the corresponding ones from NisI showed an increased nisin immunity to *L. lactis*. Therefore, the C-terminus of NisI was indicated to be essential for the immunity activity of the lipoprotein and for lantibiotic recognition (Takala and Saris, 2006). Binding of NisI and SpaI to the corresponding lantibiotics was proposed on the basis of cross-link experiments, native PAGE and surface plasmon resonance analyses (Stein *et al.*, 2003; Stein *et al.*, 2005; Takala and Saris, 2006). However, the mode of action of these lipoproteins is not completely understood. To gain insights into SpaI mechanism of action on a molecular level, the solution structure of SpaI was elucidated (Christ *et al.*, 2012).

A cooperation of the nisin immunity determinants NisEFG and NisI was proposed since each of them displays less than 20% of the full immunity when expressed alone (Ra *et al.*, 1999). Differently to native NisI and C-terminally truncated NisI, the SpaI'-'NisI fusion protein conferred the same level of immunity to *L. lactis* expressing or non-expressing NisFEG. Thus, the C-terminus of NisI was suggested to not be involved in the interaction with NisEFG (Takala *et al.*, 2006).

Cooperation between an ABC transporter and an immunity protein was deeply investigated in the lantibiotic producer *Staphylococcus warneri* ISK-1. The nukacin ISK-1 cluster encodes the ABC transporter NukFEG and the transmembrane protein NukH that were demonstrated to act cooperatively (Okuda *et al.*, 2005). Studies with fluorescent-labelled nukacin ISK-1 showed that NukH captures the lantibiotic, which is then transported to the extracellular space by NukFEG in an energy-dependent manner (Okuda *et al.*, 2008). NukH possesses three transmembrane regions, a cytoplasmic N-

terminus and an extracellular C-terminus (Okuda *et al.*, 2005). Due to its topology and function, NukH was proposed to belong to a new family of lantibiotic immunity proteins (LanH). LanH proteins are transmembrane proteins, which confer immunity to lantibiotic producers by acting in cooperation with LanFEG ABC transporters (Okuda and Sonomoto, 2011).

Other transmembrane lantibiotic immunity proteins were described, however their exact mode of action is still unclear. Few examples are SunI, LtnI, ApnI that confer immunity to sublancin 168, lacticin 3147 and subtilomycin, respectively (Dubois *et al.*, 2009; McAuliffe *et al.*, 2000; Deng *et al.*, 2014).

PepI, the protein conferring immunity to Pep5, is peculiar in the fact that it is a membrane-associated peptide. Site-directed mutagenesis studies indicated that the N-terminal is important for localization and the C-terminal for the immunity phenotype (Hoffmann *et al.*, 2004). The transport of PepI was proposed to occur together with its target, a mechanism that would provide immunity by shielding the target as soon as it emerges from the membrane (Hoffmann *et al.*, 2004).

## 1.3 The lantibiotic NAI-107

### 1.3.1 Structure and mode of action of NAI-107

NAI-107, also known as microbisporicin or 107981, is a lantibiotic produced by the actinomycete *Microbispora* ATCC PTA-5024. The compound was discovered during a screening program designed to detect classes of cell-wall inhibitors from actinomycetes, different from β-lactams and glycopeptides (Castiglione *et al.*, 2008). NAI-107 is synthesized as a precursor peptide of 57 amino acids that undergoes post-translational modifications and cleavage of the signal peptide (33 aa) to obtain the mature form. NAI-107 consists of one MeLan, three Lan, an aminovinyl-cysteine (AviCys) and two unusual lantibiotic modifications: a chlorinated tryptophan (Trp4) and a mono- or di-hydroxylated proline (Pro14) (Fig. 5) (Castiglione *et al.*, 2008). NAI-107 shares both N- and C-terminus with class I lantibiotics produced by Firmicutes. The N-terminal lanthionine rings (Val1-Ala11) resemble the lipid II-binding motif of nisin (Hsu *et al*., 2004), whereas the C-terminal AviCys is also found in epidermin (Allgaier *et al*., 1985).

Furthermore, NAI-107 shares structural elements with the class II lantibiotic mersacidin (Chatterjee *et al.*, 1992). In particular, the ring C, D and E of NAI-107 resemble the globular C-terminus of mersacidin.

NAI-107 is produced by *Microbispora* ATCC PTA-5024 as a complex of related molecules called congeners. The most abundant congeners $A_1$ and $A_2$ differ by the presence of di- or mono-hydroxy-proline, respectively (Maffioli *et al.*, 2014). F and B congeners correspond to de-chloro and oxidized derivatives. The presence of two congeners for both de-chloro and oxidized derivatives ($F_1$, $F_2$ and $B_1$, $B_2$) reflects the hydroxylation pattern of Pro14 found in $A_1$ and $A_2$. The congeners $B_1$ and $B_2$ are the result of an oxidation of the thioether of ring A. This spontaneous oxidation was observed when *Microbispora* cultures entered in the stationary phase and the pH was higher than 7 (Maffioli *et al.*, 2014). Moreover, N-terminally extended congeners of $A_1$ and $A_2$ were detected in *Microbispora* cultures in minimal medium. These congeners, designed as GPA-$A_1$ and GPA-$A_2$, possess the additional tripeptide GPA at the N-terminus of NAI-107 (Maffioli *et al.*, 2014).

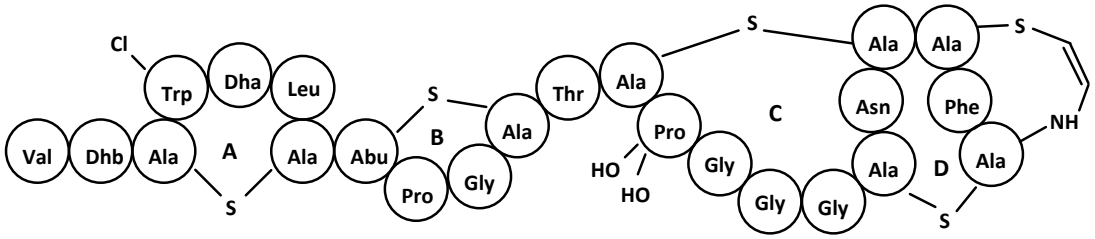


**Fig. 5. Representation of NAI-107.** Letters (A-D) indicate Lan and MeLan rings.

NAI-107 is stable in acidic conditions. The antibiotic has a half-life of more than one month in a 2-6 pH range at 40°C in methanol (Castiglione *et al.*, 2008). Besides methanol, NAI-107 is soluble in 10% DMSO and water:acetonitrile in a ratio 1:1 (Maffioli, personal communication).

NAI-107 is active against Gram-positive bacteria including methicillin-resistant *Staphylococcus aureus* (MRSA), glycopeptide-intermediate *S. aureus* (GISA), vancomycin-resistant enterococci (VRE) and penicillin-resistant *Streptococcus pneumonia,* with a higher activity than the lantibiotics nisin, actagardine and mersacidin. Furthermore, NAI-107 is active against some Gram-negative bacteria like *Moraxella catarrhalis* and

*Neisseria gonorrhoeae* (Castiglione *et al.*, 2008). The major congeners of the NAI-107 complex ($A_1$ and $A_2$) possess an identical activity whereas the B and F congeners are less active, probably due to the modifications in the ring A (Maffioli *et al.,* 2014). Because of its interesting antibacterial profile and potent antibacterial activity, NAI-107 is currently in the pre-clinical development for the treatment of multidrug-resistant Gram-positive pathogens. Although NAI-107 was tested in several *in vitro* studies against multidrug resistant pathogens no resistant mutants were observed (Jabes *et al.*, 2011). NAI-107 efficacy against MRSA, GISA and VRE was demonstrated in a lethal murine model, rat granuloma pouch model and rat endocarditis model (Jabes *et al.*, 2011) and in a murine thigh infection model induced by MRSA (Lepak *et al.*, 2014). NAI-107 is more effective when administered intravenous than subcutaneously (Jabes *et al.*, 2011). An injectable therapy for the treatment of multi-drug-resistant Gram-positive infections is being developed by Sentinella Therapeutics, the US company who acquired the rights to the compound.

The mode of action of NAI-107 was extensively studied by Münch and colleagues (Münch *et al*., 2014). Macromolecular synthesis, whole-cell and enzyme assays combined with proteomic profiling showed that NAI-107 interferes with PG biosynthesis and affects the bacterial membrane by slow depolarization. NAI-107 targets lipid II but it does not form stable nisin-like pores that cause a rapid efflux of cell metabolites. While the sequestration of lipid II leads to the block of PG biosynthesis, slow depolarization causes the disorganization of the cell wall machinery. Thus, the potency of NAI-107 is attributed to its dual mode of action. The interaction of NAI-107 with dodecylphosphocholine (DPC) micelles, used as membrane models, was analysed by NMR spectroscopy (Münch *et al*., 2014). The NMR data showed that the ring A and to lesser extent the ring B of NAI-107 interact with DPC micelles. NMR spectroscopy was also used to follow the binding of NAI-107 to lipid II. Titration experiments indicated a 1:1 NAI-107-lipid II complex that transforms into a 2:1 complex when NAI-107 was added in excess, although NAI-107 dimers in solution could not be detected. Lipid II, which is exposed to the outer leaflet of the cytoplasmic membrane, is the primary target of NAI-107. However, NAI-107 binds *in vitro* also to the bactoprenol-bound cell wall precursors lipid I, lipid III and lipid IV, precursors of the PG and WTA biosynthetic

pathways. The role *in vivo* of these potential targets was only speculated, as there is no evidence of an internalization of NAI-107.

### 1.3.2 The NAI-107 producer *Microbispora* ATCC PTA-5024 and the *mlb* cluster

*Microbispora* ATCC PTA-5024, the producer of the lantibiotic NAI-107, is a filamentous actinobacterium, which belongs to the family of the *Streptosporangiaceae*. The draft genome of *Microbispora* ATCC PTA-5024 was published with the Genbank accession number AWEV00000000. It consists of 8543819 bp, with a 71.2% G+C content. NAI-107 produced by *Microbispora* ATCC PTA-5024 was found both in the supernatant and associated with the mycelium (Castiglione *et al.*, 2008).

In addition to *Microbispora* ATCC PTA-5024, another strain, *Microbispora corallina* NRRL 30420, was described to produce NAI-107 (Lee, 2003; Foulston and Bibb, 2010). Recently, the congeners of the NAI-107 complex produced by *Microbispora* ATCC PTA-5024 and *M. corallina* NRRL 30420 were characterized (Maffioli *et al.*, 2014). The distribution of the NAI-107 congeners produced by *M. corallina* NRRL 30420 is different from the one of *Microbispora* ATCC PTA-5024. Moreover, *M. corallina* NRRL 30420 produces two congeners which are found only in traces in *Microbispora* ATCC PTA-5024: $A_0$ and $F_0$, the de-hydroxylated variants of the A and F congeners (Maffioli *et al.*, 2014).

The screening of *Microbispora* ATCC PTA-5024 genome led to the identification of the NAI-107 biosynthetic gene cluster, named *mlb* cluster (Fig. 6) (Donadio *et al*., 2009). The *mlb* cluster shows extensively syntheny with the *mib* cluster, responsible for the synthesis of NAI-107 in *M. corallina* NRRL 30420 (Foulston and Bibb, 2010). In the latter strain, the genes involved in the biosynthesis of NAI-107 were analysed (Foulston and Bibb, 2010). The *mib* cluster consists of 20 genes that comprise the genes encoding the precursor peptide (MibA), the enzymes involved in the formation of the lanthionine rings (MibB and MibC) and in the regulation (MibR, MibX, MibW). A feed-forward mechanism initiated by the master regulator MibR and mediated by the extracytoplasmic function sigma factor MibX was suggested (Foulston and Bibb, 2011). MibR initiates transcription of the *mibABCDTUV* operon by binding to the *mibA* promoter. A form of NAI-107 that lacks chlorination and hydroxylation or a low level of inhibition of PG biosynthesis were hypothesized to cause a conformational change of the

anti-sigma factor MibW and the release of the sigma factor MibX. MibX binds to the promoter sequences of *mibJ*, *mibQ*, *mibR*, *mibX* and *mibE* and activates the respective operons resulting in high-level NAI-107 production. The *mib* cluster encodes two enzymes not described before in lantibiotic gene clusters: a cytochrome P450 (MibO) and a flavin-dependent tryptophan halogenase (MibH), involved in hydroxylation of proline and chlorination of tryptophan, respectively. Furthermore, the cluster encodes three putative ABC transporters (MibYZ, MibTU, MibEF) and a predicted lipoprotein (MibQ).

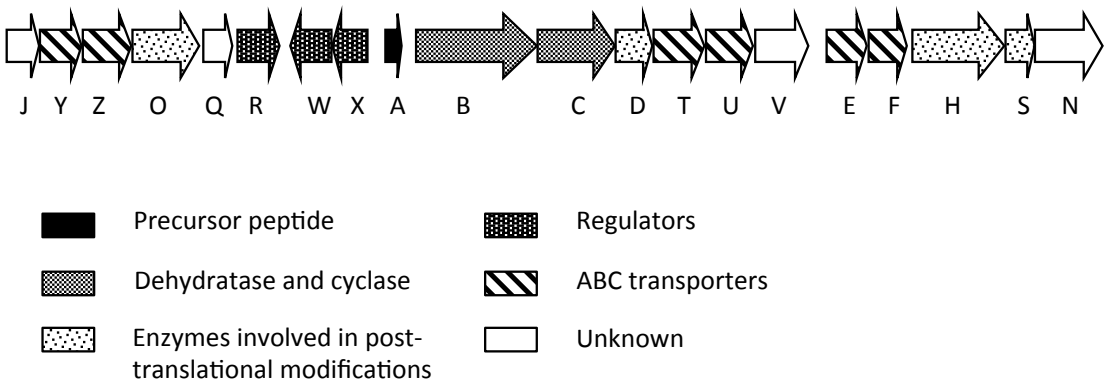


**Fig. 6. Representation of the NAI-107 biosynthetic gene cluster (*mlb*).** Genes are represented with arrows. The pattern of the arrows codes the predicted function of the gene products.

## 1.4 Aim of the work

Aim of this study was the analysis of immunity in *Microbispora* sp. 107891 to determine the mechanisms evolved in the producer strain to protect itself from the PG-targeting lantibiotic NAI-107.

Therefore the following questions had to be answered:

- Do PG modifications contribute to NAI-107 immunity?
- Does the *mlb* cluster encode immunity proteins?

# 2. MATERIAL AND METHODS

## 2.1 Culture media

Culture media were prepared with deionized water, unless stated otherwise. When reported, the pH was adjusted before autoclaving. For some media, sterile solutions of supplementary components were added after sterilization. Ultrapure water was obtained from a TKA-GenPure water purification system.

### 2.1.1 Liquid media

**Evans medium**

| | |
|---|---|
| $FeSO_4$ x $7H_2O$ | 0.09 g/l |
| MOPS | 21 g/l |
| KCl | 10 mM |
| $Na_2SO_4$ | 2 mM |
| Citric acid | 2 mM |
| $CaCl_2$ x $2H_2O$ | 0.25 mM |
| $MgCl_2$ x $6H_2O$ | 1.25 mM |
| $NaMoO_4$ x $2H_2O$ | 1 µg/l |
| Trace element solution | 5 ml/l |
| Ultrapure $H_2O$ | 903.65 ml/l |

pH 6.5

Add the following supplements after sterilization

| | |
|---|---|
| Glucose | 25 g/l (50 ml of 50% glucose) |
| $NaH_2PO_4$ | 10 mM (5 ml of 2 M $NaH_2PO_4$) |
| $NaNO_3$ | 50 mM (25 ml of 2 M $NaNO_3$) |

**GE82AB** (NAICONS)

| | |
|---|---|
| Dextrose monohydrate* | 10 g/l |
| Starch | 20 g/l |
| Soybean meal | 15 g/l |
| Yeast extract | 5 g/l |
| $CaCO_3$ | 1 g/l |
| Agar | 1 g/l |

pH 7.3

* add dextrose monohydrate (20 ml of 50% dextrose monohydrate) after sterilization

**GE82G** (NAICONS)

| | |
|---|---|
| Dextrose monohydrate* | 20 g/l |
| Starch | 20 g/l |
| Soybean meal | 15 g/l |
| Yeast extract | 5 g/l |
| $CaCO_3$ | 1 g/l |
| Agar | 1 g/l |

pH 7.3

* add dextrose monohydrate (40 ml of 50% dextrose monohydrate) after sterilization

**KV6** (NAICONS)

| | |
|---|---|
| Dextrose monohydrate | 12 g/l |
| Soy peptone | 12 g/l |
| Yeast extract | 12 g/l |
| NaCl | 2 g/l |

pH 7.5

**LB medium ready for use** (Sigma)

| | |
|---|---|
| LB powder | 20 g/l |

**M9** (Chen *et al*., 2006)

| | |
|---|---|
| $NH_4Cl$* | 0.5 g/l |
| Glucose** | 5 g/l |
| Ultrapure $H_2O$ | 700 ml/l |

Add the following supplements after sterilization

| | |
|---|---|
| $Na_2HPO_4$ | 6 g/l (100 ml 60 g/l $Na_2HPO_4$ x $H_2O$) |
| $KH_2PO_4$ | 3 g/l (100 ml 30 g/l $KH_2PO_4$) |
| NaCl | 0.5 g/l (100 ml 5 g/l NaCl) |
| $MgSO_4$ x $7H_2O$ | 2 mM (2 ml 1 M $MgSO_4$ x $7H_2O$) |
| $CaCl_2$ x $2H_2O$ | 0.01 mM (10 µl 1 M $CaCl_2$ x $2H_2O$) |
| $FeSO_4$ x $7H_2O$ | 0.01 mM (1 ml 0.01 M $FeSO_4$ x $7H_2O$) |
| Thiamine | 5 mg/l (1 ml 5 mg/ml thiamine) |
| Micronutrients | 1 ml/l |
| Vitamins | 1 ml/l |

* if $^{15}N$-minimal medium is needed, use $^{15}NH_4Cl$ in place of $NH_4Cl$. $^{15}NH_4Cl$ can be added before sterilization or cold filtered into the medium.

** if $^{13}C$-minimal medium is needed, use 2 g $^{13}C$-glucose in place of 5 g regular glucose. $^{13}C$-glucose must be cold filtered into the medium.

**Nutrient medium ready for use** (Difco)

| | |
|---|---|
| Nutrient medium powder | 8 g/l |

**R5** (Kieser *et al.*, 2000)

| | |
|---|---|
| Sucrose | 103 g/l |
| $K_2SO_4$ | 0.25 g/l |
| $MgCl_2 \times 6H_2O$ | 10.12 g/l |
| Glucose | 10 g/l |
| Casaminoacids | 0.1 g/l |
| Yeast extract | 5 g/l |
| TES | 5.73 g/l |
| Trace element solution | 2 ml/l |
| Ultrapure $H_2O$ | 900 ml/l |

pH 7.2

Add the following supplements after sterilization

| | |
|---|---|
| $KH_2PO_4$ | 0.054 g/l (10 ml of 0.54% $KH_2PO_4$) |
| $CaCl_2 \times 2H_2O$ | 2.94 g/l (80 ml of 3.68% $CaCl_2 \times 2H_2O$) |
| L-proline | 3 g/l (15 ml of 20% L-proline) |

**S medium** (Okanishi *et al.*, 1974)

| | |
|---|---|
| Pepton | 4 g/l |
| Yeast extract | 4 g/l |
| $K_2HPO_4$ | 4 g/l |
| $KH_2PO_4$ | 2 g/l |
| Glycine | 10 g/l |
| Deionized water | 800 ml |

After sterilization add 200 ml with 10 g glucose and 0.5 g $MgSO_4 \times 7H_2O$

**107P1H** (slightly modified from NAICONS' recipe)

| | |
|---|---|
| Dextrose monohydrate* | 15 g/l |
| Starch | 60 g/l |
| Soybean meal | 30 g/l |
| Yeast extract | 10 g/l |
| $CaCO_3$ | 1 g/l |
| $(NH_4)_2SO_4$ | 1 g/l |
| NaCl | 2 g/l |
| Olive oil | 10 ml/l |
| $ZnSO_4 \times 7H_2O$ | 0.1 mM |

pH 7.3

* add dextrose monohydrate (30 ml of 50% dextrose monohydrate) after sterilization

**2 x YT medium** (Kieser *et al.*, 2000)

| | |
|---|---|
| Tryptone | 16 g/l |
| Yeast extract | 10 g/l |
| NaCl | 5 g/l |

### 2.1.2 Agar media

**HA agar**

| | |
|---|---|
| Malt | 10 g/l |
| Glucose | 4 g/l |
| Yeast extract | 4 g/l |
| $CaCl_2 \times 2H_2O$ | 1.46 g/l |
| Agar | 18 g/l |

pH 7.3

**LB agar ready for use** (Roth)

| | |
|---|---|
| LB agar powder | 35 g/l |

**MS agar (Cullum)** (Kieser *et al.*, 2000)

| | |
|---|---|
| Mannitol | 20 g/l |
| Soybean meal | 20 g/l |
| Agar | 18 g/l |

Add 10 mM $MgCl_2$ x $6H_2O$ for conjugation experiments

**MV0.1 agar** (NAICONS)

| | |
|---|---|
| Dextrose monohydrate | 0.1 g/l |
| Starch | 2.4 g/l |
| Meat extract | 0.3 g/l |
| Yeast extract | 0.5 g/l |
| Tryptose | 0.5 g/l |
| Agar | 15 g/l |

pH 7.2

**S1 agar** (NAICONS)

| | |
|---|---|
| Oatmeal | 60 g/l |
| Agar | 18 g/l |
| Trace element solution | 1 ml/l |

### 2.1.3 Supplement solutions

**Micronutrients for M9 (1000x)**

| | |
|---|---|
| $(NH_4)_6Mo_7O_{24}$ x $4H_2O$ | 3 x $10^{-6}$ M |
| $H_3BO_3$ | 4 x $10^{-4}$ M |
| $CoCl_2$ x $6H_2O$ | 3 x $10^{-5}$ M |
| $CuSO_4$ x $5H_2O$ | 1 x $10^{-5}$ M |
| $MnCl_2$ x $4H_2O$ | 8 x $10^{-5}$ M |
| $ZnCl_2$ | 1 x $10^{-5}$ M |

**Vitamins for M9 (1000x)**

| | |
|---|---|
| D-biotin | 1 g/l |
| Choline chloride | 0.5 g/l |
| Folic acid | 0.5 g/l |
| Myoinositol | 1 g/l |
| Nicatinamide | 0.5 g/l |
| Panthotenic acid | 0.5 g/l |
| Pyridoxal HCl | 0.5 g/l |
| Riboflavin | 50 mg/l |
| Thiamine HCl | 0.5 g/l |

**Trace element solution for Evans medium and R5**

| | |
|---|---|
| $FeCl_3$ x $6H_2O$ | 200 mg/l |
| $MnCl_2$ x $4H_2O$ | 10 mg/l |
| $ZnCl_2$ | 40 mg/l |
| $CuCl_2$ x $2H_2O$ | 10 mg/l |
| $Na_2B_4O_7$ x $10H_2O$ | 10 mg/l |
| $(NH_4)_6Mo_7O_{24}$ x $4H_2O$ | 10 mg/l |

**Trace element solution for S1 agar**

| | |
|---|---|
| $FeSO_4$ x $7H_2O$ | 1 g/l |
| $MnCl_2$ x $4H_2O$ | 1 g/l |
| $ZnSO_4$ x $7H_2O$ | 1 g/l |

## 2.2 Buffers and solutions

### 2.2.1 Buffers and solutions for DNA and RNA methods

**Alkaline lysis**

**P1 buffer** (store at 4°C)

| | |
|---|---|
| Tris/HCl pH 8 | 50 mM |
| EDTA | 10 mM |
| RNase A | 100 µg/ml |

**P2 buffer**

| | |
|---|---|
| NaOH | 0.2 M |
| SDS | 1% |

**P3 buffer** (store at 4°C)

| | |
|---|---|
| Potassium acetate pH 5.5 | 3 M |

**Agarose gel electrophoresis**

**TAE electrophoresis buffer** (pH 7.8, adjusted with acetic acid)

| | |
|---|---|
| Tris | 40 mM |
| Sodium acetate | 10 mM |
| EDTA | 1 mM |

**DNA loading buffer**

| | |
|---|---|
| Tris pH 7.5 | 10 mM |
| Bromophenol blue | 0.04% |
| Xylene cyanole | 0.03% |
| Orange G | 0.2% |
| Glycerol | 60% |
| EDTA | 6 mM |

**RNA isolation**

**TE buffer**

| | |
|---|---|
| Tris/HCl pH 8 | 10 mM |
| EDTA | 1 mM |

**Kirby mix (2x)** (store at-20°C)

| | |
|---|---|
| Tris/HCl pH 8.3 | 50 mM |
| Sodium lauroyl sarcosinate | 2% |
| p-Aminosalicylic acid, Na-salt | 12% |
| Phenol:Chloroform:Isoamyl Alcohol (25:24:1) | 12% |

**Tris/HCl buffer**

| | |
|---|---|
| Tris/HCl pH 8.3 | 50 mM |

**Na acetate solution**

| | |
|---|---|
| Sodium acetate pH 6 | 3 M |

**RNase-killer solution**

| | |
|---|---|
| NaOH | 40 mM |
| EDTA | 1 mM |

### 2.2.2 Buffers and solutions for protein methods

**SDS-PAGE electrophoresis**

**SDS-PAGE running buffer**

| | |
|---|---|
| Tris | 0.025 M |
| Glycine | 0.192 mM |
| SDS | 0.1% |

**SDS-PAGE loading buffer (3x)** (store at 4°C)

| | |
|---|---|
| Tris/HCl pH 6.8 | 240 mM |
| SDS | 6% |
| Glycerol | 30% |
| β-mercaptoethanol | 16% |
| Bromophenol blue | 0.06% |

**Coomassie Blue staining solution**

| | |
|---|---|
| Coomassie Brilliant Blue G250 | 1 g/l |
| Methanol | 50% |
| Acetic acid | 10% |

**Destaining solution**

| | |
|---|---|
| Methanol | 12% |
| Acetic acid | 7% |

**Determination protein concentration**

**Bradford reagent** (store at -4°C)

| | |
|---|---|
| Coomassie Brilliant Blue G250 | 100 mg/l |
| Methanol | 5% |
| $H_3PO_4$ | 10% |

## Western Blot

### TBS-T buffer

| | |
|---|---|
| Tris/HCl pH 7.5 | 10 mM |
| NaCl | 150 mM |
| Tween20 | 0.05% |

### Blocking buffer

| | |
|---|---|
| TBS-T | 1x |
| Milk powder | 5% |

### Wash buffer 1

| | |
|---|---|
| TBS-T | 1x |
| Milk powder | 1% |

### Wash buffer 2

| | |
|---|---|
| Tris/HCl pH 7.35 | 50 mM |

## Protein purification

**Lysis buffer** (pH 8, prepare before usage)

| | |
|---|---|
| $NaH_2PO_4$ | 50 mM |
| NaCl | 300 mM |
| Imidazole | 10 mM |
| $MgCl_2$ x $6H_2O$ | 20 mM |
| Protease inhibitors | 1 tablet/10 ml |
| Lysozyme | 1 mg/ml |
| DNase | 0.1 mg/ml |

**Wash buffer** (pH 8)

| | |
|---|---|
| $NaH_2PO_4$ | 50 mM |
| NaCl | 300 mM |
| Imidazole | 10 mM |

**Elution buffer** (pH 8)

| | |
|---|---|
| $NaH_2PO_4$ | 50 mM |
| NaCl | 300 mM |
| Imidazole | 250 mM |

**Dialysis buffer** (pH 7.8)

| | |
|---|---|
| $NaH_2PO_4$ | 50 mM |
| NaCl | 50 mM |

**Enterokinase buffer** (pH 8)

| | |
|---|---|
| Tris/HCl | 20 mM |
| NaCl | 50 mM |
| $CaCl_2 \times 2H_2O$ | 2 mM |

**Buffer A for anion exchange**

| | |
|---|---|
| Tris/HCl pH 8 | 20 mM |

**Buffer B for anion exchange**

| | |
|---|---|
| Tris/HCl pH 8 | 20 mM |
| NaCl | 1 M |

**PBS** (pH 7.4)

| | |
|---|---|
| NaCl | 137 mM |
| KCl | 2.7 mM |
| $Na_2HPO_4$ | 10 mM |

| | |
|---|---|
| $KH_2PO_4$ | 2 mM |

## 2.3 Chemicals, antibiotics, enzymes, kits

### 2.3.1 Chemicals

| **Chemicals or additives** | **Source** |
|---|---|
| Acetic acid | Roth |
| Aceton | Sigma-Aldrich |
| Acetonitrile | J.T.Baker |
| Acrylamide/Bisacrylamide Rotiphorese Gel 30 (37.5:1) | Roth |
| Agar | Roth |
| Agarose | Genaxxon, Roth |
| Aminosalicylic acid, Na-salt | Sigma-Aldrich |
| Ammonium chloride | Merck |
| Ammonium-14N chloride | Cambridge Isotope Lab |
| Ammonium molybdate tetrahydrate | Fluka |
| Ammonium persulfate (APS) | Serva |
| Ammonium sulfate | Merck |
| Biotin (D-biotin) | Sigma-Aldrich |
| Boric acid | Merck |
| Bovine Serum Albumin (BSA) | New England Biolabs |
| Bromphenol Blue | Serva |
| Calcium chloride dihydrate | Acros Organics |
| Calcium carbonate | AppliChem |
| Casaminoacids | Difco |
| Choline chloride | Sigma-Aldrich |
| Citric acid | Roth |

| | |
|---|---|
| Cobalt(II) chloride hexahydrate | Sigma-Aldrich |
| Coomassie Brilliant Blue R-250 | Sigma-Aldrich |
| Copper chloride hexahydrate | Merck |
| Copper sulfate pentahydrate | Merck |
| Deoxynucleotides (dNTPs) | Fermentas |
| Dextrose monohydrate | Maizena Diät GmbH |
| Dimethyl sulfoxide (DMSO) | Merck |
| Dipotassium hydrogen phosphate | Roth |
| Disodium hydrogen phosphate | Roth |
| Dodecylphosphocholine (DPC) | Avanti Polar Lipids |
| EDTA | Merck |
| Ethanol | Sigma-Aldrich |
| Ethidium bromide | Roth |
| Ferric chlorure hexahydrate | Merck |
| Ferrous sulfate heptahydrate | Merck |
| Folic acid | Sigma-Aldrich |
| Formic acid | Merck |
| Glucose | Roth |
| Glucose-13C | Cambridge Isotope Lab |
| Glycerol | Roth |
| Glycine | AppliChem |
| Hydrogen fluoride | Sigma-Aldrich |
| Imidazole | Sigma-Aldrich |
| IPTG (Isopropyl–β–D–Thiogalactoside) | PeqLab |
| LB agar | Roth |
| LB broth | Sigma-Aldrich |
| Lithium chloride | Merck |

| | |
|---|---|
| Magnesium chloride hexahydrate | Roth |
| Magnesium sulfate heptahydrate | Merck |
| Malt extract | Oxoid |
| Manganese chloride tetrahydrate | Merck |
| Mannitol (D-Mannitol) | Merck |
| Meat extract dry | Merck |
| Mercaptoethanol (β-mercaptoethanol) | Merck |
| Methanol | Fisher Scientific |
| Milk powder | Saliter |
| MOPS | Roth |
| Myoinositol | Sigma-Aldrich |
| Nicatinamide | Sigma-Aldrich |
| Nutrient Broth | Becton, Dickinson and Co. |
| Oatmeal (oat flakes instant) | Kölln |
| Olive oil | Sigma-Aldrich |
| Orange G | Merck |
| Panthotenic acid | Sigma-Aldrich |
| Phenol/Chloroform Isoamyl alcohol | Roth |
| Phosphoric acid | Merck |
| Potassium acetate | Merck |
| Potassium chloride | Merck |
| Potassium dihydrogen phosphate | Roth |
| Potassium sulfate | Merck |
| Propanol (2-propanol) | Sigma-Aldrich |
| Proline (L-proline) | Sigma-Aldrich |
| Protease Inhibitor Cocktail Tablets (Complete EDTA-free) | Roche |
| Riboflavin | Sigma-Aldrich |

| | |
|---|---|
| Sodium acetate | Roth |
| Sodium borohydride | Sigma-Aldrich |
| Sodium chloride | Sigma-Aldrich |
| Sodium dihydrogen phosphate | Roth |
| Sodium dodecylsulfate Na-salt (SDS) | Serva |
| Sodium hydroxide | VWR |
| Sodium lauryl sarcosinate | Sigma-Aldrich |
| Sodium molibdate dihydrate | Merck |
| Sodium nitrate | AppliChem |
| Sodium sulphate | Merck |
| Sodium tetraborate decahydrate | Merck |
| Soybean flour (low fat) | Henselwerk GmbH |
| Soy peptone | Life Technologies |
| Starch soluble extra pure | Merck |
| Sucrose | Südzucker |
| TEMED | Roth |
| TES | Roth |
| Thiamine (HCl) | Serva |
| Tris (Trizma base) | Roth |
| Tryptone (Bacto) | Becton, Dickinson and Co. |
| Tryptose (Bacto) | Becton, Dickinson and Co. |
| Tween20 | Sigma-Aldrich |
| X-Gluc | X-Gluc DIRECT |
| Xylene cyanole | Biorad |
| Yeast extract | Oxoid |
| Zinc chloride | Merck |
| Zinc sulfate heptahydrate | Merck |

### 2.3.2 Antibiotics

| **Antibiotic (source)** | **Stock solution (mg/ml), (solvent)** | **Working concentration* (µg /ml)** |
|---|---|---|
| Ampicillin (AppliChem) | 150 ($H_2O$) | 150 (*E.c.*) |
| Apramycin (Genaxxon) | 100 ($H_2O$) | 25 (*M.*), 50 (*S.c.*), 100 (*E.c.*) |
| Bacitracin (AppliChem) | 100 ($H_2O$) | 100 (*M.*) |
| Chloramphenicol (Serva) | 50 (EtOH) | 25 (*E.c.*) |
| Epidermin | 1 (0.05% acetic acid) | up to 4 (*S.c.*) |
| Hygromycin (Roth) | 150 ($H_2O$) | 50 (*S.*), 150 (*E.c.*) |
| Kanamycin (AppliChem) | 50 ($H_2O$) | 50 (*E.c.*) |
| Nalidixic acid (AppliChem) | 25 (0.1 M NaOH) | 25 (*E.c.*) |
| NAI-107 (NAICONS) | 1 (10% DMSO) | up to 4 (*S.c.*), up to 10 (*M.*) |
| 97518 (NAICONS) | 1 (10% DMSO) | - |
| Phosphomycin (Sigma-Aldrich) | 50 ($H_2O$) | 25 (*M.*) |

*** Working concentration for *E. coli* (*E.c.*), *Streptomyces coelicolor* (*S.c.*) and *Microbispora* spp. (*M.*)

### 2.3.3 Enzymes

| **Enzyme** | **Amount/Activity** | **Source** |
|---|---|---|
| CIAP (Calf intestinal alkaline phosphatase) | 10 U/µl | NBE |
| DNase I RNase free | 1 U/µl | Fermentas |
| Enterokinase, light chain | 2.0 µg/ml | NEB |
| HotStar HiFidelity polymerase | 2.5 U/µl | Qiagen |
| KAPAHiFi polymerase | 1 U/µl | peqLab |
| Lysozyme from chicken egg white | 100 000 U/mg | Serva |
| Mutanolysin | 5 KU | Sigma-Aldrich |
| RNase I from bovine pancreas | 50-100 U/mg | Sigma-Aldrich |

| | | |
|---|---|---|
| Restriction enzymes | 5-10 U/µl | Fermentas, NEB |
| RiboLock RNase inhibitor | 40 U/µl | Fermentas |
| RevertAid Reverse Transcriptase | 200 U/µl | Fermentas |
| Trypsin from bovine pancreas | 3203 U/mg | AppliChem |
| Taq DNA polymerase | 5 U/µl | Qiagen |
| T4 ligase | 1 Weiss U/µl | Fermentas |

### 2.3.4 Kits

| **Kit** | **Source** |
|---|---|
| CloneJET PCR Cloning Kit | Fermentas |
| Gibson Assembly Master Mix | NEB |
| MiniElute Gel Extraction Kit | Qiagen |
| peqGOLD Bacterial DNA Kit | peqLab |
| pET-30 Ek/LIC Vector Kit | Novagen |
| QIAGEN Plasmid Mini/Midi Kit | Qiagen |

## 2.4 Bacterial strains

| Strain (reference, source*) | Description, application | Abbreviation |
|---|---|---|
| *Escherichia coli* XL1-Blue (Bullock *et al.*, 1987) | *endA1 gyrA96 thi-1 recA1 relA1 hsdR17 supE44 lac* [F'*proAB*$^{+}$ *lacI*$^{q}$ Δ(*lacZ*)M15 Tn*10*] ($r_K^-$ $m_K^+$), $Tet^R$, cloning host | - |
| *E. coli* Rosetta 2(DE3) (Novagen) | $F^-$ *ompT hsdS*$_B$ ($r_B^-$ $m_B^-$) *gal dcm* λ(DE3 [*lacI lacUV5*-T7 *gene1 ind1 sam7 nin5*]), pRARE, $Cm^R$, protein expression host | - |
| *E. coli* ET12567 pUZ8002 (Kieser *et al.*, 2000) | Methylation deficient *E. coli* strain containing pUZ8002, $F^-$ *dam*$^-$ 13::Tn*9 dcm-6 hsdM hsdR lacY1*, $Cm^R$; pUZ8002 is a RK2 derivative with a defective oriT ($Kan^R$), conjugation *S. coelicolor* M145 | - |
| *E. coli* S17-1 (Simon *et al.*, 1983) | Methylation proficient *E. coli* strain, *recA pro hsdR* RP4-2-Tc::Mu-Km::Tn*7*, $Tmp^R$, $Spc^R$, $Str^R$, conjugation *Microbispora* strains | - |
| *Micrococcus luteus* ATCC 10240 | Indicator strain for antibiotic bioassays | *M. luteus* |
| *Microbispora* ATCC PTA-5024 (NAICONS, Milan) | WT, NAI-107 producer | *Microbispora* sp. 107891 |
| *Microbispora* RP0 | Non-producer, disruption of *mlb* cluster by single-crossover integration of the plasmid pGusA21-*mlbAB* | - |

| | | |
|---|---|---|
| *Microbispora* Δ*mlbQ* | *mlbQ* deletion mutant of *Microbispora* ATCC PTA-5024 | - |
| *Microbispora* Δ*mlbQ* pRM4-*mlbQ* | *mlbQ* deletion mutant complemented with pRM4-*mlbQ* | *Microbispora* Δ*mlbQ*(*mlbQ*) |
| *Microbispora* pRM4-*mlbQ* | *mlbQ* overexpression in *Microbispora* ATCC PTA-5024 | *Microbispora mlbQ*$^{+}$ |
| *Microbispora* pRM4-*mlbYZ* | *mlbYZ* overexpression in *Microbispora* ATCC PTA-5024 | *Microbispora mlbYZ*$^{+}$ |
| *Microbispora* pRM4-*mlbTU* | *mlbTU* overexpression in *Microbispora* ATCC PTA-5024 | *Microbispora mlbTU*$^{+}$ |
| *Microbispora* pRM4-*mlbEF* | *mlbEF* overexpression in *Microbispora* ATCC PTA-5024 | *Microbispora mlbEF*$^{+}$ |
| *Microbispora* pRM4.3 | *egfp* expression in *Microbispora* ATCC PTA-5024 | *Microbispora egfp* |
| *Microbispora* pRM4.3-*mcherry* | *mcherry* expression in *Microbispora* ATCC PTA-5024 | *Microbispora mcherry* |
| *Microbispora* Δ*mlbQ* pRM4.3-*mlbQmcherry* | Expression of *mlbQmcherry* in *Microbispora* Δ*mlbQ* | *Microbispora* Δ*mlbQ*(*mlbQmcherry*) |
| *Microbispora* JCM 10266 (Nukajima *et al*., 1999) | WT | *Microbispora* JCM66 |
| *Microbispora* JCM 10267 (Nukajima *et al*., 1999) | WT | *Microbispora* JCM67 |
| *Microbispora* JCM 10266 pRM4-*mlbQ* | *mlbQ* expression in *Microbispora* JCM 10266 | *Microbispora* JCM *mlbQ* |
| *Microbispora* JCM 10266 pRM4-*mlbEF* | *mlbEF* expression in *Microbispora* JCM 10266 | *Microbispora* JCM *mlbEF* |

| | | |
|---|---|---|
| *Microbispora* JCM 10266<br>pRM4.3-*mcherry* | *mcherry* expression in *Microbispora* JCM 10266 | *Microbispora* JCM *mcherry* |
| *Microbispora* JCM 10266<br>pRM4.3-*mlbQmcherry* | Expression of *mlbQmcherry* in *Microbispora* JCM 10266 | *Microbispora* JCM *mlbQmcherry* |
| *S. coelicolor* M145<br>(Kieser *et al.*, 2000) | $SCP1^-$ $SCP2^-$ | *S. coelicolor* |
| *S. coelicolor* pRM4 | pRM4 in ΦC31 *attB*, control strain | *S. coelicolor* pRM4 |
| *S. coelicolor* pRM4-*mlbQ* | *mlbQ* expression in *S. coelicolor* | *S. coelicolor mlbQ* |
| *S. coelicolor* pRM4-*mlbJ* | *mlbJ* expression in *S. coelicolor* | *S. coelicolor mlbJ* |
| *S. coelicolor* pRM4-*mlbYZ* | *mlbYZ* expression in *S. coelicolor* | *S. coelicolor mlbYZ* |
| *S. coelicolor* pRM4-*mlbTU* | *mlbTU* expression in *S. coelicolor* | *S. coelicolor mlbTU* |
| *S. coelicolor* pRM4-*mlbEF* | *mlbEF* expression in *S. coelicolor* | *S. coelicolor mlbEF* |
| *S. coelicolor* pRM4-*mlbJYZ* | *mlbJYZ* expression in *S. coelicolor* | *S. coelicolor mlbJYZ* |
| *S. coelicolor* pIJ10257 | pIJ10257 in ΦBT1 *attB,* control strain | *S. coelicolor* pIJ10257 |
| *S. coelicolor* pIJ10257-*mlbQ* | *mlbQ* expression in *S. coelicolor* | *S. coelicolor* pIJ*mlbQ* |

| | | |
|---|---|---|
| *S. coelicolor* pIJ10257-*mlbJ* | *mlbJ* expression in *S. coelicolor* | *S. coelicolor* pIJ*mlbJ* |
| *S. coelicolor* pRM4-*mlbYZ* pIJ10257-*mlbQ* | Co-expression of *mlbYZ* and *mlbQ* in *S. coelicolor* | *S. coelicolor mlbYZ-mlbQ* |
| *S. coelicolor* pRM4-*mlbTU* pIJ10257-*mlbQ* | Co-expression of *mlbTU* and *mlbQ* in *S. coelicolor* | *S. coelicolor mlbTU-mlbQ* |
| *S. coelicolor* pRM4-*mlbEF* pIJ10257-*mlbQ* | Co-expression of *mlbEF* and *mlbQ* in *S. coelicolor* | *S. coelicolor mlbEF-mlbQ* |
| *S. coelicolor* pRM4-*mlbYZ* pIJ10257-*mlbJ* | Co-expression of *mlbYZ* and *mlbJ* in *S. coelicolor* | *S. coelicolor mlbYZ-mlbJ* |
| *S. coelicolor* pRM4-*mlbTU* pIJ10257-*mlbJ* | Co-expression of *mlbTU* and *mlbJ* in *S. coelicolor* | *S. coelicolor mlbTU-mlbJ* |
| *S. coelicolor* pRM4-*mlbEF* pIJ10257-*mlbJ* | Co-expression of *mlbEF* and *mlbJ* in *S. coelicolor* | *S. coelicolor mlbEF-mlbJ* |
| *S. coelicolor* pRM4-*mlbJYZQ* | Co-expression of *mlbJ, mlbYZ* and *mlbQ* in *S. coelicolor* | *S. coelicolor mlbJYZQ* |
| *S. coelicolor* pRM4-*mlbQ*Histag | Expression of C-terminal His-tagged *mlbQ* in *S. coelicolor* | *S. coelicolor mlbQ*Histag |
| *S. coelicolor* pRM4-*dagAmlbQ* | Expression of *mlbQ* fused with *dagA* (agarase from *S. coelicolor*) signal peptide in *S. coelicolor* | *S. coelicolor (dagA)mlbQ* |
| *S. coelicolor* pRM4-*vsimlbQ* | Expression of *mlbQ* fused with *vsi* (subtilisin inhibitor from *S. venezuelae*) signal peptide in *S. coelicolor* | *S. coelicolor (vsi)mlbQ* |

*Unless stated otherwise, the strains were obtained in this study.

## 2.5 Plasmids

| Plasmid (reference, source*) | Description, application |
|---|---|
| pJet1.2<br>(Thermo Scientific) | *rep* (pMB1), T7 RNA polymerase promoter, modified *Plac* promoter (*PlacUV5*) for expression of the *eco47IR* lethal gene at a level sufficient for selection of recombinant plasmids, *bla* ($Amp^R$), cloning vector |
| pGusA21<br>(Muth, unpublished) | *rep* (pMB1), *oriT*, *gusA*, *aac(3)IV* ($Apra^R$) |
| pGusA21-*mlbAB* | pGusA21 derivative, fragment of *mlbAB*, used for the interruption of the *mlb* cluster |
| pA18gus | *rep* (pMB1), *oriT*, *gusA*, *aac(3)IV* ($Apra^R$), used for the generation of the gene inactivation constructs for the deletion of *mlbQ* and *mlbYZ* |
| pA18gusΔ*mlbQ* | pA18gus derivative, upstream and downstream regions of *mlbQ* |
| pRM4<br>(Menges *et al.*, 2007) | pSET152 derivative, *rep* (pMB1), *oriT*, ΦC31 *attP*, *int*, constitutive promoter *ermE**p, artificial RBS, *aac(3)IV* ($Apra^R$), used for gene expression in *S. coelicolor* and *Microbispora* spp. |
| pRM4-*mlbQ* | pRM4 derivative, *mlbQ* |
| pRM4-*mlbJ* | pRM4 derivative, *mlbJ* |
| pRM4-*mlbYZ* | pRM4 derivative, *mlbYZ* |

| | |
|---|---|
| pRM4-*mlbTU* | pRM4 derivative, *mlbTU* |
| pRM4-*mlbEF* | pRM4 derivative, *mlbEF* |
| pRM4-*mlbQ*Histag | pRM4 derivative, *mlbQ* with a C-terminal His-tag |
| pRM4-*mlbJYZ* | pRM4 derivative, *mlbJ, mlbYZ* |
| pRM4-*mlbJYZQ* | pRM4 derivative, *mlbJ, mlbYZ*, *mlbQ* |
| pRM4-*dagAmlbQ* | pRM4 derivative, signal sequence of *dagA* (1-30 aa) fused to *mlbQ* (25-129 aa), C-terminal His-tag |
| pRM4-*vsimlbQ* | pRM4 derivative, signal sequence of *vsi* (1-28 aa) fused to *mlbQ* (25-129 aa), C-terminal His-tag |
| pRM4.3<br>(Menges, unpublished) | pRM4 derivative, *egfp* |
| pRM4.3-*mcherry*<br>(Muth, unpublished) | pRM4 derivative, *mcherry*, used for the C-terminal fusion of mCherry to MlbQ |
| pRM4.3-*mlbQmcherry* | pRM4 derivative, *mlbQmcherry* fusion gene |
| pIJ10257<br>(John Innes Institute, Norwich) | *rep* (pMB1), *oriT*, ΦBT1 *attP*, *int*, constitutive promoter *ermE**p, *hyg* ($Hyg^R$) |
| pIJ10257-*mlbQ* | pIJ10257 derivative, *mlbQ* |
| pIJ10257-*mlbJ* | pIJ10257 derivative, *mlbJ* |

| | |
|---|---|
| pET30<br>(Novagen) | *rep* (pBR322), T7 promoter, N-terminal His-tag/S-tag, thrombin and enterokinase sites, *lacI*, *aphII* ($Kan^R$), ligation independent cloning (LIC) vector, used for expression of recombinant proteins in *E. coli* |
| pET30-*mlbQ* | pET30 derivative, used for the expression of MlbQ (25-129 aa) as a N-terminal His-tag fusion protein in *E. coli* |
| 1G6<br>(NAICONS, Milan) | Cosmid containing the *mlb* cluster, *rep* (pUC), *oriT*, *cos*, *attP*, *int*, *aac(3)IV* ($Apra^R$), *bla* ($Amp^R$) |
| 4B8<br>(NAICONS, Milan) | Cosmid containing the biosynthetic gene cluster of 97518, *rep* (pUC), *oriT*, *cos*, *attP*, *int*, *aac(3)IV* ($Apra^R$), *bla* ($Amp^R$) |

* Unless stated otherwise, the plasmids were constructed in this study.

## 2.6 Primers

| Primer | Sequence (5'-3') | Experiment, restriction sites/overlaps, $T_m$ (°C) (reference*) |
|---|---|---|
| **Expression of putative lantibiotic immunity genes in *S. coelicolor* and *Microbispora* spp.** | | |
| mlbQfor1 | ACATATGACGAACACGACCAGAGCCCGCCTGTCC | *mlbQ* cloning in pRM4 and pIJ10257, *mlbQ*Histag cloning in pRM4, NdeI, 74.3 |
| mlbQrev1 | TAGAATTCCGTGTTCGTCATTCAGCCCTTTCCGCAGAG | *mlbQ* cloning in pRM4, EcoRI, 72.7 |
| mlbQrev2 | ATAAGCTTTCAGCCCTTTCCGCAGAG | *mlbQ* cloning in pIJ10257, HindIII, 64.8 |
| plnQfor | CATATGACCGGCGAACACCGGCGTCC | *plnQ* cloning in pRM4, NdeI, 71.1 |
| plnQrev | ATGAATTCTCATCGGGCGAACCGGCAGAGC | *plnQ* cloning in pRM4, EcoRI, 70.9 |
| mlbYZfor | ATCATATGACAGGCAGGTGGCTGGTCCCGCTCACG | *mlbYZ* cloning in pRM4, NdeI, >75 |
| mlbYZrev | GAATTCATTCATGGCCGCGGACCCGTGG | *mlbYZ* cloning in pRM4, EcoRI, 71 |
| mlbTUfor | ATCATATGACGGTCCCGGCGTTCGAGCTCAG | *mlbTU* cloning in pRM4, NdeI, 72.1 |
| mlbTUrev | GAATTCTCACCTCCCCACCCGCAGCCGCAG | *mlbTU* cloning in pRM4, EcoRI, 75.0 |
| mlbEFfor | ATCATATGGCGGCCCTGATATCCAC | *mlbEF* cloning in pRM4, NdeI, 64.6 |
| mlbEFrev | GAATTCTCATCTCACTGCGGAACCC | *mlbEF* cloning in pRM4, EcoRI, 64.6 |

| | | |
|---|---|---|
| mlbJfor | CATATGGAGATGGTCTCTGTCGAGTTG | *mlbJ* cloning in pRM4 and pIJ10257, NdeI, 65.0 |
| mlbJrev1 | ATGAATTCTCATACCGCCTCTCCC | *mlbJ* cloning in pRM4, EcoRI, 62.7 |
| mlbJrev2 | ATAAGCTTTCATACCGCCTCTCCC | *mlbJ* cloning in pIJ10257, HindIII, 62.7 |
| mlbJYZforGibson | CCAGGGGAGGACCCAGTGGAGATGGTCTCTGTCGAGTTGTG | *mlbJYZQ* cloning in pRM4 by Gibson assembly, overlap pRM4, >75 |
| mlbJYZrevGibson | GTTCGTCATTCATGGCCGCGGACCCGT | *mlbJYZQ* cloning in pRM4 by Gibson assembly, overlap *mlbQ*, 71.0 |
| mlbQforGibson | GGCCATGAATGACGAACACGACCAGAG | *mlbJYZQ* cloning in pRM4 by Gibson assembly, overlap *mlbZ*, 68.0 |
| mlbQrevGibson | TATCAAGCTTAGATCTCATCAGCCCTTTCCGCAGAG | *mlbJYZQ* cloning in pRM4 by Gibson assembly, overlap pRM4, 70.6 |

**Chimeric MlbQ versions**

| | | |
|---|---|---|
| mlbQfor2 | GCTAGCATGACGAACACGACCAGAGCCCGCCTGTCC | *mlbQ* cloning in pRM4.3, *mlbQmcherry* fusion, NheI, >75 |
| mlbQrev3 | CATATGGCCCTTTCCGCAGAGATTGAGGGTGGTGCTGAG | *mlbQ* cloning in pRM4.3, *mlbQmcherry* fusion, NdeI, >75 |

| | | |
|---|---|---|
| dagAfor | CATATGGTCAACCGACGTGATCTC | Cloning of *mlbQ* fused with *dagA* signal sequence in pRM4, NdeI, 62.7 |
| dagArev | GCCGCCGCCCGTGGCATGAGCGGCGGGTG | Cloning of *mlbQ* fused with *dagA* signal sequence and C-terminal His-tag in pRM4, overlap *mlbQ*, >75 |
| mlbQfor-dagA | GCCGCTCATGCCACGGGCGGCGGCAGA | Cloning of *mlbQ* fused with *dagA* signal sequence and C-terminal His-tag in pRM4, overlap *dagA*, >75 |
| vsifor | ATCATATGCGTCGCACCCTCAAG | Cloning of *mlbQ* fused with *vsi* signal sequence and C-terminal His-tag in pRM4, NdeI, 62.4 |
| vsirev | GCCGCCGCCCGTGGCCTGCGCGGTGCCTG | Cloning of *mlbQ* fused with *vsi* signal sequence and C-terminal His-tag in pRM4, overlap *mlbQ*, >75 |
| mlbQfor-vsi | ACCGCGCAGGCCACGGGCGGCGGCAGAG | Cloning of *mlbQ* fused with *vsi* signal sequence and C-terminal His-tag in pRM4, overlap *vsi*, >75 |
| mlbQhistagrev2 | GGATCCTCAGTGGTGATGGTGATGATGGCCCTTTCCG CAGAGATTG | Cloning of *dagAmlbQ, vsimlbQ* and *mlbQ* fused with C-terminal His-tag in pRM4, BamHI, >75 |

**Disruption of the *mlb* cluster**

| | | |
|---|---|---|
| mlbAfor | AAGCTTCCGGGCCGGCGGTGACGAGCTGG | Cloning of the *mlbAB* fragment in pGusA21, HindIII, >75 |
| mlbBrev | CATATGCGGTGTCTCGCTCGGCGGCCACTTG | Cloning of the *mlbAB* fragment in pGusA21, NdeI, 74.8 |

***mlbQ* gene inactivation**

| | | |
|---|---|---|
| mlbQupfor | GAATTCTCGCCGCGGTCGCCGAGGG | Amplification upstream region *mlbQ*, EcoRI, 72.8 |
| mlbQuprev | GGATCCGCCCTGTACGTAGCGTCCGGCCACCC | Amplification upstream region *mlbQ*, BamHI, >75 |
| mlbQdownfor | GGATCCGACCAGATCCGGGACCACAGG | Amplification downstream region *mlbQ*, BamHI, 72.6 |
| mlbQdownrev | AAGCTTCCGGTGCGACTACGGGGATGC | Amplification downstream region *mlbQ*, HindIII, 71.0 |
| mlbQcheckfor | ACGGATGCGGTTCCGCTCCTTGC | Verification *mlbQ* deletion, 67.8 |
| mlbQcheckrev | GGTCACGGCGTGCTCACACC | Verification *mlbQ* deletion, 65.5 |

**Verification of plasmid integration in the bacterial genome**

| | | |
|---|---|---|
| LF044F | CGAAGATCCCGTCGATGATGT | Verification of plasmid integration at the ΦC31 *attB* site in *Microbispora*, 59.8 (Foulston and Bibb, 2010) |
| LF044R | CGTTCATCCACATGGACCAGA | Verification of plasmid integration at the ΦC31 *attB* site in *Microbispora*, 59.8 (Foulston and Bibb, 2010) |
| LF045F | GAAGCGGTTTTCGGGAGTAGT | Verification of plasmid integration at the ΦC31 *attB* site in *Microbispora*, 59.8 (Foulston and Bibb, 2010) |

| | | |
|---|---|---|
| LF045R | CACAACCCCTTGTGTCATGTC | Verification of plasmid integration at the ΦC31 *attB* site in *Microbispora*, 59.8 (Foulston and Bibb, 2010) |
| Aprafor | GGCATCGCATTCTTCG | Amplification fragment of the apramycin resistance cassette, 57.0 |
| Aprarev | CATGTGCAGCTCCATCAG | Amplification fragment of the apramycin resistance cassette, 60.0 |
| Hygrofor | GACCCGGTGATCAAGCTG | Amplification fragment of the hygromycin resistance cassette, 58.2 |
| Hygrorev | CCAGGTCCACGAAGATGTTG | Amplification fragment of the hygromycin resistance cassette, 59.4 |
| ErmEXgeneFP | TTATGCTTCCGGCTCGTATG | Verification pRM4 integration in the genome, 57.3 |
| ErmExgeneRP | CTGCAAGGCGATTAAGTTGG | Verification pRM4 integration in the genome, 57.3 |

**RT-PCR**

| | | |
|---|---|---|
| mlbAforRT | CGCTGACATCCTGGAGAC | Amplification *mlbA* fragment, 58.2 (Foulston and Bibb, 2011) |
| mlbArevRT | GCACAGCGACCAGCTC | Amplification *mlbA* fragment, 56.9 (Foulston and Bibb, 2011) |
| mlbQforRT | CTGCTGGCCGGTTGCAC | Amplification *mlbQ* fragment, 60.0 |
| mlbQrevRT | CGGAGGGCAGGCACTCG | Amplification *mlbQ* fragment, 62.4 |

| | | |
|---|---|---|
| mlbYforRT | CGATACCCACGGTGTCCTAC | Amplification *mlbY* fragment, 61.4 |
| mlbYrevRT | GGTAACGCTCCGTCCAGAT | Amplification *mlbY* fragment, 58.8 |
| mlbZforRT | TCCATGTACGACGACCTGAC | Amplification *mlbZ* fragment, 59.4 |
| mlbZrevRT | GAGTAACCGCCCAGTCTCC | Amplification *mlbZ* fragment, 61.0 |
| mlbTforRT | CGACCAGATCATCATCCTCAG | Amplification *mlbT* fragment, 59.8 |
| mlbTrevRT | AGTCGATCACAGCGTCGAA | Amplification *mlbT* fragment, 56.7 |
| mlbUforRT | CGAGGAGGCTCGTCTCTG | Amplification *mlbU* fragment, 60.5 |
| mlbUrevRT | GATCCCCGGATAGACGTAGG | Amplification *mlbU* fragment, 61.4 |
| mlbEforRT | TCCTCAAAGTCGCCTACCTG | Amplification *mlbE* fragment, 59.4 |
| mlbErevRT | GATGGCGTACCAGAACGAC | Amplification *mlbE* fragment, 58.8 |
| mlbFforRT | GTGCTGAGCCTGATGAACC | Amplification *mlbF* fragment, 58.8 |
| mlbFrevRT | AGCTGGTGACTGGAGAC | Amplification *mlbF* fragment, 55.2 |
| hrdBforRT | ACTTCTGGACCTCGATGACCTTC | Amplification *hrdB* fragment, 62.4 |
| hrdBrevRT | GGTCGAGGTGATCAACAAGCTG | Amplification *hrdB* fragment, 62.1 |

**Expression of MlbQ in *E. coli***

| | | |
|---|---|---|
| mlbQhistagfor1 | GACGACGACAAGACGGGCGGCGGCAGAG | MlbQ expression in *E. coli* Rosetta 2(DE3), Ek/LIC cloning site, >75 |
| mlbQhistagrev1 | GAGGAGAAGCCCGGTTCAGCCCTTTCCGCAGAG | MlbQ expression in *E. coli* Rosetta 2(DE3), Ek/LIC cloning site, >75 |

* Unless stated otherwise, the primers were designed in this study.

## 2.7 Cultivation of bacteria

For liquid cultures, bacterial strains were grown in an Infors Multitron orbital shaker at 180 rpm, unless stated otherwise.

### 2.7.1 Cultivation and storage of *E. coli*

*E. coli* strains were grown according to Sambrook and Russel, 2001. LB medium was supplemented with the appropriate antibiotic as reported in 2.6.2. For long-term storage, strains were grown in LB medium, cells resuspended in 20% glycerol and stored at -20°C.

### 2.7.2 Cultivation, spore isolation and storage of *S. coelicolor*

*S. coelicolor* strains were cultivated as described in Kieser *et al*., 2000. LB agar with the appropriate antibiotic was used for the selection of recombinant strains, MS agar for sporulation. For spore collection, *S. coelicolor* strains were cultivated on MS agar at 28°C for up to 10 days until they appeared grey due to spore formation. Spores were harvested by filtering through a water-embedded sterile cotton pad, collected by centrifugation at 5000 rpm for 10 minutes, resuspended in 20% glycerol and stored at -20°C. The spore titre was determined by making serial dilutions in water and plating on MS agar. Resulting colonies were counted from two different plates and averaged.

### 2.7.3 Cultivation, spore isolation and storage of *Microbispora* spp.

#### 2.7.3.1 Cultivation of *Microbispora* spp.

*Microbispora* sp. 107891 and *Microbispora* JCM66 were obtained from NAICONS (Milan, Italy). For the generation of the biomass, *Microbispora* sp. 107891 was grown in GE82G, a medium suitable for a dispersed growth of *Microbispora* spp. 10 ml of medium were inoculated with 6% of a working cell bank in a 100-ml baffled Erlenmeyer flask with a coiled spring baffle and incubated at 30°C, at 180 rpm in an orbital shaker. For large-scale cultivations, a 4-days culture was used to inoculate (6% inoculum) 100 ml of GE82G in a 500-ml baffled Erlenmeyer flask with a coiled spring baffle. After 4 days of growth, *Microbispora* sp. 107891 cultures were generally ready for inoculation. Strain growth was monitored by measuring the packed mycelium volume (5-ml culture sample

centrifuged at 5000 rpm for 10 min) and by checking the culture colour. For an efficient inoculum, the packed mycelium volume (PMV) had to exceed 5% of the total culture volume and the culture had to be red/brown coloured. *Microbispora* JCM66 was grown in the same conditions as *Microbispora* sp. 107891, except the incubation time. *Microbispora* JCM66 is characterized by a faster growth rate, so the strain was usually inoculated in fresh medium at the second or third day of growth. *Microbispora* strains were grown on agar plates at 28°C, although higher temperatures (up to 37°C) are suitable for *Microbispora* spp. *Microbispora* spp. were streaked onto MV0.1 and HA agar media with the appropriate antibiotic for the selection of recombinant strains and MS agar for strain maintenance.

2.7.3.2 Spore isolation of *Microbispora* spp.

*Microbispora* spp. were streaked onto S1 agar for sporulation. Because of the slow growth, a thick mycelial suspension was plated out on plates. *Microbispora* sp. 107891 sporulates poorly and requires long incubation (10-14 days), whereas *Microbispora* JCM66 produces a high titre of spores within 7 days. Spore formation was monitored by checking the presence of a pink pigment on S1 agar plates. Spores were collected with a sterile cotton pad embedded with 10 ml sterile water. Spores were filtered through the cotton pad, centrifuged at 5000 rpm for 10 minutes, resuspended in 20% glycerol and stored at -20°C. The spore titre was determined by making serial dilutions in water and plating on MV0.1 agar. Resulting colonies were counted from two different plates and averaged.

2.7.3.3 Storage of *Microbispora* spp.

*Microbispora* spp. were stored as a working cell bank (WCB) at -80°C. For WCB preparation, the mycelium of *Microbispora* strains was scraped from a well-grown S1 plate and inoculated in 10 ml of GE82AB (30°C, 180 rpm). After 72-96 h of growth, 6 ml of culture were used to inoculate 100 ml of GE82AB. Strains were grown for 72-96h, cells harvested by centrifugation at 5000 rpm for 10 min and resuspended in sterile 0.9% NaCl supplemented with 15% glycerol (1V of mycelium and 2V of 0.9% NaCl+glycerol). The cell suspension was distributed in cryovials and stored at -80°C.

### 2.7.4 *Microbispora* sp. 107891 growth curve

The growth rate of *Microbispora* sp. 107891 was assessed my measuring the dry weight of 5-ml samples. A typical bacterial growth curve could be obtained by monitoring cultures in Evans medium. This defined medium allowed the collection of samples from the early phase of growth (8 h). NAI-107 production was checked by bioassay. HPLC analysis for the determination of NAI-107 production in this medium was not used, as the antibiotic concentration was at the limit of detection. For the generation of the biomass, *Microbispora* WT and recombinant strains were grown in GE82G in two pre-cultures for 96 h and 72 h, respectively. The second pre-culture was used to inoculate (6% inoculum) 100 ml of Evans medium in a 500-ml Erlenmeyer flask with a coiled spring baffle and incubated at 30°C, at 180 rpm in an orbital shaker. For the determination of the dry weight, 5-ml samples were taken at 8, 24, 48, 96, 120, 144, 168 h, centrifuged at 5000 rpm for 10 minutes and lyophilized.

## 2.8 General molecular biology methods

A comprehensive overview of the general methods in molecular biology is provided by the manual 'Molecular Cloning' edited by Cold Spring Harbor Laboratory Press (Sambrook and Russell, 2001). Here, a short description of the methods is reported, with an emphasis on the procedures that differ from standard protocols.

### 2.8.1 Plasmid isolation from *E. coli*

Plasmids were isolated from 1 ml of an overnight LB culture by alkaline lysis. The method is based on the ability of plasmid DNA to renature after alkaline denaturation, in contrast to chromosomal DNA and proteins. The cells were harvested by centrifugation at 8000 rpm for 1 min and the supernatant discarded. The cells were resuspended in 200 µl P1 buffer and 200 µl P2 buffer were then added. The Eppendorf tubes were carefully inverted 5 times and incubated 5 min at room temperature. After incubation, 350 µl of P3 buffer were added, the Eppendorf tubes inverted carefully for 5 times and incubated in ice for 5 min. The samples were centrifuged at 13000 rpm for 10 min and the resulting supernatant mixed with 650 µl isopropanol. After incubation in ice for 10 min, the samples were centrifuged at 13000 rpm for 20 min. The pellet was washed once with 1

ml 70% EtOH and dried for 10 min at 60°C. Plasmid DNA was resuspended in 40 µl ultrapure $H_2O$ and used for cloning or sequencing applications. For large-scale plasmid preparations, the QIAGEN Plasmid Mini/Midi Kit was used according to the manufacturer's instructions. Plasmids were stored at -20°C.

### 2.8.2 Isolation of genomic DNA

*Microbispora* spp. and *S. coelicolor* strains were grown in GE82G medium and R5 or S medium, respectively, and 0.3-0.5 ml of the cultures were used for genomic DNA (gDNA) isolation using the peqGOLD Bacterial DNA Kit. The kit is based on the reversible binding properties of DNA to silica membranes. gDNA was isolated according to the manufacturer's instructions, except for the steps reported below. For *Microbispora* spp., the lysozyme incubation was conducted at 37°C for 30-60 min instead of at 30°C for 10 min. The samples were incubated with RNase and proteinase K at 70°C until a complete lysis was achieved (no residual pellet in the Eppendorf tube). gDNA was resuspended in 50 µl ultrapure $H_2O$ and stored routinely at 4°C. For long-term storage, gDNA was stored at -20°C.

### 2.8.3 Agarose gel electrophoresis

Agarose gel electrophoresis is an easy and common technique to analyse and separate DNA after isolation, PCR amplification or digestion by restriction enzymes. This technique takes advantage of the negative charge of the DNA phosphate backbone, which allows the DNA to migrate in an electric field. The migration rate of DNA in an agarose gel is determined by the size of DNA fragment, its conformation, agarose concentration and applied current. Typically, 5 µl of DNA sample were mixed with 1.5 µl DNA loading buffer and applied on an agarose gel. The DNA loading buffer, containing glycerol and dyes, allows a better DNA loading and monitoring of DNA migration. 1-2% agarose gels were prepared with TAE buffer and electrophoresis was carried out in TAE buffer at 80 V until completion. 2% agarose gels were used for DNA fragments smaller than 500 bp. GeneRuler 1 kb DNA ladder from Thermo Scientific (250-500-750-1000-1500-2000-2500-3000-3500-4000-5000-6000-8000-10000 bp) or Easy ladder I from Bioline (100-250-500-1000-2000 bp) were used as size markers. The DNA fragments separated by gel electrophoresis were visualized with ethidium bromide, a fluorescent

compound, which intercalates between the base pairs of the DNA double helix. Gels were incubated 10 min in an ethidium bromide bath (2-4 drops of a 10% solution in 1.5 l $H_2O$) and exposed to UV light for DNA visualization. Images were viewed with the BioCaptMW software.

### 2.8.4 DNA extraction from an agarose gel

DNA extraction from agarose gels was performed to purify DNA fragments from unspecific PCR samples or after DNA digestion with restriction enzymes. In most of the cases, the purified DNA fragments were used for cloning applications. To purify the desired DNA fragment, DNA was separated by agarose gel electrophoresis and excised from the gel using a clean scalpel. In order to reduce the probability of UV mutagenesis, the gel was exposed to UV light for few seconds. DNA extraction was carried out using the MiniElute Gel Extraction Kit (Qiagen), following the manufacturer's instructions. The agarose gel slice containing the DNA fragment of interest was dissolved in a neutral pH, high salt buffer and applied to a silica gel membrane. In these conditions, DNA adsorbs to the silica membrane while contaminants pass though the column. The column was washed and the DNA fragment was eluted in elution buffer. For an efficient recovery, incubation with the elution buffer was performed for 20-30 min.

### 2.8.5 DNA digestion with restriction enzymes

Restriction enzymes are enzymes that recognize specific DNA sequences (restriction sites) and cut the DNA. For type II restriction enzymes, the recognition and the cleavage sites overlap, allowing the usage of these enzymes to manipulate DNA molecules. Indeed, type II restriction enzymes (here called restriction enzymes) became indispensable tool in recombinant DNA technology. In this work, restriction enzymes were used to digest DNA as reported below. Typically, DNA digestions were carried out at 37°C for 1 h, unless stated otherwise in the manufacturer's instructions.

| Component | Volume |
|---|---|
| Plasmid DNA | 5 µl (0.1-1 µg) |
| Restriction enzyme | 1 µl |
| 10x buffer | 2 µl |
| $H_2O$ | up to 20 µl |

To check recombinant plasmids, DNA digestions were performed with a final volume of 10 µl. For cloning applications, vectors were digested in the presence of 1 µl CIAP (10 U/µl) to dephosphorylate the 5'-end, thereby avoiding vector recircularization. Double digestions were performed according to the DoubleDigest tool from Thermo Scientific. Inactivation of the restriction enzymes was carried out following the manufacturer's instructions. In most cases, enzymes were inactivated by incubation at 65°C for 20 min. For the restriction enzymes for which heat inactivation was not possible, the desired DNA fragment was purified by DNA gel extraction.

### 2.8.6. Ligation of DNA fragments using the T4 DNA ligase

The T4 DNA ligase catalyzes the joining of two strands of DNA between the 5´-phosphate and the 3´-hydroxyl groups of adjacent nucleotides in either a cohesive-ended or blunt-ended configuration. In this work, T4 ligase-based ligation was used to obtain recombinant plasmids from restriction DNA fragments. Ligation reactions were set up as described below and conducted overnight at 4°C.

| Component | Volume |
|---|---|
| Vector* | 1 µl |
| Insert** | 2-10 µl |
| T4 ligase | 1 µl |
| 10x T4 buffer | 2 µl |
| $H_2O$ | up to 20 µl |

* restriction-digested vector
** gel-purified insert fragment

The T4 ligase was also used for the cloning of DNA fragments into the pJet1.2 vector, according to the instructions of the CloneJET PCR Cloning Kit.

### 2.8.7. Cloning strategies

#### 2.8.7.1 General cloning experiments

Typically, the cloning of a desired DNA fragment in the final vector was conducted in two cloning steps. A PCR product generated by a proofreading DNA polymerase was firstly cloned in pJet1.2 and subsequently sub-cloned in the final vector. Jet1.2 carrying the desired fragment was sequenced by GATC Biotech (Constance) using the primers pJET1.2forward and pJET1.2reverse provided by the CloneJET PCR Cloning Kit. Error-free pJet1.2 recombinant plasmids were double digested with the respective restriction enzymes and the desired DNA fragment (insert) was purified by DNA extraction from agarose gel. Ligation into the final vector was carried out with the T4 ligase as described above, using a restriction-digested vector after inactivation of the restriction enzymes. Chemically competent *E. coli* XL1-Blue cells were than transformed with the ligation mixture and recombinant clones were screened by restriction digestion.

#### 2.8.7.2 Ligation Independent Cloning (LIC) in pET vectors

The Ligation Independent Cloning (LIC) method takes advantage of the 3'-5' exonuclease activity of the T4 DNA polymerase to create specific single-stranded overhangs. The gene of interest is amplified with primers that have appropriate 5' extensions. The purified PCR product is treated with the T4 DNA polymerase in the presence of dATP to generate vector-specific overhangs. dATP limits the exonuclease activity of the T4 DNA polymerase to the first complementary T residue. The PCR product overhangs anneal to the final vector, thereby allowing a specific cloning. The joined fragments have 4 nicks that are repaired by *E.coli* during transformation. In this work, the Ek/LIC Cloning Kit from Novagen was used to clone *mlbQ* (primers: mlbQhistagfor1, mlbQhistagrev1) in the vector pET30 for heterologous expression in *E. coli*. The cloning was performed as described in the manufacturer's instructions. The recombinant plasmids were used to transform chemically competent *E. coli* XL1-Blue cells.

#### 2.8.7.3 Gibson assembly

Gibson and co-workers developed a method to assembly multiple DNA fragments in a single isothermal reaction (Gibson *et al.*, 2009). The method is based on multiple

overlapping DNA fragments and involves three different enzymatic activities. An exonuclease creates single-stranded 3' overhangs, which anneal to complementary regions, the polymerase fills the gap within each annealed fragment and the DNA ligase ligates the assembled DNA. The resulting DNA molecule is a double-stranded DNA molecule. The Gibson Assembly Master Mix (NEB) was used in the present study to clone the genes *mlbJ*, *mlbY*, *mlbZ* and *mlbQ* in pRM4 in a single-step reaction, following the manufacturer's instructions. Primers were designed with appropriate overhangs (NEBuilder web tool) and used to amplify the operon *mlbJYZ* (primers: mlbJYZforGibson and mlbJYZrevGibson) and the gene *mlbQ* (primers: mlbQforGibson and mlbQrevGibson) with a proofreading polymerase. pRM4 was digested with NdeI, taking in consideration that the restriction site is lost during the assembly. The reaction mix was set up by mixing 1.5 µl linearized pRM4, 1.5 µl *mlbJYZ* PCR product, 0.5 µl *mlbQ* PCR product, 10 µl Gibson Assembly Master Mix and 6.5 µl $H_2O$. The reaction was incubated at 50°C for 1 h and used to transform chemically competent *E. coli* XL1-Blue cells.

## 2.9 General PCR methods

The invention of the polymerase chain reaction (PCR) by K. Mullis and co-workers in the '80s (Mullis *et al.*, 1986; Saiki *et al.*, 1988) revolutionized molecular biology by allowing the amplification of DNA sequences within few hours using a thermostable DNA polymerase. In the present study, PCR was used to amplify genes for cloning applications, for generation of chimeric genes or for analytical purposes. PCR reactions were typically carried out in 0.2 ml tubes using the thermal cyclers Primus 25 advanced (peqLab) or MyCycler (BIO-RAD). Because of the high GC content of the templates, many primers had to be designed with a high melting temperature (>70°C).

### 2.9.1 High-fidelity amplification for cloning applications

High-fidelity DNA amplification is required for sequencing, cloning or site-directed mutagenesis applications. High-fidelity PCR utilizes a DNA polymerase with a low error rate (proofreading DNA polymerase) to ensure a high degree of accuracy in DNA replication. Proofreading DNA polymerases possess 3´→5´ exonuclease activity in addition to 5'→3´ DNA polymerase activity to remove mismatched nucleotides. In this

work, high-fidelity amplification was performed using either KAPAHiFi DNA polymerase or HotStar HiFidelity DNA polymerase. The KAPAHiFi polymerase is characterized by a high processivity, high DNA affinity and the ability to amplify GC- and AT-rich DNA targets. The HotStar HiFidelity DNA polymerase is chemically modified to inactivate both polymerase and exonuclease activity, preventing primers and template degradation during setup of the PCR reaction. It is activated by incubation at 95°C for 5 min and it ensures high specific and sensitive DNA amplification. PCR reaction setups and PCR programs were customized according to the kit instruction manuals. The primer annealing temperature ($T_a$) was calculated to be 10°C (KAPAHiFi DNA polymerase) or 5°C (HotStar HiFidelity DNA polymerase) below the melting temperature ($T_m$) of the primer with the lowest $T_m$. In some cases, $T_a$ was determined empirically by gradient PCR. For the amplification of the *mlb* genes, the cosmid 1G6 was used as a template instead of gDNA.

KAPAHiFi DNA Polymerase

| **Component** | **Volume** | **Final concentration** |
|---|---|---|
| 40 mM KAPA dNTPs mix (10 mM each) | 1.5 µl | 1.2 mM |
| 100 µM Forward primer | 1.5 µl | 3 µM |
| 100 µM Reverse primer | 1.5 µl | 3 µM |
| 5x KAPA HiFi GC Buffer | 10 µl | 1x |
| Template DNA | 1 | - |
| KAPA HiFi DNA polymerase | 1 µl | 0.02 U/µl |
| Ultrapure $H_2O$ | up to 50 µl | - |

| **Step** | **Temperature** | **Duration** | **Cycle** |
|---|---|---|---|
| Initial denaturation | 95°C | 5 min | 1 |
| Denaturation | 98°C | 20 sec | 30x |
| Annealing | $T_m$-10°C | 15 sec | |
| Extension | 72°C | 30 sec/kb | |
| Final extension | 72°C | 5 min | 1 |

HotStar HiFidelity DNA polymerase

| **Component** | **Volume** | **Final concentration** |
|---|---|---|
| 100 µM Forward primer | 0.5 µl | 1 µM |
| 100 µM Reverse primer | 0.5 µl | 1 µM |
| 5x HotStar PCR Buffer (contains | 10 µl | 1x |
| Template DNA | 1 µl | - |
| HotStar DNA polymerase | 1 µl | 0.05 U/µl |
| Ultrapure $H_2O$ | up to 50 µl | - |

| **Step** | **Temperature** | **Duration** | **Cycle** |
|---|---|---|---|
| Initial denaturation | 95°C | 5 min | 1 |
| Denaturation | 94°C | 15 sec | 30x |
| Annealing | $T_m$-5°C | 1 min | |
| Extension | 72°C | 1 min/kb | |
| Final extension | 72°C | 10 min | 1 |

### 2.9.2 Analytical PCR

Taq DNA polymerase is typically used for analytical purposes, where sequence accurancy is not crucial. The lack of a 3´→5´ exonuclease proofreading activity in the Taq DNA polymerase results in a relatively low replication fidelity. In the present study, Taq DNA polymerase from Qiagen was used to perform analytical PCRs from gDNA or cDNA. The kit provides a Q-solution which facilitates amplification of difficult templates by modifying the melting behaviour of nucleic acids and a CoralLoad PCR buffer which enable the loading of PCR products on agarose gels without the need to add a DNA loading buffer. PCR reaction setups and PCR programs were customized according to the kit instruction manual. The primer annealing temperature ($T_a$) was calculated to be 5°C below the melting temperature ($T_m$) of the primer with the lowest $T_m$ but in some cases it was necessary to determine the optimal $T_a$ by gradient PCR.

Taq DNA polymerase

| Component | Volume | Final concentration |
|---|---|---|
| 40 mM dNTPs mix (10 mM each) | 0.5 µl | 0.8 mM |
| 100 µM Forward primer | 0.5 µl | 2 µM |
| 100 µM Reverse primer | 0.5 µl | 2 µM |
| Q solution | 5 µl | - |
| 10x PCR Buffer (10x CoralLoad buffer) | 2.5 µl | 1x |
| Template DNA | 1 µl | - |
| Taq DNA polymerase | 0.5 µl | 0.1 U/µl |
| Ultrapure $H_2O$ | up to 25 µl | - |

| Step | Temperature | Duration | Cycle |
|---|---|---|---|
| Initial | 94°C | 2 min | 1 |
| Denaturation | 94°C | 30 sec | 30x |
| Annealing | $T_m$-5°C | 30 sec | |
| Extension | 72°C | 1 min/kb | |
| Final extension | 72°C | 1 min | 1 |

### 2.9.3 Colony PCR

Colony PCR is a quick method to screen recombinant clones for the presence of the desired gene. In this work, colony PCR was used for the screening of *Microbispora* recombinant strains, as the growth rate of the strain prevented to obtain a liquid culture from a single colony within few days. However, colony PCR was used also to screen fast-growing *S. coelicolor* recombinant clones. Mycelium from a single colony was scraped from an agar plate using a sterile toothpick and introduced into 100 µl $H_2O$ in a 1.5 ml Eppendorf tube. The mycelium was homogenized and the cell suspension boiled for 10 minutes in a water bath. The Eppendorf tube was cooled and the cell suspension was centrifuged at 10000 rpm for 5 minutes to pellet cell debris. 3 µl of the supernatant were used as template for analytical PCR (2.9.2). Alternatively to colony PCR, analytical PCR using gDNA as template was used to verify recombinant clones.

### 2.9.4 Overlap extension PCR

Overlap extension PCR is a PCR technique firstly described for site-directed mutagenesis (Ho *et al*., 1989) and subsequently reported as a method to create chimeric genes in the absence of restriction enzymes (Wurch *et al*., 1998). This technique was used to fuse the signal peptide sequence of *dagA* (agarase from *S. coelicolor*) to *mlbQ* (25-129 aa) for the generation of the chimeric gene *(dagA)mlbQ*. The signal peptide sequence of *dagA* and *mlbQ* were amplified with a proofreading polymerase from gDNA of *S. coelicolor* and the cosmid 1G6, respectively. The primers dagArev and mlbQfor-dagA were designed to overlap to each other to obtain a joined construct during the overlap extension PCR. The PCR reaction mix was set up as described below. The PCR program was designed according to 2.9.1.

| **Component** | **Volume (µl)** |
|---|---|
| PCR product *dagA* | 1 |
| PCR product *mlbQ* | 0.3 |
| 100 µM primer dagAfor | 0.5 |
| 100 µM primer mlbQhistagrev2 | 0.5 |
| 5x HotStar PCR Buffer (contains dNTPs) | 10 |
| Hotstar DNA polymerase | 1 |
| $H_2O$ | 36.7 |

## 2.10 RT-PCR analysis

RT-PCR (reverse-transcription PCR) allows a qualitative detection of gene expression by DNA amplification using cDNA as a template. cDNA transcripts are obtained from RNA thought the activity of the reverse transcriptase, an enzyme discovered in two independent works on retroviruses (Baltimore, 1970; Temin and Mizutani, 1970). In the present study, RT-PCR was used to compare the expression levels of several *mlb* genes in *Microbispora* sp. 107891 and in the non-producer strain *Microbispora* RP0.

### 2.10.1 RNA isolation

RNA was isolated according to a method based on the Kirby mix procedure (Kirby *et al.*, 1967; Kieser *et al.*, 2000), which allows the isolation of nucleic acids using phenol-chloroform extraction. Because both DNA and RNA are purified with this method, a subsequent treatment with DNase I was required. During the whole procedure, lab coat and glows were worn, double autoclaved solutions or RNase-free products were used, samples were kept in ice and centrifugation steps conducted at 4°C. Both working area and gel electrophoresis equipment were treated with the RNase-Killer solution. RNase-free loading buffer was used to load RNA on the agarose gel.

*Microbispora* was grown in Evans medium and 5-ml samples were taken after 8, 24, 50, 72 and 96 h. The cells were harvested by centrifugation at 5000 rpm for 10 min, resuspended in 1 ml ice-cold TE buffer and stored at -80°C. For RNA isolation, samples were thawed, filled in 2 ml screw cap tubes containing 0.2 ml glass beads (0.17-0.18 mm) and centrifuged at 13000 rpm for 1 min. The resulting supernatant was discarded, the cells resuspended in 0.5-0.75 ml of Kirby mix and disrupted using a Precellys Homogenizer (2x20 sec at 6500 rpm), putting the samples in ice between the two cycles. 0.5 ml of phenol:chloroform:isoamyl alcohol 25:24:1 (PC) were added and the cells disrupted with the Precellys Homogenizer as reported above. Samples were centrifuged at 14800 rpm for 5 min and the aqueous phase was transferred in a 2 ml Eppendorf tube. Nucleic acids were extracted by successive extractions with 1 ml PC until no more proteins were visible at the interphase. The aqueous phase was then transferred in a 1.5 ml Eppendorf tube and nucleic acids were precipitated by incubation at -20°C for 1 h after addition of 3 M NaAc (1/10 V) and isopropanol (1 V). After precipitation, the samples were centrifuged at 14 8000 rpm for 20 min, the supernatant discarded and the pellet washed twice with 0.5 ml 70% EtOH. The pellet was then resuspended with 100 µl RNase-free water and DNA digestion was performed at 37°C for 1 h by adding 8 µl RNase-free DNase I and 12 µl 10-fold DNase buffer. RNA quality was checked by agarose gel electrophoresis by loading 5 µl of the samples. Typically 23S and 16S bands were visible and often 5S and aggregates. The samples were stored at -80°C or further processed. Nucleic acid concentration was measured by Nanodrop and adjusted to 3-4 µg/µl. 60 µg of nucleic acid were used for an additional DNase digestion

at 37°C for 2 h (60 µg nucleic acid, 8 µl 10-fold DNase buffer, 8 µl RNase-free DNase I, RNase-free water up to 80 µl). To confirm the absence of DNA in RNA samples, PCR was carried out (2.9.2) using the primers hrdBforRT and hrdBrevRT (gDNA was used as a positive control). DNase I was deactivated by addition of 8 µl 50 mM EDTA (1/10 V) and subsequent incubation at 65°C for 10 min. The quality and quantity of RNA was determined using NanoDrop. For pure RNA a 260/280 ratio between 1.9 and 2.3 was expected and a 260/230 ratio preferably greater than 1.8. RNA was diluted to 0.3 µg/µl and controlled by agarose gel electrophoresis (10 µl sample). RNA was stored at -80°C or used directly for cDNA synthesis.

### 2.10.2 Reverse transcription of RNA to cDNA

cDNA synthesis was carried out using RevertAid Reverse Transcriptase (Fermentas) and random hexamer primers to ensure the reverse transcription of the complete transcriptome. 10 µl RNA (0.3 µg/µl) were used for cDNA synthesis. 1 µl random hexamer primers were added to the RNA samples, which were incubated for 5 min at 70°C and than cooled in ice. A master mix was prepared (4 µl 5-fold Reaction Buffer, 1 µl dNTPs, 1 µl RiboLock RNase Inhibitor, 2 µl RNase-free water) and 8 µl were added to the samples. After incubation for 5 min at 25°C, 1 µl of RevertAid Reverse Transcriptase was added, the samples incubated for 10 min at 25°C and subsequently for 60 min at 42°C. After cDNA synthesis the samples were diluted by addition of 30 µl RNase-free $H_2O$ (end volume 50 µl) and stored at -20°C.

### 2.10.3 PCR from cDNA

1 µl of cDNA was used to amplify the desired DNA sequence following the protocol for analytical PCR (2.9.2) and using the CoralLoad buffer. DNA amplification was performed in 30 cycles, using annealing temperatures between 50°C and 60°C (see below). 8 µl of the PCR products were checked on a 2% agarose gel by electrophoresis. As an internal control, a homolog of *S. coelicolor hrdB* was used. gDNA was used as a positive control and ultrapure water as a negative control.

| Gene | Primer pair | $T_a$ (°C) |
|---|---|---|
| *mlbA* | mlbAforRT, mlbArevRT | 54 |
| *mlbY* | mlbYforRT, mlbYrevRT | 54 |
| *mlbZ* | mlbZforRT, mlbZrevRT | 57 |
| *mlbQ* | mlbQforRT, mlbQrevRT | 58 |
| *mlbT* | mlbTforRT, mlbTrevRT | 54 |
| *mlbU* | mlbUforRT, mlbUrevRT | 54 |
| *mlbE* | mlbEforRT, mlbErevRT | 54 |
| *mlbF* | mlbFforRT, mlbFrevRT | 50 |
| *hrdB* | hrdBforRT, hrdBrevRT | 59 |

## 2.11 DNA transfer

Transformation, conjugation and transduction are the processes used by bacteria to uptake exogenous DNA molecules and they became precious tools in molecular biology for bacterial genetic manipulation. Transformation is the up-take of naked DNA from the extracellular environment through the cell membrane. Not all bacteria are naturally competent, therefore methods to permeabilize the cell membrane had to be established to use transformation as a DNA transfer tool. Cell membrane permeability has been enhanced either by calcium chloride treatment or by electroporation (Sambrook and Russel, 2001). Conjugation is the transfer of DNA from a donor to a recipient strain via cell-cell contact and transduction is the introduction of DNA by phage infection. The best method to introduce DNA into a bacterium depends on the properties of the single species. Standardized DNA transfer methods are available for some bacteria, however DNA transfer still remains an obstacle for the genetic manipulation of several bacterial strains.

### 2.11.1 Chemical transformation of *E. coli*

Transformation of chemically competent *E. coli* cells was firstly described by Mendel und Higa who succeeded to introduce bacteriophage λ DNA into *E. coli* cells after treatment with ice-cold solutions of calcium chloride and heat shock at 42°C (Mendel and Higa,

1970). Nowadays, transformation is a routine method to transfer plasmid DNA into *E. coli*. Chemically competent *E. coli* cells were prepared by calcium chloride treatment as described by Cohen and co-workers (Cohen *et al.*, 1972). Transformation was performed by adding 1 µl of the desired plasmid to an aliquot (200 µl) of competent cells. The cells were maintained in ice for 30 min and then incubated at 42°C for 2 min. After heat shock, the cells were incubated at 37°C for 1 h and plated out onto LB agar plates with the appropriate antibiotic selection.

### 2.11.2 Conjugation of *S. coelicolor*

One of the established methods to transfer DNA into *Streptomyces* species is the intergenic transfer of plasmids from *E. coli.* Both non-replicative and integrative plasmids, which integrate in the genome site-specifically or by homologous recombination, can be introduced into *Streptomyces* by conjugation. Conjugative plasmids contain the *oriT* (origin of transfer) from the plasmid RP4 (Mazodier *et al.*, 1989) and require transfer functions to be supplied *in trans* by the *E. coli* donor strain, typically *E. coli* ET12567 (MacNeil *et al.*, 1992) or *E. coli* S17-1 (Simon *et al.*, 1983). In the methylation deficient strain *E. coli* ET12567 the transfer functions are present in the self-transmissible plasmid pUB307 or in the non-transmissible plasmid pUZ8002. In the methylation-proficient donor *E. coli* S17-1, the transfer functions are encoded in the chromosome. Conjugation of *S. coelicolor* was conducted using *E. coli* ET12567 pUZ8002 according to Kieser *et al*., 2000. Freshly germinated spores were used for conjugation. Conjugation plates were overlaid with 750 µg nalidixic acid and the appropriate antibiotic for the selection of ex-conjugants.

### 2.11.3 Conjugation of *Microbispora* spp.

A gene transfer system for *Microbispora* sp. 107891 had to be developed, since the strain was not known to be genetically accessible. A protocol for conjugation of *Microbispora* sp. 107891 was established using the integrative plasmid pRM4.3. The DNA-transfer could be achieved using the methylation proficient donor *E. coli* S17-1 (Simon *et al.*, 1983), apramycin for the selection of *Microbispora* ex-conjugants and phosphomycin for the inihibition of *E. coli*. Indeed, an antibiotic resistant test showed that *Microbispora* sp. 107891 was partially sensitive to nalidixic acid, an antibiotic

commonly used to inhibit *E. coli* growth in conjugation experiments. The conjugation was performed using mycelium, as *Microbispora* sp. 107891 sporulates poorly. An aliquot (1 ml) of the WCB was inoculated in 10 ml of nutrient broth medium. After 20 h, the culture was sonicated for 20 min in a water bath sonicator (Branson 8200, Heinemann), the mycelium recovered by centrifugation at 5000 rpm for 10 min, washed once with the nutrient broth medium and concentrated 1:10. *E. coli* S17-1 was grown overnight, washed twice with LB and resuspended in 1/10 of the initial volume. 100 µl of *Microbispora* mycelium were mixed with 100 µl of *E. coli* and the mixture was plate on MS medium containing 10 mM $MgCl_2$. Alternatively, *Microbispora* mycelium was diluted 1:5 or 1:10 and 100 µl of it were used for conjugation. After 24 h of incubation at 30°C, each plate was overlaid with 1 ml $H_2O$ containing 1500 µg apramycin and 1250 µg phosphomycin. After about 10 days of incubation at 30°C, ex-conjugants were streaked onto HA agar plates containing 25 µg/ml apramycin and 50 µg/ml phosphomycin. Apramycin was the only selection marker used to obtain *Microbispora* recombinant strains. The recombinant strains were checked by colony PCR (2.9.3) and grown in 10 ml GE82G supplemented with 50 µg/ml apramycin. Conjugation of *Microbispora* JCM66 was conducted as described for *Microbispora* sp. 107891.

## 2.12 Generation of *Microbispora* sp. 107891 recombinant strains

To generate *Microbispora* sp. 107891 recombinant strains, plasmids were introduced by conjugation according to the protocol described above (2.11.3). The plasmids were integrated both by site-specific integration and homologous recombination. Apramycin was the only antibiotic selection marker used for *Microbispora* sp. 107891 in this study. The Gus-reporter system (2.12.4) was used to easily select the integration of the plasmids in *Microbispora* sp. 107891 genome by homologous recombination and plasmid lost due to second-event.

### 2.12.1 Generation of overexpression recombinant strains

For overexpression, the genes were cloned in pRM4 under the control of the constitutive promoter *ermE**p. The genes were amplified carrying a 5' NdeI site overlapping to the start codon (CATATG) and an EcoRI site after the stop codon. The

corresponding plasmids were integrated in *Microbispora* genome at the ΦC31 attachment site (3.1.3, Fig. 12). Plasmid integration was confirmed by PCR using the primers ErmEXgeneFP and ErmEXgeneRP that bind upstream the promoter *ermE**p and downstream the MCS.

### 2.12.2 Construction of the non-producer strain *Microbispora* RP0

The non-producer *Microbispora* RP0 strain was obtained by insertional inactivation of the *mlb* cluster. The *mlb* cluster was disrupted by single-crossover integration of the pGusA21-*mlbAB* plasmid containing the region from 34672 bp to 36222 bp (GenBank: AWEV00000000.1), which comprises part of the genes *mlbA* and *mlbB*, encoding the precursor peptide and the dehydratase, respectively (primers mlbAfor and mlbBrev). The integration of the plasmid was proved by PCR amplification of the apramycin resistant gene and by GUS-reporter assay. The production of NAI-107 was checked both by bioassay and LC/MS analysis.

### 2.12.3 Construction of *mlbQ* deletion mutant

Deletion mutants of *Microbispora* sp. 107891 were generated by in-frame deletion using recombinant plasmids carrying the 5' and 3' flanking regions (~1500 bp) of the target gene. The method consists of a multi-step process, unless the phenotype of the deletion mutant can be easily screened. Firstly, the integration of the recombinant plasmid is selected, subsequently the recombinant strain is grown non-selectively for one or more generations and than single colonies are screened for clones that have lost the plasmid. The clones would be either WT or deletion mutant depending on the position of plasmid integration and excision (Kieser *et al*., 2000). In the case of *Microbispora* sp. 107891, spore isolation was used to obtain cells with a single copy of the genome, as a method for protoplast formation could not be developed for this strain.

*mlbQ* deletion mutant was generated by double-crossover of the plasmid pA18gusΔ*mlbQ* containing a 1509 bp upstream fragment (EcoRI/BamHI) and a 1513 bp downstream fragment (BamHI/HindIII) of *mlbQ*. *mlbQ* flanking regions were cloned in pA18gus ensuring that the start and stop codons of the adjacent genes were left intact. The deletion plasmid pA18gusΔ*mlbQ* was introduced into *E. coli* S17-1 by transformation and then conjugated into *Microbispora*. The integration of pA18gusΔ*mlbQ* by single-

crossover event (apramycin resistant) was selected by GUS agar plate-based assay (2.12.4). The obtained strain was grown in GE82B medium supplemented with 50 µg/ml apramycin and plated out on S1 agar non-selectively for spore isolation. Spores were screened for the loss of pA18gusΔ*mlbQ* by GUS agar plate-based assay. A Δ*mlbQ* mutant (apramycin sensitive) was isolated with the described procedure. The correct gene deletion was confirmed by PCR (2.9.2) using the following primer pairs: mlbQforRT, mlbQrevRT; mlbQupfor, mlbQdownrev; mlbQcheckfor, mlbQcheckrev.

Δ*mlbQ* phenotype was complemented *in trans* by expressing *mlbQ* under the control of the constitutive promoter *ermE**p*.* For this purpose, the plasmid pRM4-*mlbQ* was transferred in the deletion mutant Δ*mlbQ*. To confirm plasmid integration in the genome, PCRs using the following primer pairs were performed (mlbQforRT, mlbQrevRT; ErmEXgeneFP, ErmEXgeneRP).

### 2.12.4 Selection of recombinant strains by GUS reporter system

The GUS system is a sensitive and versatile reporter system for actinomycetes described by Myronovskyi *et al.*, 2011. The GUS agar plate-based assay was reported to be an efficient method for screening recombinant clones in gene targeting. In this work, the GUS reporter system was used to screen either the integration of pA18gus and pGusA21 derivatives by homologous recombination in *Microbispora* sp. 107891 genome (blue phenotype) or the lost of pA18gus derivative plasmids in gene deletion experiments (white phenotype). *Microbispora* recombinant clones were streaked onto MV0.1 agar plates and after 7-days incubation at 30°C overlaid with 1 mg/ml X-Gluc (5-bromo-4-chloro-3-indolyl-β-D-glucopyranosiduronic acid). Clones harbouring the plasmids with the *gus* gene formed a blue halo around the colony due to the β-glucuronidase activity. Although *Microbispora* colonies have a strong red pigmentation, a blue halo could be easily detected on MV0.1 agar, a colourless agar medium.

## 2.13 Analysis of NAI-107 production

### 2.13.1 NAI-107 detection by bioassay

Bioassays for the detection of NAI-107 were conducted using *M. luteus* as indicator strain. *M. luteus* from a glycerol stock was added to LB agar ($10^5$ cfu/ml) and 15 ml poured into 90 mm standard Petri dishes or 35 ml into 120 mm square Petri dishes. To verify NAI-107 production, 20 µl of *Microbispora* culture supernatant at different time points were used. To compare NAI-107 production between different recombinant strains, the bioassay was performed with 1-3 µl of *Microbispora* cultures (120 h). In this case, a smaller volume of supernatant was used to avoid that the lantibiotic diffusion could have become a limiting factor. For *Microbispora* WT always 2 µl were used, whereas for the recombinant strains the volume of the supernatant was adjusted to the dry weight of the cultures. As reference the dry weight of the wild type was set as 100%. The supernatant of *Microbispora* cultures was pipetted on sterile paper disks, which were applied onto *M. luteus* plates. The plates were incubated at 37°C until halos were visible (approximately 24 h).

### 2.13.2 NAI-107 detection by HPLC

NAI-107 was extracted from 450 µl of liquid culture by adding two volumes of MeOH:$CH_3COOH$ 92:8 and thoroughly mixing for 1 h at 50°C (ThermoMix 50, Serva). After centrifugation, the liquid phase was analysed on a HP 1090M liquid chromatograph (Agilent) equipped with a thermostated autosampler (50°C), a reversed-phase column Reprospher 100 C18 DE (150 x 3 mm ID, 3 µm with a precolumn 10 x 3 mm ID, Dr. Maisch, Ammerbuch) and a diode-array detector (230, 268 nm) using a gradient of the two mobile phases A=75% 20 mM $HCOONH_4$, 30 mM NaCl, pH 3 (HCOOH), 25% acetonitrile and B=25% 20 mM $HCOONH_4$, 30 mM NaCl, pH 3 (HCOOH), 75% acetonitrile (time in min: $t_0$=10%B, $t_{20}$=35%B, $t_{25}$=$t_{30}$=80%B, $t_{32}$=$t_{40}$=10%B, 0.4 ml/min). The injection volume was 15 µl. The data were processed with the software LC/3D ChemStation Rev. A.08.03 (Agilent). A calibration curve was constructed by measuring the adsorbance at 230 nm or 268 nm of NAI-107 standard solutions (25, 50, 100 µg/ml in water:acetonitrile 1:1). Sample concentration was calculated by interpolation from the calibration curve.

### 2.13.3 NAI-107 detection by LC/MS

NAI-107 was extracted from *Microbispora* cultures as described in 2.13.2 and analysed with an Agilent HPLC-ESI-MS system (LC/MSD Ultra Trap System XCT 6330, Waldbronn, Germany), using a linear gradient of eluent A= 0.1% formic acid in water and eluent B= 0.06% formic acid in acetonitrile (time in min: $t_0$= 10%B, $t_{17}$=80%B, $t_{18}$=100%B, 0.4 ml/min, 40°C) on a Nucleosil 100 C18 column (100 x 2 mm ID, 3 µm, Dr. Maisch, Ammerbuch). The injection volume was 2.5 µl. Ion extracted chromatograms were obtained using Agilent DataAnalysis for 6300 Series Ion Trap LC/MS 6.1 ver. 3.4 software (Bruker-Daltonik).

## 2.14 Lantibiotic resistance assays

The lantibiotics used in this study were NAI-107, 97518 and epidermin. NAI-107 and 97518 were obtained from NAICONS and were dissolved in 10% DMSO to a final concentration of 1 mg/ml. Epidermin, isolated from *S. epidermidis* Tü 3298 (Hörner *et al.*, 1989), was dissolved in 0.05% acetic acid (1 mg/ml).

### 2.14.1 Lantibiotic resistance assays using paper disks

Resistance assays using paper disks were used to test the resistance of *S. coelicolor* and *Microbispora* spp. recombinant strains to the lantibiotics NAI-107, 97518 and epidermin. $10^6$ spores were spread onto LB agar (*S. coelicolor*) or MV0.1 agar (*Microbispora* spp.) plates to allow confluent growth. Sterile paper disks were soaked with the desired volume of lantibiotic and placed on the plates. The plates were photographed after two (*S. coelicolor*) or four-five days (*Microbispora* spp.) incubation at 30°C.

### 2.14.2 Lantibiotic resistance assays using gradient plates

Resistance assays using gradient plates were performed to test the resistance of *S. coelicolor* recombinant strains to NAI-107 and epidermin. Indeed, this method allowed a better detection of the differences in resistance between *S. coelicolor* recombinant strains. Squared Petri plates (10x10 mm) with a continuous gradient of lantibiotic were prepared as described here. Two layers of agar were poured successively into a plate to obtain a gradient from one side to the other. The desired volume of lantibiotic (final

concentration of 2 or 4 µg/ml) was added to 30 ml LB agar, which were poured into the plate. The plate was propped up just enough for the agar to cover the entire bottom using a 3 mm thick bar. In this way, the agar formed a wedge that was shallow on one side and deep on the other side of the plate. After agar solidification, the plate was placed in a horizontal position and 30 ml LB agar without lantibiotic were poured to have a homogenous agar layer. After incubation at room temperature to allow lantibiotic diffusion (1-2 h), $2x10^5$ spores of *S. coelicolor* strains were spotted at the edges of the gradient plate and streaked to the centre. The plates were incubated 2 days at 30°C.

## 2.15 Protein expression, purification, identification and structure determination

In the present study, MlbQ (25-129 aa) was expressed in *E. coli* using the plasmid pET30 to have N-terminal His- and S-tag fusion. MlbQ was purified with the Ni-NTA technology and after purification fusion sequences were removed by enterokinase digestion. To obtain high pure samples for NMR analysis, a successive purification by anion exchange chromatography was carried out.

### 2.15.1 Cultivation conditions of *E. coli* for protein expression

*E. coli* Rosetta 2(DE3) was transformed with pET30-*mlbQ* and cultivated in LB medium supplemented with 30 µg/ml kanamycin and 25 µg/ml chloramphenicol. After overnight incubation at 37°C, 250 ml LB medium containing the antibiotics were inoculated with 5 ml overnight culture (2% inoculum). Protein expression was induced by addition of 0.5 mM IPTG at an $OD_{600\ nm}$ of 0.6. After 16-18 h of cultivation at 18°C, at 180 rpm (Innova 44, New Brunswick Scientific), the cells were harvested by centrifugation at 5000 rpm for 10 min and used directly for protein purification (see below). For NMR applications, *E. coli* clones were grown in labeled M9 minimal medium and a large-scale purification was required. M9 minimal medium was either $^{15}N$-labeled or $^{13}C$,$^{15}N$-labeled, depending on the NMR applications. *E. coli* was grown overnight in LB medium, washed twice with M9 minimal medium and used to inoculate (2% inoculum) 1-2 l of labeled M9 minimal medium. Protein expression was induced as described above.

### 2.15.2 Protein purification using Ni-NTA affinity chromatography

Protein purification using the Ni-NTA technology takes advantage of the affinity of a polyhistidine sequence (Hisx6) to a nickel-charged resin (Ford *et al.*, 1991). The chelating agent NTA (nitrilotriacetric acid) insures the charge of nickel to the resin, which is used both in batch and gravity flow applications. The polyhistidine sequence can be fused either at the N- or C-terminal end of the protein of interest. Proteins can be eluted by displacement with imidazole or changing the pH (low pH buffer). In this work, Ni-NTA gravity flow columns (IBA) were used for protein purification. All the steps were performed at 4°C. The cells were resuspended in 10 ml lysis buffer and disrupted by a Bandelin Sonopuls sonicator (3x30 sec, power 60%). Cells debrids were sedimented by centrifugation at 47800 *g* for 30 min (Sorvall R6 plus, SS-34 rotor, Thermo Scientific) and the soluble fraction was used for protein purification using a 1 ml Ni-NTA Sepharose column. The supernatant was loaded on the pre-equilibrated Ni-NTA column, the resin washed twice with 5 ml wash buffer and eluted six times with 0.5 ml elution buffer. The fractions were checked for the presence of the desired protein by SDS-PAGE. 20 µl of the fractions were added to 10 µl SDS loading buffer, run on a 15% SDS-PAGE and visualized by Coomassie blue staining. Most of the protein was eluted in the fractions 3, 4 and 5 which were collected together and dialyzed overnight against the storage buffer using ZelluTrans dialysis tubes (MWCO 8000-10000, flat width 25 mm, wall thickness 28 µm, Roth). For large-scale purifications from 1-2 l cultures, the cells were resuspended in 30 ml lysis buffer and disrupted either by sonicator or by French Pressure Cell Press (SIM 3 AMINCO Spectronic Instruments, 3x 1000 Psi). A 5 ml Ni-NTA Sepharose Column was used for purification and after loading, the column was washed four times with 10 ml wash buffer. Proteins were eluted by six elution steps with 2.5 ml elution buffer.

### 2.15.3 Protein purification using anion exchange chromatography

For NMR applications, proteins were further purified by anion-exchange chromatography, a chromatography based on the electrostatic attraction between buffer-dissolved negatively charged proteins and positively charged binding sites on a solid ion exchange adsorbent (Himmelhoch, 1971). A pH higher than the isoelectric point of the proteins ensures to have negatively charged proteins. Elution is performed by

gradually increasing the ionic strength of the buffer via salt gradient. Here, protein purification was carried out using a ÄKTA purifier system and a MonoQ H55/5 column (GE Healthcare). After Ni-NTA purification and dialysis, proteins were diluted up to 50 ml with buffer A (see below) and loaded on the column. Protein purification was carried out with a linear salt gradient of buffer A: 20 mM Tris/HCl (pH 8) and buffer B: 20 mM Tris/HCl, 1 M NaCl (pH 8) (time in min: $t_0$=$t_5$=0%B, $t_{20}$= 100%B, $t_{20}$=$t_{25}$=100%B, 1 ml/min). His-MlbQ eluted at ~250 mM NaCl. The fractions containing the desired protein were collected and concentrated to 0.5 ml with 10000 MWCO Amicon Ultra centrifugal filter devices (Millipore).

### 2.15.4 Cleavage of the fusion tag by enterokinase

Proteins expressed with the pET30 vector possess a 42 aa N-terminal fusion sequence, consisting of a His- and S-tag. A thrombin site between the His- and S-tag and an enterokinase site before the first amino acid of the expressed protein allow to remove the tag by enzymatic cleavage. In this work, enterokinase digestion was performed to obtain the desired proteins without the fusion tag. The protein concentration was determined by Bradford assay (2.15.6) and digestion was carried using the enterokinase light chain from NEB. Depending on the applications, a variable amount of protein (0.2-3.5 mg) was digested with enterokinase, as described in the manufacturer's instructions (0.00016 µg of enterokinase cleave 25 µg of protein). The digestion was performed for 18 h at 4°C and checked by SDS-PAGE. The cleaved tag and the enterokinase were removed from the protein sample by Ni-NTA affinity chromatography. MlbQ without His-tag was collected in the flow through and in the washing fractions. The protein was concentrated with 3000 MWCO Amicon Ultra centrifugal filter devices (Millipore).

### 2.15.5 SDS-PAGE and Coomassie staining

SDS-PAGE (Sodium Dodecyl Sulphate – PolyAcrylamide Gel Electrophoresis) is an electrophoretic technique that allows to separate proteins according to their size. The method is based on protein denaturation by treatment with SDS. This detergent confers a negative charge to the denatured proteins, thereby allowing a migration toward a positive pole when they are placed in an electric field. Since SDS imparts a constant distribution of charge per unit mass, the proteins are separated approximately by their

size. In this work, proteins were separated on 15% SDS-PAGE gels, prepared as described below. A 5% stacking gel was poured on the top of the resolving gel. The SDS-PAGE loading buffer (3x) was added to 5-20 µl of the protein samples, which were incubated at 100°C in a water bath for 10 min and loaded on the gel. Gels were run with a Power Pac 3000 (version 4.17, BIO-RAD) at 20 mA until the migration front was at the end of the gel. Protein size was determined using the following markers from Fermentas: Prestained Protein Molecular Weight Marker (20, 27, 36, 50, 90, 118 kDa) and PageRuler Prestained Protein Ladder (10, 17, 26, 34, 43, 55, 72, 95, 130, 170 kDa).

| **Component** | **Volume*** | |
|---|---|---|
| | **Running gel** | **Stacking gel** |
| 30% Acrylamide Mix | 15 ml | 1.8 ml |
| 1.5 M Tris pH 8.8 | 7.5 ml | - |
| 1.5 M Tris pH 6.8 | - | 1.5 ml |
| 10% SDS | 0.3 ml | 0.12 ml |
| 10% APS | 0.3 ml | 0.12 ml |
| TEMED | 12 µl | 12 µl |
| $H_2O$ | 6.9 ml | 8.2 ml |

* For the preparation of four 15% SDS-PAGE gels (7x8 cm gel size).

Proteins were visualized by Coomassie staining. Gels were incubated in the Coomassie staining solution for 20 min on a horizontal shaker and destained for approximately 30-60 min with the destaining solution.

### 2.15.6 Determination of the protein concentration

To determine the concentration of protein samples, the Bradford assay was used (Bradford, 1976). This colorimetric assay is based on the Bradford reagent (Coomassie Brillian Blue G-250 in acidic solution), which binds to proteins according to their amino acid composition. Coomassie Brillian Blue G-250 binds predominantly to Arg residues and in minor extend to Trp, Tyr, His and Phe. The reagent shifts its absorbance maximum from 465 to 595 after binding to proteins. The relative protein concentration in a sample is calculated by comparison to a standard curve. Here, the samples were prepared by adding 5 µl of protein (or 5 µl of protein samples diluted 1:5 or 1:10) to 195 µl $H_2O$. For

the standard curve, 0-20 µl of 1 µg/ µl BSA were added to 5 µl protein buffer and $H_2O$ to have a final volume of 200 µl. 800 µl of Bradford reagent were added to both protein and standard samples and the absorption at 595 nm was measured. Samples were prepared in duplicate and the protein concentration was determined by comparison with a standard curve. Protein concentration was alternatively determined by measuring the absorbance at 280 nm by a NanoDrop, using an extinction coefficient determined with the online tool ProtParam Tool.

### 2.15.7 Western blot analysis

Western blot, also known as immunoblot, is a method used to identify proteins based on their specific interaction with antibodies. Proteins are separated by gel electrophoresis, transferred to a membrane, incubated with an antibody and detected by chemiluminescent, fluorescent or colorimetric methods. Here, western blot was used to verify the expression of recombinant proteins or to determine the presence of the desired proteins in certain fractions. His-tag fused proteins were detected with an anti-Histag antibody conjugated with a horseradish peroxidase (HRP), Biomol. The enzyme catalyzes the oxidation of specific substrates in the presence of hydrogen peroxide, resulting in emission of light or formation of a coloured/fluorescent product depending on the substrate used. The samples were separated on 15% SDS-PAGE and blotted onto a nitrocellulose membrane (Biotrace NT, Pall) at 400 mA for 20 min (semi-dry blotter, peqLab). The membrane was washed twice for 5 min with wash solution 1 and incubated 1 h in the blocking solution. Afterwards, the membrane was washed twice for 5 min with the wash solution 1 and incubated for 1 h with an anti-Histag antibody conjugated with HRP, Biomol (dilution 1:10000). The membrane was washed as mentioned before and a further wash step with wash solution 2 was carried out (2x 10 min). Blots were developed using the 'Western lighting *Plus* enhanced chemiluminescence system' from PerkinElmer. 1 ml of solution A and 1 ml of solution B were mixed and dropped to the membrane. After 1 min incubation, images were viewed with ChemiDoc (BIO-RAD) with an exposure time of 10 minutes.

### 2.15.8 Membrane isolation for MlbQ localization

To verify the localization of MlbQ at the membrane compartment, *mlbQ* was fused at the C-terminal with His-tag (primers: mlbQfor1, mlbQhistagrev2) and cloned into pRM4 yielding pRM4-*mlbQ*Histag. The recombinant plasmid was transferred into the heterologous host *S. coelicolor* M145, which was cultivated 3 days in R5 medium supplemented with 50 µg/ml apramycin. Membranes were isolated according to the following steps, all conducted at 4°C. The mycelium was collected, resuspended with PBS and sonicated 3 times for 30 sec (Bandelin Sonopuls sonicator). A sample of the crude extract was retained for western blot analysis and the rest was centrifuged at 14500 *g* for 30 min (Sorvall RC6 plus, SLA-600 TC rotor, Thermo Scientific). The supernatant was centrifuged at 47800 *g* for 90 min to obtain a membrane pellet, which was then washed once with PBS. Membranes were resuspended in 500 µl PBS and 10 µl of the fractions (cell extract, wash, membranes) were analysed by western blot (2.15.7).

### 2.15.9 Circular dichroism spectroscopy

Circular dichroism (CD) is the differential absorption of left- and right-handed circularly polarized light by chiral molecules. A circular dichroism signal can be positive or negative, depending on whether left-or right-handed circularly polarized light is absorbed to a greater extent. The CD signal varies depending on wavelength, so that a CD spectrum may exhibit both positive and negative peaks. CD spectroscopy is based on the CD phenomenon and it is used to study chiral molecules, in particular biological molecules. Notably, CD spectroscopy is used to predict protein secondary structure, as alpha helices and beta sheets have representative CD spectral signatures (Greenfield, 2006). CD spectroscopy is a quick method that does not require large amounts of proteins. CD spectra are recorded in few minutes in the visible and ultra-violet region of the electro-magnetic spectrum. Because each protein has a specific CD signature, CD spectroscopy is routinely used to check protein folding. Moreover, this technique turned to be a valuable tool to analyse conformational changes under different environmental conditions (temperature, pH) and in the presence of ligands. In the present work, CD spectroscopy was used to determine the folding state of the purified proteins (0.1-0.5 mg/ml). CD spectra were recorded between 210 and 300 nm. CD spectra over the

temperature range 25-95°C were recorded to determine possible unfolding intermediates. The analyses were conducted at the department of Protein Evolution at the Max Planck Institute in Tübingen in collaboration with Dirk Linke.

### 2.15.10 NMR structure determination

Traditionally, protein structures were obtained by X-ray crystallography, a technique that provides the finest visualization of protein structure currently available. The technique is based on the determination of the X-ray diffraction pattern of a protein crystal. X-rays allows to obtain high resolution protein structures, as both X-rays wavelength and covalent bonds are in the order of the nanometres. However, difficulties in the crystallization process can impose limitation in the use of this technique. NMR spectroscopy can be alternatively used to elucidate protein structure. The technique allows to determine the atomic nuclei that are closed to each other and to characterize the local conformation of atoms that are bonded together. NMR spectroscopy is unique to reveal the atomic structure of proteins in solution. Typically, a concentration of 1 mM (or 15 mg/ml for a 15 KDa protein) is required. Notably, NMR spectroscopy can be used to determine atomic structures of flexible proteins and to gain insights into the structure and dynamics of unfolded and partially folded states of proteins (Dyson and Wright, 2005). The power of NMR has greatly increased by the ability to obtain labeled proteins at specific sites ($^{13}C$, $^{15}N$, $^{2}H$) but the technique remains limited to the analysis of small and medium proteins (40 kDa). Here, NMR spectroscopy was used to elucidate the structure of a soluble version of MlbQ. MlbQ was expressed in *E. coli* (2.15.1) and purified by Ni-NTA affinity chromatography (2.15.2) and anion exchange chromatography (2.15.3). The protein samples were concentrated to about 10 mg/ml with 10000 MWCO Amicon Ultra centrifugal filter devices (Millipore). Furthermore, NMR ligand binding interaction studies using the lantibiotics NAI-107 and 97518 were attempted. The analyses were conducted at the department of Protein Evolution at the Max Planck Institute in Tübingen by Murray Coles using Bruker AVIII-600 and AVIII-800 spectrometers.

### 2.15.11 MlbQ interaction with DPC micelles and lantibiotic-protein binding studies

To determine if MlbQ interacts with membranes, dodecylphosphocholine (DPC) micelles were used as membrane models. The choice was driven by the finding that NAI-107 readly dissolves in water in the presence of 150 mM DPC (Münch *et al.*, 2013). This system was tested for the possibility to perform lantibiotic-protein binding studies in the presence of micelles. DPC was dissolved in the protein dialysis buffer at a concentration of 500 mM and added to the protein samples in a range of 5-150 mM. The binding of MlbQ to micelles was checked by NMR analysis by Murray Coles (Department of Protein Evolution, Max Planck Institute, Tübingen). Lantibiotic-protein binding studies in the presence of micelles were carried out by bioassay (2.13.1). 4 µl 0.1 mg/ml NAI-107 were added to 1.6 µl 5 mM DPC and 1.2-2.4 µl ~1 mg/ml MlbQ, the latter purified by anion exchange chromatography and cleaved with enterokinase. The total volume was 40 µl. The mix was incubated at 30°C for 10 min and 20 µl were used for bioassay.

## 2.16 Methods to analyse the peptidoglycan

Methods for PG isolation were established immediately after the discovery of the cell wall of *E. coli* by Weidel and co-workers (Weidel *et al.*, 1960). In the meantime, lots of different methods were developed, all based on the following steps: cell disruption, digestion of proteins, RNA, DNA and release of muropeptides by enzymatic reaction. Detailed analysis of muropeptides became possible with the advent of high performance liquid chromatography (HPLC) in the early 1980s. Before that time, information about cell components were mainly obtained by amino acid analysis and thin layer chromatography (Schleifer and Kandler, 1972).

In this work, PG was isolated as previously described (Bera *et al.*, 2005, Schäberle *et al.*, 2011). Bacterial cell wall (PG-teichoic acids complex) was isolated after boiling the bacteria in SDS, a step required for the solubilisation of the cell membrane and a high proportion of proteins. The insoluble cell wall was recovered by centrifugation and washed from SDS. The cell wall was mechanically broken and residual DNA, RNA and proteins were enzymatically removed by incubation with DNase, RNase and trypsin. Pure cell wall was obtained by successive purification steps involving extractions with SDS, LiCl, EDTA and acetone. To obtain pure peptidoglycan, WTAs were solubilized by

treatment with HF. Muropeptides were released by incubation with mutanolysin, a muralytic enzyme that cleaves the β-N-acetylmuramyl-(1→4)-N-acetylglucosamine linkage of PG polymer. Prior to HPLC analysis, muropeptides were reduced with sodium borohydride. In particular, the anomeric carbon (C1) of N-acetylmuramic acid was reduced to the corresponding alcohol. The presence of the reduced sugar instead of the two anomeric forms, which would have different retention times, allowed a HPLC separation with high resolution. A recent review (Desmarais *et al.,* 2013) describes the applications of HPLC in PG analysis with a particular focus on PG chemical features and morphological aspects. For a detailed PG structure determination, ion fragmentation by tandem mass spectrometry (MS/MS) and amino acid analysis were conducted in this study. Moreover, UDP-linked PG precursor analysis was performed to determine the composition of soluble PG precursors. In the next paragraphs, the methods for PG and UDP-linked PG precursor analyses are described in details.

### 2.16.1 Peptidoglycan isolation

For peptidoglycan isolation*, Microbispora* spp. were grown in GE82G medium for the generation of biomass (2.7.3) and than inoculated (6% inoculum) in a 1000-ml baffled Erlenmeyer flask with a coiled spring baffle, filled with 300 ml KV6 medium. Cells were grown for 72 h (exponential phase) or 120 h (stationary phase) at 28°C and harvested by centrifugation at 5000 rpm for 10 min. The cells were resuspended in the smallest volume of 50 mM Tris/HCl pH 7 and the cell suspension was added drop-wise to 4% boiling SDS (120 ml) with vigorous stirring. SDS was boiled for 15 minutes and than cooled to room temperature. The crude cell wall material was collected by centrifugation at 13000 *g* for 10 min at room temperature (Sorvall RC6 plus, SLA-600 TC rotor, Thermo Scientific), the pellet washed twice with 1 M NaCl and then with $H_2O$ until no foam could be observed (around 15 washes). The pellet was resuspended in 2-4 ml $H_2O$ and filled in 2 ml screw cap tubes containing 0.2 ml glass beads (0.17-0.18 mm). Cell walls were mechanically broken with a Precellys Homogenizer (2 cycles: 2x20 sec at 6500 rpm). After every second pulse, the samples were cooled in ice for 5 min. Glass beads were removed by centrifugation at 2000 *g* for 5 min and the broken cell walls were sedimented by centrifugation at 25000 g for 15 min. The pellet was resuspended in 3 ml 100 mM Tris/HCl pH 7.5 supplemented with 20 mM $MgSO_4$. DNase (10 µg/ml)

and RNase (50 µg/ml) were added and the samples were incubated for 1 h at 37°C. A second digestion was performed after addition of trypsin (100 µg/ml) for 18 h at 37°C. After trypsin incubation, SDS was added (1%) and the samples were incubated at 80°C for 15 min. The volume was adjusted with $H_2O$ to 20 ml and cell walls were sedimented by centrifugation at 25000 rpm for 30 min. The pellet was resuspended in 10 ml 8 M LiCl and incubated at 37°C for 15 min. After centrifugation (25000 rpm, 30 min), the pellet was resuspended in 10 ml 100 mM EDTA pH 7.0 and incubated at 37°C for 15 min. Cell walls were sedimented as described before and successively washed with 20 ml $H_2O$, 20 ml acetone and 20 ml $H_2O$. The obtained pellet consisted of purified cell walls. To obtain pure peptidoglycan, cell walls were treated with 48% HF for 48 h at 4°C. This step was carried out by Mulugeta Nega (Department of Microbial genetics, University of Tübingen). As HF is a very aggressive and toxic acid, samples were handled carefully and the Eppendorf tubes were covered with parafilm. After HF treatment, peptidoglycan was sedimented by centrifugation at 13000 rpm for 10 min and washed with $H_2O$ until no HF residues were present (pH was checked with litmus paper). Peptidoglycan was immediately digested or lyophilized and stored at -20°C.

### 2.16.2 Analysis of muropeptides

The isolated PG was digested with mutanolysin to release muropeptide monomers, dimers and multimers. 5 µg of PG were resuspended in 80 µl of 25 mM Na phosphate buffer (pH 6.8) and 20 µl 5 KU mutanolysin were added. Digestion was carried out at 37°C for 18 h (180 rpm). Samples were centrifuged and the muropeptides present in the supernatant were reduced with sodium borohydride. The supernatant was mixed with the same volume of 0.5 M sodium borate pH 9.0 and 1-2 mg sodium borohydride were added. After a 30-minutes incubation at room temperature, the excess of borohydride was destroyed by successive addition of few drops of 20% phosphoric acid until a pH of 2 was reached. Muropeptides were analysed either by HPLC, HPLC/MS or stored at -20°C. Muropeptides were separated by HPLC on an Agilent 1200 HPLC using a linear gradient of eluent A= 5% MeOH in 100 mM sodium phosphate buffer (pH 2.5) and eluent B= 30% methanol in 100 mM sodium phosphate buffer (pH 2.8) for 150 min (time in min: $t_0$=$t_5$=0%B, $t_{150}$=100%B, 0.5 ml $min^{-1}$, 52°C) on a Prontosil 120 C18 column (250 × 4.6 mm, 3 µm, Bischoff Chromatography, Leonberg, Germany). The injection volume

was 100 µl. Muropeptides were detected at 205 nm. HPLC-MS analyses of muropeptide samples were performed with an Agilent HPLC-ESI-MS system (LC/MSD Ultra Trap System XCT 6330, Waldbronn, Germany), using a linear gradient of eluent A= 0.1% formic acid in water and eluent B= 0.06% formic acid in methanol (time in min: $t_0$=$t_5$=5%B, $t_{155}$=$t_{180}$=30%B, 0.5 ml $min^{-1}$, 52°C) on a Reprosil Gold 300 C18 column (250 x 4.6 mm ID, 5 µm, Dr. Maisch, Ammerbuch). The injection volume was 90 µl. Detection of m/z values was conducted with Agilent DataAnalysis for 6300 Series Ion Trap LC/MS 6.1 ver. 3.4 software (Bruker-Daltonik). $MS^2$ and $MS^3$ data were acquired with electrospray ionization in the positive mode. $MS^3$ spectra were annotated using the software mMass (Niedermeyer and Strohalm, 2012).

### 2.16.3 Amino acid analysis of muropeptides

The analysis of muropeptide amino acids was performed by HPLC using Opa derivatization. Opa (o-phthaldialdehyde) reacts with primary amines of amino acids enabling fluorescent detection and quantification. A pre-column derivatization was performed using an Agilent 1200 HPLC. HPLC purified individual muropeptides were hydrolysed with 6 N HCl at 110°C for 16 h. After removal of HCl using a vacuum desiccator, the muropeptide hydrolysates were resuspended in water and subjected to HPLC analysis using the O-phtaldialdehyde (OPA) pre-column derivatization method. Hydrolysates and OPA reagent (Alltec Grom, Germany) were mixed in a 2.3:1 ratio and derivatization was carried out in the Agilent 1200 HPLC injection needle for 90 seconds before injection. Separation was made on a Grom-Sil OPA-3 column (4 x 150 mm, 5 µm, Alltec Grom, Rottenburg-Hailfingen, Germany) using a gradient of eluent A: 25 mM Na-Phosphate buffer supplemented with 0.75% THF and eluent B=50% buffer A mixed with 35% methanol and 15% acetonitrile (time in min: $t_0$=0%B, $t_{10}$=50%B, $t_{15}$=60%B, $t_{20}$= $t_{25}$=100%B, 1.1 ml $min^{-1}$, 30°C). Detection was made at 340 nm. 2.5 mM amino acid solutions were prepared and used as standard.

### 2.16.4 UDP-linked peptidoglycan precursor analysis

A method for UDP-linked PG precursor purification was firstly described by Kohlrausch and Holtje, 1991. PG precursors were accumulated by treatment with vancomycin (pentapeptide precursors) or D-cycloserine (tripeptide precursors) and separated on a

reverse-phase HPLC. In the present study, the analysis was carried out according to Schärberle *et al.,* 2011, using bacitracin for the accumulation of UDP-linked PG precursors and LC/MS analysis for the detection of PG precursors. Bacitracin is an antibiotic that interferes with the dephosphorylation of $C_{55}$-isoprenyl pyrophosphate, thereby preventing its recycling. In this way, UDP-linked PG precursors are accumulated in the cytoplasm, as the lipid carrier is not anymore available on the inner-leaflet of the cytoplasmic membrane. For the accumulation of UDP-linked PG precursor, *Microbispora* sp. 107891 and *Microbispora* RP0 were grown in 100-ml baffled Erlenmeyer flask with a coiled spring baffle filled with 50 ml KV6 medium. After 72 h of growth at 28°C, cultures were treated with 100 µg/ml bacitracin for 1 h. The cells were collected by centrifugation, resuspended in 20 ml of water and boiled for 20 minutes. The supernatant was lyophilized, resuspended in 1 ml water and analysed by HPLC-MS with an Agilent HPLC-ESI-MS system (LC/MSD Ultra Trap System XCT 6330, Waldbronn, Germany), using a linear gradient of eluent A= 0.1% formic acid in water and eluent B= 0.06% formic acid in methanol (time in min: $t_0$=0%B, $t_{25}$=10%B, $t_{27}$=$t_{30}$=100%B, 0.4 ml $min^{-1}$, 40°C) on a Nucleosil 100 C18 column (100 x 2 mm ID, 3 µm, Dr. Maisch, Ammerbuch). Ion extracted chromatograms were obtained using Agilent DataAnalysis for 6300 Series Ion Trap LC/MS 6.1 ver. 3.4 software (Bruker-Daltonik).

## 2.17 Microscopy

### 2.17.1 Phase contrast microscopy

Samples were placed on 76x26 mm glass slides (VWR international) and covered with a glass cover slip (18x18 mm; VWR international). Slides were observed at 400 or 1000 times magnification with a Zeiss DM5500B microscope equipped with a Leica DFC360FX camera. ImageJ was used for image processing.

### 2.17.2 Fluorescence microscopy

Fluorescence microscopy was used to monitor MlbQ-mCherry localization in *Microbispora* Δ*mlbQ* and in the heterologous strains *Microbispora* JCM66 and *S. coelicolor*. The same strains expressing mCherry were used as controls. *Microbispora*

mycelium and *S. coelicolor* spores were plated on S1 and MS agar respectively and sterile coverslips were inserted at a 45° angle into the agar. Coverslips were removed after 1-14 days (*Microbispora* spp.) or 1-3 days (*S. coelicolor*) of incubation at 30°C and mounted on slides coated 1% agarose in water. Fluorescent microscopy was performed with a Zeiss DM5500B microscope equipped with a Leica DFC360FX camera using the filters 41017-Endow GFP/EGFP Bandpass for GFP fluorescence and F46-008 TxRed ET Filterset for mCherry fluorescence (Chroma Technology). ImageJ was used for image processing.

### 2.17.3 Transmission electron microscopy

Transmission electron microscopy (TEM) of *Microbispora* sp. 107891 and *Microbispora* RP0 was performed to compare the cell wall thickness of the two strains. *Microbispora* strains were grown on HA agar plates and after 6 days incubation at 30°C, the mycelium was scraped and used for sample preparation. Sample preparation and electron microscopy were carried out by Iris Maldenar and Claudia Menzel at the Microbiology/Organismic Interactions Department at the University of Tübingen. The samples were examined with a Philips Tecnai electron microscope at 80 kV. ImageJ was used for image processing.

## 2.18 Scientific Software and www-services

ChemSketch 12.0 for Microsoft Windows
Clone Manager Professional Suite for Microsoft Windows
ImageJ 1.46r for Macintosh
mMass 5.5.0 for Microsoft Windows
6300 Series Ion Trap LC/MS Software 6.1
http://www.cbs.dtu.dk/services/SignalP
http://www.cbs.dtu.dk/services/TatP
https://www.cebitec.uni-bielefeld.de/gendb
http://www.ebi.ac.uk/Tools/msa/clustalw2
http://web.expasy.org/protparam
http://harrier.nagahama-i-bio.ac.jp/sosui/sosui_submit.html

http://www.ncbi.nlm.nih.gov

http://nebuilder.neb.com

http://www.thermoscientificbio.com/fermentas

http://toolkit.tuebingen.mpg.de/hhpred

http://toolkit.tuebingen.mpg.de/quick2_d

http://www.uniprot.org

# 3. RESULTS

## 3.1 *Microbispora* spp.: growth, morphological differentiation, lantibiotic production, NAI-107 susceptibility and DNA transfer

### 3.1.1 Characterization of *Microbispora* sp. 107891

#### 3.1.1.1 Growth and differentiation of *Microbispora* sp. 107891

*Microbispora* sp. 107891 is a slow-growing actinomycete, which takes about 10 days to form a workable mycelium form a single colony. When grown on agar media, *Microbispora* sp. 107891 formed a mycelium strongly anchored to the agar and coloured from orange to red/brown depending on the medium (Fig. 7A). In liquid media, the mycelium was orange/red/brown and a soluble orange/red pigment was produced (Fig. 7B). *Microbispora* sp. 107891 grew quite dispersed in media containing insoluble components like soybean meal (GE82AB and GE82G media). Reproducible growth curves were obtained in Evans medium (3.1.1.2). Sporulation of *Microbispora* sp. 107891 was occasionally observed on S1 agar plates after 10-14 days. Firstly, white aerial mycelium was formed and then pinkish spores.

To investigate the sporulation state of *Microbispora* sp. 107891, phase contrast microscopy (2.17.1) was carried out. The strain produced branched mycelium (Fig. 7C left). After a long period of incubation, bulges at the tip of the hyphae were formed, which were considered immature spores (Fig. 7C right). Mature spores were rarely detected by phase contrast microscopy, confirming the inefficient sporulation of *Microbispora* sp. 107891.

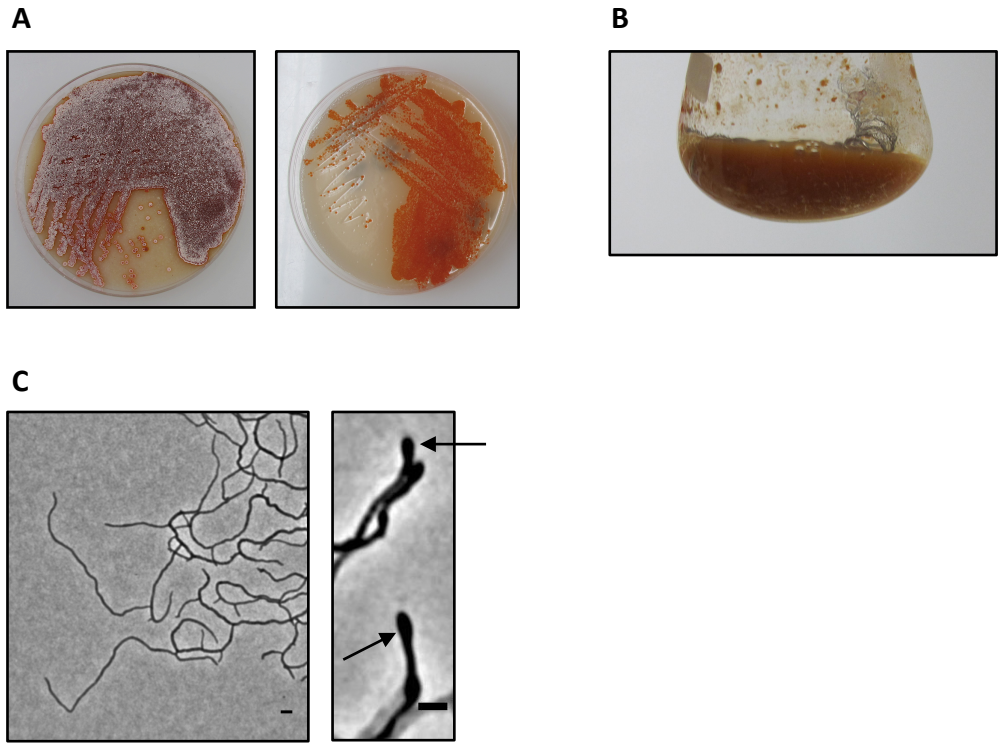


**Fig. 7. Growth and differentiation of *Microbispora* sp. 107891.** (A) Growth of *Microbispora* sp. 107891 on S1 (left) and MS (right) agar media. (B) Growth of *Microbispora* sp. 107891 in GE82G. *Microbispora* sp. 107891 produced an orange/red soluble pigment in liquid cultures. (C) Images from phase contrast microscopy of *Microbispora* sp. 107891. Overview of the mycelium (left) and apical tips characterized by immature spores indicated by arrows (right). Scale bars represent 2 µm.

### 3.1.1.2 NAI-107 production in *Microbispora* sp. 107891

*Microbispora* sp. 107891 produced NAI-107 under all conditions used in this study, both in liquid and on solid media. NAI-107 production was typically monitored by a bioassay using *M. luteus* as indicator strain (2.13.1). LC/MS analysis was carried out to confirm the identity of the antibiotic compound by comparison with a NAI-107 standard. MS signals at *m/z* 1116 and 1124 were detected in the supernatant of *Microbispora* sp. 107891. They represent the double-protonated ions $[M+2H]^{2+}$ of the A2 and A1 congeners (mono- and di-hydroxylated proline) of the NAI-107 complex (Castiglione *et al.*, 2008; Maffioli *et al.*, 2014). NAI-107 production was monitored from 8 h to 168 h in Evans medium (Fig. 8). NAI-107 was firstly detected at about 48 h post-inoculation (mid-

exponential phase). The major increase of NAI-107 production was observed between 48 h and 72 h of growth. At the latter time point, the strain entered the stationary phase, where a slight increase of NAI-107 was observed (Fig. 8).

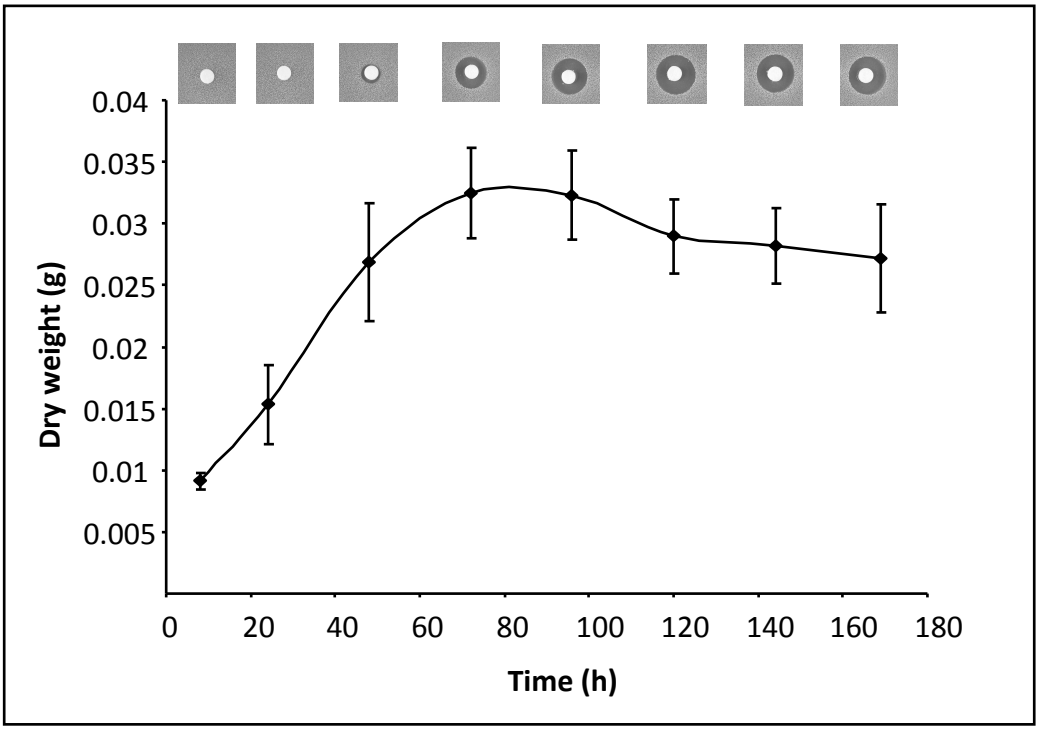


**Fig. 8. Growth and NAI-107 production of *Microbispora* sp. 107891 in Evans medium.** The y-axis represents the dry weight of 5-ml samples. n=3, three technical replicates. Images are representative of bioassays against *M. luteus* using 2 µl of the supernatant of samples collected at different time points.

NAI-107 production in Evans medium was usually checked by bioassay, as the NAI-107 concentration was at limit of HPLC detection in the conditions used in this study (2.13.2). In contrast, HPLC was used to monitor NAI-107 production of *Microbispora* sp. 107891 cultures in 107PH1 medium. In this medium, *Microbispora* sp. 107891 is able to produce up to 1 g/l NAI-107 (Monciardini, NAICONS, personal communication). The growth rate of *Microbispora* sp. 107891 in 107PH1 was monitored from 72 h post-inoculum, as at earlier time points the insoluble components of the medium interfered with the biomass measurement. At 72 h, *Microbispora* sp. 107891 was already in the stationary phase and a decrease of biomass was observed during time (up to 192 h) (Fig. 9A). However,

although the biomass did not increase, NAI-107 concentration increased up to 350 mg/l (Fig. 9B).

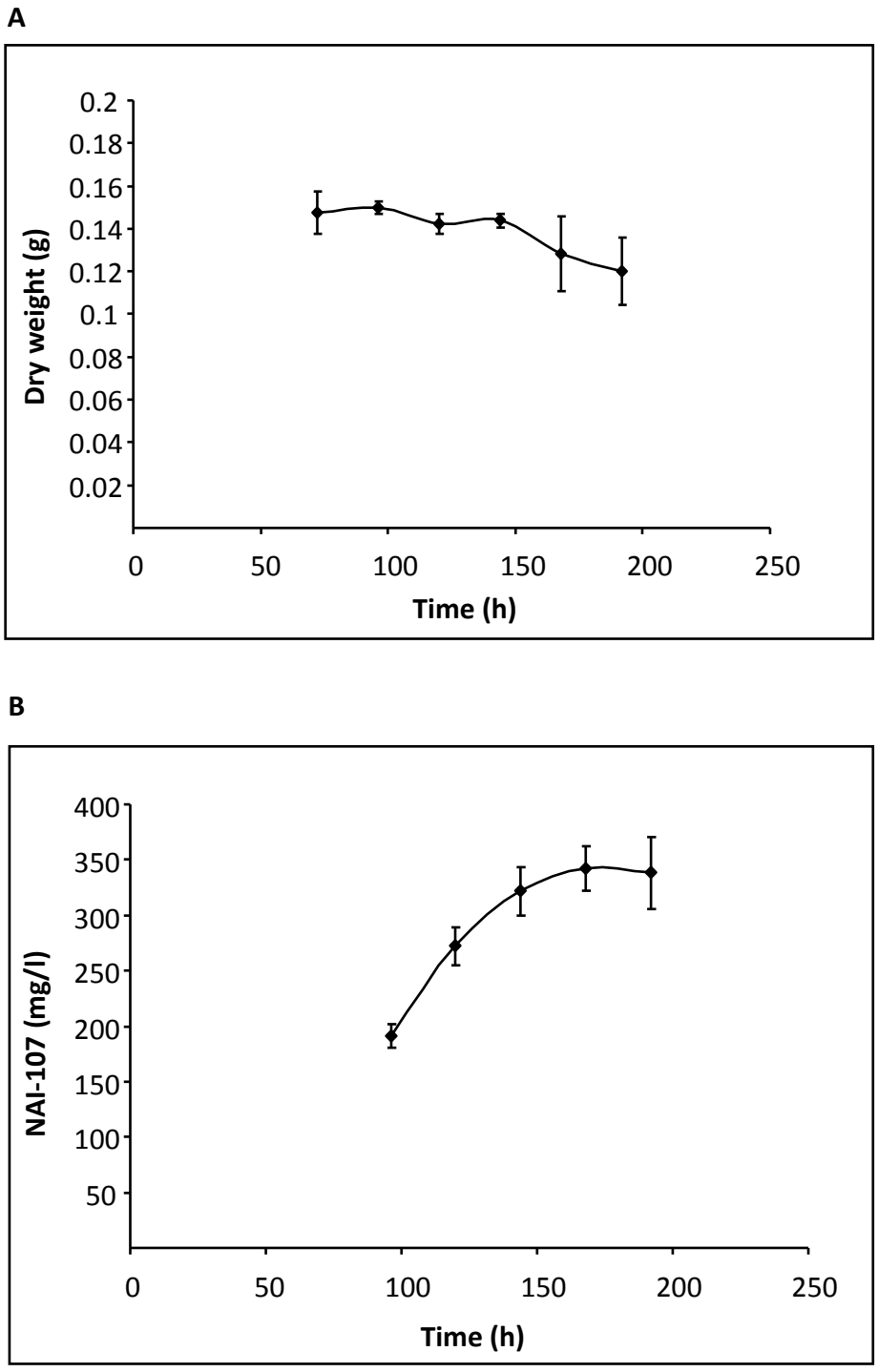


**Fig. 9. Growth and NAI-107 production of *Microbispora* sp. 107891 in 107PH1 medium.** (A) Growth from 72 h and (B) NAI-107 production from 96 h. Traces of NAI-107 were detected by HPLC at 72 h. The y-axis in (A) represents the dry weight of 5-ml samples. n=1, two technical replicates.

### 3.1.2 Characterization of *Microbispora* JCM66 and *Microbispora* JCM67

*Microbispora* JCM 10266 (*Microbispora* JCM66) and *Microbispora* JCM 10267 (*Microbispora* JCM67) are two *Microbispora* spp. isolated from soil and taxonomically characterized by Nukajima *et al.*, 1999. In the present study, these two *Microbispora* spp. were compared with *Microbispora* sp. 107891 concerning NAI-107 production, lantibiotic resistance and PG structure. Moreover, *Microbispora* JCM66 was used as a host strain for heterologous expression.

*Microbispora* JCM66 and *Microbispora* JCM67 were grown in the conditions used for *Microbispora* sp. 107891 and checked for lantibiotic production. *Microbispora* JCM66 and *Microbispora* JCM67 grew faster than *Microbispora* sp. 107891 both in liquid and on agar media. *Microbispora* JCM66 sporulated abundantly on S1 agar medium within 7 days (Fig. 10A). Spore formation was verified by phase contrast microscopy (2.17.1). Longitudinally pairs of spores attached to the aerial mycelium were observed (Fig. 10B), as described by Nakajima *et al.*, 1999. Production of antibacterial compounds was analysed by bioassay using *M. luteus* as indicator strain (2.13.1). Neither *Microbispora* JCM66 nor *Microbispora* JCM67 was able to produce antibacterial molecules that inhibited *M. luteus* growth (Fig. 11).

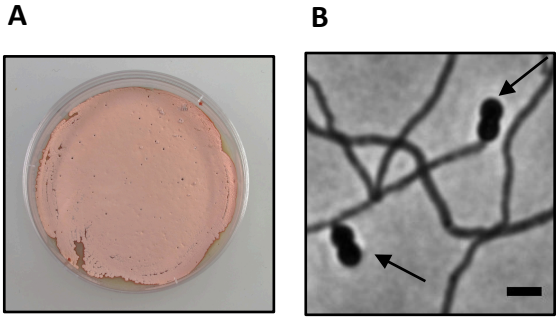


**Fig. 10. Growth and differentiation of *Microbispora* JCM66.** (A) Growth of *Microbispora* JCM66 on S1 agar medium. (B) Image from phase contrast microscopy of *Microbispora* JCM66. Longitudinally pair of spores attached to the aerial mycelium (indicated by arrows). Scale bar represents 2 µm.

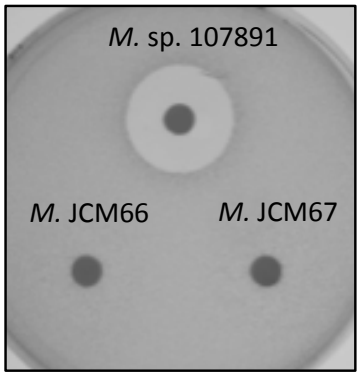


**Fig. 11. Bioassay of *Microbispora* JCM66 and *Microbispora* JCM67 against the indicator strain *M. luteus*.** *Microbispora* sp. 107891 was used as a positive control.

### 3.1.3 Development of a DNA transfer protocol for *Microbispora* sp. 107891

*Microbispora* sp. 107891 was not known to be genetically accessible, thus a DNA transfer system had to be developed. A conjugation protocol using the methylation deficient *E. coli* strain ET10257 pUZ8002 was previously reported for *Microbispora corallina* NRRL 30420 (Foulston and Bibb, 2010) but attempts to conjugate *Microbispora* sp. 107891 with the described method were not successful. Therefore, an alternative conjugation protocol had to be established. To determine which antibiotics could be used as markers, *Microbispora* sp. 107891 sensitivity to several antibiotics was tested. *Microbispora* sp. 107891 was sensitive to apramycin (3 µg/ml), hygromycin (<1 µg/ml), erythromycin (3 µg/ml), kanamycin (3 µg/ml) and thiostrepton (<1 µg/ml), markers typically used for streptomycetes (Kieser *et al.*, 2000). *Microbispora* sp. 107891 was partially sensitive to nalidixic acid (25-50 µg/ml), an antibiotic commonly used to inhibit *E. coli* growth in conjugation experiments, but resistant to phosphomycin and spectinomycin.

A protocol for conjugation of *Microbispora* sp. 107891 was established using the integrative plasmid pRM4.3, which contains an apramycin resistance cassette, the reporter gene *egfp* under the control of the *ermE** promoter (*ermE**p) and the *attP* site of the phage ΦC31. The *Microbispora* sp. 107891 genome possesses a ΦC31 attachment site (*attB*), whose sequence differs from the one of *S. coelicolor* (Combes *et al.*, 2002) by 4 nt (Fig. 12A). Conjugation experiments were performed by varying the *E. coli* donor (*E. coli* ET10257 pUZ8002 or *E. coli* S17-1), the period of incubation before overlay (10-24 h) and the antibiotic used to inhibit *E. coli* growth (nalidixic acid, phosphomycin or spectinomycin). These attempts to introduce DNA into *Microbispora* sp. 107891 were performed with *Microbispora* sp. 107891 mycelium, as *Microbispora* sp. 107891 sporulates poorly (3.1.1.1). The DNA-transfer could be achieved using the methylation proficient donor *E. coli* S17-1, apramycin for the selection of *Microbispora* ex-conjugants and phosphomycin for the inhibition of *E. coli* (2.11.3). About 20 clones were obtained and two of them (*Microbispora egfp* 1 and 2) were checked by PCR using the primers Aprafor and Aprarev (2.6) for the amplification of a fragment of the apramycin resistance cassette. The integration of pRM4.3 in *Microbispora* sp. 107891 genome was proved by PCR using the primer pairs LF044F, LF045R and LF045F, LF044R (2.6), as

described for *M. corallina* (Foulston and Bibb, 2010). Both PCR amplifications confirmed the integration of pRM4.3 at the *attB* site in *Microbispora egfp* clone 1 and 2 (Fig. 12B).

**A**

*S. coelicolor* CGGTGCGGGTGCCAGGGCGTGCCC**TT**GGGCTCCCCGGGCGCGTACTC

*M.* sp. 107891 CGGTGCGGGTGCCACGGCGTGCCC**TT**GGGCTCGCCCGGGGCGTACTC

**B**

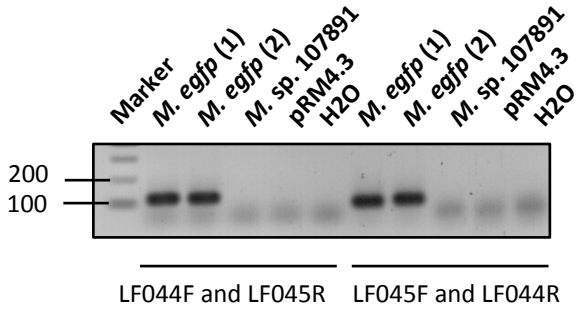


**Fig. 12. pRM4.3 integration in *Microbispora* sp. 107891 genome.** (A) Alignment of the ΦC31 attachment site (*attB*) of *S. coelicolor* with the one of *Microbispora* sp. 107891. The site of integration is in bold. (B) Verification of pRM4.3 integration in *Microbispora* sp. 107891 genome by PCR using the primer pairs LF044F, LF045R and LF045F, LF044R according to Foulston and Bibb, 2010. The primers were expected to amplify 118 bp and 94 bp products across the site of integration. Genomic DNA from *Microbispora egfp* clone 1 and 2 was used as template. *Microbispora* sp. 107891, pRM4.3 and $H_2O$ were used as negative controls.

### 3.1.4 Construction and characterization of the non-producer strain *Microbispora* RP0

A non-producer strain of *Microbispora* sp. 107891 was generated and compared with the WT regarding NAI-107 resistance (3.1.5.2), PG structure (3.2.4) and expression of immunity genes (3.3.2).

#### 3.1.4.1 Generation of the non-producer strain *Microbispora* RP0

To obtain the non-producer strain *Microbispora* RP0, insertional inactivation *via* a single-crossover event was preferred instead of *mlbA* deletion (gene encoding the precursor peptide). The chosen approach overcame the difficulties encountered in

obtaining deletion mutants (3.4.1.1), since a single-crossover event generated the desired phenotype (3.1.4.2). *Microbispora* RP0 was obtained by disruption of the NAI-107 biosynthetic gene cluster (*mlb*) by integration of the plasmid pGusA21-*mlbAB* (2.12.2). The plasmid contains a region of about 1500 bp covering part of *mlbA* and *mlbB*, the genes encoding the precursor peptide and the dehydratase, respectively (Fig. 6). The GUS reporter system facilitated the identification of recombinant clones carrying the plasmid pGusA21-*mlbAB*. The GUS agar plate-based assay (2.12.4) allowed the identification of two clones, which were verified by PCR using the primers Aprafor and Aprarev (2.6). PCR analysis confirmed the integration of pGusA21-*mlbAB* in both clones. One of them was chosen for phenotypic characterization (3.1.4.2) and was subjected to further analyses.

### 3.1.4.2 Phenotype of *Microbispora* RP0

The *Microbispora* RP0 clone obtained by integration of pGusA21-*mlbAB* was checked for NAI-107 production by LC/MS (2.13.3) and bioassay (2.13.1). *Microbispora* RP0 did not produce neither NAI-107 (Fig. 13A) nor any other antibacterial compound that affected *M. luteus* growth (Fig. 13B). *Microbispora* RP0 sporulated poorly. Immature spores at the tip of vegetative hyphae were observed by phase contrast microscopy, as reported for *Microbispora* sp. 107891 (3.1.1.1).

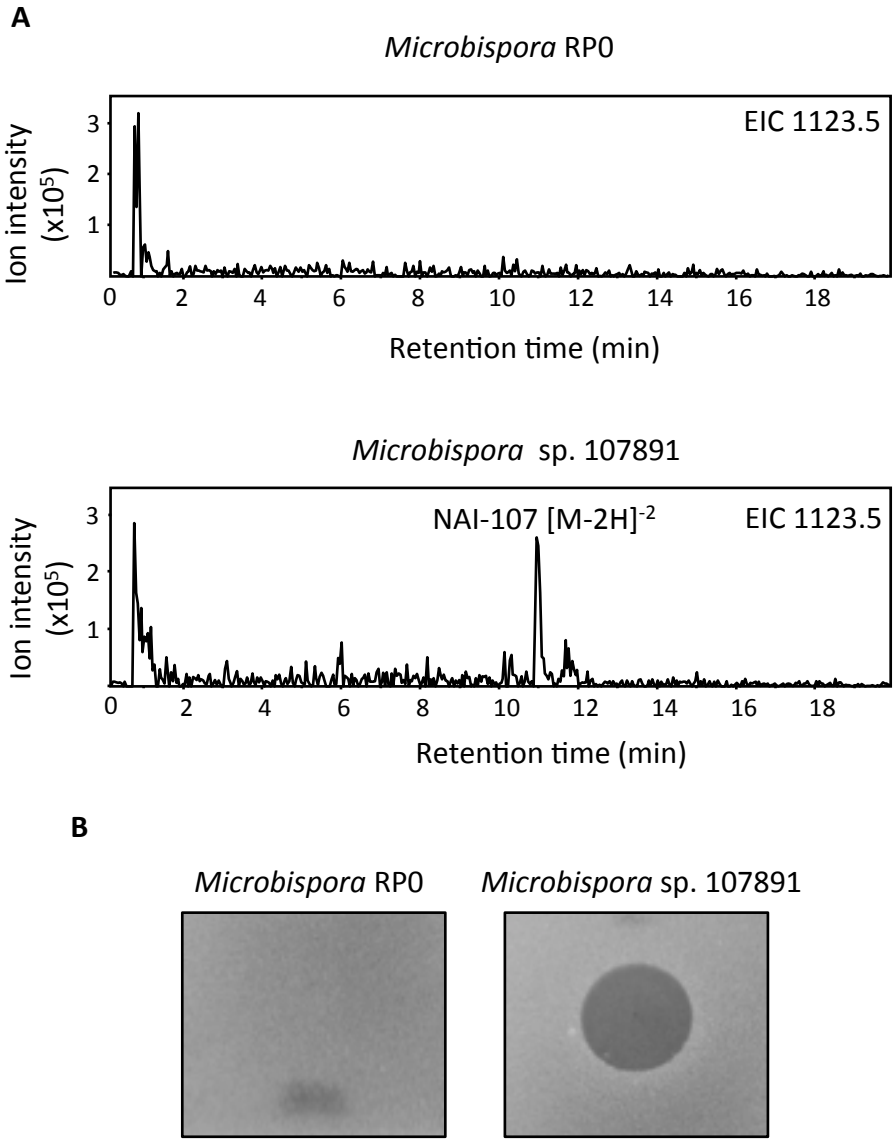


**Fig. 13. Phenotypic characterization of *Microbispora* RP0. (A)** Determination of NAI-107 production by LC/MS. EIC of 1123.5 for *Microbispora* RP0 and *Microbispora* sp. 107891 (positive control). *m/z* 1123.5 corresponds to $[M-2H]^{-2}$. (B) Determination of antibiotic production by bioassay. Bioassay against the indicator strain *M. luteus* using 20 µl of supernatant of *Microbispora* RP0 and *Microbispora* sp. 107891 (positive control).

### 3.1.5 Determination of NAI-107 resistance of *Microbispora* strains

#### 3.1.5.1 *Microbispora* sp. 107891

*Microbispora* sp. 107891 possesses likely immunity mechanisms to prevent growth inhibition by NAI-107. During initial characterization of *Microbispora* sp. 107891, the resistance to NAI-107 was determined. The mycelium of a 72 h-old culture in Evans medium was plated onto MV0.1 agar containing increasing concentrations of NAI-107 (0-5 µg/ml) and the colony forming units (CFU) were counted after 7 days of incubation. The CFU in absence of NAI-107 (CFU0) were considered 100% and the other CFU values were expressed in percentage referring to CFU0 (Fig. 14). The CFU rapidly decreased at 0.1 µg/ml NAI-107 (64% of CFU0). A further significant reduction of *Microbispora* sp. 107891 growth was observed at 1.5 µg/ml NAI-107 (12% of CFU0). At 5 µg/ml NAI-107, the CFU were about the 10% (Fig. 14). *Microbispora* sp. 107891 was grown on higher NAI-107 concentrations (data not shown). *Microbispora* sp. 107891 did not grow at 10 µg/ml NAI-107, which was considered the minimal inhibitory concentration (MIC).

This preliminary test showed that *Microbispora* sp. 107891 is not highly resistant to its own product NAI-107. *Microbispora* sp. 107891 spores were also tested for the ability to grow in presence of NAI-107. *Microbispora* sp. 107891 spores were grown on increasing concentrations of NAI-107 as described above and the MIC was calculated to be 0.5-1 µg/ml. The MIC of *Microbispora* sp. 107891 spores was about 10 times lower than the one of *Microbispora* sp. 107891 mycelium.

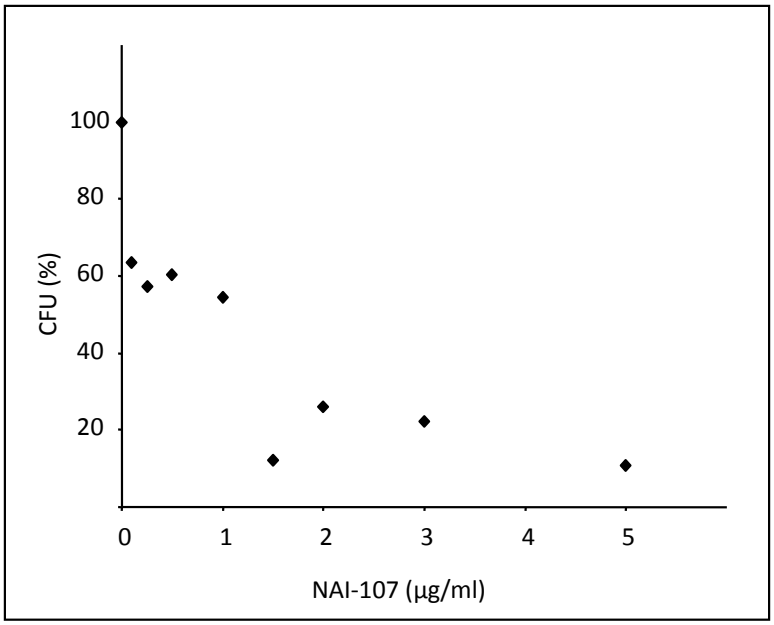


**Fig. 14. Analysis of NAI-107 resistance of *Microbispora* sp. 107891 mycelium.** *Microbispora* sp. 107891 mycelium from a 72h-old culture in Evans medium was plated onto MV0.1 with increasing concentrations of NAI-107 (0-5 µg/ml). y-axis represents the colony forming units (CFU) expressed in percentage.

### 3.1.5.2 *Microbispora* RP0

NAI-107 resistance was tested also for the non-producer strain *Microbispora* RP0, which was obtained by disruption of the *mlb* cluster (3.1.4). A high variability between experiments precluded reproducible resistance assays using mycelium. Here and in the assays reported below (3.1.5.3), spores were used to compare the NAI-107 resistance of different *Microbispora* strains (2.14.1). In this way, the variability due to differential mycelial growth was excluded. $10^6$ spores of *Microbispora* RP0 were plated onto MV0.1 agar (30 ml) and paper disks containing different amounts of NAI-107 were placed on the plate. In parallel, *Microbispora* sp. 107891 resistance was assessed. The assay revealed a higher resistance of *Microbispora* RP0 than *Microbispora* sp. 107891 (Fig. 15). 5 and 10 µg of NAI-107 formed smaller inhibition halos on RP0 plates than on *Microbispora* sp. 107891 ones (Fig. 15). Probably, the higher resistance of *Microbispora* RP0 is due to the absence of self-produced NAI-107. Thus, *Microbispora* RP0 would be able to resist to a higher amount of exogenous NAI-107 than *Microbispora* sp. 107891.

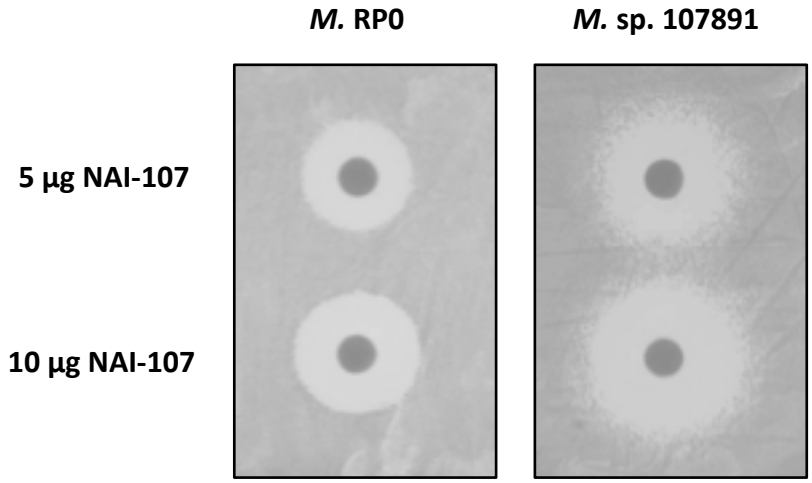


**Fig. 15. Resistance assay of *Microbispora* RP0 and *Microbispora* sp. 107891 to NAI-107.**

3.1.5.3 *Microbispora* JCM66

*Microbispora* JCM66 is a *Microbispora* strain not producing NAI-107 nor any other lantibiotic (3.1.2). *Microbispora* JCM66 resistance to NAI-107 was tested to verify if the strain behaves as *Microbispora* RP0 in presence of NAI-107. The resistance assay was performed as described for *Microbispora* RP0 (2.14.1). *Microbispora* JCM66 was susceptible to low amounts of NAI-107. 0.5 and 1 µg of NAI-107 produced remarkable inhibition halos on *Microbispora* JCM66 plates in comparison to *Microbispora* sp. 107891 (Fig. 16).

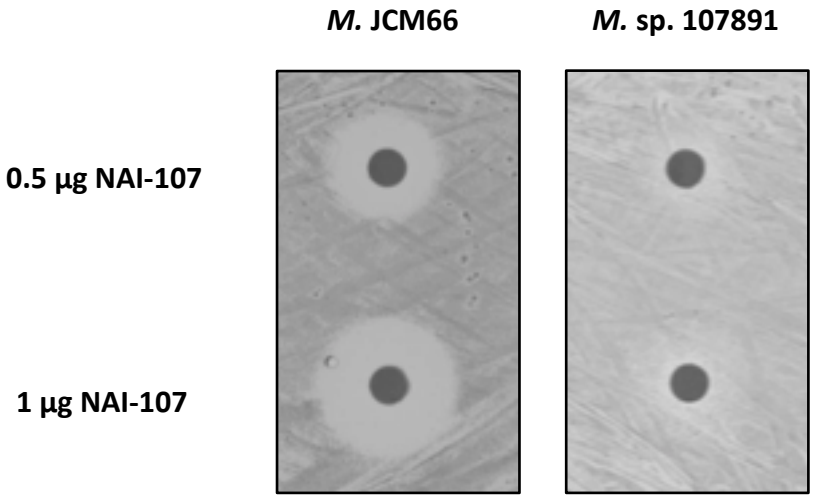


**Fig. 16. Resistance assay of *Microbispora* JCM66 and *Microbispora* sp. 107891 to NAI-107.**

Successively, the NAI-107 MIC for *Microbispora* JCM66 was determined. *Microbispora* JCM66 spores were more sensitive to NAI-107 (MIC 0.1 µg/ml) than *Microbispora* sp. 107891 ones (MIC 0.5-1 µg/ml) (3.1.5.1). In contrast, *Microbispora* RP0 was more resistant than *Microbispora* sp. 107891 (3.1.5.2). Thus, it was hypothesized that the determinants that contribute to NAI-107 resistance are characteristic of *Microbispora* sp. 107891 strain, both in production (*Microbispora* sp. 107891) and in non-production (*Microbispora* RP0) conditions.

To verify the specificity of *Microbispora* sp. 107891 resistance to NAI-107, *Microbispora* sp. 107891 and *Microbispora* JCM66 were tested against the lantibiotics 97518 and epidermin. 97518, also called planosporicin, is a NAI-107-like lantibiotic produced by a *Planomonospora* sp. (Maffioli *et al.*, 2009) and epidermin a lantibiotic produced by *S. epidermidis* (Allgaier *et al.*, 1985). Paper disks were soaked with 1 µg (NAI-107) or 5 µg (97518 and epidermin) of lantibiotics and placed on plates were $10^6$ spores of the tester strain were spread. *Microbispora* JCM66 was considerably more sensitive to 97518, as observed for NAI-107 (Fig. 17). Notably, epidermin formed the same inhibition halo on *Microbispora* sp. 107891 and *Microbispora* JCM66 plates (Fig. 17), indicating that the resistance of *Microbispora* sp. 107891 is specific to NAI-107-like lantibiotics. Epidermin was used as a negative control in successive resistance assays to exclude an influence of spore preparation on lantibiotic sensitivity.

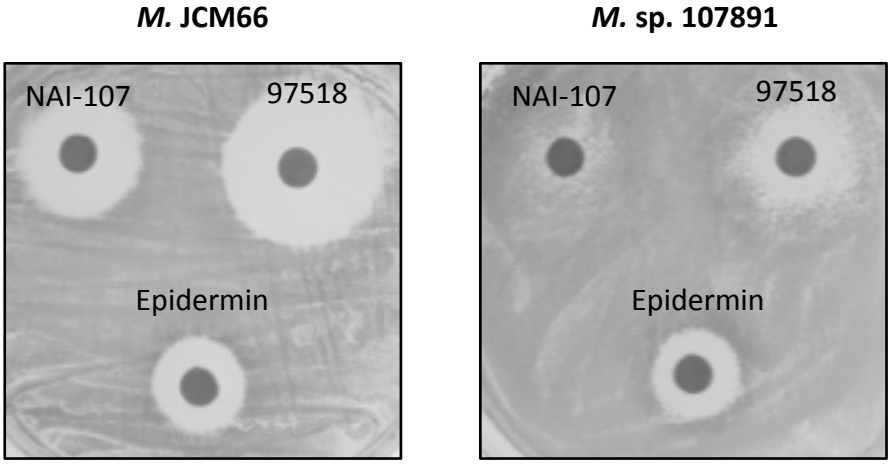


**Fig. 17. Resistance assay of *Microbispora* JCM266 and *Microbispora* sp. 107891 to the lantibiotics NAI-107, 97518 and epidermin.** Paper disks with 1 µg NAI-107, 5 µg 97518 and 5 µg epidermin.

## 3.2 Cell wall analysis of *Microbispora* sp. 107891 and of the non-producer strains *Microbispora* RP0, *Microbispora* JCM66 and *Microbispora* JCM67

### 3.2.1 Peptidoglycan analysis of *Microbispora* sp. 107891

3.2.1.1. Establishment of a protocol for peptidoglycan analysis

The lantibiotic NAI-107 interferes with the late stages of PG biosynthesis by binding the bactoprenol-pyrophosphate coupled PG precursors (Münch *et al.*, 2014). Thus, the study of lantibiotic immunity in the NAI-107 producer strain *Microbispora* sp. 107891 started with the analysis of PG in order to determine the structure of the muropeptides and possible PG modifications. PG was purified from exponentially growing bacteria (72 h) in KV6 medium (Fig. 18), as described in 2.16.1.

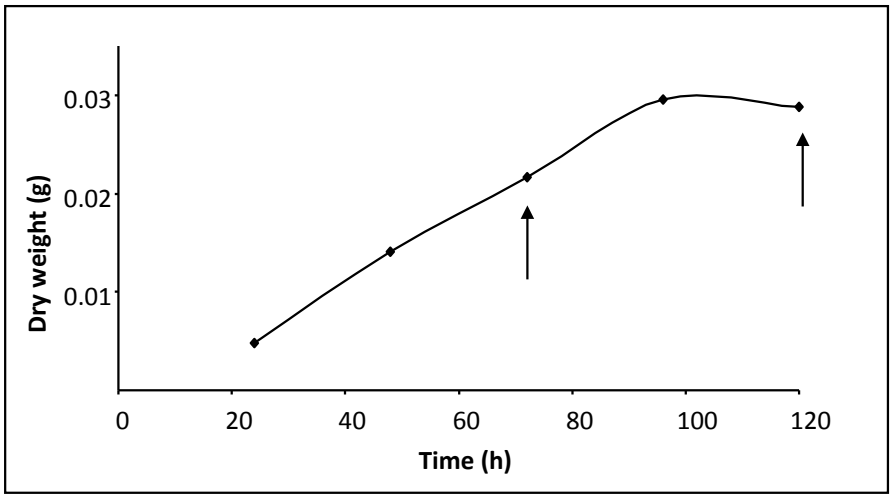


**Fig. 18. Growth of *Microbispora* sp. 107891 in KV6.** Arrows indicate the samples collected for PG isolation at 72 h and 120 h. n=1.

The muropeptides were released by PG digestion with the muramidase mutanolysin, reduced with sodium borohydride and separated by HPLC (2.16.2). HPLC is an efficient and sensitive procedure to analyse muropeptides prior to more extensive analysis by mass spectroscopy. The technique allows to determine the right conditions for PG isolation and digestion and to compare the PG of different strains or mutants. HPLC analysis of mutanolysin digested PG from *Microbispora* sp. 107891 showed a good separation of the muropeptides (Fig. 19A). The HPLC chromatogram revealed early eluting fractions (RT 12.5-30 min), probably consisting of monomeric muropeptides, and

fractions that eluted at later retention times (30-120 min), presumably multimers (Fig. 19A). *Microbispora* sp. 107891 PG was also isolated from a stationary phase culture (120 h) in KV6 medium (Fig. 18) and analysed as reported above. The HPLC profile of muropeptides at 120 h showed a huge hump at the end of the chromatogram (RT 50-120 min) (Fig. 19B), which is characteristic of samples containing undigested multimers that are not completely separated. Muropeptides were detected in the first 50 min of the HPLC chromatogram and their elution profile was comparable to the one of the muropeptides from the PG sample at 72 h. The presence of the huge hump precluded the use of the PG sample at 120 h for further analyses, therefore all PG analyses were conducted with PG isolated from exponentially growing bacteria (72 h).

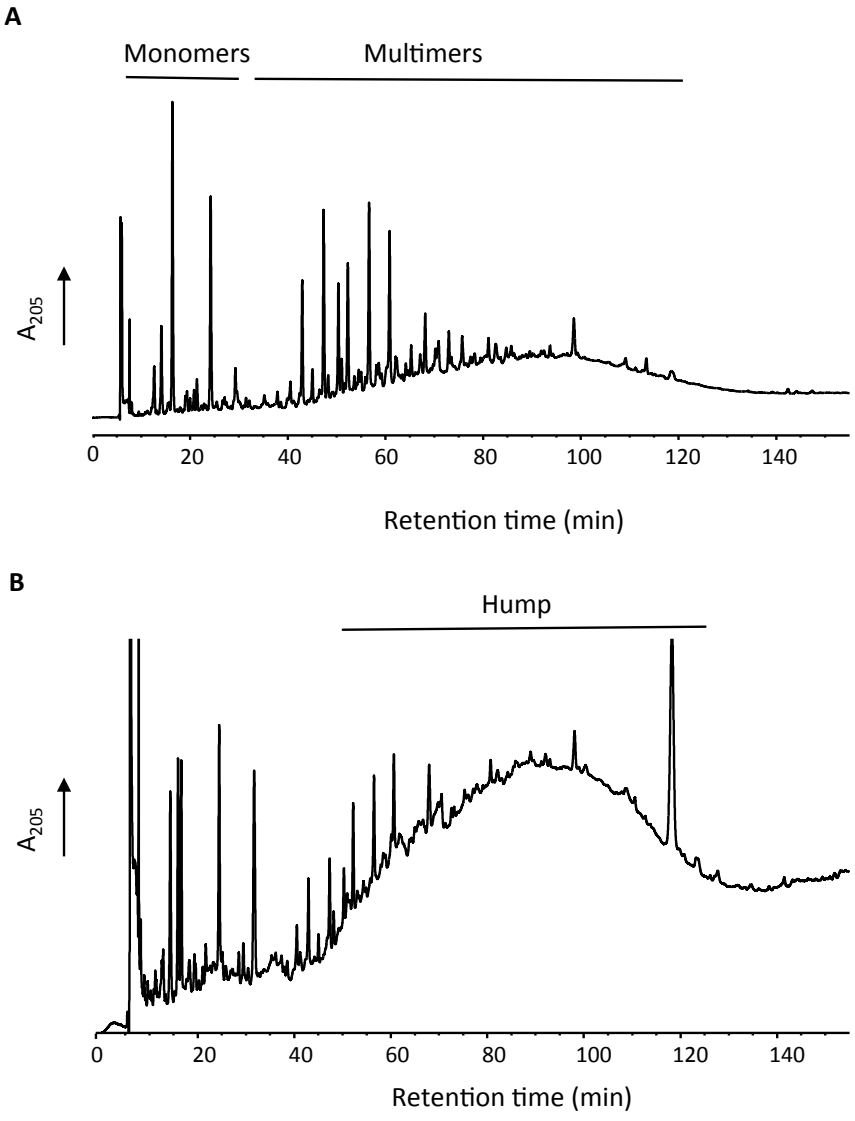


**Fig. 19. HPLC separation of the muropeptides from *Microbispora* sp. 107891.** Muropeptides from samples at (A) 72 h and (B) 120 h.

Analysis of the amino acid composition of *Microbispora* sp. 107891 PG was carried out by comparison with amino acid standard solutions. The amino acids were released from PG by acid hydrolysis and analysed by HPLC upon derivatization with the fluorescent reagent Opa (2.16.3). This procedure allowed the identification of the following amino acids: Ala, Glu, Ser, Gly and $A_2$pm (2,6-diaminopimelic acid). The amino acid configuration was deduced from the PG chemotype of *Microbispora* JCM67 (Nukajima *et al*., 1999): D- and L-Ala, D-Glu and meso-$A_2$pm. Notably, Nukajima and co-workers did not report the presence of the amino acids Gly and Ser in the PG of *Microbispora* JCM67.

3.2.1.2 Structure of the muropeptide monomers from *Microbispora* sp. 107891

Mutanolysin digested PG from *Microbispora* sp. 107891 was analysed by mass spectroscopy (LC/MS) to determine the structure of the muropeptides according to their mass. The ion chromatogram (Fig. 20A) had a similar profile to the UV chromatogram (Fig. 19A). In the conditions used in this study, few peaks of the ion chromatogram (e.g. peaks of the muropeptides 1 and 2) were not resolved as in the UV chromatogram. However, the analysis of the mass spectra of these peaks allowed the identification of the muropeptides eluting at the same time. In this way, digested PG samples were analysed directly by LC/MS, thereby allowing the detection of the muropeptides present in minor amounts. The spectra in the positive mode were characterized by *m/z* values corresponding to the protonated muropeptide $[M+H]^+$ (+1 Da), to the sodium adduct $[M+Na]^+$ (+22 Da) and to the muropeptide without the GlcNAc residue $[M\text{-}GlcNAc]^+$ (-203 Da). All these species were formed during sample ionization. The MS analysis of monomeric muropeptides showed the presence of tri- (*m/z* 870.4) **(1)**, tetra- (*m/z* 941.4) **(7)** and pentapeptides (*m/z* 1012.5) **(8)** (Fig. 20, Table 1). The structure of the pentapeptide was considered to be GlcNAc-MurNAc-L-Ala-γ-D-Glu-*meso*-$A_2$pm-D-Ala-D-Ala, according to the chemotype of *Microbispora* JCM67 (Nukajima *et al*., 1999). However, the *m/z* values of the muropeptide monomers of *Microbispora* sp. 107891 were 1 Da lower than the predicted ones. This observation suggested an amidation of the α-carboxylic group of $Glu^2$ or ε-carboxylic group of $A_2pm^3$, as previously reported for other Gram-positive bacteria (Vollmer *et al.*, 2008a). To verify this hypothesis, $MS^3$ fragmentation of monomeric pentapeptides (*m/z* 1012.4) was performed. The amidation was considered to be at $Glu^2$, as the fragments b3-$H_2O$ (*m/z* 459.4), y3 (*m/z* 333.2) and

y3-$H_2O$ (*m/z* 315.2) could be detected (5.2.1). Non-amidated muropeptides (+1 Da to the corresponding amidated muropeptides) were not observed by MS analysis. The monomeric muropeptides were therefore considered fully amidated at $Glu^2$ and the structure of the pentapeptide monomers to be GlcNAc-MurNAc-L-Ala-γ-D-iGln-*meso*-$A_2$pm-D-Ala-D-Ala.

**Table 1. Proposed structure of the muropeptides from *Microbispora* sp. 107891**

| **Muropeptides**[a] | **Proposed structure**[b] | ***m/z* [M+H]$^+$** | |
|---|---|---|---|
| | | **Observed** | **Calculated** |
| 1 | Tri | 870.4 | 870.39 |
| 2 | Tetra(Ser) | 957.5 | 957.42 |
| 3 | Tetra (Gly) | 927.4 | 927.42 |
| 4 | Penta(Ser) | 1028.5 | 1028.46 |
| 5 | Di | 698.3 | 698.31 |
| 6 | Penta(Gly) | 998.5 | 998.45 |
| 7 | Tetra(Ala) | 941.4 | 941.43 |
| 8 | Penta(Ala) | 1012.5 | 1012.47 |
| 9 | Tri-Tetra(Ser)** | 1808.9 | 1808.80 |
| 10 | Tri-Tetra(Gly)** | 1778.9 | 1778.79 |
| 11a,b* | Tetra-Tetra(Ser) and Tri-Penta(Ser)** | 1879.9 | 1879.84 |
| 12a,b* | Tetra-Tetra(Gly) and Tri-Penta(Gly)** | 1849.9 | 1849.83 |
| 13a,b* | Tetra-Tri and Tri-Tetra(Ala)** | 1792.8 | 1792.81 |
| 14a,b* | Tetra-Tetra(Ala) and Tri-Penta(Ala)** | 1863.8 | 1863.84 |

[a] Muropeptide numbers refer to Fig. 20.

[b] In branckets the amino acids in the fourth or fifth position in monomers and in the acceptor peptide in dimers. The dimers are indicated with the donor and acceptor peptides.

* muropeptides a and b have the same *m/z*

** dimers with a proposed 3-3 cross-link

**A**

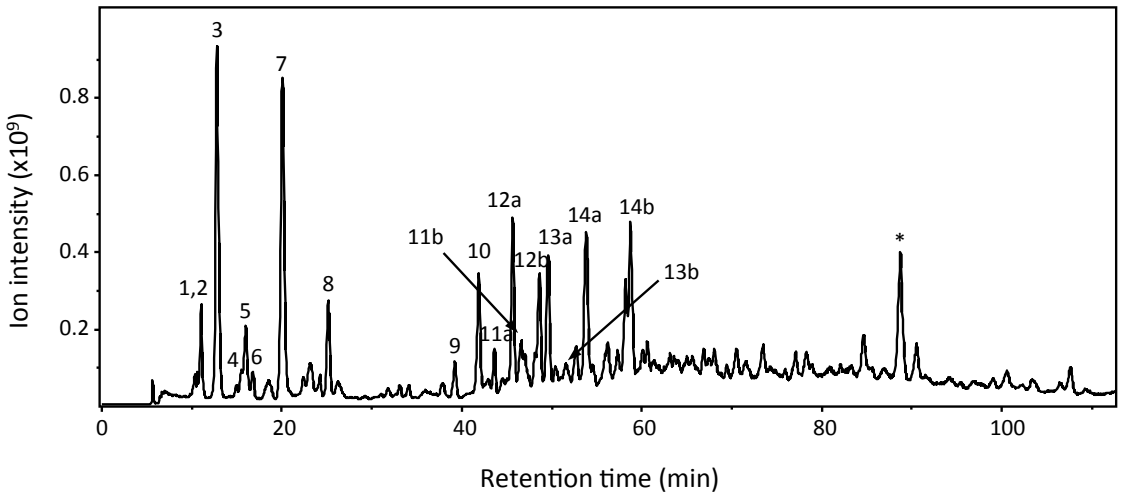
Ion intensity (x10⁹)
0.8
0.6
0.4
0.2
0
20
40
60
80
100
Retention time (min)
1,2
3
4,6
5
7
8
9
10
11a
11b
12a
12b
13a
13b
14a
14b
*

**B**

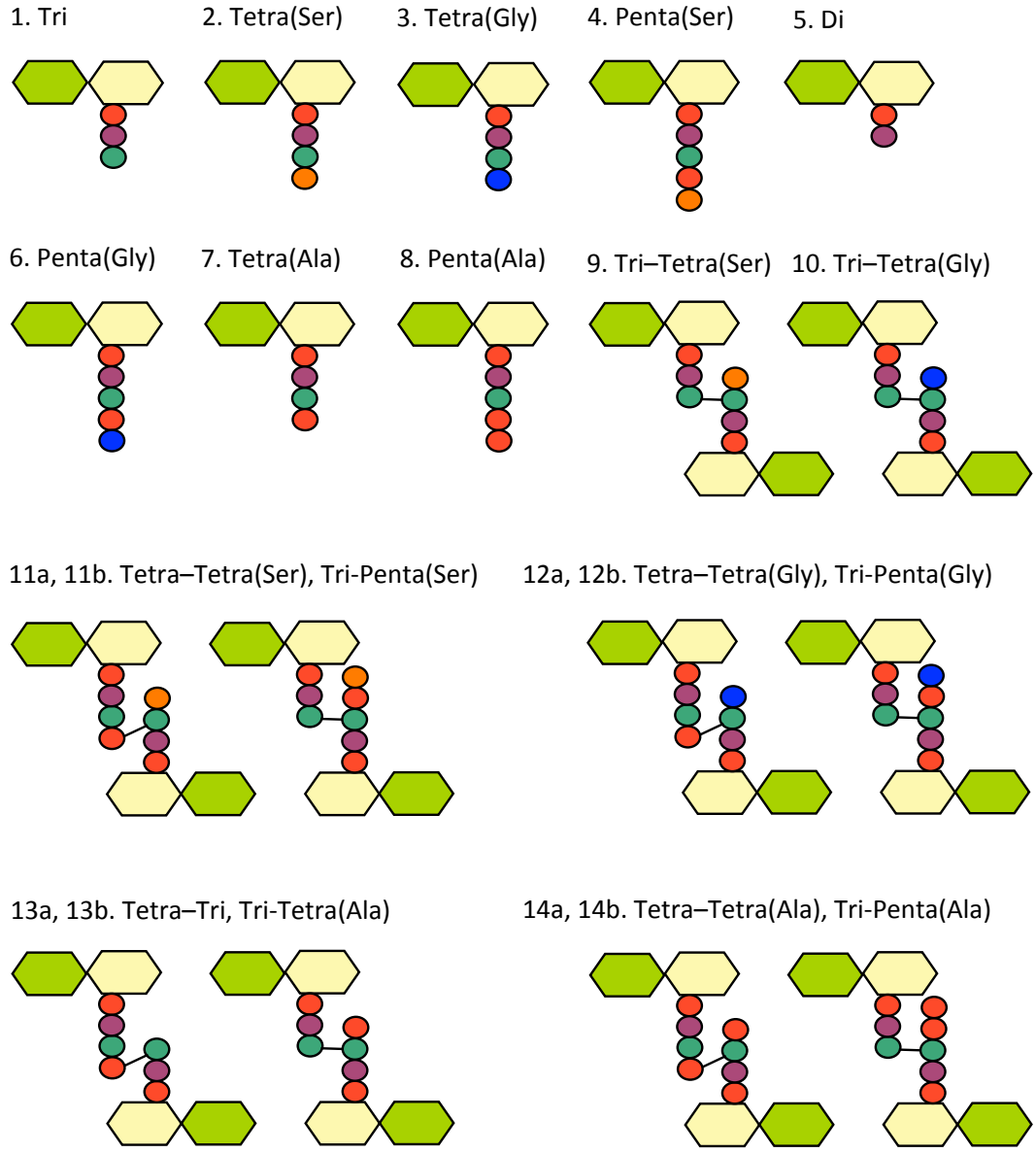
1. Tri
2. Tetra(Ser)
3. Tetra(Gly)
4. Penta(Ser)
5. Di
6. Penta(Gly)
7. Tetra(Ala)
8. Penta(Ala)
9. Tri–Tetra(Ser)
10. Tri–Tetra(Gly)
11a, 11b. Tetra–Tetra(Ser), Tri-Penta(Ser)
12a, 12b. Tetra–Tetra(Gly), Tri-Penta(Gly)
13a, 13b. Tetra–Tri, Tri-Tetra(Ala)
14a, 14b. Tetra–Tetra(Ala), Tri-Penta(Ala)

**Fig. 20. Muropeptides from *Microbispora* sp. 107891.** (A) LC/MS chromatogram of the muropeptides from *Microbispora* sp. 107891 in the positive mode. Numbers refer to Table 1. Peaks 1 and 2 overlap. Peaks a and b correspond to muropeptides with the same *m/z*. The peak indicated by a star corresponds to muropeptides monomers at *m/z* 1017.5 and 1039.5 whose structure was not determined. (B) Proposed structure of the muropeptides of *Microbispora* sp. 107891. Numbers refer to Fig. 20A and Table 1. GlucNAC (green hexagon), MurNAC (yellow hexagon), Ala (red circle), iGln (purple circle), $A_2$pm (green circle), Gly (blue circle), Ser (orange circle).

MS analysis showed that *Microbispora* sp. 107891 muropeptides possess isoglutamine (iGln) at the second position of the peptide stem, in contrast to the amino acid analysis, where only Glu residues were detected. Since the PG sample was treated with 6 N HCl to release the amino acids, iGln could have been converted to Glu by acid hydrolysis. To prove this hypothesis, a standard solution of Gln was hydrolysed in the same conditions used for the PG sample and analysed by HPLC after Opa derivatization. As expected, Gln converted to Glu upon acid hydrolysis (Fig. 21).

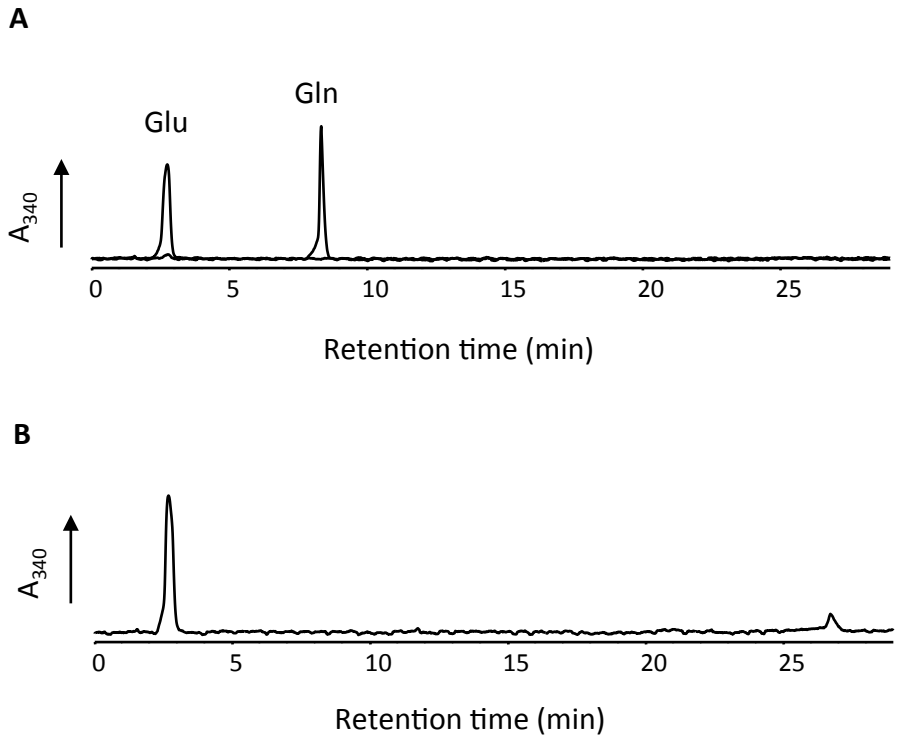


**Fig. 21. HPLC analysis of amino acids derivatized with Opa.** (A) Glu and Gln standard solutions and (B) Gln after acid hydrolysis (6 N HCl).

Since iGln was not available, Gln was used instead of iGln for this control experiment. However, similarly to Gln, iGln can be expected to be converted to Glu after acid hydrolysis. In addition to the described monomeric muropeptides, a major peak at *m/z* 927.4 **(3)** was present in the ion chromatogram (Fig. 20, Table 1). The difference in mass (14 Da) with the monomer tetrapeptide at *m/z* 941.4 **(7)** (Fig. 20, Table 1) strongly suggested a substitution of an Ala with a Gly. The presence of Gly was confirmed by amino acid analysis of the monomer tetrapeptide **3** which contained Glu, Ala and Gly in a molar ratio 1.0:0.8:1.2, calculated by defining the amount of glutamic acid as 1.0 (Fig. 22A). As a control, the monomer tetrapeptide **7** was analysed. The amino acids Glu and Ala were found in a ratio 1.0:1.7, whereas Gly was present in minor amounts (Glu:Gly 1:0.3) (Fig. 22B).

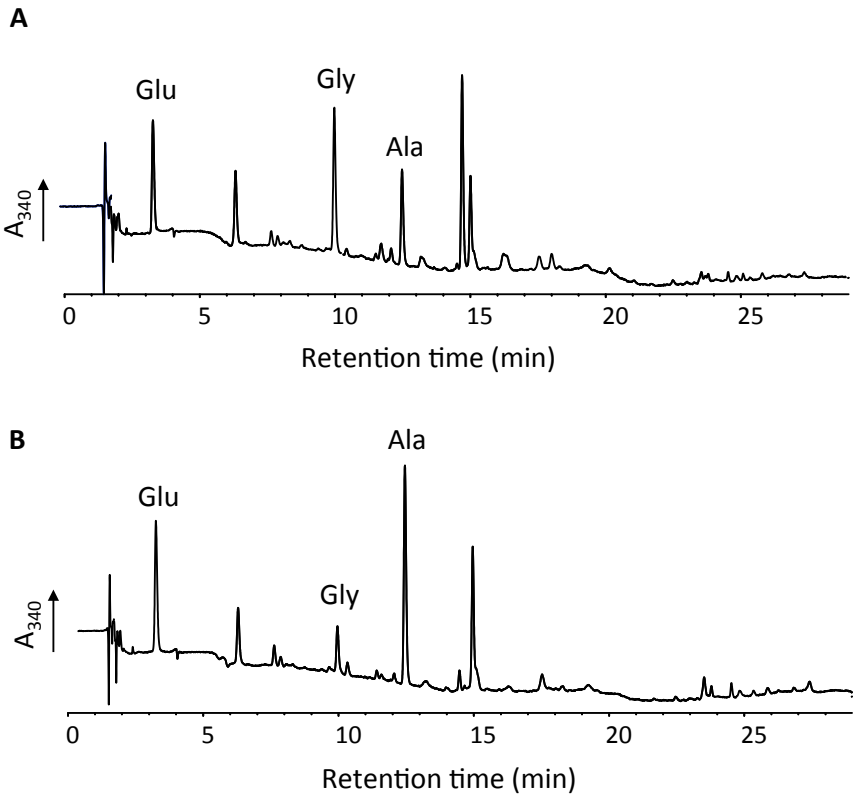


**Fig. 22. Amino acid analysis of monomer tetrapeptides**. Amino acids of the monomer tetrapeptide at (A) *m/z* 927.4 and (B) 941.4 after acid hydrolysis and Opa derivatization. Molar ratio of the amino acids (A) Glu:Ala:Gly 1:0.8:1.2, (B) Glu:Ala:Gly 1:1.7:0.3

To determine the position of Gly in the monomer tetrapeptide **3** (*m/z* 927.4), $MS^3$ fragmentation was performed. The fragmentation patterns of the monomer

tetrapeptide **3** (*m/z* 927.4) and **7** (*m/z* 941.4) revealed different C-terminal y2, y3, y4 ions (Fig. 23, 5.2.2 and 5.2.4), which suggested the presence of Gly in the fourth position of the peptide in the monomer **3** instead of D-Ala.

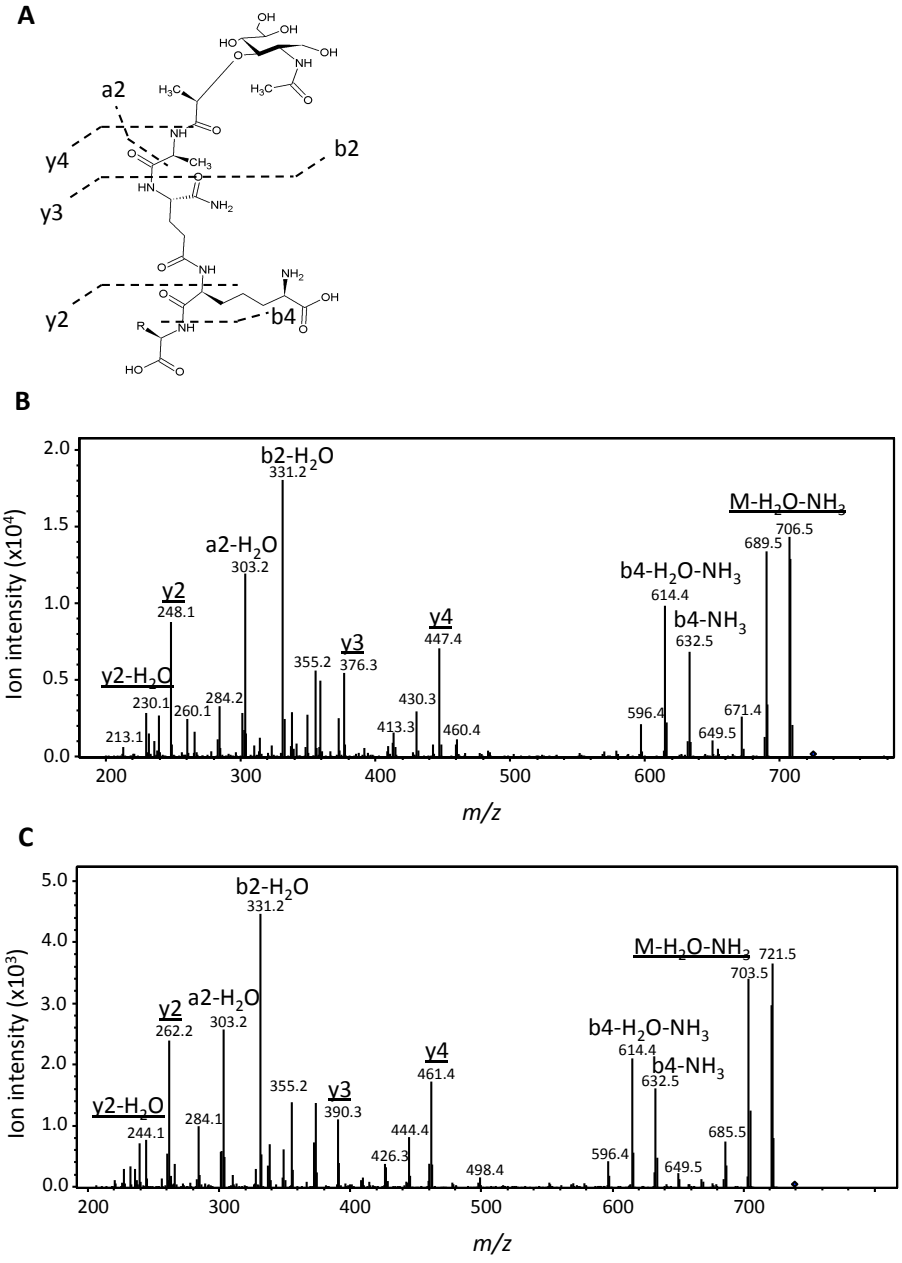


**Fig. 23. MS fragmentation analysis of the monosaccharide tetrapeptides from *Microbispora* sp. 107891.** (A) Structure and fragmentation pattern of the reduced monosaccharide tetrapeptides at *m/z* 724.5 (R:-H) and *m/z* 738.5 (R:-$CH_3$). $MS^3$ spectrum of the reduced monosaccharide tetrapeptides (B) *m/z* 724.5 (parental ion *m/z* 927.4) and (C) *m/z* 738.5 (parental ion *m/z* 941.4) in the positive mode. The different fragments between the two tetrapeptide monomers are underlined.

However, MS fragmentation analysis could not exclude the presence of a Gly branch at $A_2$pm, as reported for *S. coelicolor* (Hong *et al.*, 2005). To exclude this possibility, the PG of *S. coelicolor* was analysed and compared to *Microbispora* sp. 107891 PG. The most represented muropeptide monomers in *S. coelicolor* PG were tripeptide_Gly (*m/z* 927.6), tetrapeptide_Gly (*m/z* 998.6) and pentapeptide_Gly (*m/z* 1069.7) (Fig. 24, Table 2), according to Hugonett *et al.*, 2014. The different composition of *Microbispora* sp. 107891 muropeptide monomers suggested a *Microbispora* sp. 107891 PG structure different than the one of *S. coelicolor.* Notably, the muropeptide at *m/z* 998 was present in minor amount in *Microbispora* sp. 107891 and the one at m/z 1069 was absent. The monomer at *m/z* 941, one of the major monomers in *Microbispora* sp. 107891 PG, was present in little amount in *S. coelicolor* PG. The different composition of the muropeptide monomers and the different PG cross-link type in *Microbispora* sp. 107891 (3.2.1.3), confirmed the presence of Gly at the 4$^{th}$ position of the stem peptide instead of a branch at $A_2$pm.

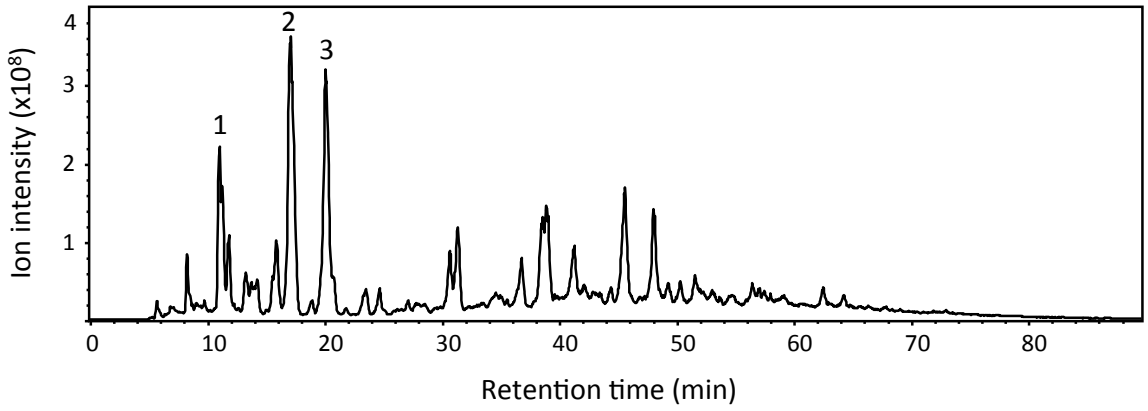


**Fig. 24. LC/MS chromatogram of the muropeptides from *S. coelicolor* in the positive mode.** Numbers refer to Table 2.

**Table 2. Structure of the more representative muropeptide monomers of *S. coelicolor***

| Muropeptides[a] | Structure[b] | *m/z* $[M+H]^+$ | |
|---|---|---|---|
| | | **Observed** | **Calculated** |
| 1 | Tri_Gly | 927.6 | 927.42 |
| 2 | Tetra_Gly | 998.6 | 998.45 |
| 3 | Penta_Gly | 1069.7 | 1069.48 |

[a] Muropeptide numbers refer to Fig. 24.

[b] Gly is linked to the side-chain amine of $A_2$pm

Tetrapeptides ending in D-Ser **(2)** (Fig. 20, Table 1) were also detected in *Microbispora* PG, though in minor amounts. Moreover, besides the pentapeptide GlcNAc-MurNAc-L-Ala-γ-D-iGln-*meso*-$A_2$pm-D-Ala-D-Ala **(8)**, pentapeptides ending in Gly **(6)** and D-Ser **(4)** were found in *Microbispora* PG (Fig. 20, Table 1). The structure of these muropeptides was proved by $MS^3$ fragmentation and annotation with mMass (5.2.3, 5.2.5 and 5.2.6).

3.2.1.3 Peptidoglycan cross-linking in *Microbispora* sp. 107891

To determine the cross-link type of *Microbispora* sp. 107891 PG, the muropeptide dimers were analysed by LC/MS. The MS spectra in the positive mode were characterized by mono- $[M+H]^+$ and di-protonated $[M+2H]^{2+}$ ions. Information about the protonation state was obtained by analysing the isotopic pattern of the ion of interest. In addition, *m/z* values corresponding to the loss of one or two GluNAc residues were detected. The structure of the dimers, which was suggested inferring to their masses, reflected the different combinations of the detected monomers. MS analysis showed the presence of muropeptide dimers with Ala (*m/z* 1792.8 and 1863.8) **(13, 14)**, Gly (*m/z* 1778.9 and 1849.9) **(10, 12)** or Ser (*m/z* 1808.9 and 1879.9) **(9, 11)** in the fourth or fifth position of the acceptor peptides (Fig. 20, Table 1). The *m/z* values suggested dimers with direct 4-3 cross-links between the carboxylic group of the donor and the amino group of the acceptor muropeptide (Table 1). However, the structure of the dimers **9** and **10** could be explained exclusively by the presence of 3-3 cross-links rather than 4-3 cross-links. Dimers with a disaccharide tripeptide as acyl donor were in fact considered to contain direct 3-3 cross-links. Moreover, the presence of two isomers (**a** and **b**) for

the muropeptides at *m/z* 1879.9, 1849.9, 1792.8 and 1863.8 (**11**, **12**, **13** and **14**) may be the result of the two cross-link types (Fig. 20, Table 1). In addition, a major peak eluting at late retention time (88.6 min) was analysed (Fig. 20A, peak indicated with a star). The corresponding spectrum showed the presence of two muropeptides at *m/z* 1017.5 and 1039.5. Surprisingly, the *m/z* values corresponded to monocharge ions, thus to muropeptide monomers with molecular masses 1016.5 and 1038.5 Da. This was in contrast to the expectations, as the characterized monomers eluted at earlier retention time. A structure for the monomers at *m/z* 1017.5 and 1039.5 could not be proposed.

### 3.2.2 UDP-linked PG precursors analysis of *Microbispora* sp. 107891

The analysis of mature peptidoglycan from *Microbispora* sp. 107891 revealed a PG structure characterized by muropeptide monomers that had different amino acids (Ala, Gly or Ser) in the fourth or fifth position of the stem peptide. To determine if the muropeptide diversity is introduced in the early- or late-stage of PG synthesis, the analysis of UDP-linked PG precursors was carried out. The PG precursors were accumulated in the cytoplasm of exponentially growing bacteria (72 h) by treatment with bacitracin (2.16.4). For the identification of UDP-linked PG precursors, ion chromatograms of the desired *m/z* values were extracted in the positive mode. MS analysis identified UDP-linked PG precursors at *m/z* 1194.4, corresponding to UDP-MurNAc pentapeptides (UDP-MurNAc-L-Ala-γ-D-Glu-*meso*-$A_2$pm-D-Ala-D-Ala) (Fig. 25, Table 3). Besides UDP-MurNAc pentapeptides, UDP-MurNAc tetrapeptides at *m/z* 1123.4 (UDP-MurNAc-L-Ala-γ-D-Glu-*meso*-$A_2$pm-D-Ala) were also detected (Fig. 25, Table 3). The structure of both PG precursors was confirmed by $MS^2$ fragmentation (5.3.1, 5.3.2). Moreover, the MS data were analysed to search for UDP-MurNAc pentapeptides and tetrapeptides ending in Gly or Ser. Extracted ion chromatograms (EIC) of the calculated *m/z* values showed the presence of UDP-MurNAc pentapeptides ending in Gly (*m/z* 1180.4) or Ser (*m/z* 1210.4) (Fig. 25, Table 3), whose structure was verified by $MS^2$ fragmentation (5.3.3 and 5.3.4). In contrast, UDP-MurNAc tetrapeptides ending in Gly (calculated *m/z* 1109.29) or Ser (calculated *m/z* 1139.30) were not detected (Fig. 25, Table 3). Moreover, MS data were analysed to determine if *Microbispora* sp. 107891 synthesises UDP-linked PG precursors with a Gly branch at $A_2$pm. No peak was found at

*m/z* 1251.5, demonstrating that *Microbispora* sp. 107891 does not produce UDP-linked PG precursors with a Gly branch, as reported for *S. coelicolor* (Hong *et al.*, 2005).

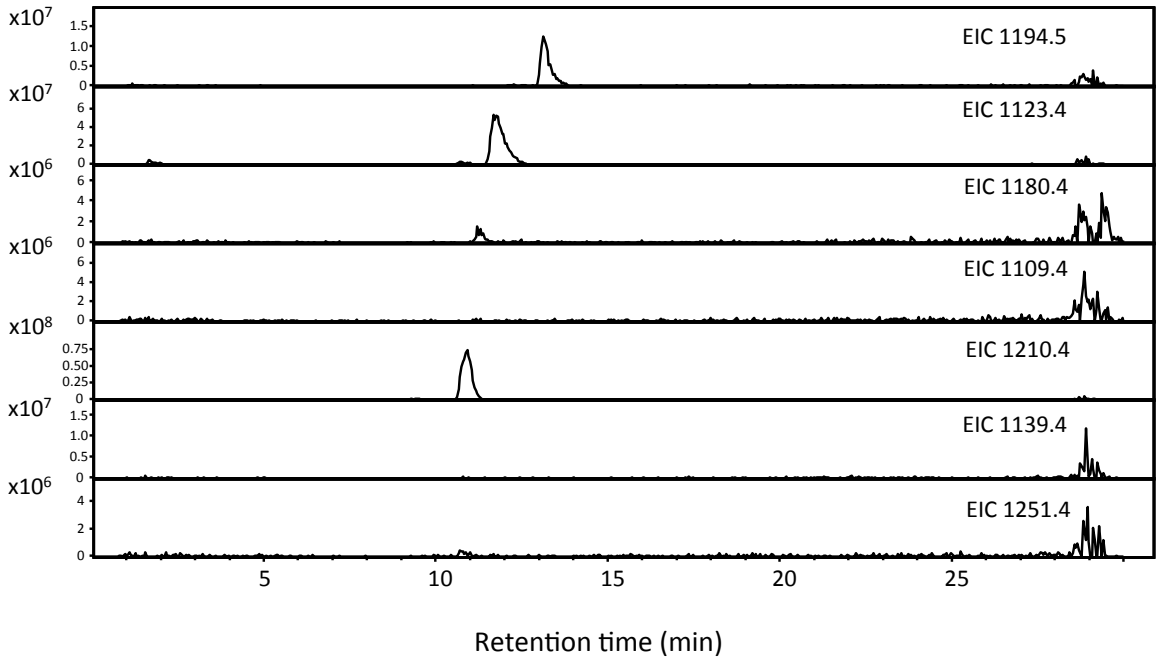


**Fig. 25. UDP-linked peptidoglycan precursor analysis of *Microbispora* sp. 107891.** Extracted ion chromatogram (EIC) in the positive mode of the peptidoglycan precursors. y-axis represents ion intensity. *m/z* values refer to Table 3. Peaks from the top: UDP-MurNAc-L-Ala-D-γ-Glu-*meso*-$A_2$pm-D-Ala-D-Ala (*m/z* 1194.4), UDP-MurNAc-L-Ala-D-γ-Glu-*meso*-$A_2$pm-D-Ala (*m/z* 1123.4), UDP-MurNAc-L-Ala-D-γ-Glu-*meso*-$A_2$pm-D-Ala-Gly (*m/z* 1180.4) and UDP-MurNAc-L-Ala-D-γ-Glu-*meso*-$A_2$pm-D-Ala-Ser (*m/z* 1210.4).

**Table 3. UDP-linked PG precursors of *Microbispora* ATCC PTA-5024**

| **Structure**[a] | ***m/z* [M+H]$^+$** | |
|---|---|---|
| | **Observed** | **Calculated** |
| UDP-MurNAc penta(Ala) | 1194.4 | 1194.34 |
| UDP-MurNAc tetra(Ala) | 1123.4 | 1123.30 |
| UDP-MurNAc penta(Gly) | 1180.4 | 1180.32 |
| UDP-MurNAc tetra(Gly) | - | 1109.29 |
| UDP-MurNAc penta(Ser) | 1210.4 | 1210.34 |
| UDP-MurNAc tetra(Ser) | - | 1139.30 |
| UDP-MurNAc penta_Gly[b] | - | 1251.36 |

[a] In brackets the amino acid at the terminal position of the peptide chain

[b] Gly is linked to the side-chain amine of $A_2$pm

Since the muropeptides containing Gly were highly represented in *Microbispora* sp. 107891 PG, KV6 medium was analysed to determine a possible accumulation of Gly during *Microbispora* sp. 107891 growth. KV6 samples were taken before the inoculum ($t_0$) and after 72 h of *Microbispora* sp. 107891 growth ($t_{72}$). The samples were treated with Opa and analysed by HPLC (2.16.3). Gly was detected in both samples at 9.7 min by comparison with a standard (Fig. 26). Accumulation of Gly was not observed in KV6 during *Microbispora* sp. 107891 growth, as the sample at $t_0$ and $t_{72}$ had Gly peaks with comparable areas (Fig. 26). The concentration of Gly was 2.8 and 2.9 mM in the samples $t_0$ and $t_{72}$, calculated by comparison with a 2.5 mM Gly standard solution.

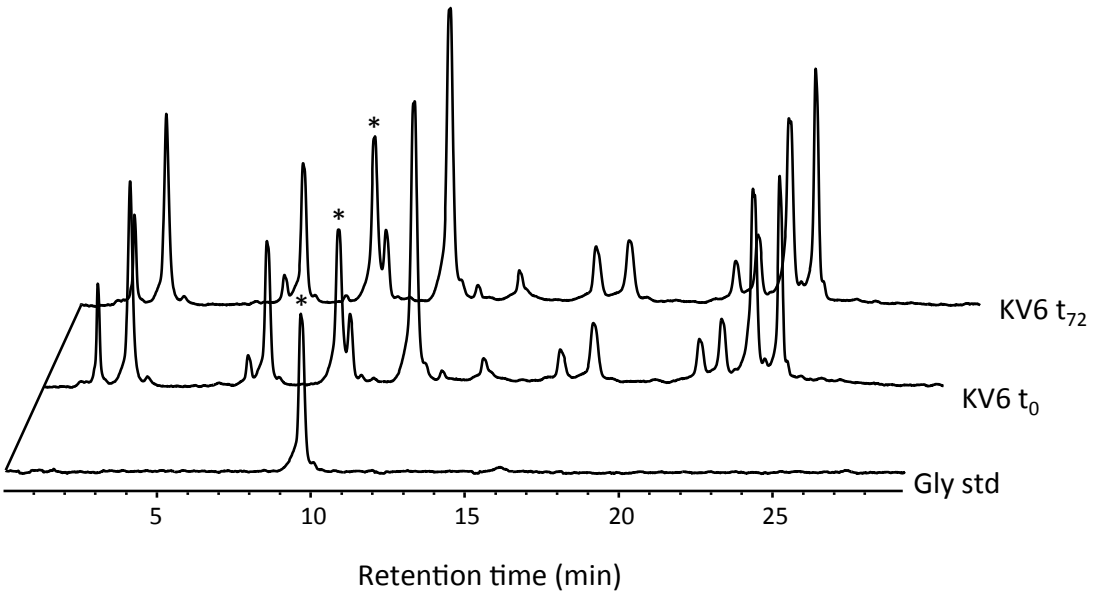


**Fig. 26. Detection of Gly in KV6 medium.** Gly in KV6 medium before inoculum ($t_0$) and after 72 h *Microbispora* sp. 107891 growth ($t_{72}$). A 2.5 mM Gly solution was used as standard. Samples were derivatized with Opa. Stars indicate Gly peaks.

### 3.2.3 Identification of a D,D-carboxypeptidase and L,D-transpeptidases in *Microbispora* sp. 107891 by bioinformatic analysis

The presence of UDP-MurNAc tetrapeptides in the cytoplasm of *Microbispora* sp. 107891 suggested the action of a D,D-carboxypeptidase for the cleavage of the D-Ala$^4$-D-Ala$^5$ peptide bond of UDP-MurNAc pentapeptides. D,D-carboxypeptidases were previously characterized in vancomycin-resistant *Enterococcus faecium* (Wright *et al.*, 1992), in the glycopeptide producers *Nonomurea* ATCC 39727 (Binda *et al.*, 2012) and *Amycolatopsis bahimycina* (Schäberle *et al*., 2011) and in *Mycobacterium tuberculosis* (Kumar *et al.*, 2012). A putative metallo-D,D-carboxypeptidase in *Microbispora* sp. 107891 was identified by BLAST analysis (ETK37916.1). The protein has a predicted transmembrane domain and two motifs (SxHxxGxAxD, ExxH), which were previously reported to be conserved motifs in VanY-like proteins (Binda *et al*., 2012). The protein has a high amino acid identity to VanY$_b$ (206 aa) from *A. balhimycina* (66% identity over 164 residues). Interestingly, the gene encoding ETK37916.1 is adjacent to two genes encoding a putative two-component regulatory system (ETK37914.1: sensor histidine

kinase, ETK37915.1: transcriptional regulator). A similar gene organization was already reported for $VanY_b$ from *A. balhimicina* (Schäberle *et al*., 2011) and DcdY from *Enterococcus faecium* (Sacco *et al.*, 2010). The activity of a D,D-carboxypeptidase is required to produce the substrate for L,D-transpeptidases (LDT) (Mainardi *et al.*, 2005). These enzymes are responsible for the formation of 3-3 cross-links between muropeptide monomers, a cross-link type also found in *Microbispora* sp. 107891 (3.2.1.3). Bioinformatic analysis was carried out to search for putative LDTs in *Microbispora* sp. 107891 genome. Blast analysis was conducted using the sequence of LDT2 from *Mycobacterium tuberculosis* (Swissprot: O53223) as a query. The analysis identified 5 putative LDTs (ETK30841.1, ETK34769.1, ETK36279.1, ETK36315.1, ETK37869.1.) that contain the catalytic domain of YkuD (Bielnicki *et al.*, 2006), including the active site cysteine residue within the invariant SHGC motif. Notably, ETK36315.1 possesses a PG binding domain and ETK30841.1, ETK34769.1, ETK36279.1, ETK37869.1 IgD-like domains that were found in a tandem repeat arrangement at the N-terminal of LDT2 from *M. tuberculosis* (LDT_IgD_like_2, NCBI CDD cd13432). The presence of genes encoding putative LDTs in *Microbispora* sp. 107891 genome indicates the potential of *Microbispora* sp. 107891 to form 3-3 cross-links besides 4-3 cross-links, as suggested from the analysis of dimeric muropeptides (3.2.1.3).

### 3.2.4 Peptidoglycan analysis of the non-producer *Microbispora* strains *Microbispora* RP0, *Microbispora* JCM66 and *Microbispora* JCM67

To determine if the PG composition of *Microbispora* sp. 107891 is linked to NAI-107 production, the PG of the non-producer strain *Microbispora* RP0 was analysed. *Microbispora* RP0 was obtained by disruption of the *mlb* cluster (3.1.4). The PG was isolated at 72 h and analysed by LC/MS. The ion chromatogram of mutanolysin digested *Microbispora* RP0 PG had a similar profile than the one of *Microbispora* sp. 107891 (Fig. 27). The muropeptides detected in *Microbispora* sp. 107891 (Table 1) were also found in *Microbispora* RP0 (Fig. 27).

The PG structure of *Microbispora* sp. 107891 was than compared to the one of *Microbispora* JCM66 and *Microbispora* JCM67, two *Microbispora* spp. that do not produce the lantibiotic NAI-107 nor any other antibacterial compound (3.1.2). PG

analysis of *Microbispora* JCM66 and *Microbispora* JCM67 by LC/MS identified the same muropeptides found in in *Microbispora* sp. 107891 PG (Fig. 28, Table 1). The MS ion chromatograms of *Microbispora* sp. 107891, *Microbispora* JCM66 and *Microbispora* JCM67 PG did not show any significant difference (Fig. 28). These results demonstrated that the muropeptide diversity found in *Microbispora* sp. 107891 is an intrinsic characteristic of *Microbispora* genus and it is not linked to lantibiotic production.

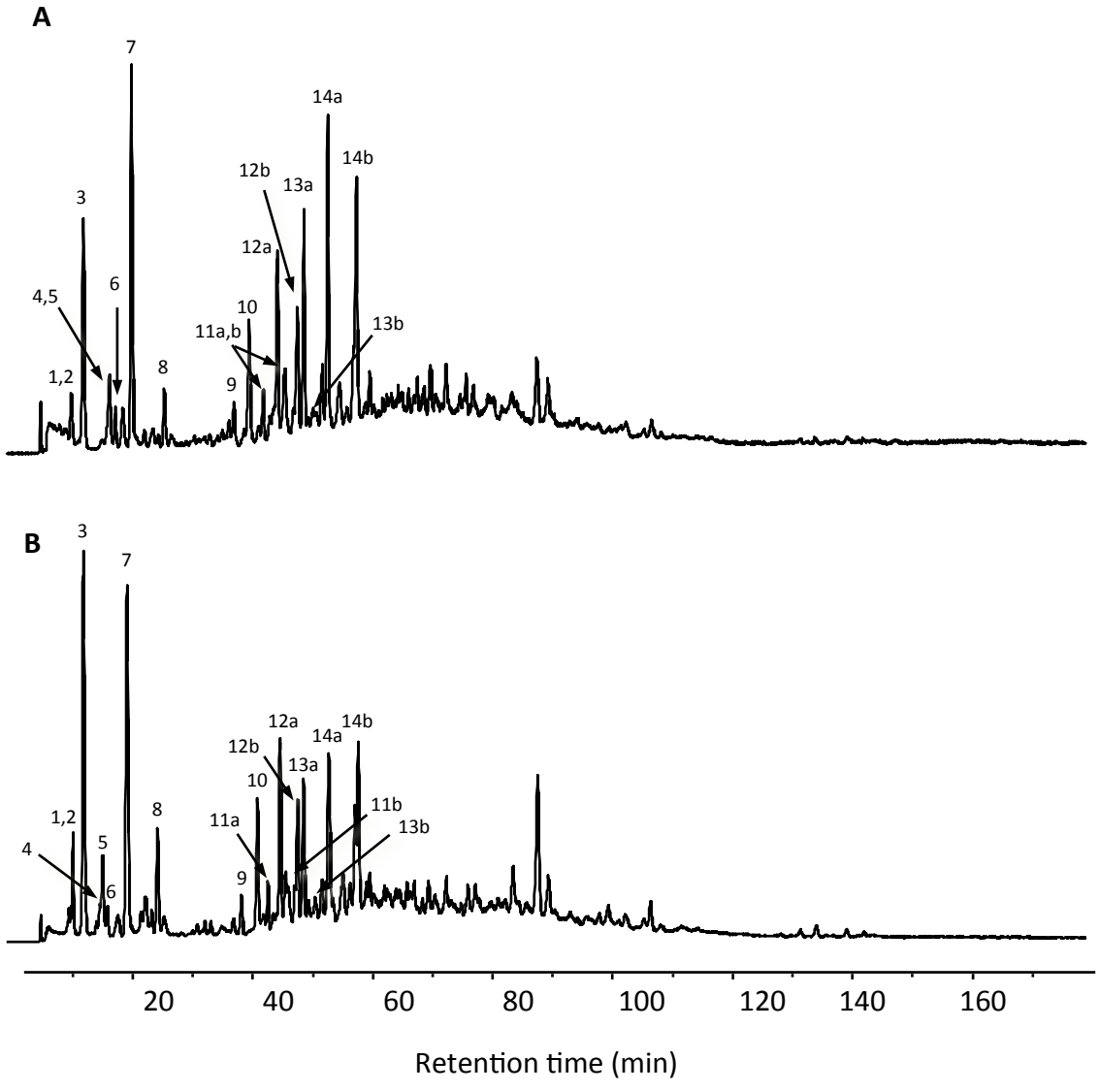


**Fig. 27. Muropeptides from *Microbispora* RP0.** LC/MS chromatogram of the muropeptides from (A) *Microbispora* RP0 and (B) *Microbispora* sp. 107891. Numbers refers to Table 1.

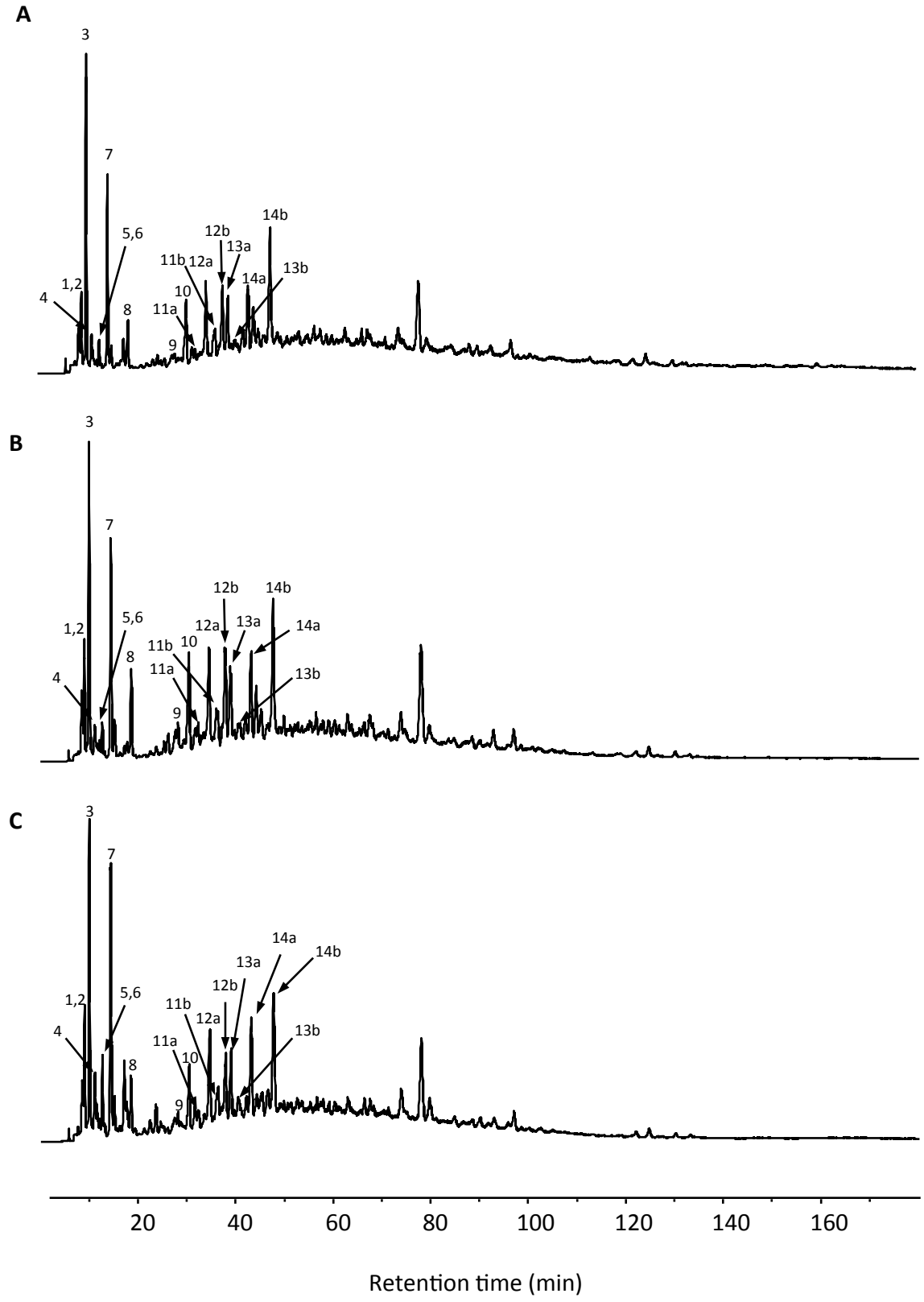


**Fig. 28. Muropepties from *Microbispora* JCM67 and *Microbispora* JCM66.** LC/MS chromatogram of the muropeptides from (A) *Microbispora* JCM67, (B) *Microbispora* JCM66 and (C) *Microbispora* sp. 107891. Numbers refers to Table 1.

### 3.2.5 Comparison of the cell wall thickness of *Microbispora* sp. 107891 and *Microbispora* RP0 by electron microscopy

The analysis of PG from *Microbispora* sp. 107891 and the non-producer *Microbispora* RP0 did not show significant difference in the composition of the muropeptides (3.2.4). One of the mechanisms reported for glycopeptide resistance is the activation of cell wall synthesis leading to an increase of cell wall thickness, as described for vancomycin-resistant *S. aureus* clinical isolates (Hanaki *et al.*, 1998). To exclude that *Microbispora* sp. 107891 and *Microbispora* RP0 differ in the cell wall ultrastructure, transmission electron microscopy (TEM) was performed. Both strains were grown on HA agar medium and after 6 days of growth, the mycelium was collected and used for sample preparation (2.17.3), which was carried out by Claudia Menzel and Iris Maldenar at the Microbiology/Organismic Interactions Department at the University of Tübingen. TEM images were obtained from longitudinal and transverse sections of mycelium (Fig. 29). The images showed an identical cell wall envelope for *Microbispora* sp. 107891 and *Microbispora* RP0, characterized by a high-density zone closer to the cytoplasmic membrane, and a more external low-density zone (Fig. 29). The two zones were suggested to be the PG and teichoic acid layer, respectively. The observation of *Microbispora* sp. 107891 and *Microbispora* RP0 TEM images did not underline any difference in the cell wall thickness (Fig. 29). To verify this, images were analysed by ImageJ. Measurements of the thickness of the high-density zone and the layer comprising both high- and low-density zone were taken. In particular, the measurement of the low-density zone was arduous, as the thickness of this layer was not uniform. For each strain, ten measurements were taken and the mean value and standard deviation calculated. Significant differences in the cell wall thickness between *Microbispora* sp. 107891 and *Microbispora* RP0 could not be detected (Table 4).

**Table 4. Thickness of *Microbispora* sp. 107891 and *Microbispora* RP0 cell wall.** The values refer to ten measurements.

| | *Microbispora* sp. 107891 | *Microbispora* RP0 |
|---|---|---|
| High-density zone | 16.0 nm ±2.0 | 13.5 nm ±1.3 |
| High- and low-density zone | 31.2 nm ±3.3 | 29.9 nm ±5.2 |

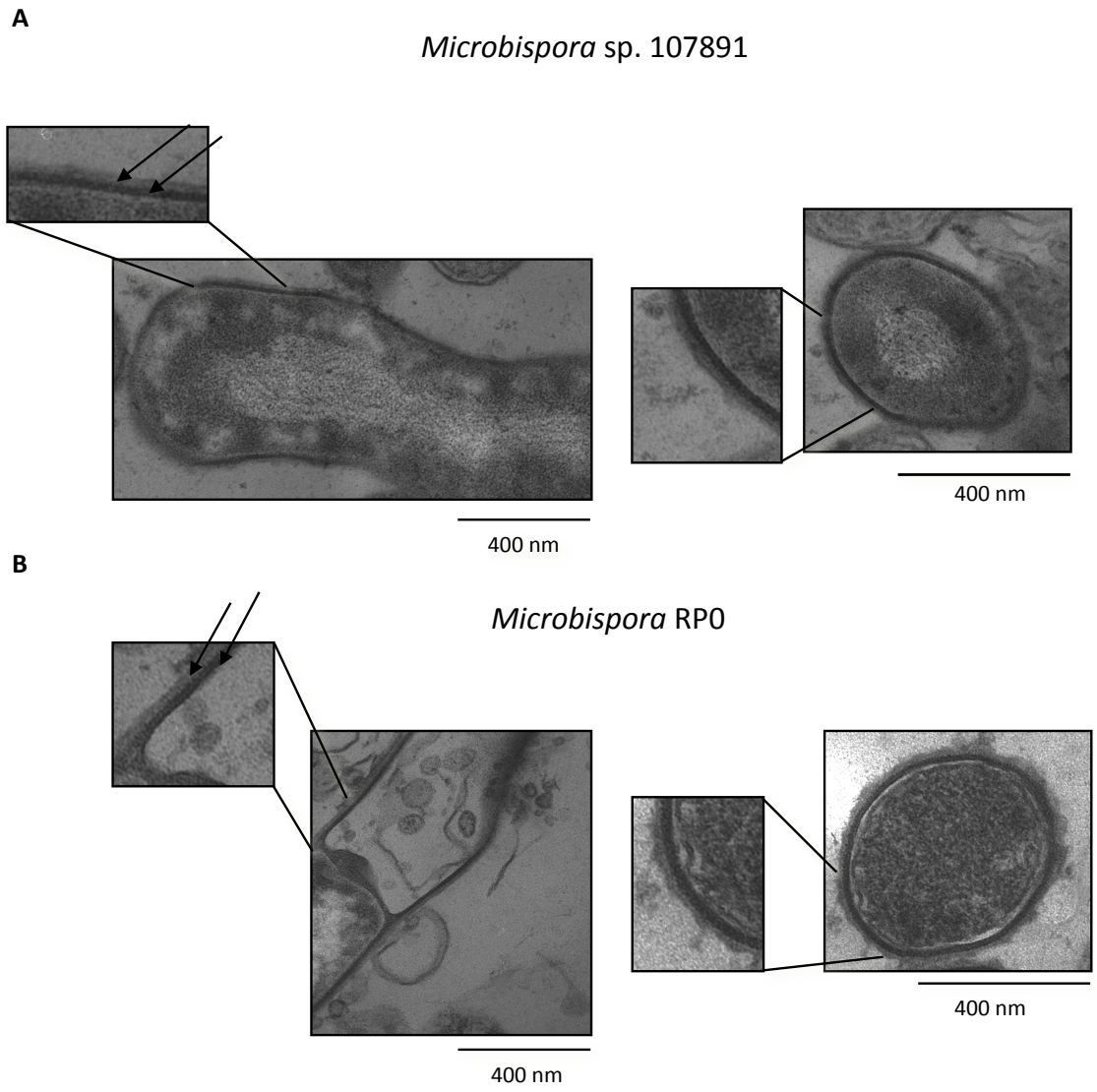


**Fig. 29. Comparison of the cell wall ultrastructure of *Microbispora* sp. 107891 and *Microbispora* RP0 by TEM.** (A) *Microbispora* sp. 107891 and (B) *Microbispora* RP0. Images of longitudinal (left) and transverse (right) sections. Arrows indicate the high- and low-dense zone.

## 3.3 Analysis of the NAI-107 immunity proteins encoded in the *mlb* cluster

The NAI-107 producer *Microbispora* sp. 107891 is about 10 times more resistant than the non-producer *Microbispora* JCM66 (3.1.5). The fact that *Microbispora* sp. 107891 and *Microbispora* JCM66 possess the same muropeptides (3.2.4) suggested that *Microbispora* sp. 107891 protects itself from NAI-107 by mechanisms that exclude target modification. Protection to lantibiotics is typically achieved by the expression of immunity proteins like lipoproteins, membrane-associated peptides, membrane proteins and ABC transporters encoded in lantibiotic biosynthetic gene clusters (Draper *et al.*, 2008; Okuda and Sonomoto, 2011). The difference in resistance between *Microbispora* sp. 107891 and *Microbispora* JCM66 was suggested to be due to the action of immunity proteins encoded in the NAI-107 gene cluster (*mlb*) (Fig. 6).

### 3.3.1 *In silico* identification of putative NAI-107 immunity proteins

BlastP analysis of the proteins encoded by the *mlb* cluster led to the identification of the putative immunity proteins MlbQ, MlbYZ, MlbTU and MlbEF.

MlbQ is a lipoprotein of 129 amino acids with a conserved lipobox motif (LAGC) (Fig. 30). The lipobox contains a cysteine (C24), which presumably becomes the N-terminal residue of the mature protein (24-129 aa) after lipidation by a lipoprotein diacylglyceryl transferase (Lgt) and cleavage of the signal peptide by a signal peptidase II (SpII). A SpII cleavage site between G23 and C24 was identified by LipoP 1.0, a tool that predicts the presence and location of lipoprotein signal peptides. The nearest MlbQ homolog is MibQ (GenBank: ADK32550.1), a protein encoded by the *mib* cluster from *M. corallina* (Foulston and Bibb, 2010), which has a single conserved amino acid substitution (N46S). BlastP analysis identified proteins of unknown function from actinomycetes spp. that have high amino acid sequence identity (62-77%) to MlbQ (YP_003654016.1 from *Thermobispora bispora* DSM 43833, WP_016906189.1 from *Streptomyces* sp., CCQ18689.1 from *Planomonospora alba*).

MTNTTRARLSGAGLLAAALL**LAGC**TGGGRADPAHRSPVPLPSPTSNKQDISEANLAYLWPLTVD
HGTIECLPSDNAVFVAPDGTTYALNDRAEKAGHPPITPIRAKGSGGGYISLGALLSTTLNLCGKG

**Fig. 30. Amino acid sequence of MlbQ.** The N-terminal signal peptide is underlined. The lipobox motif, characteristic of lipoproteins, is in bold.

MlbYZ, MlbTU, MlbEF are putative ABC transporters. The ABC transporters encoded by lantibiotic biosynthetic gene clusters were classified in SunT-, NisT- and LanFEG-type transporters according to their domain structure and phylogeny (Gebhard, 2012). SunT transporters possess an ATPase domain (also called nucleotide binding domain, NBD) fused to the permease domain and an N-terminal peptidase domain that is responsible for the processing of precursor peptides. NisT transporters are similar to the SunT-type ones but they do not contain a peptidase domain. In the LanFEG transporters, separate proteins encode the ATPase (LanF) and the permeases (LanE and LanG).

MlbYZ, MlbTU and MlbEF do not contain a N-terminal peptidase domain. In the Mlb transporters, the permease and the ATPase are encoded by two genes, in contrast to both SunT- and NisT-type transporters. Permeases are encoded by *mlbY*, *mlbU*, *mlbE*, whereas *mlbZ*, *mlbT* and *mlbF* encode ATPases. Each pair of genes seemed to be transcriptionally coupled, as the genes overlap (*mlbY-mlbZ* and *mlbT-mlbU*) or they are in close proximity (1 nt between *mlbE* and *mlbF*). LanFEG-type ABC transporters consist of two permeases (LanG and LanE) and an ATPase (LanF), which assemble to form the functional ABC transporter $F_2GE$. In the case of *Microbispora* sp. 107891, the ABC transporters encoded in the *mlb* cluster probably assemble as tetramers of two heterodimers ($Y_2Z_2$, $T_2U_2$, $E_2F_2$). This domain architecture was found in BcrAB, an ABC transporters involved in bacitracin resistance (Podlesek *et al.*, 1995). Phylogeny analysis revealed that the BcrAB-type transporters are ancestral to the LanFEG-type group (Gebhard, 2012). The permeases MlbY, MlbU, MlbE were predicted to have 6-7 membrane-spanning regions (TM) by Quick2D (Bioinformatics Toolkit, Max Planck Institute for Developmental Biology, Tübingen). Since permeases of the LanFEG-type transporters possess 6 TMs, MlbY, MlbU, MlbE were considered to have six membrane-spanning regions. The N-terminal sequence before the first predicted TM is longer in MlbU (about 60 aa) than in MlbY and MlbE (15-20 aa).

The ATPases of the Mlb transporters contain the conserved motifs Walker A, Walker B, Signature motif and H-loop (Fig. 31). MlbZ, MlbT and MlbF were checked for the presence of a Q/E-loop. While most of the ABC transporters contain a Q-loop, this loop is substituted with an E-loop (E85) in NukF of *S. warneri*. Mutagenesis analysis indicated that the E-loop is required for nukacin ISK-1 resistance but not for ATPase activity

(Okuda *et al*., 2010). Moreover, the E-loop was found to be conserved in LanF proteins (Okuda *et al*., 2010). Notably, MlbF contains an E-loop, in contrast to MlbZ and MlbT, which possess a Q-loop (Fig. 31).

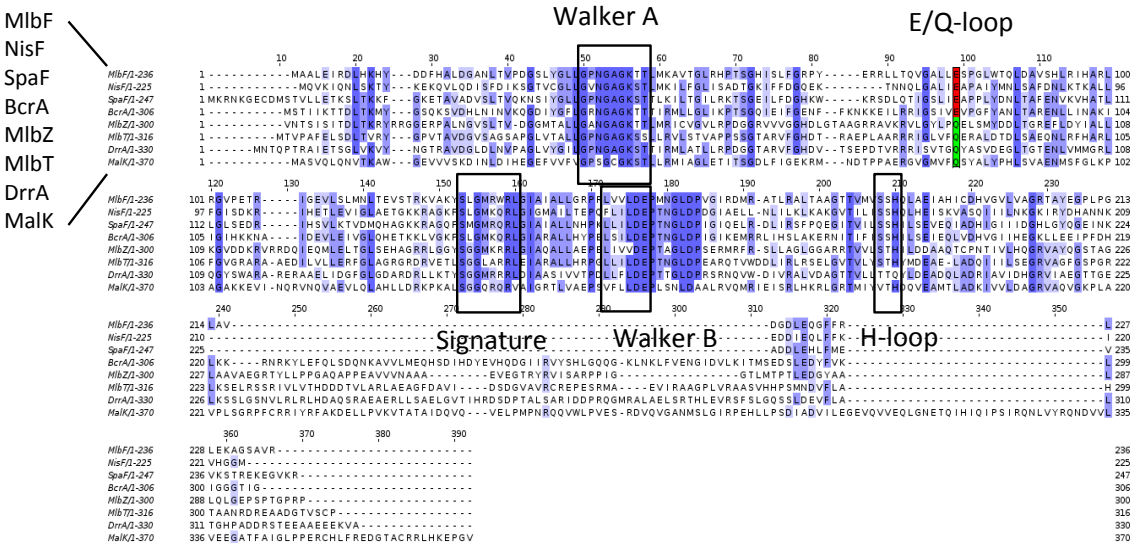


**Fig. 31. Multiple sequence alignment of NBDs (nucleotide binding domain) of the ABC transporters encoded in the *mlb* cluster (MlbZ, MlbT, MlbF) and of other ABC transporters.** The alignment was constructed using ClustalW (Chenna *et al.,* 2003), according to Okuda *et al.*, 2010. The residues involved in conserved motifs (Walker A, the Signature motif, Walker B and H-loop) are shown. The E-loop is underlined in red, the Q-loop in green. The amino acids conserved in at least four of eight sequences are underlined with degree of blue. Name of the proteins are given on the left. MlbF, MlbZ, MlbT: ATPases of the ABC transporters encoded in the *mlb* cluster. ATPases of the nisin immunity system (NisF), subtilin immunity system (SpaF), bacitracin resistance system (BcrA), daunorubicin/doxorubicin resistance system (DrrA), maltose transport system (MalK).

### 3.3.2 Expression analysis of putative NAI-107 immunity genes in *Microbispora* sp. 107891 and *Microbispora* RP0

To verify the transcription of the putative immunity genes identified *in silico*, gene expression analysis of *Microbispora* sp. 107891 was carried out. *Microbispora* sp. 107891 was grown in Evans medium and samples were collected at 8, 24 h (early-exponential growth phase), 50 h (middle-exponential growth phase), 72 h (late-exponential growth

phase) and 96 h (stationary phase). RNA was isolated as described in 2.10.1 and RNA integrity was checked by visualization of 23S and 16S ribosomal RNA bands on agarose gel (Fig. 32). DNA-free RNA samples were then retro-transcribed to cDNA (2.10.2). *Microbispora* sp. 107891 genome was screened to identify a homolog of *hrdB* from *S. coelicolor*. *hrdB* encodes the vegetative sigma factor σ70 (Shiina *et al.*, 1991) and it is commonly used as a control in RT-PCR analysis. A homolog of *hrdB* was identified in *Microbispora* sp. 107891 (ETK32198.1, 91% nucleotide identity across 749 nt) and was named $hrdB_M$. $hrdB_M$ was expressed at equal levels during growth (8-96 h), thus it was used as an internal control (Fig. 32). The expression of the genes *mlbQ*, *mlbY*, *mlbZ*, *mlbT*, *mlbU*, *mlbE*, *mlbF* was verified by PCR using primers that were designed to obtain DNA fragments of about 130-230 bp for an efficient amplification. All the analysed genes were expressed in *Microbispora* sp. 107891 already at 8 h. No significant differences in gene expression were observed during growth up to 96 h. As a control, the expression of the gene encoding the precursor peptide (*mlbA*) was verified (Fig. 32).

The non-producer strain *Microbispora* RP0 was also analysed for gene expression and compared to *Microbispora* sp. 107891. *Microbispora* RP0 was grown in Evans medium and RNA isolation was conducted as reported for *Microbispora* sp. 107891. The transcription of the *mlb* genes in *Microbispora* RP0 was detected from 8 h to 96 h (Fig. 32). The samples at 50 and 96 h had weak signals for almost all the analysed genes and for $hrdB_M$. *mlbA* was also expressed in *Microbispora* RP0 (Fig. 32), indicating that the integration of pGusA21-*mlb*AB for the disruption of the *mlb* cluster (2.12.2) did not occur in the DNA fragment amplified by RT-PCR. Overall, the putative immunity genes *mlbQ*, *mlbY*, *mlbZ*, *mlbT*, *mlbU*, *mlbE*, *mlbF* were expressed in *Microbispora* RP0 as in *Microbispora* sp. 107891. This result indicated that NAI-107 production does not impact the transcription of the analysed genes.

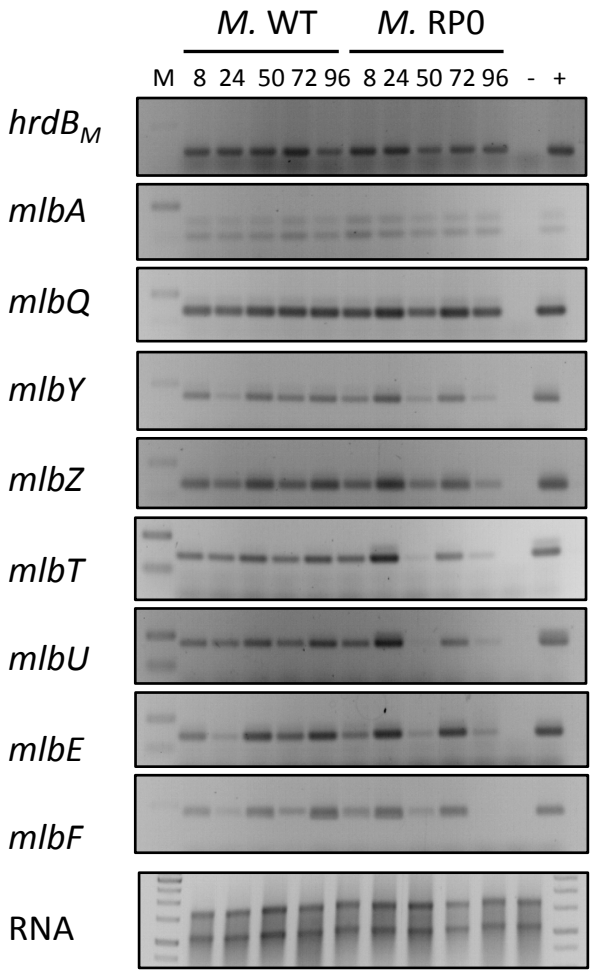


**Fig. 32. Expression analysis of *mlbA*, *mlbQ*, *mlbY*, *mlbZ*, *mlbT*, *mlbU*, *mlbE* and *mlbF* in *Microbispora* sp. 107891 (*M.* WT) and *Microbispora* RP0 (*M.* RP0).** $hrdB_M$ was used as internal control, $H_2O$ as a negative control (-) and genomic DNA from *Microbispora* sp. 107891 as positive control (+). Marker (M): 100 and 250 bp (Easy ladder I). The 1 kb DNA ladder was used for RNA samples (lower band: 16S rRNA, upper band: 23S rRNA). Size of the PCR products in bp: $hrdB_M$ 131, *mlbA* 115 (first band from the bottom), *mlbQ* 163, *mlbY* 198, *mlbZ* 155, *mlbT* 161, *mlbU* 215, *mlbE* 161, *mlbF* 230.

### 3.3.3 Overexpression of putative NAI-107 immunity genes in *Microbispora* sp. 107891

The genes encoding MlbQ, MlbYZ, MlbTU and MlbEF were overexpressed in *Microbispora* sp. 107891 in order to verify the effect on NAI-107 resistance and production. ABC transporters encoded by lantibiotic gene clusters can be involved either in lantibiotic secretion or immunity (Sonomoto and Okuda, 2011; Gebhard, 2012). Thus, overexpression of the ABC transporters in *Microbispora* sp. 107891 could directly or indirectly lead to an increase in lantibiotic production, by increasing the export of the lantibiotic to the extracellular space or by conferring a higher resistance to the producer strain, respectively. Here, the integrative plasmid pRM4 containing the constitutive promoter *ermE**p was chosen for gene overexpression in *Microbispora* sp. 107891.

#### 3.3.3.1 Verification of the functionality of the *ermE** promoter in *Microbispora* sp. 107891

The promoter of *ermE*, a gene encoding a 23S RNA methylase from the erythromycin-producing strain *Saccharopolyspora erythraea*, was firstly described 30 years ago (Bibb *et al.*, 1985). Its upregulated variant *ermE**p is still widely used for strong constitutive gene expression in *Streptomyces* and related bacteria (Schmitt-John and Engels, 1992; Kieser *et al.*, 2000). For gene overexpression in *Microbispora* sp. 107891, the integrative plasmid pRM4 containing the *ermE** promoter was chosen. To verify *ermE**p functionality in *Microbispora* sp. 107891, expression of the reporter gene *egfp* was checked. The plasmid pRM4.3, containing *egfp* under the control of the *ermE**p was transferred into *Microbispora* sp. 107891 yielding *Microbispora egfp* (3.1.3). *Microbispora egfp* was grown in GE82G for 4 days and *egfp* expression was checked by fluorescence microscopy (2.17.2). The fluorescence of *Microbispora egfp* was intense, suggesting a strong expression of the fluorescence protein eGFP. To confirm the result, two clones of *Microbispora egfp* were compared to *Microbispora* sp. 107891 by measuring the eGFP fluorescence with a POLARstar Galaxy microplates reader ($\lambda_{ex}/\lambda_{em}$: 485/520 nm). The fluorescence signals of *Microbispora egfp* clones were about 150 and 200 times higher than for *Microbispora* sp. 107891. Hence, the promoter *ermE**p was considered functional in *Microbispora* sp. 107891 and was chosen for gene overexpression.

3.3.3.2 Growth and NAI-107 production of the overexpression *Microbispora* strains

To overexpress *mlbQ*, *mlbYZ*, *mlbTU* and *mlbEF* in *Microbispora* sp. 107891, the genes were amplified with primers harbouring a 5' NdeI site and 3' EcoRI site (2.6) and cloned into pRM4 (2.12.1). The obtained plasmids pRM4-*mlbQ*, pRM4-*mlbYZ*, pRM4-*mlbTU* and pRM4-*mlbEF* were introduced in *Microbispora* sp. 107891 by conjugation (2.11.3) and the corresponding recombinant strains (*Microbispora mlbQ*$^+$, *Microbispora mlbYZ*$^+$, *Microbispora mlbTU*$^+$, *Microbispora mlbEF*$^+$) were confirmed by PCR using the primers ErmEXgeneFP, ErmEXgeneRP (2.6). The overexpression strains were then characterised concerning NAI-107 resistance and production. To perform resistance assays using spores (2.14.1), the overexpression strains were checked for sporulation. Unfortunately, spores could not be obtained for these strains, as they sporulate even more poorly than the WT. Resistance assays using mycelium were attempted but reproducible results could not be obtained. However, significant differences between the WT and the recombinant strains overexpressing one of the ABC transporters were not detected (data not shown).

Growth and NAI-107 production was verified in Evans medium (2.7.4, 2.13.1) as reported for *Microbispora* sp. 107891 (3.1.1.2). After two pre-cultures in GE82B, *Microbispora* overexpression strains were inoculated in 100 ml Evans medium in triplicate and samples were collected at 8, 24, 48, 72, 96, 120, 144, 168 h for dry weight determination. The overexpression strains did not significantly differ from the WT in growth (Fig. 33). Moreover, bioassays against *M. luteus* were performed with the supernatants collected at 120 h (volume adjusted to the dry weight of the WT). No significant differences were observed in the inhibition halos, indicating that NAI-107 production in the overexpression strains is comparable to the WT (Fig. 33). Overall, *Microbispora mlbQ*$^+$, *Microbispora mlbYZ*$^+$, *Microbispora mlbTU*$^+$ and *Microbispora mlbEF*$^+$ did not show a different phenotype than *Microbispora* sp. 107891.

**A**

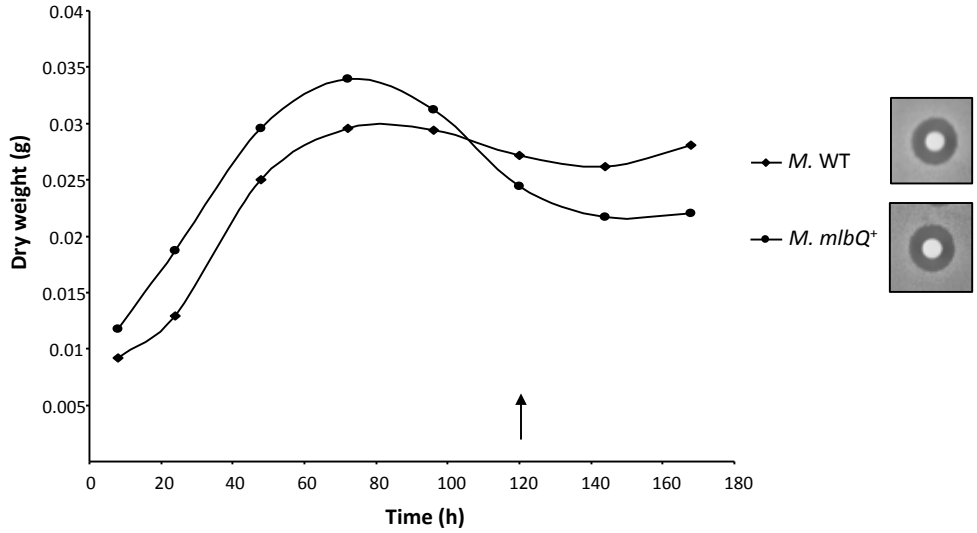
0.04
0.035
0.03
0.025
0.02
0.015
0.01
0.005
Dry weight (g)
0
20
40
60
80
100
120
140
160
180
Time (h)
M. WT
M. mlbQ+

**B**

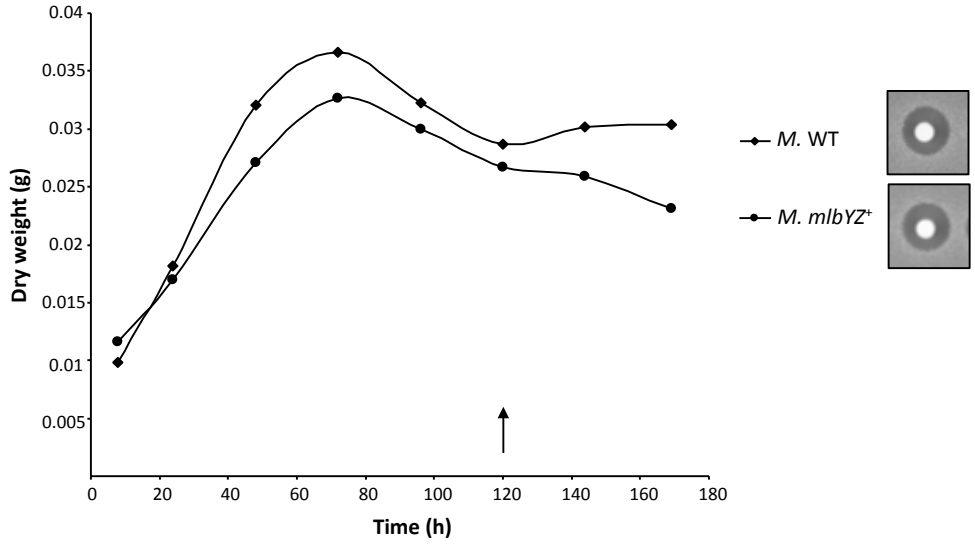
0.04
0.035
0.03
0.025
0.02
0.015
0.01
0.005
Dry weight (g)
0
20
40
60
80
100
120
140
160
180
Time (h)
M. WT
M. mlbYZ+

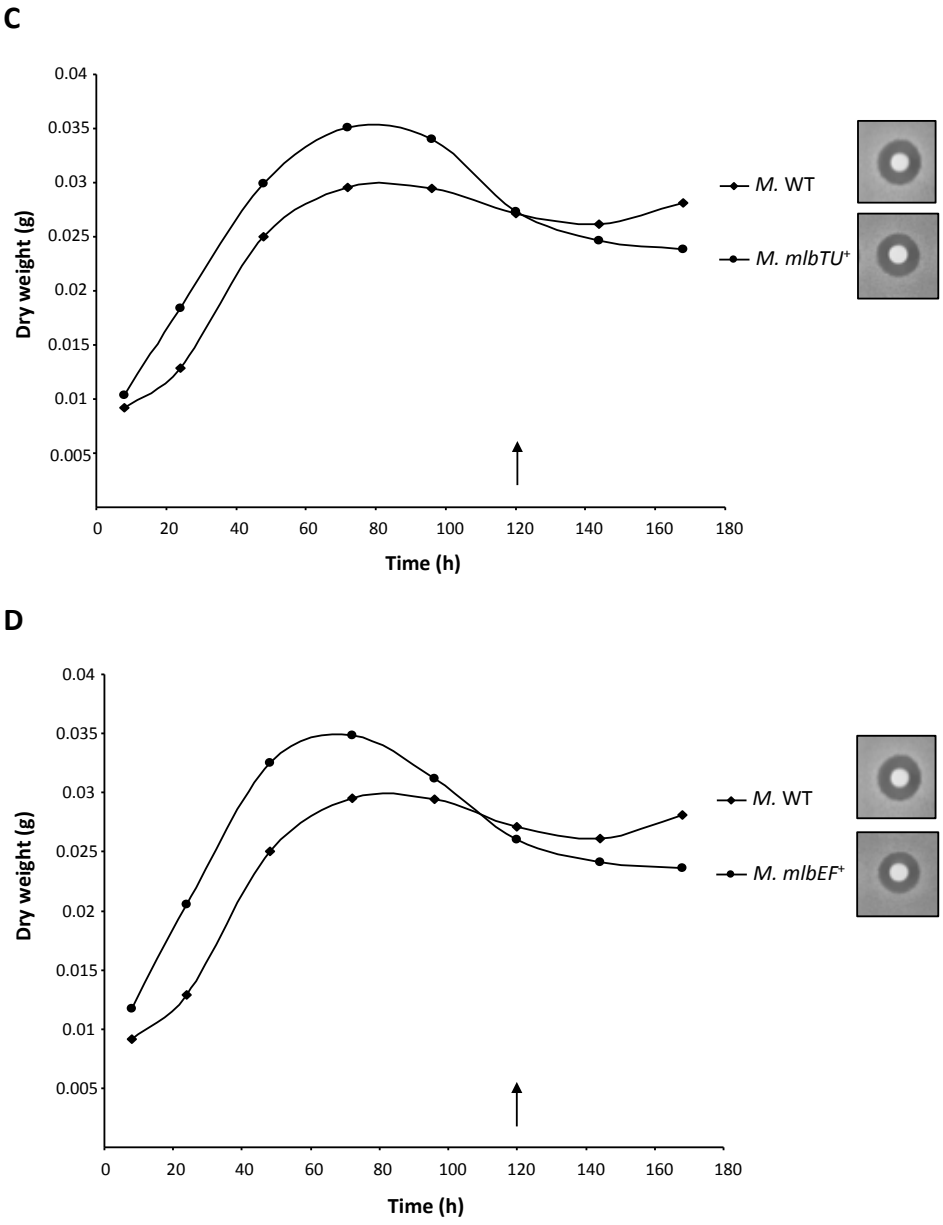


**Fig. 33. Growth and NAI-107 production of *Microbispora* sp. 107891 overexpression strains.** *Microbispora* sp. 107891 (*M.* WT) (diamond) and the overexpression strains (A) *M. mlbQ*$^{+}$, (B) *M. mlbYZ*$^{+}$, (C) *M. mlbTU*$^{+}$ and (D) *M. mlbEF*$^{+}$ (circle). *M. mlbQ*$^{+}$*, M. mlbTU*$^{+}$ and *M. mlbEF*$^{+}$ were grown in parallel and were compared to *M.* WT. Samples for the bioassay were taken at 120 h (arrow). The y-axis represents the dry weight of 5-ml samples. n=1, three technical replicates, except for *M. mlbEF*$^{+}$ (two technical replicates).

### 3.3.4 Heterologous expression of putative NAI-107 immunity genes in *S. coelicolor*

To assess the role of MlbQ, MlbYZ, MlbTU and MlbEF in NAI-107 resistance, the corresponding genes were heterologously expressed in *S. coelicolor*. The plasmids pRM4-*mlbQ*, pRM4-*mlbYZ*, pRM4-*mlbTU* and pRM4-*mlbEF,* which were introduced into *Microbispora* sp. 107891 to obtain overexpression strains (3.3.3.2), were used for heterologous expression in *S. coelicolor. S. coelicolor* recombinant strains were checked by PCR with the primers ErmEXgeneFP, ErmEXgeneRP (2.6) and spores were collected (2.7.2). For each recombinant strain, two independent clones were analysed by lantibiotic resistance assay (2.14.2). The figures reported below show one representative clone. *S. coelicolor* carrying the empty plasmid pRM4 was used as a negative control. *S. coelicolor* expressing the lipoprotein MlbQ was more resistant to NAI-107 than the WT (Fig. 34A). Notably, the plates were prepared with a low NAI-107 gradient (0-4 µg/ml) to detect an effect of MlbQ on NAI-107 resistance. This is in accordance with the low resistance of *Microbispora* sp. 107891 to NAI-107 (3.1.5.1). In contrast to MlbQ, none of the ABC transporters encoded in the *mlb* cluster (MlbYZ, MlbTU, MlbEF) conferred NAI-107 protection to *S. coelicolor* (Fig. 34B). The recombinant strains expressing the ABC transporters were plated onto plates with a low NAI-107 gradient (0-2 µg/ml) to exclude the possibility of a minimal effect on NAI-107 resistance. However, no effect was observed. The heterologous expression of the *mlb* genes in *S. coelicolor* revealed that the *mlb* cluster encodes at least one immunity protein, namely the lipoprotein MlbQ.

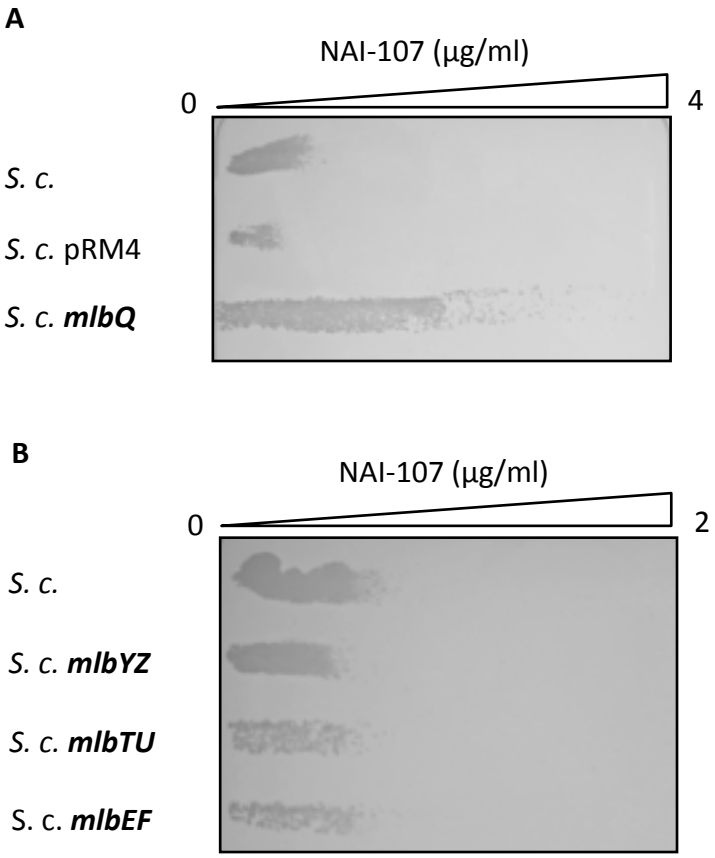


**Fig. 34. Resistance of *S. coelicolor* (*S.c.*) recombinant strains expressing the lipoprotein- and the ABC-transporter-genes to NAI-107.** (A) *S. coelicolor* WT, containing the empty vector pRM4 and expressing *mlbQ.* (B) *S. coelicolor* WT and expressing *mlbYZ*, *mlbTU* or *mlbEF*. NAI-107 gradient plates (0-4, 0-2 µg/ml).

### 3.3.5 Heterologous expression of *mlbQ* and *mlbEF* in *Microbispora* JCM66

To further analyse the effect of MlbQ, MlbYZ, MlbTU and MlbEF on NAI-107 immunity, heterologous expression was carried out in *Microbispora* JCM66 (3.1.2), a heterologous host closely related to *Microbispora* sp. 107891. *Microbispora* JCM66 was manipulated as reported for *Microbispora* sp. 107891 (2.11.3). The introduction of the plasmid pRM4-*mlbQ* and pRM4-*mlbEF* was successful and was confirmed by PCR using the primers ErmEXgeneFP, ErmEXgeneRP (2.6). Spores were isolated from the corresponding recombinant strains *Microbispora* JCM *mlbQ* and *Microbispora* JCM *mlbEF* and lantibiotic resistance assays were performed using paper disks soaked with 0.5 µg NAI-107 (2.14.1). The recombinant strains were compared to the WT. *Microbispora* JCM

*mlbQ* was considerably more resistant than the WT to NAI-107 (Fig. 35A). The MlbQ effect on NAI-107 resistance was even clearer than in the heterologous host *S. coelicolor* (3.3.4). In contrast, expression of *mlbEF* did not show any effect on NAI-107 resistance (Fig. 35B).

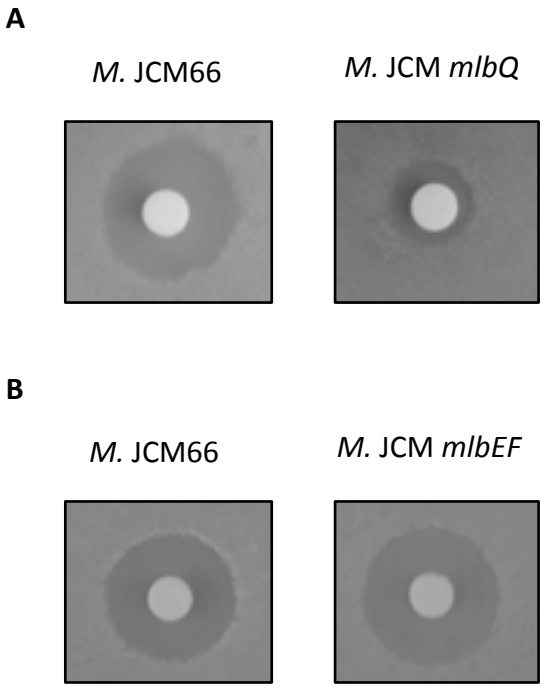


**Fig. 35. Resistance of *Microbispora* JCM66 WT and expressing (A) *mlbQ* and (B) *mlbEF* to NAI-107.** Paper disks with 0.5 µg NAI-107.

### 3.3.6 Analysis of the cooperativity between NAI-107 immunity proteins

Several ABC transporters of antimicrobial peptides (AMPs) are functional in association with accessory proteins whose mechanism of action is mostly unknown (Gebhard, 2012). To determine whether any of the ABC transporters in the *mlb* cluster is involved in resistance by acting in cooperation with other proteins, co-expression studies were performed. MlbYZ, MlbTU, MlbEF were co-expressed in the heterologous host *S. coelicolor* either with the lipoprotein MlbQ (3.3.6.1) or the transmembrane protein MlbJ (3.3.6.2).

3.3.6.1 Co-expression of *mlbQ* with the ABC transporters *mlbYZ*, *mlbTU* and *mlbEF* in *S. coelicolor*

MlbYZ, MlbTU, MlbEF were co-expressed with the lipoprotein MlbQ in the heterologous host *S. coelicolor*. For co-expression studies, the integrative plasmid pIJ10257 was chosen, as it contains an *attP* site (*attP* site of the phage ΦBT1) and an antibiotic resistant cassette ($hyg^R$) different from pRM4. *mlbQ* was amplified with the primers mlbQfor1 and mlbQrev2 (2.6) and cloned into pIJ10257 under the control of the constitutive promoter *ermE**p. The resulting plasmid pIJ10257-*mlbQ* was transferred by conjugation (2.11.2) to *S. coelicolor* harbouring one of the recombinant plasmids pRM4-*mlbYZ*, pRM4-*mlbTU* and pRM4-*mlbEF* ($apra^R$) (3.3.4), respectively. The *S. coelicolor* recombinant strains were proved by PCR using the primers Hygrofor and Hygrorev (2.6). For the determination of a possible cooperative effect of the expressed proteins, the recombinant strains were tested against NAI-107 using gradient plates (0-2 µg/ml NAI-107) (2.14.2). To distinguish the cooperative effect of an ABC transporter with MlbQ from the protective effect of MlbQ alone (3.3.4), *S. coelicolor* carrying the plasmid pIJ10257-*mlbQ* (*S. coelicolor* pIJ*mlbQ*) was used as a control. The NAI-107 resistance assay did not show any cooperative effect of the tested ABC transporters with the lipoprotein MlbQ (Fig. 36). Notably, the strains co-expressing one of the ABC transporter and MlbQ were resistant to NAI-107 as the control strain *S. coelicolor* pIJ*mlbQ*, with exception of *S. coelicolor mlbYZ-mlbQ* which was not as resistant as *S. coelicolor* pIJ*mlbQ* (Fig. 36). The resistance assays against NAI-107 showed that MlbYZ, MlbTU and MlbEF do not work in cooperation with MlbQ. Since the immunity effect of MlbQ did not increase by co-expressing any of the Mlb transporters, an MlbQ-mode of action independent from the ABC transporters MlbYZ, MlbTU and MlbEF was assumed (3.4).

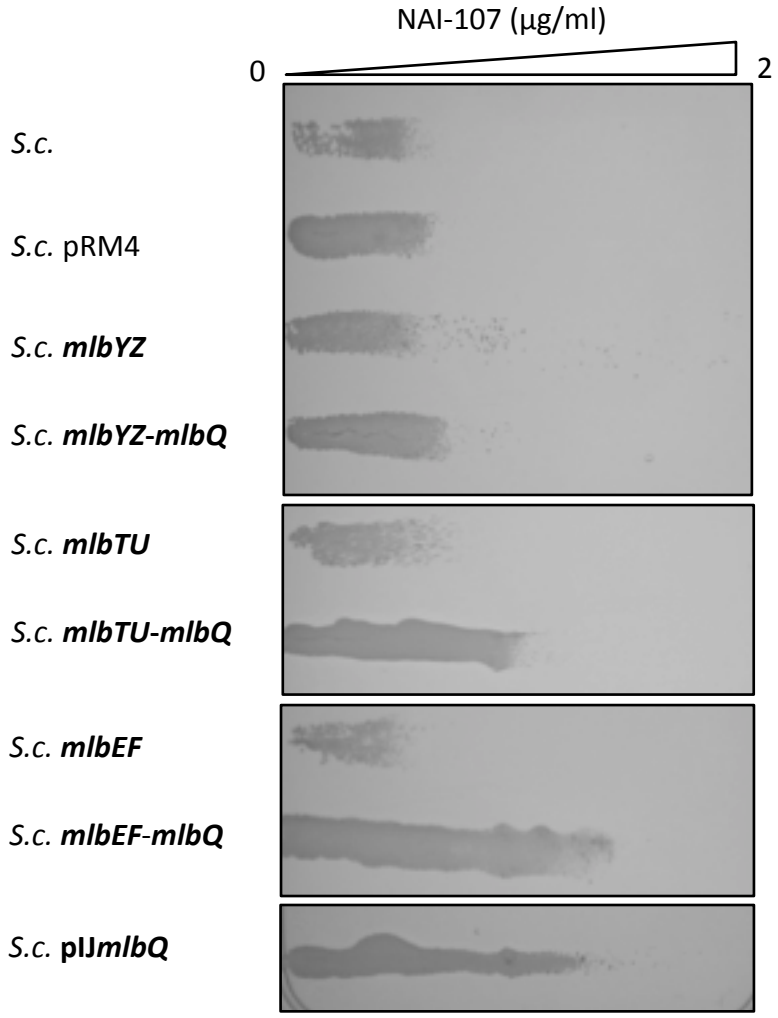


**Fig. 36. Resistance of *S. coelicolor* (*S.c.*) recombinant strains co-expressing *mlbQ* and the ABC-transporter-genes to NAI-107.** *S. coelicolor* WT, containing the empty vector pRM4, expressing *mlbYZ*, *mlbYZ* and *mlbQ*, *mlbTU*, *mlbTU* and *mlbQ*, *mlbEF*, *mlbEF* and *mlbQ*. *S.c.* carrying the plasmid pIJ10257-*mlbQ* (*S.c.* pIJ*mlbQ*) was used as control. NAI-107 gradient plates (0-2 µg/ml).

### 3.3.6.2 Co-expression of *mlbJ* with the ABC transporters *mlbYZ*, *mlbTU* and *mlbEF* in *S. coelicolor*

*In silico* analysis of the *mlb* cluster revealed the presence of a gene named *mlbJ* upstream the genes encoding the ABC transporter MlbYZ. The stop codon of *mlbJ* overlaps with the start codon of *mlbY*, thereby *mlbJ* was assumed to form an operon with *mlbYZ*. Analysis of the amino acid sequence by SOSUI ver. 1.11 (Hirokawa *et al.*, 1998) and Quick2D (Bioinformatics Toolkit, Max Planck Institute for Developmental

Biology, Tübingen) predicted several membrane-spanning regions for MlbJ. To determine whether MlbJ plays a role in NAI-107 resistance, *mlbJ* was expressed in *S. coelicolor* using the vector pRM4 as described before (3.3.4). *S. coelicolor mlbJ* was compared with the WT and *S. coelicolor* pRM4 by resistance assay using NAI-107 gradient plates (0-2 µg/ml) (2.14.2). *S. coelicolor mlbJ* was slightly more resistant than the WT and *S. coelicolor* pRM4 to NAI-107 (Fig. 37A).

Since none of the ABC transporters encoded in the *mlb* cluster showed a role in NAI-107 resistance in heterologous expression experiments (3.3.4, 3.3.6.1), *mlbYZ*, *mlbTU* and *mlbEF* were co-expressed with *mlbJ* to determine whether MlbJ acts as an accessory protein for these ABC transporters. The strategy used was the same as for the co-expression of the ABC transporters with *mlbQ* (3.3.6.1). *mlbJ* was cloned into the integrative plasmid pIJ10257 ($hyg^R$) under the constitutive promoter *ermE**p and the resulting plasmid pIJ10257-*mlbJ* was transferred into *S. coelicolor* harbouring one of the recombinant plasmids pRM4-*mlbYZ*, pRM4-*mlbTU* and pRM4-*mlbEF* ($apra^R$), respectively. *S. coelicolor* recombinant strains were proved by PCR (primers Hygrofor and Hygrorev) and resistance assays using NAI-107 gradient plates (0-2 µg/ml) (2.14.2) were carried out. Interestingly, an effect of the co-expression of MlbJ with MlbYZ was observed (Fig. 37A). *S. coelicolor mlbYZ-mlbJ* was more resistant than *S. coelicolor* pRM4 and *S. coelicolor mlbJ*. This effect was specific with MlbYZ, as no effect was observed by co-expressing *mlbTU* and *mlbEF* with *mlbJ* (Fig. 37B).

To confirm the result, the operon *mlbJYZ* was amplified with the primers mlbJfor and mlbYZrev (2.6) and cloned into pRM4 yielding pRM4-*mlbJYZ*. The obtained plasmid was transferred by conjugation into *S. coelicolor* giving *S. coelicolor mlbJYZ* and resistance assays with NAI-107 gradient plates (0-2 µg/ml) were performed. *S. coelicolor* expressing the operon *mlbJYZ* under the control of *ermE**p was more resistant than the WT, *S. coelicolor* containing the empty plasmid and expressing *mlbJ* and *mlbYZ* separately (Fig. 38). The heterologous expression of *mlbJ* in *S. coelicolor* revealed a role of MlbJ in NAI-107 immunity and co-expression studies indicated a co-operative action with MlbYZ. MlbJ and MlbYZ were suggested to be immunity proteins.

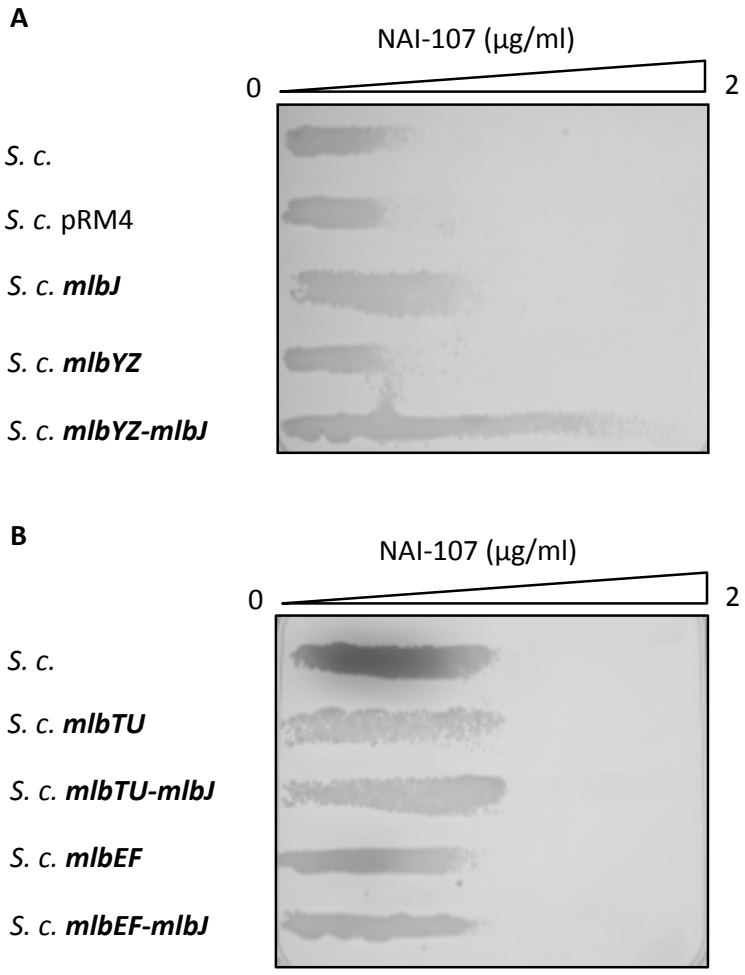


**Fig. 37. Resistance of *S. coelicolor* (*S. c.*) recombinant strains co-expressing *mlbJ* and the ABC-transporter-genes to NAI-107.** (A) *S. coelicolor* WT, containing the empty vector pRM4, expressing *mlbJ*, *mlbYZ* or co-expressing *mlbJ* and *mlbYZ.* (B) *S. coelicolor* WT, expressing *mlbTU*, *mlbTU* and *mlbJ*, *mlbEF* or *mlbEF* and *mlbJ*. NAI-107 gradient plates (0-2 µg/ml).

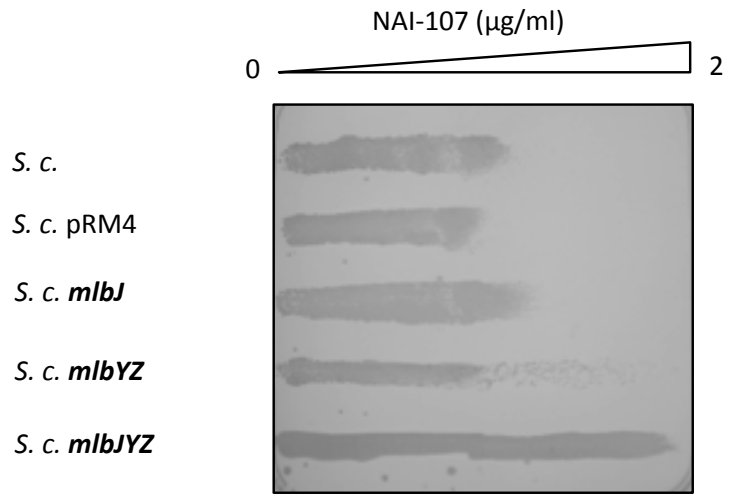


**Fig. 38. Resistance of *S. coelicolor* (*S.c.*) expressing the operon *mlbJYZ* to NAI-107.** *S. coelicolor* WT, containing the empty vector pRM4, expressing *mlbJ*, *mlbYZ* or *mlbJYZ*. NAI-107 gradient plate (0-2 µg/ml).

### 3.3.7 Construction and analysis of the synthetic immunity operon *mlbJYZQ*

Heterologous expression studies indicated that *Microbispora* sp. 107891 possesses distinct immunity proteins: the lipoprotein MlbQ (3.3.4), the ABC transporter MlbYZ and the transmembrane protein MlbJ (3.3.6.2). *mlbJ, mlbY* and *mlbZ* form the operon *mlbJYZ,* which is separated from *mlbQ* by *mlbO*, a gene encoding an oxygenase, probably involved in the hydroxylation of NAI-107 (Donadio *et al*., 2009) (Fig. 6). To note, *mlbZ* overlaps with *mlbO*. MlbJ, MlbY, MlbZ and MlbQ homologs were found in the planosporicin gene cluster (*psp*) of *Planomonospora alba* and in uncharacterized lantibiotic gene clusters of *Nocardia brasiliensis* and *Actinomyces sp.* ZP_061621 (Sherwood *et al.*, 2013). In *Planomonospora alba* and *Actinomyces sp.* ZP_061621, the *mlbQ* homologs lay downstream of the *mlbZ* homologs. To mimic the synthenous arrangement of the *mlb* homologs and to determine the effect on NAI-107 resistance of the co-expression of MlbJ, MlbYZ and MlbQ, the synthetic operon *mlbJYZQ* was constructed and used in heterologous expression studies.

#### 3.3.7.1 Construction of the *mlbJYZQ* synthetic immunity operon

To obtain the synthetic operon *mlbJYZQ*, *mlbJYZ* and *mlbQ* were joined by Gibson assembly (Gibson *et al.*, 2009). *mlbJYZ* (2335 nt) was amplified with the primers mlbJYZforGibson and mlbJYZrevGibson and *mlbQ* (416 nt) with the primers mlbQforGibson and mlbQrevGibson (2.8.7.3). The primers mlbJYZrevGibson and mlbQforGibson were designed to overlap with *mlbQ* and *mlbZ*, respectively. *mlbQ* was joined to *mlbJYZ* to have the *mlbQ* start codon (ATG) directly downstream the stop codon (TGA) of *mlbZ*. The Gibson assembly was also used to clone the *mlbJYZQ* operon in the linearized plasmid pRM4 (NdeI), chosen for heterologous expression in *S. coelicolor*. Thus, the construction of the *mlbJYZQ* operon and its cloning into pRM4 were successfully obtained by a single reaction (2.8.7.3).

#### 3.3.7.2 Heterologous expression of the *mlbJYZQ* operon in *S. coelicolor*

To determine the effect of the immunity proteins identified in *Microbispora* sp. 107891 on NAI-107 resistance, the operon *mlbJYZQ* was expressed in *S. coelicolor* under the control of the constitutive promoter *ermE**p. pRM4-*mlbJYZQ* was transferred in *S. coelicolor* by conjugation (2.11.2) to obtain *S. coelicolor mlbJYZQ* which was checked by

PCR using the primers ErmEXgeneFP and ErmEXgeneRP (2.6). *S. coelicolor mlbJYZQ* spores were then collected (2.7.2) and used for NAI-107 resistance assay (2.14.1). 0-4 µg/ml NAI-107 gradient plates were prepared for the determination of NAI-107 resistance of *S. coelicolor mlbJYZQ* in comparison with the one of the WT, *S. coelicolor mlbQ, S. coelicolor mlbYZ and S. coelicolor mlbYZ-mlbJ*. *S. coelicolor mlbJYZQ* was more resistant than *S. coelicolor* and *S. coelicolor mlbYZ* to NAI-107 (Fig. 39). The NAI-107 resistance conferred by the immunity operon *mlbJYZQ* was slightly higher than for *S. coelicolor mlbYZ-mlbJ* and comparable to the one of *S. coelicolor mlbQ* (Fig. 39). Although an effect of *mlbJYZQ* expression on NAI-107 resistance was detected, the effect of the co-expression of the NAI-107 immunity proteins MlbJ, MlbYZ and MlbQ was not the result of the additional effects of the single immunity determinants (MlbJYZ and MlbQ). This is probably due to an inefficient translation or instability of the transcript. Because *mlbQ* is located at the end of the operon, *mlbQ* expression does not probably contribute to NAI-107 resistance as observed in *S. coelicolor* expressing exclusively *mlbQ*.

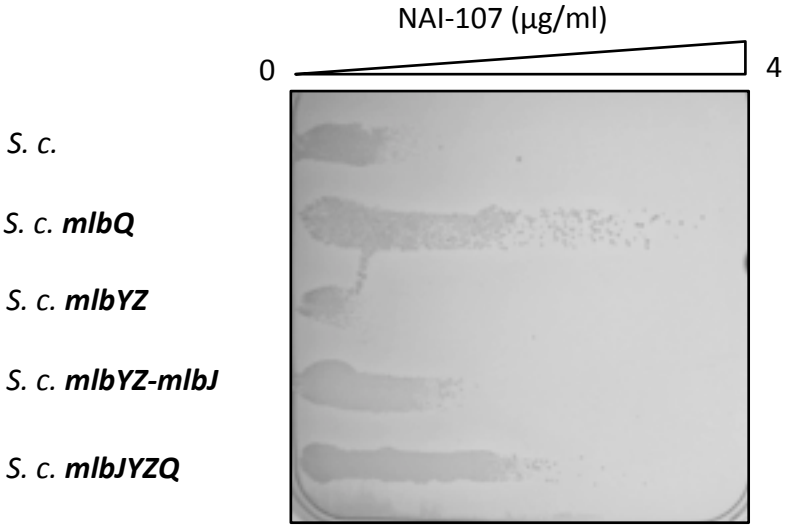


**Fig. 39. NAI-107 resistance of *S. coelicolor* (*S. c.*) expressing the immunity operon *mlbJYZQ*.** *S. coelicolor* WT, expressing *mlbQ*, *mlbYZ*, co-expressing *mlbJ* and *mlbYZ* or *mlbJYZQ*. NAI-107 gradient plate (0-4 µg/ml).

## 3.4 Characterization of MlbQ

The lipoprotein MlbQ confers NAI-107 resistance to *S. coelicolor* (3.3.4). Co-expression studies (3.3.6.1) did not show any cooperativity of MlbQ with the ABC transporters encoded in the *mlb* cluster. To gain insights into the role of MlbQ in NAI-107 immunity and MlbQ-mode of action, MlbQ was further investigated both by genetic and biochemical analyses.

### 3.4.1 *mlbQ* gene inactivation and complementation

#### 3.4.1.1 Construction of an *mlbQ* deletion mutant

To determine the effect of MlbQ-mediated immunity in the NAI-107 producer strain *Microbispora* sp. 107891, the markerless deletion mutant *Microbispora* Δ*mlbQ* was constructed. Because of the low efficiency of homologous recombination in *Microbispora* sp. 107891, several conjugations had to be performed to obtain the integration of pA18gusΔ*mlbQ* into *Microbispora* sp. 107891 genome by single-crossover event. pA18gusΔ*mlbQ* is a non-replicative plasmid containing the *mlbQ* flanking regions, constructed as described in 2.12.3. Even more efforts were put in the selection of a double-crossover event to gain *mlbQ* deletion. Single and double-crossover events were selected using the GUS reporter system (2.12.4). One *Microbispora* Δ*mlbQ* clone was obtained and checked by PCR. Firstly, amplification of an *mlbQ* fragment using the primers mlbQforRT (P1) and mlbQrevRT (P2) was carried out (Fig. 40A). No band was observed in the *Microbispora* Δ*mlbQ* sample, whereas *Microbispora* sp. 107891 possessed the expected DNA fragment at 163 bp (Fig. 40B). In addition, PCR analyses were performed with primers binding to the flanking regions of *mlbQ,* either contained in the recombinant plasmid pA18gusΔ*mlbQ* or not (Fig. 40A). PCRs were performed with the primer pairs mlbQupfor/mlbQdownrev (P3/P4) and mlbQcheckfor/mlbQcheckrev (P5/P6) (Fig. 40A), using genomic DNA from *Microbispora* Δ*mlbQ* and *Microbispora* sp. 107891. Correct gene deletion was proved by both PCR reactions. In both cases the fragment amplified from *Microbispora* Δ*mlbQ* was about 400 bp smaller than the one from *Microbispora* sp. 107891 (Fig. 40C and 40D). PCR analyses confirmed the correct deletion of *mlbQ*.

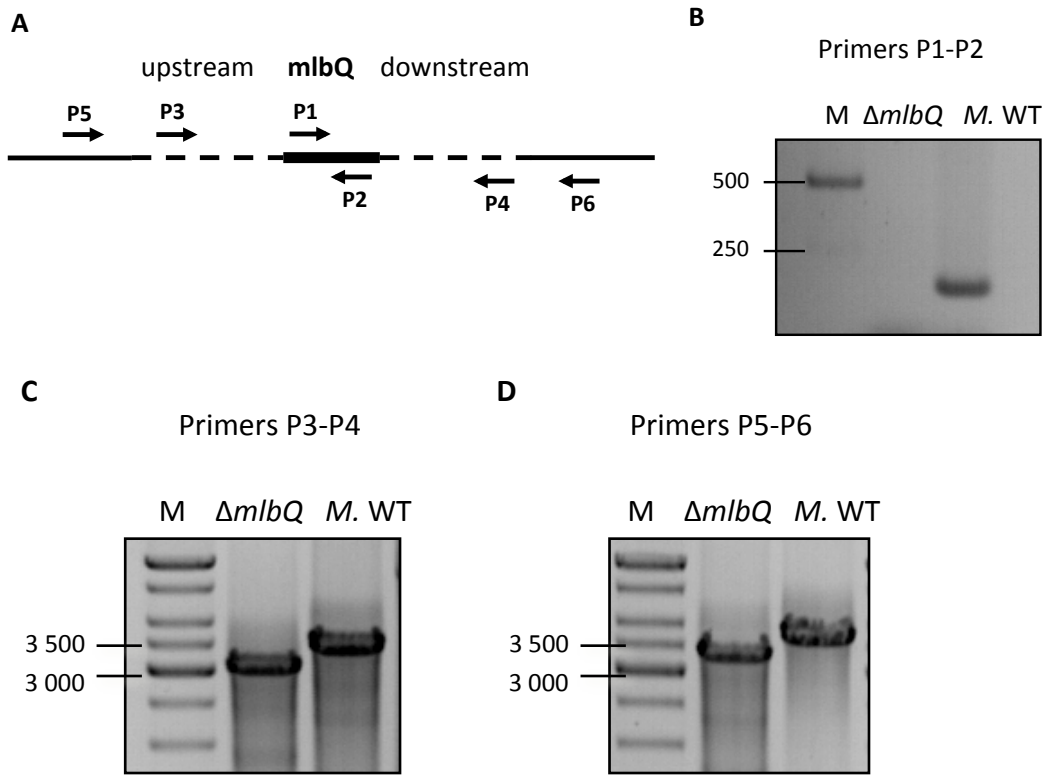


**Fig. 40. Verification of *Microbispora* Δ*mlbQ* by PCR**. PCRs were carried out with genomic DNA from *Microbispora* Δ*mlbQ.* Genomic DNA from *Microbispora* sp. 107891 (*M.* WT) was used as a control. (A) Schematic representation of *mlbQ*, its flanking regions and the primers used to check *Microbispora* Δ*mlbQ.* P1: mlbQforRT, P2: mlbQrevRT, P3: mlbQupfor, P4: mlbQdownrev, P5: mlbQcheckfor, P6: mlbQcheckrev. (B) Amplification of a fragment of *mlbQ* using the primers P1 and P2. Expected PCR product: 163 bp. M: Easy ladder I, 2% agarose gel. (C) and (D) Amplification of DNA fragments from *Microbispora* Δ*mlbQ* and *Microbispora* sp. 107891 with the primers P3-P4 (C) and P5-P6 (D). (C) P3 and P4 bind to the *mlbQ* flanking regions (upstream and downstram regions) cloned in pA18gusΔ*mlbQ.* Expected PCR products: 3016 bp for Δ*mlbQ,* 3400 bp for *M.* WT. (D) P5 and P6 bind to *mlbQ* flanking regions not contained in pA18gusΔ*mlbQ.* Expected PCR products: 3311 bp for Δ*mlbQ,* 3695 bp for *M.* WT. M: GeneRuler 1 kb DNA ladder, 1% agarose gel.

### 3.4.1.2 Characterization of *Microbispora* Δ*mlbQ* phenotype and complementation

*Microbispora* Δ*mlbQ* was characterized concerning NAI-107 resistance, growth and production. *Microbispora* Δ*mlbQ* sporulated poorly, so a NAI-107 resistance assay using spores (2.14.1) could not be performed. Alternatively, mycelium grown in Evans medium for 72 h or 120 h was plated onto MV0.1 agar plates containing increasing amounts of

NAI-107 (0-2 µg/ml) and colony forming units (CFU) were counted. Unfortunately, a high standard deviation between replicates precluded a comparison with *Microbispora* sp. 107891. Thus, it was not possible to determine if *Microbispora* Δ*mlbQ* differs from *Microbispora* sp. 107891 in NAI-107 resistance. Even if *Microbispora* Δ*mlbQ* was more sensitive than *Microbispora* sp. 107891 to NAI-107, this difference was minimal and it could not have been observed.

To further characterize *Microbispora* Δ*mlbQ*, the growth and NAI-107 production in Evans medium were analysed. *Microbispora* Δ*mlbQ* and *Microbispora* sp. 107891 were grown in Evans medium as described in 2.7.4 and samples were collected from 8 h to 168 h of growth. The supernatant (2 µl) of *Microbispora* Δ*mlbQ* and *Microbispora* sp. 107891 at different time points was used to check NAI-107 production by bioassay (2.13.1). Both *Microbispora* Δ*mlbQ* and *Microbispora* sp. 107891 initiate to produce NAI-107 at about 48 h (Fig. 41A). Growth was monitored by measuring the dry weight of 5-ml samples (2.7.4). *Microbispora* Δ*mlbQ* was impaired in growth compared to the WT strain (Fig. 41B). Notably, the difference in growth between *Microbispora* Δ*mlbQ* and *Microbispora* sp. 107891 was significant from the start of NAI-107 production (from 48 h to 168 h) (Fig. 41B). *Microbispora* Δ*mlbQ* and *Microbispora* sp. 107891 were then compared regarding NAI-107 production. The supernatant of *Microbispora* sp. 107891 (2 µl) and *Microbispora* Δ*mlbQ* (volume adjusted to the dry weight of the culture) at 120 h was used for bioassays against the indicator strain *M. luteus* (2.13.1). The inhibition halo produced by *Microbispora* Δ*mlbQ* was not significant different from the one of *Microbispora* sp. 107891. Hence, NAI-107 productivity of *Microbispora* Δ*mlbQ* and *Microbispora* sp. 107891 were comparable. *Microbispora* Δ*mlbQ* seemed to differ from *Microbispora* sp. 107891 exclusively in growth. To exclude that the observed phenotype was due to polar effects caused by the deletion of *mlbQ*, the mutant was complemented *in trans* by expressing *mlbQ* under the control of the constitutive promoter *ermE**p. pRM4-*mlbQ* was introduced into *Microbispora* Δ*mlbQ* by conjugation (2.11.3) yielding *Microbispora* Δ*mlbQ*(*mlbQ*). The complemented mutant *Microbispora* Δ*mlbQ*(*mlbQ*) grew and produced as the WT (Fig. 41B). Complementation of *mlbQ* demonstrated that the impaired growth of the *mlbQ* mutant is a consequence of *mlbQ* deletion.

**A**

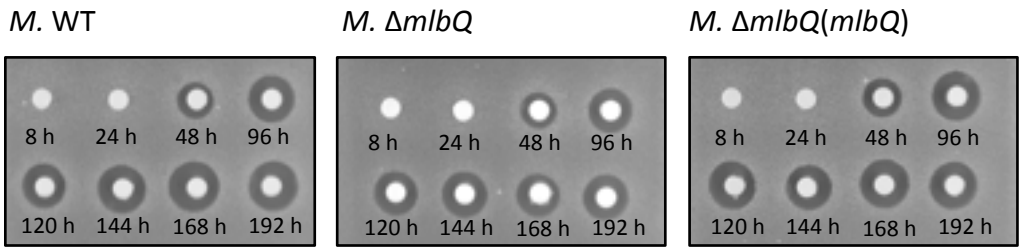


**B**

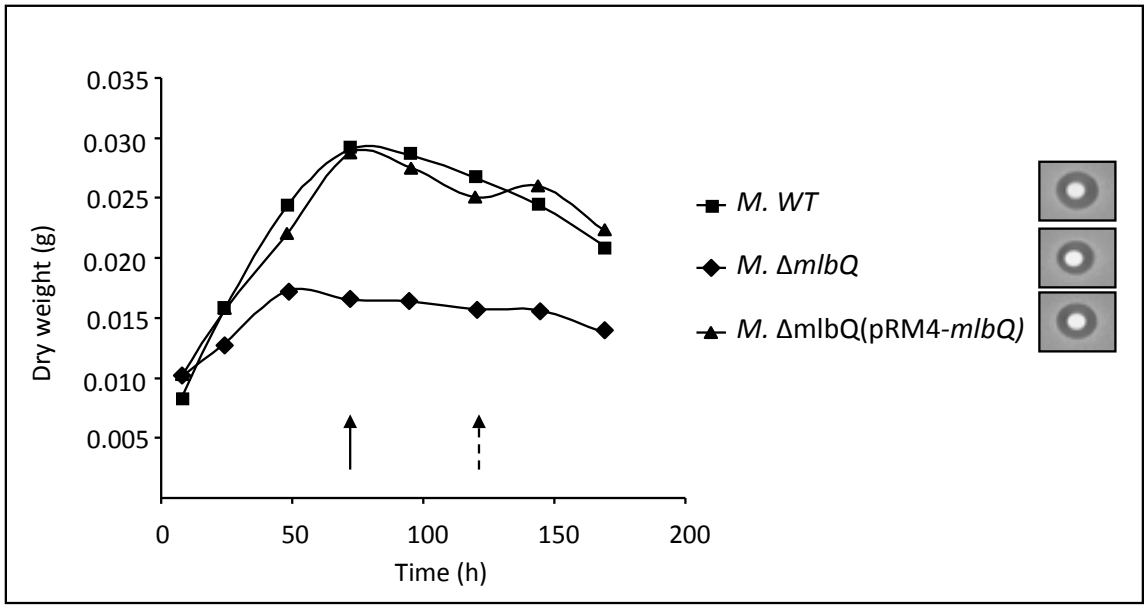


**Fig. 41. Characterization of the phenotype of *Microbispora* Δ*mlbQ* and of the complementation strain *Microbispora* Δ*mlbQ*(*mlbQ*).** (A) Representative bioassays of *Microbispora* sp. 107891 (*M.* WT), *Microbispora* Δ*mlbQ* and *Microbispora* Δ*mlbQ*(*mlbQ)* supernatants at 8, 24, 48, 72, 96, 120, 144, 168 and 192 h. (B) Growth and NAI-107 production of *Microbispora* sp. 107891 (*M.* WT) (square) *Microbispora* Δ*mlbQ* (diamond) and *Microbispora* Δ*mlbQ*(*mlbQ*) (triangle). NAI-107 production starts at 48 h (black arrow). Samples for the bioassay were taken at 120 h (dashed arrow). The y-axis represents the dry weight of 5-ml samples. n=1, four technical replicates.

### 3.4.2 Analysis of MlbQ-specificity to NAI-107-like lantibiotics

To explore the specificity of MlbQ-mediated immunity, *S. coelicolor mlbQ* was tested against the lantibiotic 97518 and epidermin. The lantibiotic 97518 is a NAI-107-like

lantibiotic that has an identical arrangement of thioether rings to NAI-107 and a similar antibacterial spectrum, but is considerably less potent than NAI-107 (Maffioli *et al*., 2009). To determine if MlbQ confers resistance also to 97518, a resistance assay using paper disks was performed (2.14.1). *S. coelicolor mlbQ* was grown on a LB agar plate where a sterile paper disk soaked with 20 µg of 97518 was applied. *S. coelicolor mlbQ* was more resistant against 97518 than the WT and *S. coelicolor* pRM4 (Fig. 42A). To confirm the specificity of MlbQ to NAI-107-like lantibiotics, a resistance test against epidermin was performed. Epidermin is a class I lantibiotic which presents a N-terminal nisin-like lipid II binding motif and a C-terminal aminovinyl cysteine (Allgaier *et al*., 1985). Epidermin differs from NAI-107 and 97518 in the central region where the flexible 12-15 amino acids are substituted in NAI-107 and 97518 by the ring C (Fig. 4 and 5). The resistance of *S. coelicolor mlbQ* to epidermin was tested on 0-4 µg/ml epidermin gradient plates (2.14.2). *S. coelicolor* expressing MlbQ possessed the same level of resistance to epidermin than the WT and *S. coelicolor* pRM4 (Fig. 42B). Hence, the resistance assays against 97518 and epidermin revealed that MlbQ-action is specific to NAI-107-like lantibiotics.

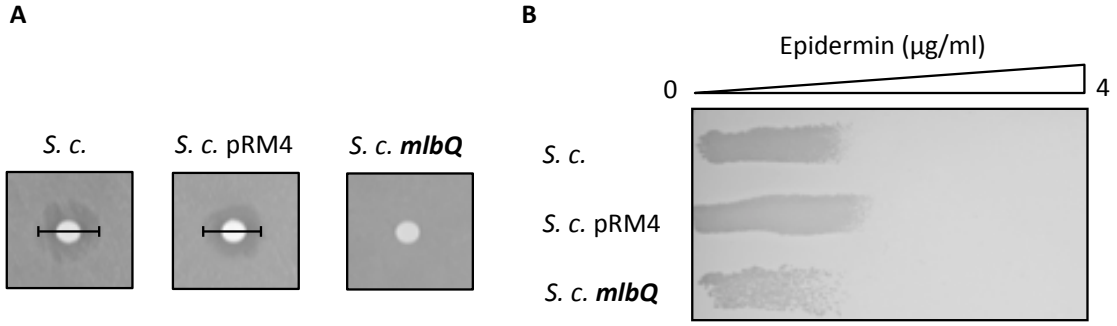


**Fig. 42. Resistance of *S. coelicolor* (*S.c.*) expressing *mlbQ* to the lantibiotics 97518 and epidermin.** (A) Resistance of *S.c.*, containing the empty vector and expressing *mlbQ* to 97518 (20 µg). (B) Resistance of *S.c.*, containing the empty vector and expressing *mlbQ* to epidermin (gradient plate 0-4 µg/ml).

### 3.4.3 Heterologous expression of the MlbQ homolog PlnQ in *S. coelicolor*

One of the closest homolog of MlbQ is PlnQ, a lipoprotein encoded by *Planomonospora* spp., producers of 97518 (also known as planosporicin) (Maffioli *et al.*, 2009; Sherwood *et al.*, 2013). *S. coelicolor* expressing MlbQ was more resistant than the WT to both NAI-107 and 97518 (3.4.2). To further investigate cross-resistance to the lantibiotics NAI-107 and 97518, lantibiotic immunity conferred by PlnQ was analysed. *plnQ* was amplified with the primers plnQfor and plnQrev (2.6), using the cosmid 4B8 (NAICONS) as template. *plnQ* was cloned into pRM4 to yield pRM4-*plnQ* which was introduced into *S. coelicolor* by conjugation (2.11.2). Firstly, *S. coelicolor plnQ* was tested against the lantibiotic 97518 (2.14.1). The lantibiotic resistance assay showed that *S. coelicolor* expressing PlnQ was more resistant to 97518 than the WT (Fig. 43A). Cross-resistance to NAI-107 was then checked by resistance assay using gradient plates (2.14.2). *S. coelicolor plnQ* was compared to the WT and *S. coelicolor mlbQ*. PlnQ conferred NAI-107 resistance to *S. coelicolor* but in minor extent than the lipoprotein MlbQ (Fig. 43B).

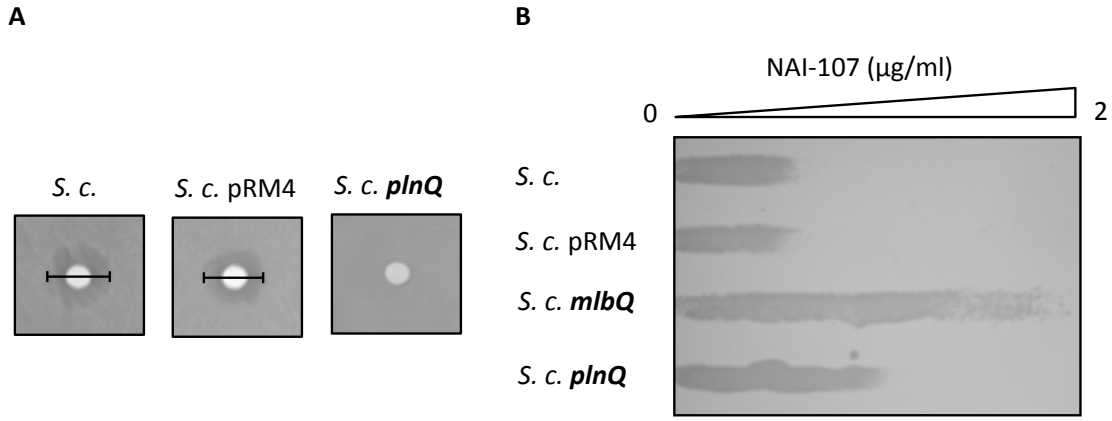


**Fig. 43. Resistance of *S. coelicolor* expressing *plnQ* to the lantibiotics 97518 and NAI-107.** (A) Resistance of *S. coelicolor* WT, containing the empty vector, and expressing *plnQ* to 97518 (20 µg). (B) Resistance of *S. coelicolor* WT, containing the empty vector, expressing *mlbQ* or *plnQ* to NAI-107 (gradient plate 0-2 µg/ml).

### 3.4.4 MlbQ localization at the membrane compartment in *S. coelicolor*

MlbQ contains a N-terminal signal sequence and a lipobox motif (Fig. 30) that suggest an export of the protein through the cytoplasmic membrane and the attachment to it via lipidation. To verify the membrane localization of MlbQ, C-terminal His-tagged MlbQ was expressed in *S. coelicolor*. *mlbQ* was amplified with the primers mlbQfor1 and mlbQhistagrev2 (2.6), the latter designed to fuse a C-terminal His-tag to MlbQ. *mlbQ*Histag was cloned into pRM4 by NdeI and BamHI restriction sites to obtain pRM4-*mlbQ*Histag (2.15.8), which was transferred into *S. coelicolor* by conjugation (2.11.2). The functionality of MlbQHistag was tested by resistance assay using NAI-107 gradient plates (0-2 µg/ml) (2.14.2). *S. coelicolor mlbQ*Histag was more resistant than the WT (Fig. 44A), indicating that the C-terminal His-tag does not interfere with MlbQ action.

After verification of MlbQHistag functionality, membrane localization of MlbQHistag in *S. coelicolor* was verified. *S. coelicolor mlbQ*Histag was cultivated in R5 medium for 3 days and membranes were isolated as described in 2.15.8. The cell extract, the wash and the membrane fractions were analysed by Western Blot using an anti-Histag antibody (2.15.7). Western blot analysis showed signals in the cell extract and in the membrane fraction (Fig. 44B). MlbQHistag was successfully expressed in *S. coelicolor* and its membrane localization was confirmed.

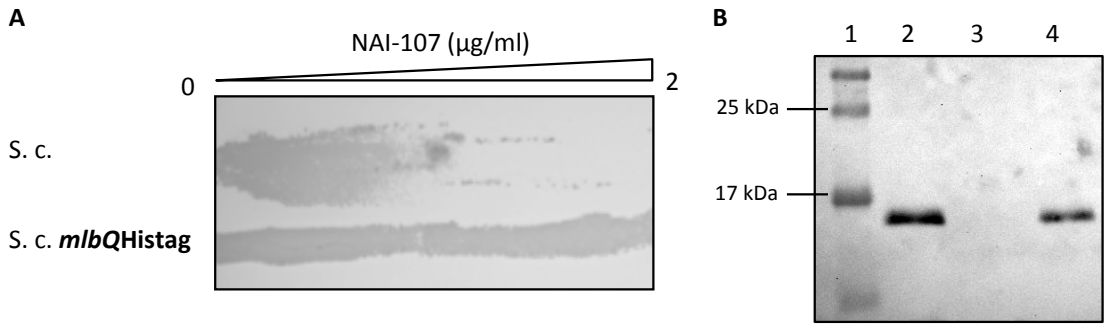


**Fig. 44. Expression of MlbQHistag in *S. coelicolor*.** (A) Resistance of *S. coelicolor* (*S.c.*) expressing *mlbQ*Histag to NAI-107 in comparison to the WT (0-2 µg/ml NAI-107 gradient plates). (B) Western Blot analysis of *S. coelicolor mlbQ*Histag. (1) protein marker, (2) cell extract, (3) PBS wash, (4) membrane fraction. Detection by anti-Histag antibodies conjugated with HRP.

### 3.4.5 Attempts to generate MlbQ secreted variants

The immunity protein NisI was shown to be secreted into the extracellular space. About half of NisI escapes lipid modification, thus it is not anchored to the cytoplasmic membrane (Koponen *et al.*, 2004). To determine whether the lipid anchor is required for MlbQ-action, generation of secreted variants of MlbQ was attempted.

Lipoproteins were initially thought to be translocated exclusively by the Sec general secretory pathway (Sec) in their unfold state. In the last decade, few reports indicated also the Tat pathway as a system for lipoprotein translocation (Valente *et al.*, 2007; Thompson, *et al.*, 2010). In *S. coelicolor*, the Tat system plays a major role in lipoprotein translocation. About 25% of the lipoproteins were predicted to be putative Tat substrates, as they possess Tat translocation motifs (RR-X-ΦΦ, where Φ represents a hydrophobic amino acid) (Thompson *et al.*, 2010). In contrast to the Sec system, the Tat system recognizes folded proteins (Delisa *et al.*, 2003). Both translocation systems are used by secreted proteins.

For the generation of MlbQ secreted variants, the MlbQ signal peptide was substituted with signal sequences of characterized secreted proteins. Since the folding state of the protein is crucial for the route of translocation, the MlbQ signal peptide was analysed to predict the secretory pathway. The fact that the signal peptide of MlbQ does not include a Tat translocation motif RR-X-ΦΦ indicated the Sec system as the most probable translocation system for MlbQ.

#### 3.4.5.1 MlbQ fusion to a Sec-dependent signal peptide

The MlbQ signal peptide (1-23 aa) was substituted with the Sec-dependent signal peptide of Vsi, the subtilisin inhibitor from *Streptomyces venezuelae.* The Vsi signal peptide is well characterized, as it was used for the secretion of TNFα (Tumor Necrosis Factor α) in *Streptomyces lividans* and to evaluate the impact of the number of positive charges on protein secretion efficiency (Lammertyn *et al.*, 1997; Schaerlaekens *et al.*, 2004). Amplification of the sequence encoding the Vsi signal peptide, here indicated as *vsi*, was attempted (primers vsifor, vsirev). The genomic DNA of a *S. venezuelae* sp. was used as a template but no PCR product was obtained. Therefore, the chimeric gene *vsimlbQ* was synthesized by Eurofins. The gene was designed to fuse *vsi* to *mlbQ* lacking

its own signal peptide. In addition, a C-terminal His-tag was introduced to allow the detection of the secreted protein by Western Blot and NdeI/EcoRI sites for cloning into pRM4. The obtained plasmid pRM4-*vsimlbQ* was introduced into *S. coelicolor* by conjugation (2.11.2) to yield *S. coelicolor (vsi)mlbQ* and checked by PCR using the primers Aprafor and Aprarev (2.6). *S. coelicolor (vsi)mlbQ* was then tested for the ability to confer NAI-107 resistance, in comparison with *S. coelicolor mlbQ*, expressing the native MlbQ. NAI-107 resistance assay was performed using NAI-107 gradient plates (0-4 µg/ml) (2.14.2). *S. coelicolor (vsi)mlbQ* was not more resistant than the WT to NAI-107 (Fig. 45). The expression of *(vsi)mlbQ* seemed to be rather toxic for *S. coelicolor*, as *S. coelicolor (vsi)mlbQ* did not grow as well as the WT (Fig. 45). *S. coelicolor (vsi)mlbQ* was grown in liquid medium and the supernatant used for protein precipitation with TCA (trichloroacetic acid) for detection of secreted MlbQ. The sample was then analysed by Western Blot using anti-Histag antibody (2.15.7) to determine if the protein was secreted in the extracellular space. All the attempts to detect the secreted variant of MlbQ were not successful (data not shown). MlbQ was neither detected in the supernatant nor in the cell extract. The result of the resistant assay was attributed to the lack of expression of this MlbQ variant.

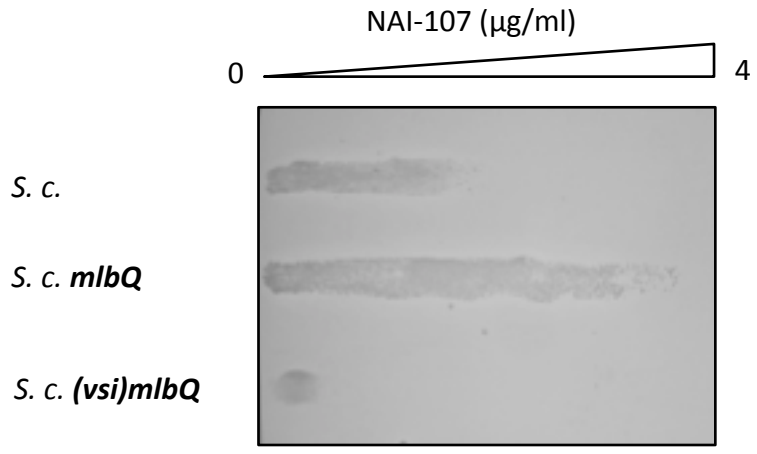


**Fig. 45. NAI-107 resistance of *S. coelicolor* expressing *(vsi)mlbQ.*** Resistance of *S. coelicolor* WT, expressing *mlbQ* and *(vsi)mlbQ* to NAI-107 (gradient plate: 0-4 µg/ml NAI-107).

### 3.4.5.2 MlbQ fusion to a Tat-dependent signal peptide

The fusion of a Sec-dependent signal peptide to MlbQ was not a successful approach to generate a secreted variant of MlbQ (3.4.5.1). Even if MlbQ was predicted to be translocated by the Sec system, it was not excluded that Tat translocation may occur. Indeed, the Tat machinery allows some exceptions in the Tat translocation motif, as reported for the tetrathionate reductase from *Salmonella enterica*, which was found to lack an arginine (Hinsley *et al.*, 2001). Thus, the ability of a Tat-dependent signal peptide to obtain a secreted variant of MlbQ was tested. For this purpose, the signal peptide of DagA, an agarase from *S. coelicolor* (Buttner *et al.*, 1997), was chosen. Overlap extension PCR was used to generate the chimeric gene *(dagA)mlbQ* (2.9.4). *dagA* was amplified from *S. coelicolor* genomic DNA using the primers dagAfor and dagArev (2.6). *mlbQ* lacking the sequence encoding the signal peptide was amplified with the primers mlbQfor-dagA and mlbQhistagrev2 using *Microbispora* sp. 107891 genomic DNA as template. The primers dagArev and mlbQfor-dagA were designed to overlap and mlbQhistagrev2 to contain a His-tag sequence, useful for the detection of the expressed protein. The chimeric gene *(dagA)mlbQ* was cloned in pRM4 using NdeI and EcoRI sites. The resulting plasmid pRM4-*dagAmlbQ* was introduced into *S. coelicolor* by conjugation (2.11.2) and spores were isolated (2.7.2). *S. coelicolor (dagA)mlbQ* was characterized for NAI-107 resistance and MlbQ secretion as reported for *S. coelicolor (vsi)mlbQ* (3.4.5.1). *S. coelicolor (dagA)mlbQ* grew like the WT and *S. coelicolor* pRM4 on 0-4 µg/ml NAI-107 gradient plates (Fig. 46). *(dagA)mlbQ* expression did not confer NAI-107 resistance as the expression of *mlbQ* with its native signal peptide. Also in this case, the protein was detected neither in the supernatant nor in the cell extract by Western Blot analysis (2.15.7).

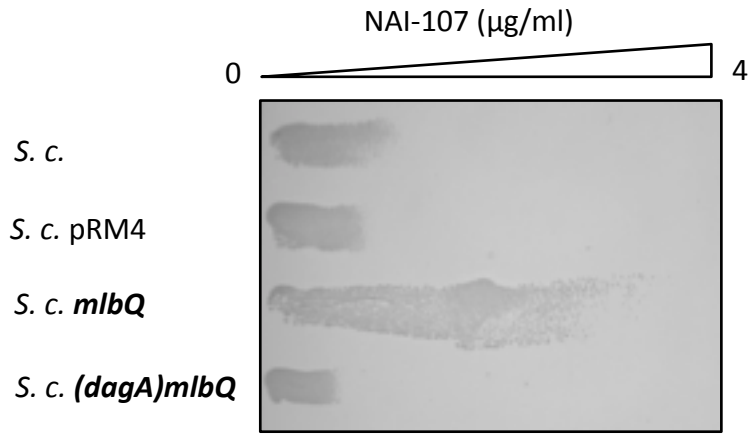


**Fig. 46. NAI-107 resistance of *S. coelicolor* expressing *(dagA)mlbQ*.** Resistance of *S. coelicolor* WT, expressing *mlbQ* and *(dagA)mlbQ* to NAI-107 (gradient plate: 0-4 µg/ml NAI-107).

### 3.4.6 MlbQ purification

To characterize MlbQ biochemically, MlbQ was expressed in *E. coli* using the pET30 vector (2.15.1). His-MlbQ expression was successfully achieved in *E. coli* Rosetta 2(DE3). Purification by Ni-NTA gravity columns allowed to obtain considerable amounts of protein (Fig. 47).

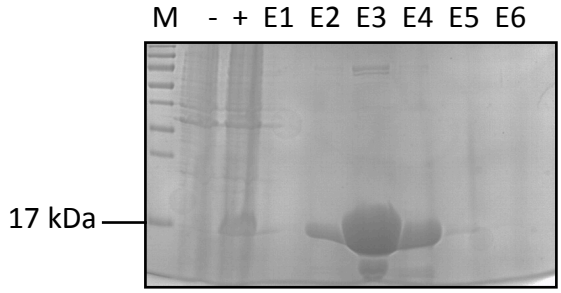


**Fig. 47. SDS-PAGE of His-MlbQ expressed in *E. coli* Rosetta 2(DE3) and purified by affinity chromatography.** M: Prestained PAGE Ruler Protein Marker. Cell extract before (-) and after (+) IPTG induction. E1-E6: elution fractions. The protein concentration of E3 was about 50 mg/ml.

Prior to functional analyses, His-MlbQ folding was checked by circular dichroism (2.15.9), performed at the Max Planck Institute in Tübingen in cooperation with Dirk Linke. The CD spectrum of His-MlbQ had a characteristic signal at 230-240 nm (Fig. 48). To determine the folding state of His-MlbQ, CD spectra were recorded at 95°C. The spectrum at 95°C missed the signal at 230-240 nm (Fig. 48). This signal is presumably characteristic of a His-MlbQ secondary structure, as it is lost during denaturation. The

protein sample was cooled to 25°C and CD spectra recorded. Interestingly, the signal at 230-240 reappeared and the CD spectrum was similar to the one recorded before protein denaturation (Fig. 48). Although CD spectroscopy analysis did not ensure that the purified protein was in the folding state, His-MlbQ was considered folded because of the different profile of the CD spectra recorded at 25°C and 95°C. Moreover, it was suggested that the protein could self-assemble, since the signal at 230-240 nm reappeared when the sample was cooled after denaturation.

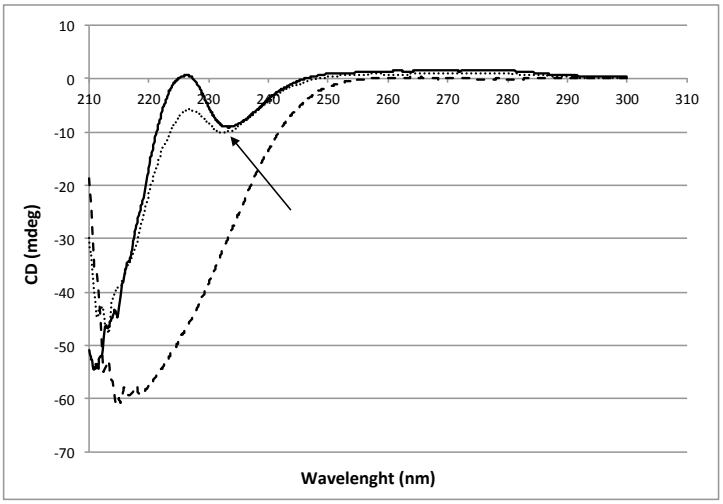


**Fig. 48. CD spectra of His-MlbQ.** CD spectra recorded at 25°C (solid line) and 95°C (dashed line). The dotted line represents the CD spectra recorded at 25°C after protein denaturation. The arrow indicates a characteristic signal at 230-

### 3.4.7 MlbQ structure determination by NMR

CD spectroscopy suggested a folding state for the purified His-MlbQ (3.4.6). To date, only one structure of a lantibiotic immunity lipoprotein (SpaI) was reported (Christ *et al.*, 2012). To analyse MlbQ fold and to gain insights into its mode of action, MlbQ protein structure was determined by NMR spectrometry. C- and N-labelled His-MlbQ was expressed in *E. coli* Rosetta 2(DE3) and purified to obtain a highly pure protein sample (2.15.1). *E. coli* Rosetta 2(DE3) carrying the plasmid pET30-*mlbQ* was able to express appropriate amount of $^{15}N$, $^{13}C$-labelled protein in M9 medium supplemented with $^{15}NH_4Cl$ and $^{13}C$-glucose. A pure protein sample was obtained by two chromatographic steps consisting of a Ni-NTA chromatography followed by an anion-exchange chromatography (2.15.2, 2.15.3). About 15 mg of pure protein were obtained after anion-exchange chromatography (Fig. 49) and were used for NMR analysis.

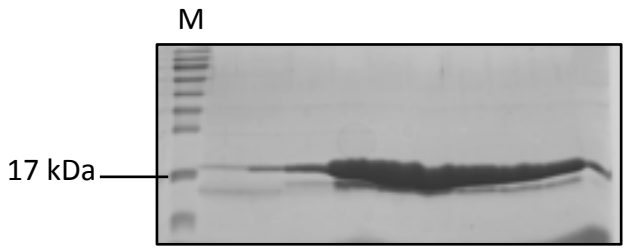


**Fig. 49. SDS-PAGE of His-MlbQ after anion exchange purification.** Prestained PAGE Ruler Protein Marker (M) and fractions 40-48.

Elucidation of MlbQ structure was carried out by Murray Coles (MPI, Tübingen). MlbQ is divided into an unstructured N-terminal region followed by a globular domain consisting of a C-terminal helix (α3) packed at an angle against a four-stranded β-sheet, with a disulphide bond connecting the helix to the sheet at its C-terminal end (Fig. 50A). MlbQ possesses an unusual structured β1-β2 loop, including a short helix (α1) that runs perpendicular to the sheet. A conserved tryptophan residue (W35) anchors the loop into the hydrophobic core of the fold formed by the aromatic rings of F54 and Y62 (numbers refer to the protein sequence without tag) (Fig. 51A). MlbQ possesses a surface hydrophobic patch bounded by the β1-β2 loop, α3 and the structured region of the N-terminal loop (Fig. 50B).

The MlbQ homologs identified in the *psp* cluster (Sherwood *et al*., 2013) and in the uncharacterized lantibiotic biosynthetic gene cluster in *Nocardia brasiliensis* (named NocQ) and *Actinomyces sp.* ZP_061621 (named ActQ) were aligned with MlbQ using ClustalW (Chenna *et al.*, 2003). W35, F54, Y62 and the C residues forming a disulphide bond in MlbQ were conserved (Fig. 51B). The sequence alignment suggested that these residues are important for the action of MlbQ homologs and/or for their folding.

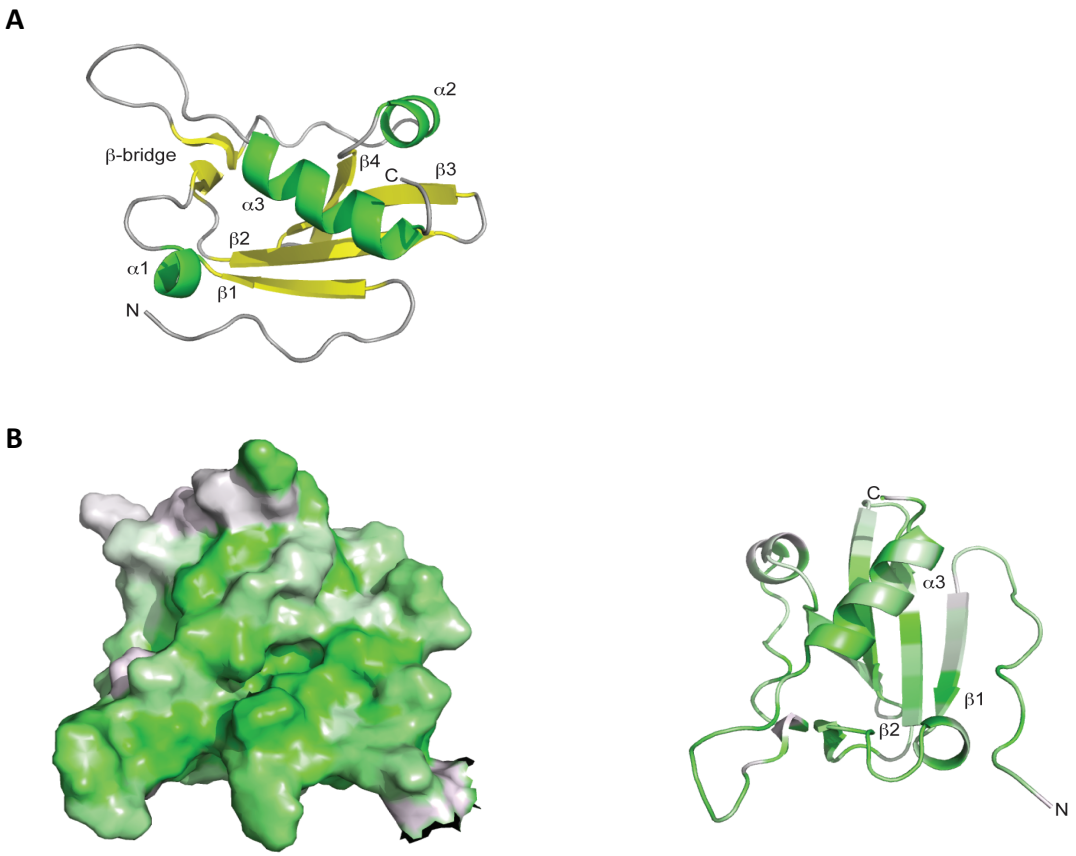


**Fig. 50. Solution structure of MlbQ.** (A) A cartoon view of the globular domain of the protein. β-strands are in yellow and helices in green. (B) The surface of MlbQ globular domain colored from white to green according to increasing residue hydrophobicity. A distinct hydrophobic patch runs across this face of the protein. The cartoon view on the left shows this patch is bounded by α3, the β1-β2 loop, and the structured region of the N-terminal loop.

A

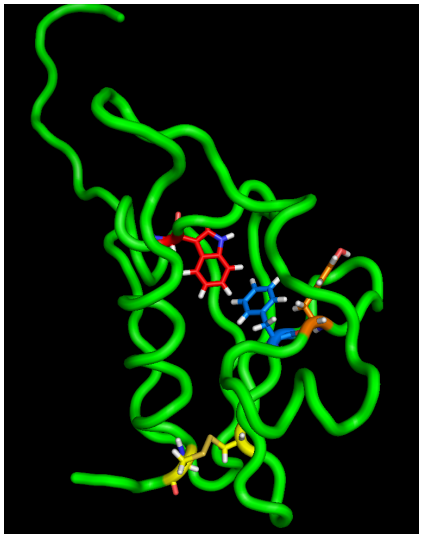

B

```
MlbQ            -TGGGRADPAHRSPVPLPSPTSNKQDISEANLAYLWPLTVDHGTIECLPSDN----AVFV
PspQ            -GGSGQADPATREPVALPSPTAAAQQVSERNFGYTWPLTVDHGTAECRDGDR----AVFT
NocQ            GGGSGPKDPAHRDGVALPEPTSSSQAVGSENLGYLWPFTVDRGTIECRAGEQ----ATFT
ActQ            --GMLHPEDYPTDTAKLPKATSNPAKISKATFRHSWNLTVDHGTVYCKLNSAGDPILYFT
                  *    :    . . **..*:    :.. .: : * :***:**  *  ..       *.

MlbQ            APDGTTYALNDRAEKAGHPPITPIRAKGSGGGYISLGALLSTTLNLCGKG-
PspQ            APDGTTYALNERAREAGYAAVDPVRLSGEGGGKVSLGPLLSRTMKLCRFAR
NocQ            APDGKIYALNEKAEQSGLPGVEPLRATGAGGDKISLGALRSRAMQLCRFAN
ActQ            APNGTEYALNSVTGNGGRPNIEDIADG-------SVGPIRSFAFSVCDVK-
                **:*. ****. : :.* . :  :          *:*.: * ::.:*
```

**Fig. 51. Conserved amino acids in MlbQ and MlbQ homologs.** (A) MlbQ structure with the characteristic residues W35 (red), F54 (blue), Y62 (orange). The C residues that form the disulphide bond are in yellow. (B) Sequence alignment of MlbQ, PspQ, NocQ and ActQ obtained with ClustalW. Amino acid sequences without the signal peptides were used for the alignment. The conserved residues that form the hydrophobic core of MlbQ and the C residues are indicated.

### 3.4.8 MlbQ interaction studies

#### 3.4.8.1 MlbQ interaction studies with NAI-107

MlbQ conferred resistance to *S. coelicolor* against the structurally related lantibiotics NAI-107 and 97518 (3.4.2). Thus, an MlbQ-mode of action based on lantibiotic

recognition was hypothesized. His-MlbQ purified from *E. coli* Rosetta 2(DE3) (3.4.6) was used for interaction studies with NAI-107. Cross-linking reactions were performed as described for the lantibiotic subtilin and the immunity protein SpaI (Stein *et al*., 2005). The N-terminal His-tag was complexed with $Ni^{2+}$, which was successively oxidized to $Ni^{3+}$ by treatment with MMPP (magnesium monoperoxyphthalate), forming reactive radicals that led to cross-link. Cross-linking experiments were performed varying the amount of protein, of lantibiotic, the incubation time and the pH of the Tris/HCl buffer. Although several different conditions were used for the cross-link reactions, no interaction between MlbQ and NAI-107 was observed. Cross-link experiments were also carried out with glutaraldehyde but no interaction was detected. Since the structure of the soluble MlbQ was successfully solved (3.4.7), attempts to detect an MlbQ interaction with NAI-107 by NMR spectroscopy were carried out (Murray Coles, MPI, Tübingen). Unfortunately, NAI-107 precipitation in the protein buffer (50 mM Tris/HCl, 20 mM NaCl, pH 8) precluded the possibility to perform the interaction studies. Although several buffers were tested for NAI-107 solubilization, none of them was able to solubilize NAI-107 to obtain at least a solution of about 1 mg/ml. Münch *et al.*, 2014 reported the interaction of NAI-107 with DPC (dodecylphosphocholine) micelles, thus DPC micelles were thought suitable to keep NAI-107 in solution and to use in NMR interaction studies. Interaction studies of MlbQ with NAI-107 in presence of DPC micelles were planned. Firstly, MlbQ interaction with DPC micelles was tested. To be sure that the N-terminal tag did not interfere with the analysis, His-MlbQ was cleaved by enterokinase (2.15.4) to obtain a 10.7 kDa protein, designed as cMlbQ. The cleavage was verified by SDS-PAGE (2.15.5) (Fig. 52).

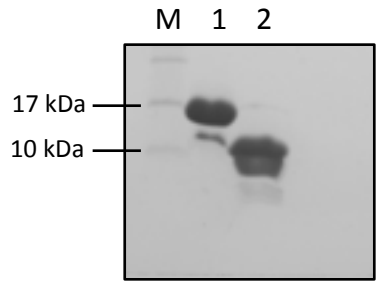


**Fig. 52. Verification of tag removal from His-MlbQ by enterokinase.** His-MlbQ before (1) and after (2) enterokinase digestion. M: protein marker.

cMlbQ was tested with increasing concentration of DPC (5-150 mM) but NMR spectroscopy did not evidence any interaction of cMlbQ with the micelles. Therefore,

NMR analysis with labelled protein and deuterated-DPC was not set up. Alternatively, cMlbQ was tested by bioassay against the indicator strain *M. luteus* in presence of DPC and NAI-107 (2.15.11). The inhibition halos of NAI-107 did not decrease by adding cMlbQ (Fig. 53). All the studies carried out to assess an MlbQ-NAI-107 interaction did not prove any MlbQ interaction with the lantibiotic. Moreover, the poor solubility of NAI-107 precluded to perform more detailed interaction studies.

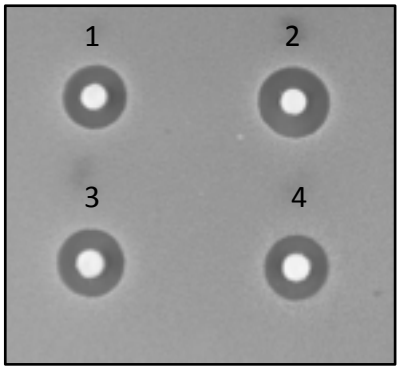


**Fig. 53. Verification of NAI-107 interaction with cMlbQ in presence of DPC micelles.** NAI-107 (1), NAI-107 + DPC (2), NAI-107 + DPC + MlbQ (3 and 4). cMlbQ (MlbQ without tag) was used for the bioassay.

### 3.4.8.2 MlbQ interaction studies with 97518

To overcome the insolubility of NAI-107 in protein buffers, 97518 was used for interaction studies. 97518 is a NAI-107 like lantibiotic which is more soluble than NAI-107 due to the additional negative charge of Glu, which substitutes the hydroxylated proline in position 14 of NAI-107 (Maffioli *et al.*, 2009). 97518 was dissolved in phosphate buffer (50 mM $NaH_2PO_4$, 50 mM NaCl, pH 8) and used for interaction studies with MlbQ by NMR spectroscopy (Murray Coles, MPI, Tübingen). After adding 97518, perturbations of the NMR spectra were not observed, indicating no interaction of MlbQ with 97518.

### 3.4.9 MlbQmCherry localization studies by fluorescence microscopy

To gain more insights into the role of MlbQ in immunity and its membrane localization, fluorescence microscopy studies were conducted in the NAI-107 producer strain and in the heterologous hosts *Microbispora* JCM66 and *S. coelicolor*.

#### 3.4.9.1 MlbQmCherry localization in *Microbispora* Δ*mlbQ*

The lipoprotein MlbQ was detected at the membrane compartment in *S. coelicolor* (3.4.4). To determine if MlbQ preferentially localizes in specific regions of the cytoplasmic membrane, fluorescence microscopy was performed. MlbQ was fused at the C-terminus with the fluorescent protein mCherry. The primers mlbQfor2 and mlbQrev3 were used to amplify *mlbQ*, which was cloned in pRM4.3-*mcherry* downstream the constitutive promoter *ermE**p to yield the plasmid pRM4.3-*mlbQmcherry*. The recombinant strain *Microbispora* Δ*mlbQ*(*mlbQmcherry*) was obtained by transfer of pRM4-*mlbQmcherry* in the *mlbQ* null mutant (*Microbispora* Δ*mlbQ*) by conjugation (2.11.3). mCherry fluorescence was then monitored as described in 2.17.2. An mCherry fluorescent signal was detected, indicating the successful expression of the fusion protein in *Microbispora* Δ*mlbQ(mlbQmcherry*). However, *Microbispora* Δ*mlbQ(mlbQmcherry*) did not reveal any specific localization of MlbQmCherry, rather a diffuse fluorescence in the mycelium, suggesting a a localization in the cytoplasm of the recombinant strain (Fig. 54).

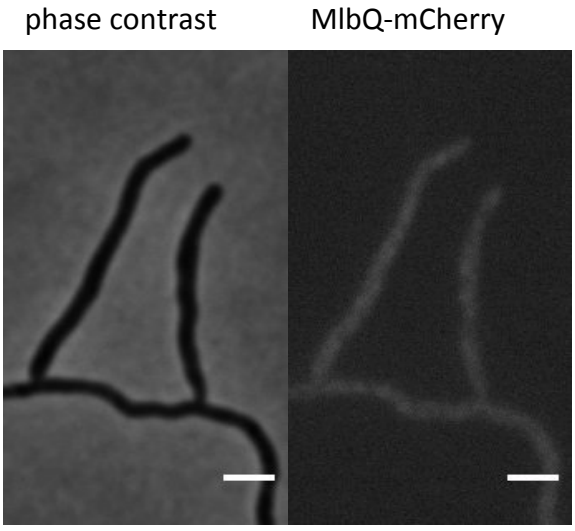


**Fig. 54. Monitoring MlbQ-mCherry localization in *Microbispora* Δ*mlbQ*(*mlbQmcherry*).** Diffuse fluorescence in the all mycelium. The strain was grown on S1 medium for 6 days. Scale bars represent 2 µm.

3.4.9.2 MlbQmCherry localization in *Microbispora* JCM66

pRM4.3-*mlbQmcherry* (3.4.9.1) was introduced also in *Microbispora* JCM66 to obtain *Microbispora* JCM *mlbQmcherry*. *Microbispora* JCM66 does not possess MlbQ homologs (according to PCR analysis) and sporulates abundantly, in contrast to *Microbispora* sp. 107891 (3.1.2). The spore morphology of *Microbispora* JCM *mlbQmcherry* resembled that of *Microbispora* JCM66, indicating no interference of MlbQmCherry with the spore formation process. MlbQmCherry fluorescence was monitored as for *Microbispora* Δ*mlbQ*(*mlbQmcherry*) (3.4.9.1). Interestingly, fluorescence microscopy revealed a strong signal in *Microbispora* JCM *mlbQmcherry* spores where MlbQmCherry was localized around the surface, forming a ring-like structure (Fig. 55A). In contrast to the spores, the mycelium showed no fluorescence signal (Fig. 55A). As a control, the plasmid pRM4.3-*mcherry* was introduced in *Microbispora* JCM66 and mCherry fluorescence was monitored. In this case, a strong fluorescence signal was observed in the mycelium after 3 days of growth (Fig. 55B).

Finally, *Microbispora* JCM *mlbQmcherry* was compared to *Microbispora* JCM66 by lantibiotic resistance assay (2.14.1). Spores were plated onto MV0.1 agar and paper disks containing 0.5 µg NAI-107 were placed on the plates. The inhibition halo of *Microbispora* JCM *mlbQmcherry* was comparable to the one of *Microbispora* JCM66 (Fig. 56). In contrast to the expression of MlbQ (3.3.5), MlbQmCherry expression did not confer NAI-107 resistance to *Microbispora* JCM66.

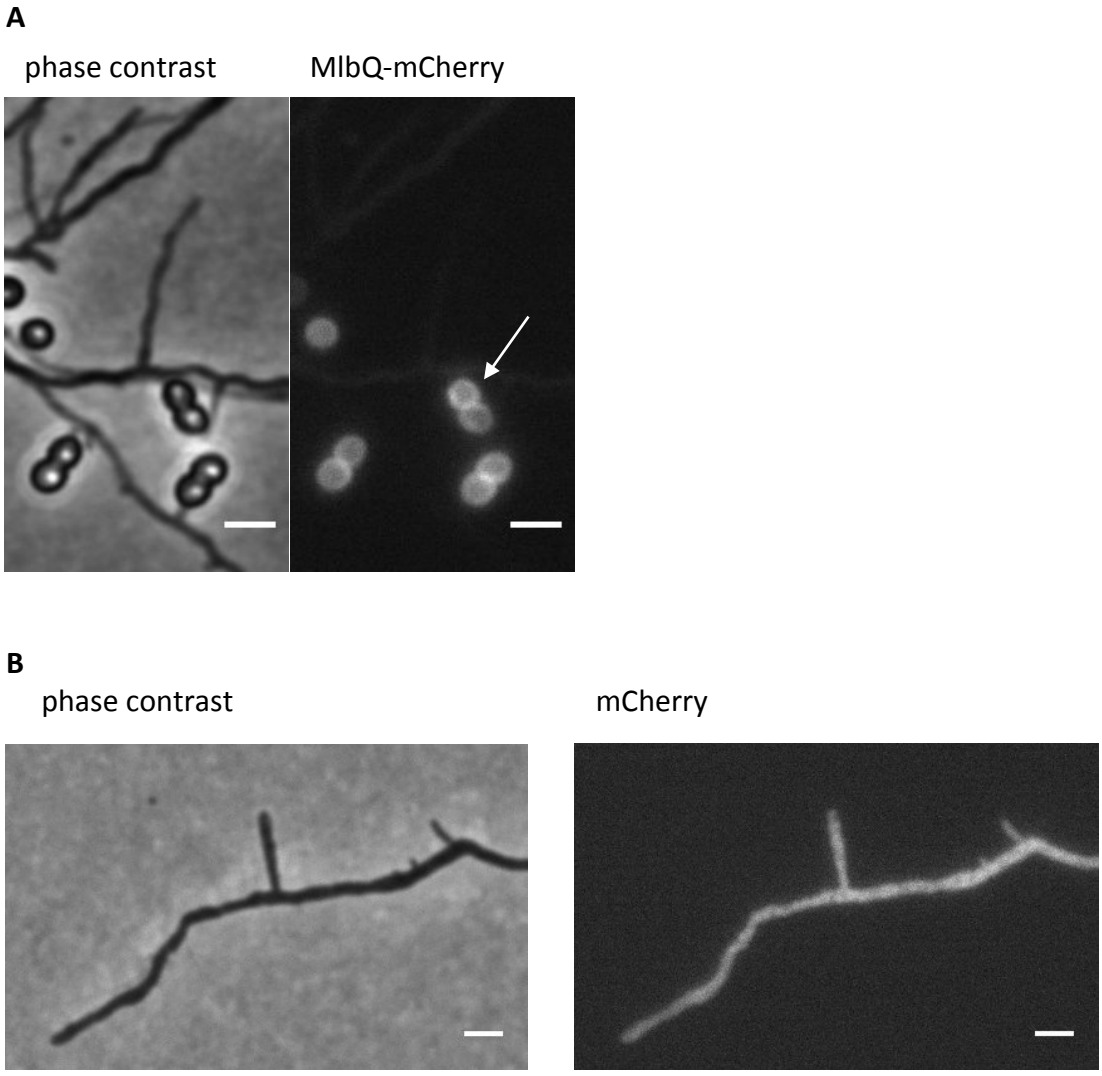


**Fig. 55. Monitoring mCherry fluorescence in *Microbispora* JCM *mlbQmcherry* and in *Microbispora* JCM *mcherry.*** (A) *Microbispora* JCM *mlbQmcherry* on S1 medium after 5 days. The arrow shows the fluorescent ring of MlbQ-mCherry. Scale bars represent 2 µm. (B) *Microbispora* JCM *mcherry* on S1 medium after 3 days. Strong fluorescent signal in the all mycelium. Scale bars represent 2 µm.

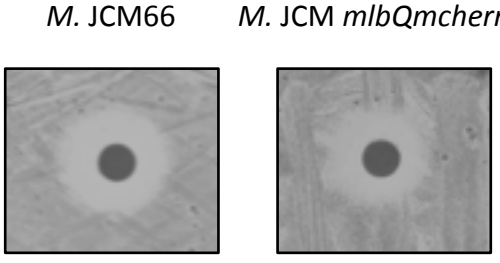


**Fig. 56. Resistance of *Microbispora* JCM66 WT and expressing *mlbQmcherry* to NAI-107.** Paper disks with 0.5 µg NAI-107.

3.4.9.3 MlbQmCherry localization in *S. coelicolor*

To further investigate the spore localization of MlbQ, pRM4.3-*mlbQmcherry* was introduced in *S. coelicolor* (*S. coelicolor mlbQmcherry*). In this heterologous host, MlbQmCherry was detected exclusively in spore chains. Any fluorescence signal was observed neither in the vegetative mycelium nor in the non-sporogenic part of the aerial mycelium (Fig. 57A). As observed in *Microbispora* JCM66, the fluorescent signal of MlbQmCherry was ring-like (Fig. 57A), probably due to the localization of the recombinant protein at the spore cytoplasmic membrane. In contrast to *S. coelicolor mlbQmcherry*, *S. coelicolor* expressing mCherry not fused to MlbQ showed a fluorescent signal already in young mycelium (Fig. 57B). Moreover, lantibiotic resistance assays were performed to compare *S. coelicolor mlbQmcherry* and the WT. As reported for *Microbispora* JCM *mlbQmcherry* (3.4.9.2), the expression of MlbQmCherry in *S. coelicolor* did not confer NAI-107 resistance (data not shown).

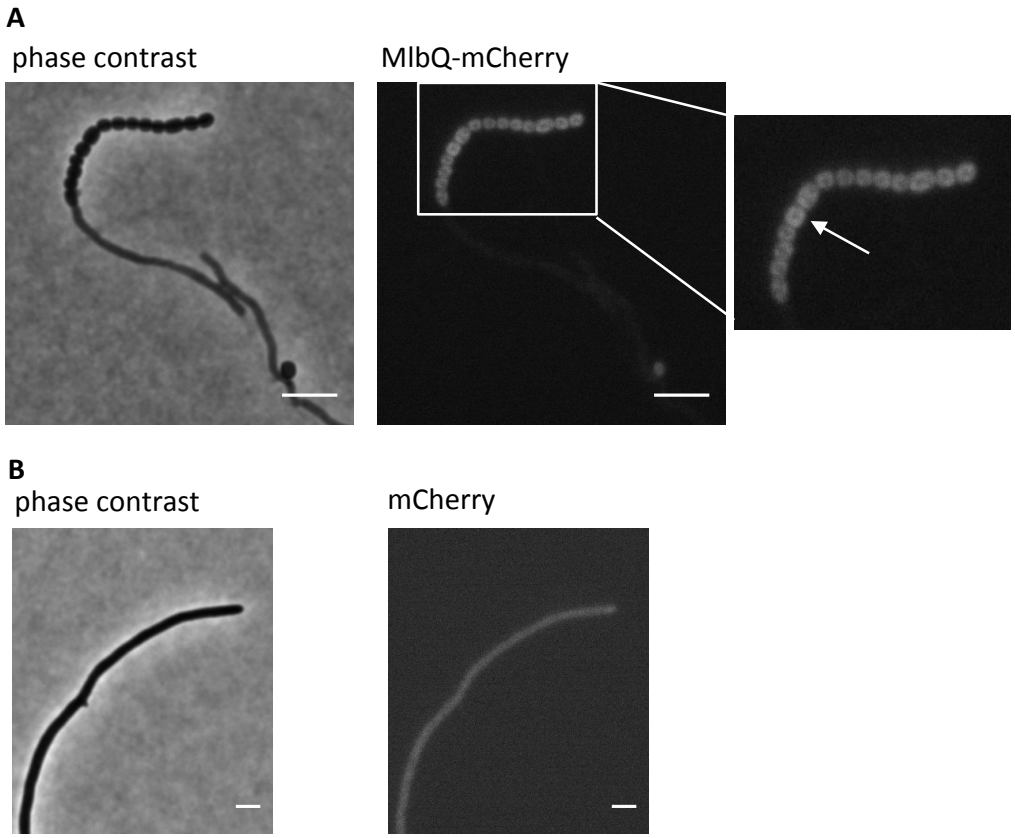


**Fig. 57. Monitoring mCherry fluorescence in *S. coelicolor mlbQmcherry* and in *S. coelicolor mcherry*.** (A) *S. coelicolor mlbQmcherry* on MS medium after 2 days. The arrow shows the fluorescent ring of MlbQ-mCherry. Scale bars represent 4 µm. (B) *S. coelicolor mcherry* on MS medium after 24 h. Strong fluorescent signal in the all mycelium. Scale bars represent 2 µm.

# 4. DISCUSSION

The development of antibiotic resistance in clinically relevant pathogens is one major obstacle to effective treatment of bacterial infections and the main reason for the urgent need of new therapeutic strategies. Lantibiotics have drawn attention as potential antibacterial drugs because of their activity in the nM range against drug-resistant Gram-positive bacteria (Cotter *et al.*, 2005). The effectiveness of lantibiotics reflects their mode of action, for most of them based on lipid II binding. A deeper understanding of lantibiotic biosynthesis has allowed to exploit this class of antibiotics by both *in vitro* and *in vivo* engineering to improve their pharmacological properties and to broaden their antibacterial spectrum (Field *et al.*, 2010). To date, few lantibiotics are reported to be in pre- or clinical phase for the treatment of bacterial infections (www.pmlive.com/pharma_news/meeting_with_resistance_ 262262).

Considering that lantibiotics might be introduced into the clinic as antibacterial agents in the next years, emerging resistance in pathogens has to be taken into account. The only example of lantibiotic present on the market is nisin, used since over 50 years as food preservative. Despite the wide use of this compound, no cases of resistance in food spoilage bacteria had been described. However, *in vitro* studies have shown a high nisin resistance potential for *Listeria monocytogenes* and *S. aureus* (Gravesen *et al.*, 2002; Blake *et al.*, 2011). The fact that nisin is still considered safe for food preservation indicates that the development of resistance is minimal in food systems.

## 4.1 NAI-107 resistance and production in *Microbispora* sp. 107891

The interest in the lantibiotic NAI-107 as therapeutic agent has been arisen because of its superior antibacterial potency against resistant Gram-positive bacteria in comparison with vancomycin and linezolid (Jabes *et al.*, 2011). Pre-clinical studies proved the efficacy of NAI-107 treatment in animal models of infection with MRSA and VRE (Jabes *et al.*, 2011; Lepak *et al*., 2015). Moreover, NAI-107 resistant mutants were not observed during *in vitro* studies with multidrug resistant pathogens. Considering as a long-term

goal the introduction of NAI-107 into the clinic, efforts have to be focused in the prediction of resistance mechanisms in pathogenic bacteria.

Since antibiotic-producing bacteria have been indicated as the natural reservoir of resistance determinants (Wright, 2010), in the present study an analysis of NAI-107 resistance in the NAI-107 producer *Microbispora* sp. 107891 was conducted. In contrast to glycopeptides and β-lactams, for which resistance gene determinants were firstly studied in pathogenic bacteria, the research of lantibiotic resistance genes initially focused on producer strains (Draper *et al.*, 2008).

Determination of the minimal inhibitory concentration (MIC) of NAI-107 showed that *Microbispora* sp. 107891 is not highly resistant to its own lantibiotic. The mycelium is sensitive to 10 µg/ml NAI-107 and a significant decrease in the colony forming units is observed already at 0.1 µg/ml NAI-107. The spores are 10 times more sensitive to NAI-107 (MIC 1 µg/ml) than the mycelium. This observation is not unexpected, since the germination of spores is inhibited by some antibiotics. For instance, the peptidoglycan-targeting antibiotics nisin and oritavancin have been shown to interfere with spore germination and outgrowth (Gut *et al.*, 2011; Chilton *et al.*, 2013). *Microbispora* sp. 107891 does not sporulate as observed for *Microbispora* JCM66, a *Microbispora* sp. producing neither NAI-107 nor any other lantibiotic. *Microbispora* sp. 107891 forms bulges at the tip of the hyphae resembling immature spores that might indicate the capability of NAI-107 to interfere with sporulation. The low resistance level of *Microbispora* sp. 107891 is not unexpected. Other lantibiotic producer strains are partially susceptible to their own products. *Staphylococcus epidermidis* Tü3298 grows up to 1.8 µg/ml epidermin (Peschel and Götz, 1996), while the MIC of nisin A for *L. lactis* NZ9700 is 25 µg/ml (Kuipers *et al.*, 1993). This could reflect the efficacy of these antibacterials, thus the difficulty of the producer strains to counteract their action.

Lantibiotic autotoxicity has represented an obstacle for the improvement of fermentation processes. To overcome this problem, a two-step process was established for the overproduction of gallidermin. Gallidermin was produced as inactive precursor peptide and successively activated by enzymatic cleavage of the leader peptide (Valsesia *et al.*, 2007). In the case of NAI-107, the partial sensitivity of *Microbispora* sp. 107891 to NAI-107 does not obstacle NAI-107 production to high titres. In optimized conditions,

*Microbispora* sp. 107891 is able to produce up to 1 g/l in the 107PH1 medium (Monciardini, personal communication). Experiments conducted in flasks showed that NAI-107 concentration increased upon time (96-168 h), although the biomass did not. The ability of *Microbispora* sp. 107891 to produce high NAI-107 titres in 107PH1 is probably medium-dependent. 107PH1 contains high amounts of hydrophobic components (olive oil and soybean meal), which may capture NAI-107 from the medium and allow *Microbispora* sp. 107891 to reach high NAI-107 titres during fermentation. 107PH1 medium is indeed able to sequester about 85% of NAI-107. The hydrophobic components of the medium would function as an adsorbent resin, apparently allowing *Microbispora* sp. 107891 to overcome its sensitivity to NAI-107.

## 4.2 Gene manipulation of *Microbispora* sp. 107891

Gene manipulation is an alternative strategy to enhance antibiotic productivity besides improvement of culture conditions. In this regard, one of the exploited approaches is the increase of resistance by overexpression of resistance determinants, a strategy employed by bacteria to adapt to antibiotics (Sandegren and Andersson, 2009). A similar strategy was pursued for *Microbispora* sp. 107891. In order to conduct genetic analyses and gene overexpression experiments, *Microbispora* sp. 107891 had to be genetically manipulated. DNA transfer in *Microbispora* sp. 107891 was achieved by a conjugation protocol set up in this study.

Several conjugation experiments were performed varying the *E. coli* donor, the period of incubation before overlay and the antibiotic used to inhibit *E. coli* growth. A successful DNA transfer was achieved using *E. coli* S17-1 as a donor strain and phosphomycin to inhibit *E. coli* growth. The protocol set up in this work differs from the one used for the model organism *S. coelicolor* (Kieser *et al.*, 2000) in the donor strain (*E. coli* S17-1 instead of *E. coli* ET12567 pUZ8002) and the antibiotic used to inhibit *E. coli* growth (phosphomycin instead of nalidixic acid).

The only strains from the *Streptosporangiaceae* family that could be genetically manipulated were *Nonomurea* ATCC 39727 and *Microbispora corallina*, for which conjugation protocols similar to the one described by Kieser *et al*., 2000 were used

(Marcone e*t al.*, 2010; Foulston and BIbb, 2010). DNA transfer in *Nonomurea* ATCC 39727 was achieved also by protoplast transformation (Marcone e*t al.*, 2010) but this protocol could not be used for *Microbispora* sp. 107891 since no protoplasts could be produced.

With the conjugation protocol established in this study, DNA transfer of a pSET152 derivative plasmid (pRM4) could be easily obtained. Thus, gene overexpression could be achieved by transfer of the integrative plasmid pRM4 carrying the gene of interest under the control of the *ermE** promoter. In contrast, gene deletion was more difficult to achieve. The common difficulties encountered in obtaining deletion mutants in *Actinomycetes* spp. were exacerbated by the poor sporulation and low frequency of homologous recombination in *Microbispora* sp. 107891. In addition, the slow growth rate of the strain did not support the construction of deletion mutants. About 10-15 days are required to obtain a considerable amount of *Microbispora* sp. 107891 mycelium from a single colony. Hence, the GUS reporter system (Myronovskyi *et al.*, 2011) was used to facilitate clone selection and to avoid the tedious and time-consuming work of colony picking.

## 4.3 The peptidoglycan of *Microbispora* sp. 107891

An important target of antibiotic therapy is peptidoglycan, a fundamental component of the bacterial cell wall. Several steps of PG biosynthesis have been widely exploited for the development of new or improved antibacterial agents and they are still a main focus of antibiotic research (Bugg *et al.*, 2011; Ling *et al.*, 2015). Among the targets under investigation, lipid II is playing an important role, being target of several classes of antibacterials including lantibiotics (Breukink and de Kruijff, 2006). The search for new antibiotics is driven by the emergence of resistant pathogens that do not respond to the antibacterial treatments currently employed in clinic. Several mechanisms conferring resistance to PG targeting antibiotics have been well documented (Rice, 2012). One of the strategies to overcome antibiotic efficacy is target modification. In this regard, reprogramming of PG biosynthesis leading to glycopeptide resistance has been described (Healy *et al.*, 2000).

### 4.3.1 Muropeptide composition and cell wall ultrastructure of *Microbispora* sp. 107891

The lantibiotic NAI-107 interferes with the late stages of PG biosynthesis by binding lipid II (Münch *et al.*, 2014). Analysis of immunity in the producer strain *Microbispora* sp. 107891 initially focused on PG structure to determine if PG modifications are responsible for the protection of *Microbispora* sp. 107891 from NAI-107. Therefore, a detailed PG structural analysis combining amino acid analysis, high performance liquid chromatography (HPLC) and mass spectrometry (LC/MS) was carried out.

Amino acid analysis of PG was performed taking advantage of amino acid derivatization with the fluorescent reagent Opa. The analysis revealed the presence of the following amino acids: Ala, Glu, $A_2$pm, Gly and Ser. In contrast, Nukajima and co-workers reported only the presence of the amino acids Ala, Glu and $A_2$pm during a taxonomical study of *Microbispora* JCM66 and *Microbispora* JCM67 (Nukajima *et al.*, 1999). The different amino acids composition of PG was speculated to be due to the media used for bacterial growth. However, Nukajima and co-workers grew *Microbispora* spp. in a complex medium (10 g/l glucose, 10 g/l yeast extract, pH 7.2) similar in composition to KV6, the medium used to grow *Microbispora* sp. 107891. Thus, it is unlikely that the presence of Gly and Ser in the PG of *Microbispora* sp. 107891 is medium-dependent, rather the two amino acids are specifically incorporated in the PG of *Microbispora* sp. 107891. Alternatively, Gly and Ser could not be identified by Nukajima and co-workers, since they used the less sensitive ninhydrin reagent for amino acid analysis.

To explore the diversity of *Microbispora* sp. 107891 PG structure, PG from exponentially growing bacteria was digested with mutanolysin and the resulting muropeptides were analysed by HPLC and LC/MS. The structure of the muropeptides was initially assigned according to their *m/z* values. LC/MS analysis showed the presence of a muropeptide at *m/z* 1012.5, which was considered to be the monomer pentapeptide GlcNAc-MurNAc-L-Ala-γ-D-iGln-*meso*-$A_2$pm-D-Ala-D-Ala, according to the PG composition reported for *E. coli* and *Microbispora* spp. (Schleifer and Kandler, 1972; Nukajima *et al.*, 1999). The structure of the monomer pentapeptide was confirmed by $MS^3$ fragmentation and the corresponding tri- (*m/z* 870.4) and tetrapeptides (*m/z* 941.4) were detected in the ion chromatogram. In addition, tetrapeptides and pentapeptides ending in Gly or Ser were identified. The muropeptide monomers from *Microbispora* sp. 107891 were fully

amidated at $Glu^2$. This PG modification was described to reduce the susceptibility of *S. aureus* towards the defensin plectasin (Münch *et al*., 2012). To determine if the amidation of $Glu^2$ contributes to immunity in *Microbispora* sp. 107891, Daniela Münch (Institute of Medical Microbiology, University of Bonn) tested the complex formation of NAI-107 with a lipid II variant containing iGln instead of Glu. The *in vitro* studies showed no effects of iGln on the binding affinity of NAI-107 to lipid II (Münch D., personal communication). Thus, the α-carboxylic group of $Glu^2$ is not crucial for NAI-107 binding and its amidation was not considered to be a resistance mechanism.

Besides the PG composition, the cell wall ultrastructure of *Microbispora* sp. 107891 was analysed. A previous work on nisin resistant variants of *Listeria innocua* showed a marked thickening of the cell wall, which possessed an irregular surface (Maisnier-Patin and Richard, 1996). A thicker cell wall might reduce lantibiotic diffusion, thereby decreasing the number of molecules that reach the cytoplasmic membrane. To verify this hypothesis for *Microbispora* sp. 107891, transmission electron microscopy was performed. The cell wall thickness of *Microbispora* sp. 107891 was compared with the one of the non-producer strain *Microbispora* RP0 but no differences in the cell envelope were detected.

### 4.3.2 The origin of PG muropeptides diversity

The variety of muropeptide monomers found in *Microbispora* sp. 107891 PG could be explained by diversification of PG biosynthesis at both early and late stages of PG assembly. To assess if Gly and Ser are introduced into the PG at the early step of PG biosynthesis, UDP-linked PG precursors analysis was carried out. UDP-linked PG precursors were accumulated in the cytoplasm of *Microbispora* sp. 107891 by bacitracin treatment and analysed by LC/MS. The composition of the stem peptide of UDP-linked PG precursors was then compared with the one of PG muropeptides. *Microbispora* sp. 107891 possesses UDP-MurNAc pentapeptides ending in Ala, Gly or Ser that reflect the diversity of monomeric pentapeptides found in the PG. The presence of different amino acids at the fifth position of the stem peptide of muropeptides was explained by an unspecific activity of the Ddl ligase, as previously described (Sato *et al.*, 2006).

The analysis of UDP-linked PG precursors revealed also the presence of UDP-MurNAc tetrapeptides. Differently from UDP-MurNAc pentapeptides, the PG precursors UDP-

MurNAc tetrapeptides contain exclusively Ala at the terminal position of the stem peptide. The presence of Gly and Ser at the fourth position of monomeric tetrapeptides in the PG was therefore considered the result of reactions that occur at later stage of PG biosynthesis instead of the activity of a MurF homolog lacking substrate specificity.

### 4.3.3 L,D-transpeptidase action and PG remodelling

The dimeric muropeptides detected in *Microbispora* sp. 107891 PG reflect the variety found in monomeric muropeptides. Dimeric muropeptides containing a disaccharide tripeptide as acyl donor were suggested to harbour 3-3 cross-links instead of the classical 4-3 cross-links. For these muropeptides any other structure could not be hypothesized. Besides these muropeptides, *Microbispora* sp. 107891 possesses muropeptides with 4-3 cross-links.

The action of LDTs in the formation of 3-3 cross-links was suggested, thus the genome of *Microbispora* sp. 107891 was screened to identify LDT homologs. BlastP analysis revealed that *Microbispora* sp. 107891 possesses at least five genes encoding putative LDTs. The activity of LDTs was previously reported for some members of the order *Actinomycetales* (Lavollay *et al.*, 2008; Hugonnet *et al.*, 2014) but not described before for lantibiotic producers. In *Mycobacterium tuberculosis,* the increased level of 3-3 cross-links during the stationary phase suggested a role of LDTs in the adaptation of the strain to the absence of *de-novo* synthesized PG precursors (Lavollay *et al.*, 2008). On the other hand, *Nonomurea* ATCC 39727 has a significant proportion of 3-3 cross-links both in exponential and stationary phase, similarly to *Microbispora* sp. 107891. In *Nonomurea* ATCC 39727 the formation of 3-3 cross-links besides the classical 4-3 cross-links was suggested to be a mechanism of tolerance to the produced glycopeptide A40926 (Hugonnet *et al.*, 2014). In *Microbispora* sp. 107891, LDTs activity was attribute to a general mechanism of resistance against PG-targeting antibiotics (4.3.5).

LDTs were also reported to catalyse the exchange of D-Ala$^4$ for Gly or other D-amino acids, a reaction in competition with the formation of 3-3 cross-links. In *Microbispora* sp. 107891, LDTs might be responsible for the substitution of D-Ala$^4$ for Gly or D-Ser. PG remodelling would therefore contribute to the diversification of *Microbispora* muropeptides.

Since the exchange of D-Ala$^4$ for Gly or D-Ser catalysed by LDTs occurs in the extracellular space, the concentration of Gly in the supernatant of *Microbispora* sp. 107891 was checked to determine if the incorporation of Gly in the stem peptide of muropeptides is due to the high amount of Gly in the medium. Amino acid analysis did not show an increasing concentration of Gly during exponential phase (0-72 h), therefore Gly incorporation in the PG was not considered linked to an accumulation of Gly in the extracellular space during growth. High concentrations of Gly in the culture medium (0.05-1.33 M) were demonstrated to affect the growth of different bacteria by altering PG composition (Hammes *et al.*, 1973). In the present study, the concentration of Gly in the medium used for PG isolation (KV6) was significantly lower (about 2.8 mM). This value suggested that the presence of muropeptides containing Gly in the fourth position of the stem peptide is not a consequence of high amounts of Gly in the medium and the same conclusion could be drawn for D-Ser. PG analysis of *Microbispora* sp. 107891 grown in different media could be planned to totally exclude an influence of medium composition on the incorporation of Gly in the PG.

*Vibrio cholera* is known to release and accumulate non-canonical D-amino acids like D-Met and D-Leu during stationary phase. The incorporation of these amino acids into the PG is important to resist to osmotic stress and to control the amount of PG per cell (Cava *et al.*, 2011). In the case of *Microbispora* sp. 107891, no significant differences were observed between mutanolysin digested PG from bacteria in the exponential or stationary phase. This observation led to the conclusion that the variety of *Microbispora* muropeptides in not dependent on the bacterial growth phase.

### 4.3.4 Formation of LDT substrates

To form 3-3 cross-links, LDTs use tetrapeptides as acyl donors instead of pentapeptides (Mainardi *et al.*, 2005). The D,D-carboxypeptidase VanY$_n$ ensures the presence of LDTs substrates in *Nonomurea* ATCC 39727 by cleaving the D-Ala$^4$-D-Ala$^5$ peptide bond of PG precursors (Binda *et al.*, 2012). UDP-linked PG precursors analysis of *Microbispora* sp. 107891 demonstrated the presence of cytoplasmic UDP-MurNAc tetrapeptides. *Microbispora* sp. 107891 encodes a D,D-carboxypeptidase with high homology to VanY proteins, which was proposed to be responsible for the generation of UDP-MurNAc tetrapeptides.

In *Enterococcus faecium*, the contribution of LDTs to PG cross-linking was demonstrated to be controlled by the availability of the substrate by the action of the D,D-carboxypeptidase DdcY. The expression of DdcY is controlled by a two-component regulatory system (DdcRS), which is encoded by genes forming the *ddc* locus, together with *ddcY* (Sacco *et al.*, 2010). Interestingly, the gene encoding the putative D,D-carboxypeptidase in *Microbispora* sp. 107891 is adjacent to genes encoding a regulatory two-component system.

### 4.3.5 PG of non-producing *Microbispora* strains

A link between PG remodelling and bacteriocin resistance was described for *L. lactis* (Roces *et al*., 2012). The hypothesis that PG remodelling found in *Microbispora* sp. 107891 plays a role in lantibiotic resistance led to the idea that a non-producer strain might consist of muropeptides different to that of the NAI-107 producer. To verify this hypothesis, the PG of the non-producer strains *Microbispora* RP0 and *Microbispora* spp. JCM66 and JCM67 was analysed. LC/MS analysis revealed the presence of the same muropeptides detected in *Microbispora* sp. 107891.

The PG structure found in *Microbispora* spp. seemed to be an intrinsic characteristic of *Microbispora* genus, rather than a mechanism of NAI-107 resistance. However, an effect of the variety of muropeptide structure on the binding affinity of NAI-107 to the target cannot be excluded. Alternatively, PG remodelling in *Microbispora* could be a general attempt to counteract the action of cell wall-targeting antibiotics produced by soil-dwelling bacteria. Overall, PG analyses indicated a high diversity of muropeptides that could not be directly associated with a mechanism of lantibiotic resistance in the producer strain *Microbispora* sp. 107891.

## 4.4 Resistance determinants encoded in the *mlb* cluster

The identification of the first lantibiotic gene clusters in the early 90's led to the discovery of lantibiotic resistance determinants encoded in biosynthetic gene clusters. A role of these genes in lantibiotic immunity was initially determined by heterologous expression experiments (Klein and Entian, 1994; Siegers and Entian, 1995; Peschel and

Götz, 1996). Successively, several lantibiotic gene clusters and cognate immunity proteins were identified (Draper *et al.*, 2008).

In the present study, the resistance determinants encoded in the NAI-107 biosynthetic gene cluster *mlb* were identified and analysed. The *mlb* cluster encodes the immunity proteins MlbQ, MlbJ and MlbYZ.

### 4.4.1 The immunity lipoprotein MlbQ

MlbQ sequence analysis revealed the presence of a conserved lipobox motif (LAGC) at the end of a predicted signal peptide, thus MlbQ was considered to be a putative lipoprotein. As part of the bacterial cell envelope, lipoproteins are involved in a variety of mechanisms like nutrient scavenging, host cell adhesion, virulence, environmental signalling and antibiotic resistance (Sutcliffe and Russell, 1995). Lipoproteins involved in lantibiotic immunity were previously described. The well studied NisI and SpaI were demonstrated to protect the respective producer strains from their own produced lantibiotic (Okuda and Sonomoto, 2011).

The function of MlbQ could not be predicted on the basis of sequence similarity, since the closest proteins found by BlastP analysis had unknown functions. Therefore, to verify the role of *mlbQ* in lantibiotic immunity, heterologous expression in *S. coelicolor* was conducted. *S. coelicolor* expressing *mlbQ* under the control of the constitutive promoter *ermE**p was compared to the WT by NAI-107 resistance assay. *mlbQ* expression conferred resistance to *S. coelicolor* against NAI-107. *mlbQ* conferred NAI-107 resistance also to *Microbispora* JCM66, a heterologous host close related to the NAI-107 producer *Microbispora* sp. 107891. Moreover, *mlbQ* gene inactivation was carried out. The *mlbQ* null mutant produced NAI-107 like the WT but its growth was impaired.

In Gram-positive bacteria, lipoproteins are anchored to the outer leaflet of the cytoplasmic membrane. After translocation *via* Sec or Tat system, proteins are anchored to the membrane by lipidation of the conserved Cys in the lipobox, a reaction catalysed by the enzyme lipoprotein diacylglycerol transferase (Lgt). Successively, a lipoprotein signal peptidase (Lsp) cleaves the signal peptide, so that the modified Cys becomes the N-terminal amino acid of the mature protein. *S. coelicolor* possesses two Lgts (SCO2034, SCO7822) and one Lsp (SCO2074) (Thompson *et al.*, 2010). BlastP analysis of *Microbispora* sp. 107891 genome revealed that *Microbispora* sp. 107891 encodes two

Lgts (ETK36501.1, WP_036323688.1) and one Lsp (WP_036321388.1), thus it possesses the genetic potential to process lipoproteins. To verify the membrane localization of MlbQ, heterologous expression of C-terminally His-tagged MlbQ in *S. coelicolor* and successive Western Blot analysis of purified membranes were carried out. The chimeric protein MlbQ-Histag was detected in *S. coelicolor* membranes and was still able to display its functionality. Apparently, MlbQ-Histag did not interfere with bacterial growth and sporulation.

Lipoproteins can be detached from the cytoplasmic membrane or can escape lipid-modification. A lipid-free version of NisI (LF-Nis) was found in the supernatant of *L. lactis* (Koponen *et al.*, 2004). A role of LF-Nis in nisin immunity was suggested, as LF-Nis has been shown to interact with nisin by surface plasmon resonance analysis (Takala *et al.*, 2006). To determine if a lipid-free form of MlbQ mediates NAI-107 immunity, secreted variants of MlbQ were generated by the substitution of the signal peptide of MlbQ with the one of Vsi (subtilisin inhibitor) or DagA (agarase), substrates of the Tat and Sec translocation system, respectively. Signal peptides of both routes of translocation were chosen because it was not known whether MlbQ was translocated *via* Tat or Sec system. MlbQ fused to Vsi or DagA signal peptide was expressed in *S. coelicolor* and the supernatant was checked by Western Blot to verify the presence of secreted MlbQ. However, MlbQ could be detected neither in the culture supernatant nor in the cell extract. The most probable explanation of this result is that the chimeric proteins were degraded due to not correct processing.

In Gram-positive bacteria, lipoproteins seem to have an equivalent role to periplasmic proteins in Gram-negative bacteria (Hutchings *et al*., 2009). This hypothesis is mostly sustained by the fact that, in Gram-positive bacteria, substrate binding proteins (SBPs) of ATP-binding cassette (ABC) transporters are typically lipoproteins (Nielsen and Lampen, 1982). To assess if the immunity role of MlbQ is fully displayed by acting as substrate-binding protein, co-expression studies with the three ABC transporters encoded in the *mlb* cluster were performed in *S. coelicolor*. *S. coelicolor* expressing MlbQ with MlbYZ, MlbTU or MlbEF was resistant to NAI-107 as the recombinant strain expressing exclusively MlbQ. This result demonstrated that MlbQ does not work in cooperation

with any of the ABC transporters that were investigated. Thus, an MlbQ mode of action independent from MlbYZ, MlbTU and MlbEF was postulated.

To verify cross-resistance, resistance bioassays using the lantibiotics 97518 and epidermin were performed. 97518 is a NAI-107-like lantibiotic with the same ring organization of NAI-107 but no 2-aminovinyl-D-cysteine motif (AviCys) at its C-terminus. Epidermin differs from NAI-107-like lantibiotics in the central region where the flexible 12-15 amino acids are substituted by a lanthionine ring in NAI-107 and 97518. Similarly to NAI-107, epidermin contains an AviCys motif. The expression of MlbQ in *S. coelicolor* conferred 97518 resistance, while no effect was observed with epidermin. This result suggests that MlbQ displays its immunity activity by recognizing the lantibiotic. The fact that epidermin, but not 97518, possesses AviCys at its C-terminal, indicates that MlbQ does not recognize this lantibiotic motif. The recognition motif was speculated to be comprised in the lanthionine rings conserved both in NAI-107 and 97518.

The 97518 biosynthetic gene cluster encodes a lipoprotein, named PlnQ, which shares amino acid sequence identity (62%) with MlbQ. Heterologous expression in *S. coelicolor* and resistance assay using the cognate lantibiotic confirmed the hypothesis. To further investigate cross-immunity, *S. coelicolor plnQ* was tested against NAI-107. PlnQ conferred resistance also to NAI-107, even in a lesser extend compared to MlbQ. Although an effect of PlnQ on NAI-107 resistance was observed, PlnQ was not as efficient as MlbQ. Notably, NAI-107 is a lantibiotic that possesses more post-translational modifications than 97518 (e.g. Cl-Trp and OH-Pro), thus PlnQ might not be able to interact with NAI-107 like MlbQ. Lantibiotic cross-resistance was previously reported for the membrane-associated proteins PepI and EciI encoded in the Pep5 and epicidin 280 lantibiotic clusters from *Staphylococcus epidermidis* 5 and *Staphylococcus epidermidis* BN280, respectively (Heidrich *et al*., 1998). In contrast, NisI did not confer resistance to subtilin, a lantibiotic with an identical organization of the thioether rings (Stein *et al*., 2003).

These studies indicate that the structure of the lantibiotic is crucial for the immunity mechanism of MlbQ. To investigate MlbQ mechanism on a molecular level, the structure of MlbQ was solved by NMR. MlbQ fused to an N-terminal His-tag was expressed in *E. coli* as a $^{15}N$,$^{13}C$-labelled protein. Purification steps were optimized to obtain a high

amount of pure protein to subject to NMR analysis, which was carried out at the MPI in Tübingen. MlbQ possesses an unstructured N-terminal region followed by a globular domain. A hydrophobic core built around a Trp residue (W77) is characteristic of the protein structure, which does not shares similarity to known folds (Fig. 51A). W77 is conserved in PlnQ and in MlbQ homologs encoded by uncharacterized lantibiotic gene clusters. F54 and Y62, whose aromatic rings appear to border the hydrophobic core on one site, are also conserved. Moreover, 2 conserved Cys residues form a disulphide bond that presumably stabilizes the structure. MlbQ does not show structural similarity to SpaI from *B. subtilis*, the only other lantibiotic immunity protein of known structure (Christ *et al*., 2012). SpaI consists mainly of β-sheet. It possesses an unstructured and flexible N-terminus in solution followed by a structured core of six β-strands and two α-helices. The N-terminus interacts with membranes and seems to form α-helices in presence of liposome. SpaI was proposed to bind its cognate lantibiotic, subtilin, via an extended hydrophobic patch on its surface. Looking for a similar feature on MlbQ, an analogous surface patch was located bounded by the β1-β2 loop, α3 and the structured, conserved hydrophobic section of the N-terminal loop (P55-N64), which runs antiparallel to β1 (Fig. 50B). The extended shape of the patch and its length (~16 Å) are comparable to that in SpaI. The low solubility of the lantibiotic in the NMR buffers precluded mapping of the potential interaction sites for SpaI (Christ *et al*., 2012). Similar problems were encountered for MlbQ, thus interaction studies were attempted with the more soluble lantibiotic 97518. Under the conditions used in this study, no interaction between MlbQ and 97518 was detected. To get insights into the mechanism of action of MlbQ, interaction experiments between the MlbQ homolog PlnQ and its cognate lantibiotic 97518 were carried out. Despite several attempts to obtain the protein, PlnQ could not be purified in its folded state. The expression as an N-terminal His-tag protein in *E. coli* using the vector pET30 was successful but the protein was not correctly folded, as shown by CD spectroscopy and NMR analysis. Alternatively, MlbQ expression using the vector pJOE2275 was pursued to obtain a C-terminal His-tag protein. This approach failed since no protein expression could be detected. The difficulties encountered to perform interaction studies could not be overcame, especially because of the extreme poor solubility of NAI-107 in aqueous buffers. In any case, the solving of MlbQ structure

provided interesting insights of a possible MlbQ mode of action. The conserved amino acids W35, F54 and Y62 seem to be important for MlbQ functionality by forming a hydrophobic pocket, which might capture NAI-107. Mutagenesis studies could be performed in future studies considering that the indicated amino acids might be crucial not only for MlbQ action but also for its folding.

To monitor MlbQ localization by fluorescence microscopy, MlbQ was fused at the C-terminal with mCherry. The chimeric fluorescent protein was expressed in *Microbispora* Δ*mlbQ* and in the heterologous hosts *Microbispora* JCM66 and *S. coelicolor*. *Microbispora* Δ*mlbQ* was chosen instead of the WT to avoid competition between the chimeric protein and the native one for the lipoprotein processing enzymes. The expression of MlbQ-mCherry did not show a strong fluorescence signal in *Microbispora* Δ*mlbQ mlbQmcherry* mycelium. Unexpectedly, the fusion protein localized at spores in *Microbispora* JCM66 and *S. coelicolor*. The fact that a ring-like fluorescent signal was detected confirmed the membrane localization of the protein. A similar ring-like fluorescent signal was observed for the lantibiotic immunity peptide PepI fused to GFP in *Staphylococcus carnous* (Hoffmann *et al.*, 2004). Differently to spores, the mycelium of *Microbispora* JCM66 and *S. coelicolor* showed a weak or none fluorescent signal.

The spore localization of MlbQ initially suggested an involvement of MlbQ in spore formation. Lipoproteins involved in sporulation were described in both *Firmicutes* and *Actinobacteria* (Bagyan *et al.*, 1998; Tzanis *et al.*, 2014). However, since *Microbispora* sp. 107891 does not efficiently sporulate and *Microbispora* JCM66 does, a role in spore formation in *Microbispora* spp. was discarded. Indeed, *Microbispora* JCM66 does not possess MlbQ homologs.

MlbQ-mCherry localization preferentially in spores might be due to protein interaction or protein recruitment to specific membrane regions. The fact that MlbQ loses its immunity activity by mCherry fusion, might argue against a physiological localization of the fusion proteins. However, it is not surprising that the fusion of a 106 aa protein with mCherry (235 aa) affects its functionality. If MlbQ plays a role in the spore compartment is not clear. In this regards, further investigations are complicated by the fact that *Microbispora* sp. 107891 does not sporulate under standard laboratory conditions. However, the strain could still be able to sporulate in the natural environment upon

adverse conditions. The production of NAI-107 appeared to impair sporulation. If this is the case, the localization of the immunity protein MlbQ in spores could be an extreme attempt to protect the strain from its product. In any case, the fluorescent localization experiments carried out in this study led to the following considerations. First, MlbQ-mcherry spore localization does not depend on the presence of the lantibiotic, as the heterologous host *Microbispora* JCM66 does not produce NAI-107. Second, MlbQ-action is independent from the NAI-107 target lipid II, because MlbQ could not be detected at the apical tips of mycelium. Fluorescent vancomycin staining of nascent PG of *S. coelicolor* showed that the PG precursor lipid II is prevalently localized at the apical tips (Sigle *et al.*, 2015), where PG biosynthesis in filamentous bacteria occurs (Flärdh *et al*., 2012).

### 4.4.2 The immunity proteins MlbJ, MlbY and MlbZ

Heterologous expression studies in *S. coelicolor* revealed a role of MlbJ and MlbYZ in NAI-107 immunity. The expression of *mlbJ* conferred a slight NAI-107 resistance to *S. coelicolor*, whereas *mlbYZ* did no show any effect. Notably, the effect of MlbJ on NAI-107 resistance significantly increased in presence of MlbYZ, thus cooperativity between these immunity proteins was suggested. In this study, a model in which MlbJ acts as substrate-binding protein was proposed. The fact that the expression of MlbJ alone confers a low NAI-107 resistance, suggests that MlbJ might intercept the lantibiotic from the extracellular space. MlbJ contains several predicted membrane-spanning regions. According to its hydrophobicity profile and function, MlbJ was classified in the LanH proteins.

LanH proteins are accessory proteins that act with the immunity ABC transporters LanFEG. These proteins do not share amino acid sequence similarity and the classification is only based on their functionality (Okuda and Sonomoto, 2011). One of the best characterized LanH protein is NukH, a transmembrane protein from *Staphylococcus warneri* encoded downstream *nukFEG*. NukH recognizes the lantibiotic nukacin ISK-1 at its C-terminal and was proposed to transfer the lantibiotic to the ABC transporter NukFEG. The latter one was shown to contribute to immunity by pumping the lantibiotic to the extracellular space in an energy-dependent manner, thereby

decreasing the lantibiotic concentration in proximity of the cytoplasmic membrane (Okuda *et al*., 2008).

The hypothesis that MlbJ acts as substrate-binding protein for MlbYZ implies an interaction between proteins. The interaction of MlbJ, MlbY and MlbZ was analysed by bacterial two-hybrid system (Karimova *et al.*, 1998) by Paul Schwarz during an internship in our laboratory. All the tested chimeric protein combinations did not show any interaction. Since MlbJ and MlbY are transmembrane proteins with several membrane-spanning regions, truncated variants of *mlbJ* and *mlbY* were used but also in this case any interaction could not be observed. Despite this result, an interaction of MlbJ and mlbYZ could not be excluded, since the bacterial two-hybrid system often fails to detect interaction between transmembrane proteins. Alternatively, protein interactions could be analysed by Blue Native PAGE, cross-linking experiments or co-immunoprecipitation.

*mlbJ*, *mlbY* and *mlbZ* lay in an operon with *mlbO*, a gene encoding a cytochrome P450, considered to hydroxylate Pro14 in NAI-107. This observation suggested an immunity role of *mlbJYZ* against the hydroxylated congeners of NAI-107. However, this hypothesis was discarded by the observation that the planosporicin cluster (*psp*) contains *mlbJYZ* homologs (*pspJYZ*) but it does not include an *mlbO* homolog (Sherwood *et al*., 2013).

PspJ and PspYZ were proposed to be involved in the regulation of lantibiotic biosynthesis (Sherwood and Bibb, 2013). The conservation of *pspJYZ* and *pspXW* homologs in actinomycetes genomes (e.g. *Nocardia brasiliensis*, *Thermobispora bispora*, *Streptosporangium roseum*, *Frankia* sp.) and their close proximity strongly suggested a functional linkage. *pspX* encodes an extracytoplasmic function (ECF) sigma factor and *pspW* an anti-sigma factor which were described to control lantibiotic biosynthesis. Planosporicin was suggested to increase in a feed-forward mechanism the lantibiotic production by activating the sigma factor PspX. The lantibiotic was suggested to provoke conformational changes of the anti-sigma factor PspW directly or indirectly (through cell wall stress), thereby leading to the release of PspX (Sherwood and Bibb, 2013). A more complex regulatory model was hypothesized for the release of MlbX, homolog of PspX (Foulston, 2010). The model is based on the regulated intramembrane proteolysis of sigma factors, well studied for RsiW in *Bacillus subtilis* (Heinrich *et al.*, 2009). In this model, the release of the sigma factor is obtained by the action of two proteases (PrsW

and RasP) that cleave RsiW and by an ABC transporter (EcsAB), whose exact function is still unknown. Therefore, a model for microbisporicin regulation that implies the action of MibJ and MibYZ in the proteolitic degradation of MibW was proposed. The role suggested for PspJ and MibJ is speculative, rather than based on genetic and/or biochemical analyses.

In contrast, the co-expression studies reported in this work demonstrated a role of MlbJ in lantibiotic resistance. The fact that *pspJYZ* and *pspWX* homologs are present in several *Actinobacteria* (Sherwood *et al*., 2013), either in NAI-107-like putative lantibiotic biosynthetic gene clusters or as independent system, suggests a role of *pspJYZ* homologs in NAI-107-like lantibiotic resistance. The presence of *pspJYZ* homologs in close proximity to *pspXW* homologs may be explained by a sigma factor-dependent transcriptional regulation of *pspJYZ* homologs. Thus, the ECF sigma factor/anti-sigma factor complex (XW) may sense the lantibiotic in the extracellular space and activate the transcription of the *JYZ* immunity operon.

### 4.4.3 The *mlb* cluster encodes two resistance determinants

NAI-107 immunity in *Microbispora* sp. 107891 is based at least on the two distinct resistance determinants MlbJYZ and MlbQ, both encoded in the *mlb* cluster. The action of two resistance determinants, which work independently, might reflect the extreme attempt of *Microbispora* sp. 107891 to counteract the action of the potent lantibiotic NAI-107. Despite the expression of these immunity proteins, *Microbispora* sp. 107891 does not reach a high immunity level (4.1).

Two resistance determinants were also identified in lantibiotic-producing *Firmicutes*. The nisin cluster (nis) encodes the lipoprotein NisI and the ABC transporter NisFEG, both contributing to nisin immunity (Stein *et al*., 2003). NisI and NisFEG homologs were found in the subtilin cluster (*spa*) (Stein *et al*., 2005). NisFEG and SpaFEG do not require the action of another immunity protein to be functional, differently to MlbYZ, for which an effect on NAI-107 resistance was observed only in the presence of MlbJ. Other lantibiotic gene clusters encode a single resistance determinant. For instance, the epidermin cluster (*epi*) encodes a LanFEG homolog (Peschel and Götz, 1996) whereas the pep5 gene cluster (*pep*) expresses exclusively the membrane-associated peptide PepI, which confers full immunity to the producer (Hoffmann *et al.*, 2004).

## 4.5 The ABC transporters MlbTU, MlbEF and the BcrA homolog ETK33189.1

Besides MlbYZ, the *mlb* cluster encodes the ABC transporter MlbTU and MlbEF. To determine if *mlbTU* and *mlbEF* play a role in lantibiotic immunity, heterologous expression in *S. coelicolor* was conducted. The expression of MlbTU and MlbEF did not showed any effect on NAI-107 resistance, neither alone nor in presence of MlbJ or MlbQ. To gain insights into the role of *mlbTU* and mlbEF, RT-PCR analysis was performed in *Microbispora* sp. 107891 and in the non-producer strain *Microbispora* RP0 to assess whether *mlbTU* and *mlbEF* expression is dependent on NAI-107 production. In both strains, gene expression was observed from 8 h to 96 h. *mlbTU* and *mlbEF* expression was considered not dependent on NAI-107 production, since it was detected both in the non-producer strain *Microbispora* RP0 and in the early exponential phase of the WT.

MlbEF and MlbTU homologs were previously described (Foulston and Bibb, 2010, Sherwood *et al.*, 2013). The microbisporicin cluster from *Microbispora corallina* NRRL 30420 (*mib*) encodes the MlbEF homolog MibEF. The deletion of *mibEF* results in a delayed and markedly reduced level of lantibiotic production, thus it was initially speculated a MibEF involvement in either immunity or lantibiotic export (Foulston and Bibb, 2010). MIbF and MibF, the ATPases of the two homologs ABC transporters, contain an E-loop, motif that is conserved in ABC transporters involved in lantibiotic immunity (Okuda *et al.*, 2010). This observation supported the idea that MlbEF and MibEF are immunity proteins. MibEF expression in *S. coelicolor* conferred a certain degree of NAI-107 resistance (Fernardez-Martinez, personal communication). A similar result was obtained by expressing the MlbEF-homolog ABC transporter PspEF from *P. alba* in *S. coelicolor* and testing the recombinant strain against the lantibiotic planosporicin (Sherwood *et al.*, 2013). As reported above, the expression of MlbEF in *S. coelicolor* did not shown any effect on NAI-107 resistance and the same result was obtained expressing MlbEF in *Microbispora* JCM66. The role of MlbEF in *Microbispora* sp. 107891 is still unclear. Although a role in lantibiotic immunity seems most likely, this study did not provide any experimental evidence. Further investigations on MlbEF and MlbEF homologs would enable a better understanding of the function of these ABC transporters.

In the microbisporicin cluster the *mibT* and *mibU* genes are co-transcribed with genes encoding synthesizing enzymes, forming the operon *mibBCDTUV* (Foulston and Bibb, 2010). Since the gene organisation in the *mlb* gene cluster is identical, the same transcriptional unit could be supposed and therefore, a role of MlbTU as exporter was speculated.

Overexpression studies in *Microbispora* sp. 107891 were performed to check if the overexpression strains produce more NAI-107. An increase in lantibiotic production was expected considering a role of the overexpressed genes in either lantibiotic immunity or export. However, a significant difference between the WT and the overexpression strains in NAI-107 production was not detected. The expression of *epiFEG*, an ABC transporter from the epidermin biosynthetic gene cluster involved in lantibiotic immunity, in the heterologous host *S. carnosus* led to a fivefold increase of the amount of epidermin detected in the culture supernatant (Peschel and Götz, 1996). The observed effect have been attributed to the action of EpiFEG rather than to an increased lantibiotic production, which would have been more correctly estimated by measuring the total amount of lantibiotic, both in the supernatant and attached to the membrane.

Proteomic analysis of *Microbispora* sp. 107891 revealed an up-regulation of MlbZ and MlbF during NAI-107 production (Gallo G., personal communication). Up-regulation was also observed for the BcrA homolog ETK33189.1 in *Microbispora* sp. 107891. BcrA is the ATPase of the ABC transporter involved in bacitracin immunity. The up-regulation of ETK33189.1 in *Microbispora* sp. 107891 during NAI-107 production suggests a role of this ABC transporter in NAI-107 resistance. Phylogenetic tree analysis indicates that BcrAB-type transporters are ancestral to LanFEG-type ones. Since no experimental evidences are available on the mechanism of transport for BcrAB, a transport mechanism similar to the one of LanFEG-type transporters was assumed (Gebhard, 2012). The expression of BcrAB in *Bacillus licheniformis* was demonstrated to be regulated by the two-component regulatory system BacRS (Neumüller *et al.*, 2001). The hypothesis that the regulation of ETK33189.1 is mediated by a two-component system is plausible. In this case, cell-wall stress induced by NAI-107 could activate the regulatory system. If BcrAB is really involved in NAI-107 resistance, its activity would support the action of the immunity proteins encoded in the *mlb* cluster.

# 5. SUPPLEMENTARY MATERIAL

## 5.1 General Abbreviations

| | |
|---|---|
| **A** | Adenine |
| **aa** | Amino acid |
| **Abu** | α-aminobutyrate |
| **AC** | Adenylate Cyclase |
| **ADP** | Adenosine diphosphate |
| **Amp** | Ampicillin |
| **$A_2$pm** | Diaminopimelic acid |
| **Apra** | Apramycin |
| **APS** | Ammonium persulfate |
| **ATP** | Adenosine triphosphate |
| **AviCys** | S-aminovinyl-D-cysteine |
| **BLAST** | Basic Local Alignment Search Tool |
| **Bp** | Base pair(s) |
| **BPB** | Bromophenol blue |
| **BSA** | Bovine Serum Albumin |
| **C** | Cytosine |
| **cAMP** | Cyclic adenosine monophosphate |
| **CD** | Circular Dichroism |
| **cDNA** | Complementary DNA |
| **CFU** | Colony Forming Unit |
| **CIAP** | Calf Intestinal Alkaline Phosphatase |
| **Cm** | Chloramphenicol |
| **C-terminal** | Carboxy-terminal |
| **Da** | Dalton |
| **Dha** | 2,3-didehydroalanine |

| | |
|---|---|
| **Dhb** | (Z)-2,3-didehydrobutyrine |
| **DMSO** | Dimethyl sulfoxide |
| **DNA** | Deoxyribonucleic acid |
| **DNase** | Deoxyribonuclease |
| **dNTP** | Deoxyribonucleoside triphosphate |
| **DPC** | n-dodecylphosphocholine |
| **ECF** | Extracytoplasmic function |
| **EDTA** | Ethylenediaminetetraacetic acid |
| **EIC** | Extracted Ion Chromatogram |
| **EtBr** | Ethidium bromide |
| **EtOH** | Ethanol |
| **G** | Guanine |
| **g** | Gram |
| ***g*** | Acceleration of gravity |
| **gDNA** | Genomic DNA |
| **GISA** | Glycopeptide-intermediate *Staphylococcus aureus* |
| **GlucNAc** | N-acetyl glucosamine |
| **h** | Hour |
| **HPLC** | High Pressure Liquid Chromatography |
| **HRP** | Horseradish Peroxidase |
| **Hyg** | Hygromycin |
| **iGln** | Isoglutamine |
| **IPTG** | Isopropyl-β-D-thiogalactopyranoside |
| **k** | Kilo |
| **Kan** | Kanamycin |
| **kb** | Kilobase |
| **kDa** | Kilodalton |
| **l** | Liter |
| **Lan** | Lanthionine |
| **LB** | Luria-Bertani |
| **LDT** | L,D-transpeptidase |

| | |
|---|---|
| **Lgt** | Diacylglycerol transferase |
| **Lsp** | Lipoprotein signal peptidase |
| **M** | Marker |
| **M** | Molar |
| **mA** | Milliampere |
| **MCS** | Multiple-cloning site |
| **MeLan** | Methyllanthionine |
| **MIC** | Minimal Inhibition Concentration |
| **min** | Minute |
| **mRNA** | Messenger RNA |
| **MRSA** | Methicillin-resistant *Staphylococcus aureus* |
| **MS** | Mass spectrometry |
| **MurNAc** | N-acetyl muramic acid |
| **MW** | Molecular weight |
| ***m/z*** | Mass-to-charge ratio |
| **Nal** | Nalidixic acid |
| **NBD** | Nucleotide-Binding Domain |
| **nm** | Nanometer |
| **NMR** | Nuclear Magnetic Resonance |
| **N-terminal** | Amino-terminal |
| **nt** | Nucleotides |
| **OD** | Optical density |
| **Opa** | *o*-phthaldialdehyde |
| **PBP** | Penicillin Binding Protein |
| **PC** | Phenol:chloroform:isoamyl alcohol |
| **PCR** | Polymerase Chain Reaction |
| **PG** | Peptidoglycan |
| **PMV** | Packed Mycelium Volume |
| **RNA** | Ribonucleic acid |
| **rRNA** | Ribosomal RNA |
| **RNase** | Ribonuclease |

| | |
|---|---|
| **rpm** | Revolution per minute |
| **RT** | Retention time |
| **RT-PCR** | Reverse Transcriptase Polymerase Chain Reaction |
| **s** | Second |
| **SBP** | Substrate Binding Protein |
| **SDS** | Sodium Dodecyl Sulfate |
| **Spc** | Spectinomycin |
| **Str** | Streptomycin |
| **T** | Thymine |
| **TCA** | Trichloroacetic acid |
| **TEM** | Transmission Electron Microscopy |
| **TEMED** | N,N,N',N'-tetramethylethylenediamine |
| **TMB** | Transmembrane Domain |
| **Tmp** | Trimethoprim |
| **Tris** | Tris(hydroxymethyl)aminomethane |
| **U** | Unit |
| **UV** | Ultraviolet |
| **v** | Volume |
| **V** | Volt |
| **VRE** | Vancomycin-resistant enterococci |
| **WCB** | Working Cell Bank |
| **WT** | Wild-type |
| **WTA** | Wall Teichoic Acids |
| **X-Gluc** | 5-bromo-4-chloro-3-indolyl-β-D-glucopyranosiduronic acid |
| **Δ** | Deletion |
| **µg** | Microgram |
| **µl** | Microliter |

## 5.2 MS$^3$ of *Microbispora* sp. 107891 muropeptide monomers

### 5.2.1 MS$^3$ of the monomeric pentapeptide Penta(Ala)

**A**

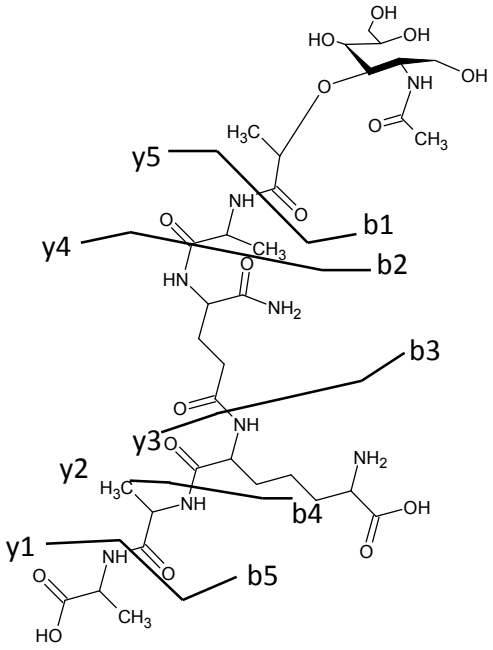


**B**

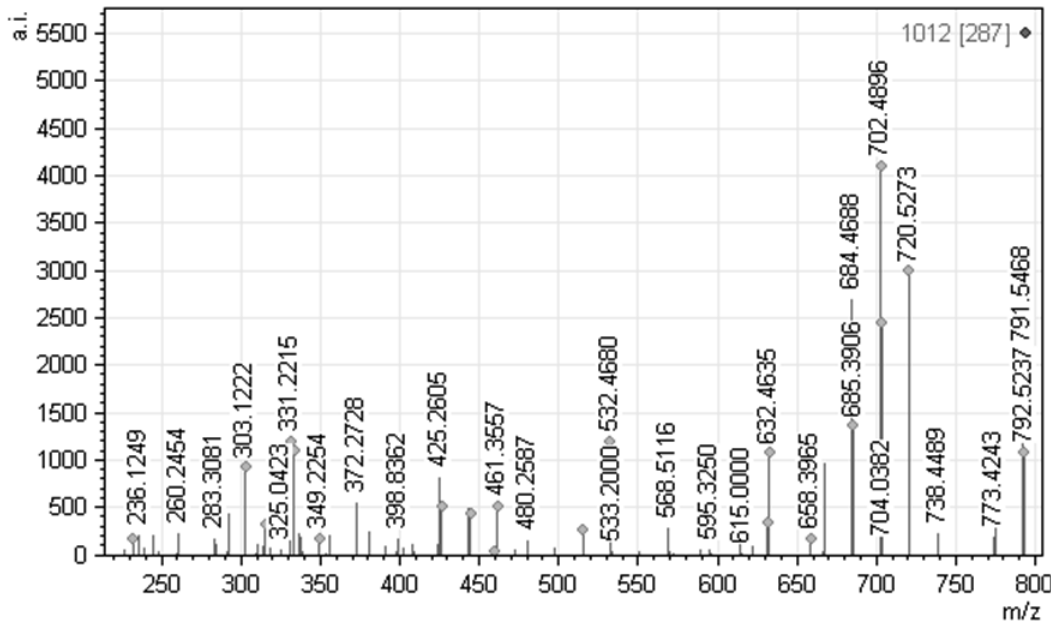


**Fig. 58. MS$^3$ of the pentapeptide Penta(Ala) at *m/z* 1012.5.** (A) Structure and fragmentation pattern of the reduced monosaccharide pentapeptide at *m/z* 809.4 (parental ion *m/z* 1012.5). (B) MS$^3$ spectrum (positive mode) annotated with mMass.

**Table 5. List of the matched fragments of the ion at *m/z* 809.4 annotated with mMass.**

M: molecular ion, b-ions: N-terminal fragments, y-ions: C-terminal fragments.

| Meas. m/z | Calc. m/z | δ (Da) | δ (ppm) | Rel. Int. (%) | z | Annotation | Formula |
|---|---|---|---|---|---|---|---|
| 232.1020 | 232.1179 | -0.0159 | -68.6 | 4.17 | 1 | im1 -H2O [1-1] | C10H17NO5 |
| 303.1222 | 303.1551 | -0.0329 | -108.4 | 22.59 | 1 | a2 -H2O [1-2] | C13H22N2O6 |
| 315.2018 | 315.1663 | 0.0355 | 112.5 | 8.02 | 1 | y3 -H2O [4-6] | C13H22N4O5 |
| 331.2215 | 331.1500 | 0.0715 | 215.9 | 29.33 | 1 | b2 -H2O [1-2] | C14H22N2O7 |
| 333.2315 | 333.1769 | 0.0547 | 164.1 | 26.62 | 1 | y3 [4-6] | C13H24N4O6 |
| 349.2254 | 349.1605 | 0.0649 | 185.8 | 4.16 | 1 | b2 [1-2] | C14H24N2O8 |
| 426.3723 | 426.1983 | 0.1740 | 408.3 | 12.69 | 1 | y4 -H2O -NH3 [3-6] | C18H27N5O7 |
| 444.2773 | 444.2089 | 0.0684 | 154.0 | 10.49 | 1 | y4 -NH3 [3-6] | C18H29N5O8 |
| 459.4000 | 459.2086 | 0.1914 | 416.9 | 0.87 | 1 | b3 -H2O [1-3] | C19H30N4O9 |
| 461.3557 | 461.2354 | 0.1203 | 260.8 | 12.59 | 1 | y4 [3-6] | C18H32N6O8 |
| 515.3589 | 515.2460 | 0.1129 | 219.1 | 6.49 | 1 | y5 -NH3 [2-6] | C21H34N6O9 |
| 532.4680 | 532.2726 | 0.1954 | 367.1 | 29.19 | 1 | y5 [2-6] | C21H37N7O9 |
| 614.4310 | 614.2668 | 0.1642 | 267.3 | 15.85 | 1 | b4 -H2O -NH3 [1-4] | C26H39N5O12 |
| 631.4618 | 631.2933 | 0.1684 | 266.8 | 8.13 | 1 | b4 -H2O [1-4] | C26H42N6O12 |
| 632.4635 | 632.2774 | 0.1861 | 294.4 | 26.13 | 1 | b4 -NH3 [1-4] | C26H41N5O13 |
| 658.3965 | 658.2930 | 0.1035 | 157.3 | 4.19 | 1 | a5 -NH3 -NH3 [1-5] | C28H43N5O13 |
| 685.3906 | 685.3039 | 0.0867 | 126.4 | 33.19 | 1 | b5 -H2O -NH3 [1-5] | C29H44N6O13 |
| 702.4896 | 702.3305 | 0.1591 | 226.5 | 100.00 | 1 | b5 -H2O [1-5] | C29H47N7O13 |
| 703.4618 | 703.3145 | 0.1473 | 209.5 | 59.64 | 1 | b5 -NH3 [1-5] | C29H46N6O14 |
| 720.5273 | 720.3410 | 0.1863 | 258.7 | 72.97 | 1 | b5 [1-5] | C29H49N7O14 |
| 774.5414 | 774.3516 | 0.1899 | 245.2 | 12.60 | 1 | M -H2O -NH3 [1-6] | C32H51N7O15 |
| 791.5468 | 791.3781 | 0.1686 | 213.1 | 52.32 | 1 | M -H2O [1-6] | C32H54N8O15 |
| 792.5237 | 792.3622 | 0.1615 | 203.9 | 26.54 | 1 | M -NH3 [1-6] | C32H53N7O16 |

### 5.2.2 $MS^3$ of the monomeric tetrapeptide Tetra(Ala)

**A**

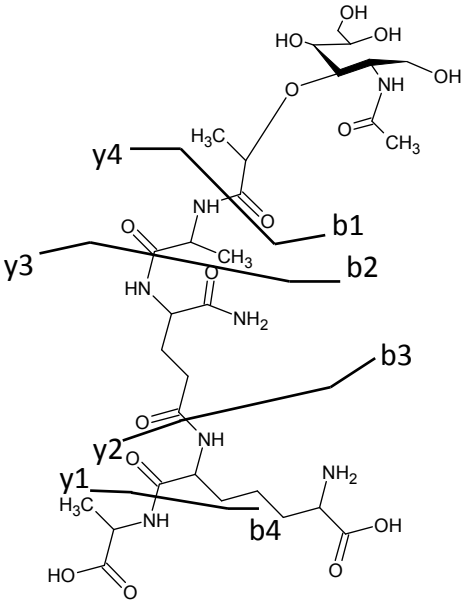


**B**

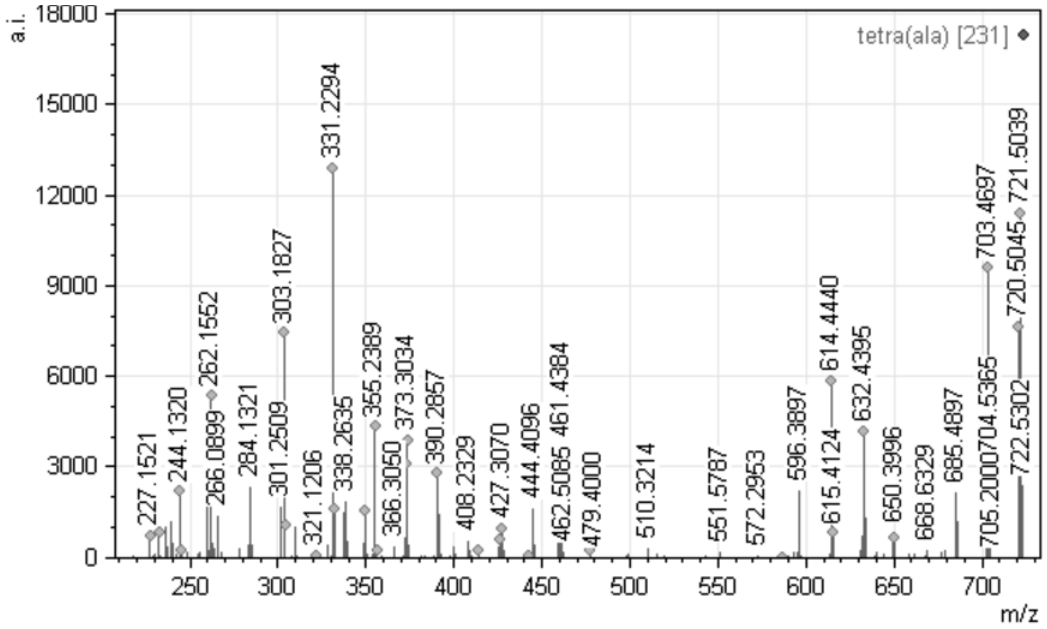


**Fig. 59. $MS^3$ of the tetrapeptide Tetra(Ala) at *m/z* 941.4.** (A) Structure and fragmentation pattern of the reduced monosaccharide tetrapeptide at *m/z* 738.5 (parental ion *m/z* 941.4). (B) $MS^3$ spectrum (positive mode) annotated with mMass.

**Table 6. List of the matched fragments of the ion at *m/z* 738.4 annotated with mMass.**

M: molecular ion, b-ions: N-terminal fragments, y-ions: C-terminal fragments.

| Meas. m/z | Calc. m/z | δ (Da) | δ (ppm) | Rel. Int. (%) | z | Annotation | Formula |
|---|---|---|---|---|---|---|---|
| 227.1521 | 227.1026 | 0.0495 | 218.0 | 5.58 | 1 | y2 -H2O -NH3 [4-5] | C10H14N2O4 |
| 232.1267 | 232.1179 | 0.0087 | 37.7 | 6.58 | 1 | im1 -H2O [1-1] | C10H17NO5 |
| 244.1320 | 244.1292 | 0.0028 | 11.6 | 16.90 | 1 | y2 -H2O [4-5] | C10H17N3O4 |
| 245.2247 | 245.1132 | 0.1115 | 455.0 | 1.68 | 1 | y2 -NH3 [4-5] | C10H16N2O5 |
| 262.1552 | 262.1397 | 0.0155 | 59.0 | 41.43 | 1 | y2 [4-5] | C10H19N3O5 |
| 303.1827 | 303.1551 | 0.0277 | 91.3 | 57.55 | 1 | a2 -H2O [1-2] | C13H22N2O6 |
| 304.1672 | 304.1391 | 0.0281 | 92.5 | 8.55 | 1 | a2 -NH3 [1-2] | C13H21NO7 |
| 321.1206 | 321.1656 | -0.0451 | -140.3 | 0.67 | 1 | a2 [1-2] | C13H24N2O7 |
| 331.2294 | 331.1500 | 0.0794 | 239.8 | 100.00 | 1 | b2 -H2O [1-2] | C14H22N2O7 |
| 332.1971 | 332.1340 | 0.0631 | 190.0 | 12.32 | 1 | b2 -NH3 [1-2] | C14H21NO8 |
| 349.2668 | 349.1605 | 0.1063 | 304.4 | 12.20 | 1 | b2 [1-2] | C14H24N2O8 |
| 355.2389 | 355.1612 | 0.0777 | 218.6 | 33.62 | 1 | y3 -H2O -NH3 [3-5] | C15H22N4O6 |
| 356.2142 | 356.1452 | 0.0689 | 193.6 | 1.66 | 1 | y3 -NH3 -NH3 [3-5] | C15H21N3O7 |
| 372.2756 | 372.1878 | 0.0878 | 236.0 | 23.85 | 1 | y3 -H2O [3-5] | C15H25N5O6 |
| 373.3034 | 373.1718 | 0.1316 | 352.7 | 30.10 | 1 | y3 -NH3 [3-5] | C15H24N4O7 |
| 390.2857 | 390.1983 | 0.0874 | 224.0 | 21.49 | 1 | y3 [3-5] | C15H27N5O7 |
| 414.0767 | 414.1871 | -0.1104 | -266.6 | 1.95 | 1 | a3 -H2O -NH3 [1-3] | C18H27N3O8 |
| 426.2893 | 426.1983 | 0.0910 | 213.4 | 4.71 | 1 | y4 -H2O -NH3 [2-5] | C18H27N5O7 |
| 427.3070 | 427.1823 | 0.1247 | 291.9 | 7.46 | 1 | y4 -NH3 -NH3 [2-5] | C18H26N4O8 |
| 442.2900 | 442.1820 | 0.1080 | 244.2 | 0.67 | 1 | b3 -H2O -NH3 [1-3] | C19H27N3O9 |
| 460.3296 | 460.1926 | 0.1370 | 297.8 | 13.62 | 1 | b3 -NH3 [1-3] | C19H29N3O10 |
| 477.3723 | 477.2191 | 0.1532 | 321.0 | 1.66 | 1 | b3 [1-3] | C19H32N4O10 |
| 586.2762 | 586.2719 | 0.0043 | 7.3 | 0.18 | 1 | a4 -H2O -NH3 [1-4] | C25H39N5O11 |
| 614.4440 | 614.2668 | 0.1772 | 288.5 | 45.34 | 1 | b4 -H2O -NH3 [1-4] | C26H39N5O12 |
| 615.4124 | 615.2508 | 0.1616 | 262.7 | 6.36 | 1 | b4 -NH3 -NH3 [1-4] | C26H38N4O13 |
| 632.4395 | 632.2774 | 0.1622 | 256.5 | 32.37 | 1 | b4 -NH3 [1-4] | C26H41N5O13 |
| 649.4482 | 649.3039 | 0.1443 | 222.2 | 5.02 | 1 | b4 [1-4] | C26H44N6O13 |
| 703.4697 | 703.3145 | 0.1552 | 220.7 | 74.37 | 1 | M -H2O -NH3 [1-5] | C29H46N6O14 |
| 720.5045 | 720.3410 | 0.1635 | 227.0 | 59.31 | 1 | M -H2O [1-5] | C29H49N7O14 |
| 721.5039 | 721.3250 | 0.1789 | 248.0 | 88.32 | 1 | M -NH3 [1-5] | C29H48N6O15 |

### 5.2.3 MS$^3$ of the monomeric pentapeptide Penta(Gly)

**A**

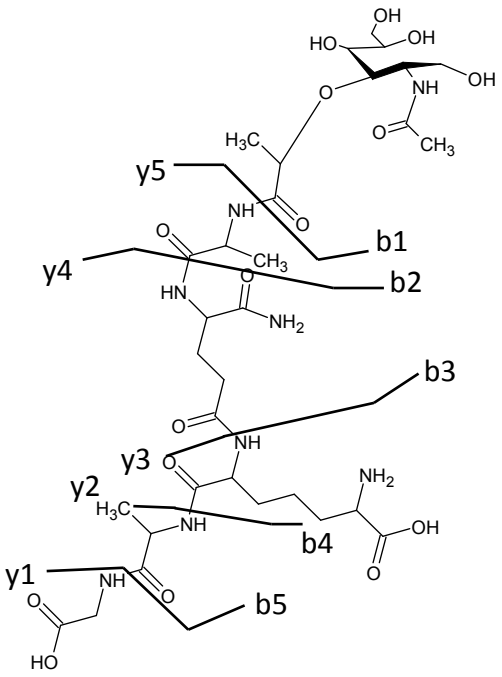


**B**

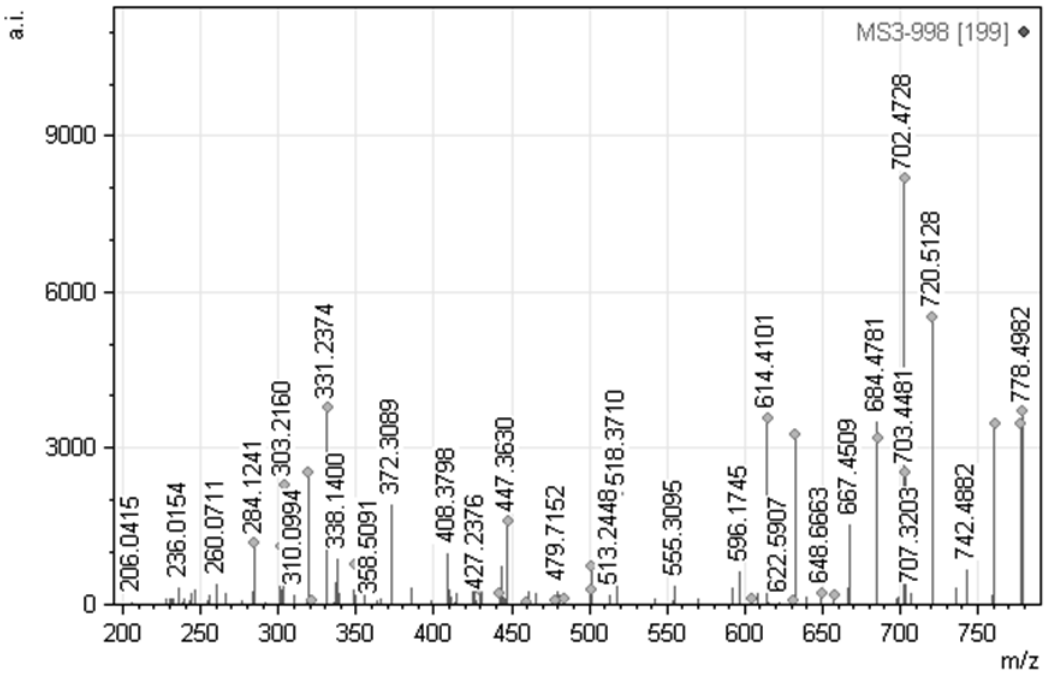


**Fig. 60. MS$^3$ of the pentapeptide Penta(Gly) at *m/z* 998.5.** (A) Structure and fragmentation pattern of the reduced monosaccharide pentapeptide at *m/z* 795.4 (parental ion *m/z* 998.5). (B) MS$^3$ spectrum (positive mode) annotated with mMass.

**Table 7. List of the matched fragments of the ion at *m/z* 795.4 annotated with mMass.**

M: molecular ion, b-ions: N-terminal fragments, y-ions: C-terminal fragments.

| Meas. m/z | Calc. m/z | δ (Da) | δ (ppm) | Rel. Int. (%) | z | Annotation | Formula |
|---|---|---|---|---|---|---|---|
| 284.1241 | 284.1241 | -0.0000 | -0.0 | 14.25 | 1 | y3 -H2O -NH3 [4-6] | C12H17N3O5 |
| 301.1079 | 301.1506 | -0.0428 | -142.0 | 13.65 | 1 | y3 -H2O [4-6] | C12H20N4O5 |
| 303.2160 | 303.1551 | 0.0609 | 201.0 | 27.99 | 1 | a2 -H2O [1-2] | C13H22N2O6 |
| 319.1964 | 319.1612 | 0.0352 | 110.3 | 31.05 | 1 | y3 [4-6] | C12H22N4O6 |
| 321.2906 | 321.1656 | 0.1250 | 389.1 | 0.74 | 1 | a2 [1-2] | C13H24N2O7 |
| 331.2374 | 331.1500 | 0.0874 | 263.9 | 46.14 | 1 | b2 -H2O [1-2] | C14H22N2O7 |
| 349.2478 | 349.1605 | 0.0873 | 250.0 | 9.36 | 1 | b2 [1-2] | C14H24N2O8 |
| 429.3404 | 429.2092 | 0.1311 | 305.5 | 3.52 | 1 | y4 -H2O [3-6] | C17H28N6O7 |
| 430.3762 | 430.1932 | 0.1830 | 425.3 | 11.23 | 1 | y4 -NH3 [3-6] | C17H27N5O8 |
| 442.2910 | 442.1820 | 0.1090 | 246.5 | 2.70 | 1 | b3 -H2O -NH3 [1-3] | C19H27N3O9 |
| 447.3630 | 447.2198 | 0.1432 | 320.2 | 19.49 | 1 | y4 [3-6] | C17H30N6O8 |
| 459.2550 | 459.2086 | 0.0464 | 101.2 | 0.56 | 1 | b3 -H2O [1-3] | C19H30N4O9 |
| 477.2949 | 477.2191 | 0.0758 | 158.8 | 0.82 | 1 | b3 [1-3] | C19H32N4O10 |
| 483.3137 | 483.2198 | 0.0939 | 194.3 | 1.38 | 1 | y5 -H2O -NH3 [2-6] | C20H30N6O8 |
| 500.4092 | 500.2463 | 0.1629 | 325.6 | 3.38 | 1 | y5 -H2O [2-6] | C20H33N7O8 |
| 501.3983 | 501.2304 | 0.1679 | 335.0 | 8.71 | 1 | y5 -NH3 [2-6] | C20H32N6O9 |
| 518.3710 | 518.2569 | 0.1141 | 220.2 | 25.87 | 1 | y5 [2-6] | C20H35N7O9 |
| 604.3433 | 604.2824 | 0.0608 | 100.6 | 1.13 | 1 | a4 -NH3 [1-4] | C25H41N5O12 |
| 614.4101 | 614.2668 | 0.1433 | 233.3 | 43.75 | 1 | b4 -H2O -NH3 [1-4] | C26H39N5O12 |
| 631.3854 | 631.2933 | 0.0921 | 145.9 | 1.05 | 1 | b4 -H2O [1-4] | C26H42N6O12 |
| 632.4155 | 632.2774 | 0.1382 | 218.5 | 39.76 | 1 | b4 -NH3 [1-4] | C26H41N5O13 |
| 649.4361 | 649.3039 | 0.1322 | 203.6 | 2.64 | 1 | b4 [1-4] | C26H44N6O13 |
| 657.4579 | 657.3090 | 0.1489 | 226.6 | 2.17 | 1 | a5 -H2O -NH3 [1-5] | C28H44N6O12 |
| 685.4224 | 685.3039 | 0.1185 | 172.9 | 38.99 | 1 | b5 -H2O -NH3 [1-5] | C29H44N6O13 |
| 702.4728 | 702.3305 | 0.1424 | 202.7 | 100.00 | 1 | b5 -H2O [1-5] | C29H47N7O13 |
| 703.4481 | 703.3145 | 0.1336 | 190.0 | 30.78 | 1 | b5 -NH3 [1-5] | C29H46N6O14 |
| 720.5128 | 720.3410 | 0.1718 | 238.5 | 67.47 | 1 | b5 [1-5] | C29H49N7O14 |
| 760.5209 | 760.3359 | 0.1850 | 243.3 | 42.62 | 1 | M -H2O -NH3 [1-6] | C31H49N7O15 |
| 777.5067 | 777.3625 | 0.1442 | 185.5 | 42.30 | 1 | M -H2O [1-6] | C31H52N8O15 |
| 778.4982 | 778.3465 | 0.1517 | 194.9 | 45.36 | 1 | M -NH3 [1-6] | C31H51N7O16 |

### 5.2.4 MS$^3$ of the monomeric tetrapeptide Tetra(Gly)

**A**

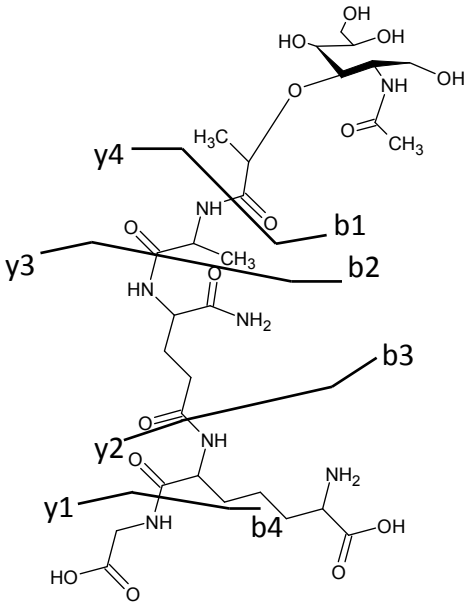


**B**

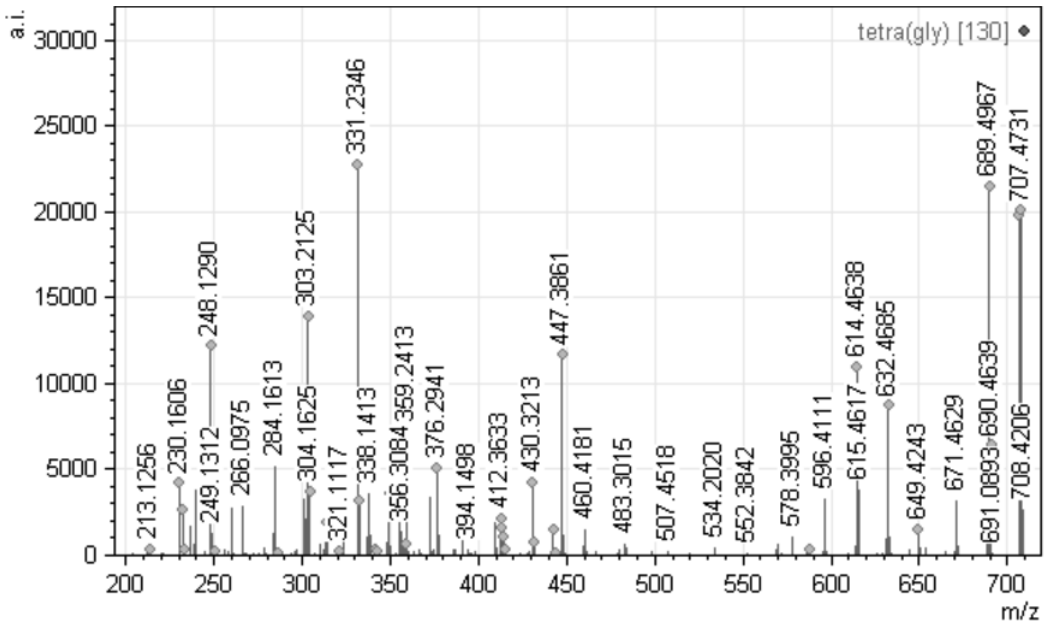


**Fig. 61. MS$^3$ of the tetrapeptide Tetra(Gly) at *m/z* 927.4.** (A) Structure and fragmentation pattern of the reduced monosaccharide tetrapeptide at *m/z* 724.5 (parental ion *m/z* 927.4). (B) MS$^3$ spectrum (positive mode) annotated with mMass.

**Table 8. List of the matched fragments of the ion at *m/z* 724.5 annotated with mMass.**

M: molecular ion, b-ions: N-terminal fragments, y-ions: C-terminal fragments.

| Meas. m/z | Calc. m/z | δ (Da) | δ (ppm) | Rel. Int. (%) | z | Annotation | Formula |
|---|---|---|---|---|---|---|---|
| 213.1256 | 213.0870 | 0.0386 | 181.2 | 1.45 | 1 | y2 -H2O -NH3 [4-5] | C9H12N2O4 |
| 230.1606 | 230.1135 | 0.0471 | 204.5 | 18.39 | 1 | y2 -H2O [4-5] | C9H15N3O4 |
| 232.1185 | 232.1179 | 0.0006 | 2.6 | 11.35 | 1 | im1 -H2O [1-1] | C10H17NO5 |
| 233.0778 | 233.1020 | -0.0242 | -103.6 | 1.23 | 1 | im1 -NH3 [1-1] | C10H16O6 |
| 248.1290 | 248.1241 | 0.0049 | 19.9 | 53.58 | 1 | y2 [4-5] | C9H17N3O5 |
| 250.2381 | 250.1285 | 0.1096 | 438.1 | 0.75 | 1 | im1 [1-1] | C10H19NO6 |
| 286.0546 | 286.1285 | -0.0739 | -258.2 | 0.45 | 1 | a2 -H2O -NH3 [1-2] | C13H19NO6 |
| 303.2125 | 303.1551 | 0.0574 | 189.3 | 61.22 | 1 | a2 -H2O [1-2] | C13H22N2O6 |
| 304.1625 | 304.1391 | 0.0234 | 76.9 | 16.34 | 1 | a2 -NH3 [1-2] | C13H21NO7 |
| 314.2032 | 314.1234 | 0.0798 | 254.0 | 8.31 | 1 | b2 -H2O -NH3 [1-2] | C14H19NO7 |
| 321.1117 | 321.1656 | -0.0540 | -168.0 | 1.03 | 1 | a2 [1-2] | C13H24N2O7 |
| 331.2346 | 331.1500 | 0.0846 | 255.5 | 100.00 | 1 | b2 -H2O [1-2] | C14H22N2O7 |
| 332.1579 | 332.1340 | 0.0239 | 72.0 | 13.84 | 1 | b2 -NH3 [1-2] | C14H21NO8 |
| 341.2774 | 341.1456 | 0.1319 | 386.6 | 1.27 | 1 | y3 -H2O -NH3 [3-5] | C14H20N4O6 |
| 342.2541 | 342.1296 | 0.1245 | 363.8 | 0.81 | 1 | y3 -NH3 -NH3 [3-5] | C14H19N3O7 |
| 349.2222 | 349.1605 | 0.0617 | 176.6 | 15.70 | 1 | b2 [1-2] | C14H24N2O8 |
| 358.2839 | 358.1721 | 0.1118 | 312.0 | 2.65 | 1 | y3 -H2O [3-5] | C14H23N5O6 |
| 359.2413 | 359.1561 | 0.0852 | 237.2 | 31.60 | 1 | y3 -NH3 [3-5] | C14H22N4O7 |
| 376.2941 | 376.1827 | 0.1114 | 296.1 | 22.36 | 1 | y3 [3-5] | C14H25N5O7 |
| 412.3633 | 412.1827 | 0.1806 | 438.1 | 9.32 | 1 | y4 -H2O -NH3 [2-5] | C17H25N5O7 |
| 413.3021 | 413.1687 | 0.1354 | 327.6 | 7.11 | 1 | y4 -NH3 -NH3 [2-5] | C17H24N4O8 |
| 414.3176 | 414.1871 | 0.1305 | 315.1 | 4.71 | 1 | a3 -H2O -NH3 [1-3] | C18H27N3O8 |
| 415.3153 | 415.1711 | 0.1442 | 347.3 | 1.24 | 1 | a3 -NH3 -NH3 [1-3] | C18H26N2O9 |
| 430.3213 | 430.1932 | 0.1280 | 297.6 | 18.55 | 1 | y4 -NH3 [2-5] | C17H27N5O8 |
| 431.4041 | 431.2136 | 0.1905 | 441.7 | 3.03 | 1 | a3 -H2O [1-3] | C18H30N4O8 |
| 442.3292 | 442.1820 | 0.1472 | 332.9 | 6.43 | 1 | b3 -H2O -NH3 [1-3] | C19H27N3O9 |
| 443.2315 | 443.1660 | 0.0655 | 147.8 | 0.23 | 1 | b3 -NH3 -NH3 [1-3] | C19H26N2O10 |
| 447.3861 | 447.2198 | 0.1663 | 371.9 | 51.16 | 1 | y4 [2-5] | C17H30N6O8 |
| 587.3378 | 587.2559 | 0.0819 | 139.5 | 1.52 | 1 | a4 -NH3 -NH3 [1-4] | C25H38N4O12 |
| 614.4638 | 614.2668 | 0.1970 | 320.7 | 48.09 | 1 | b4 -H2O -NH3 [1-4] | C26H38N5O12 |
| 632.4685 | 632.2774 | 0.1911 | 302.3 | 38.19 | 1 | b4 -NH3 [1-4] | C26H41N5O13 |
| 649.4243 | 649.3039 | 0.1203 | 185.3 | 6.55 | 1 | b4 [1-4] | C26H44N6O13 |
| 689.4967 | 689.2988 | 0.1979 | 287.1 | 94.34 | 1 | M -H2O -NH3 [1-5] | C28H44N6O14 |
| 690.4639 | 690.2828 | 0.1811 | 262.3 | 28.11 | 1 | M -NH3 -NH3 [1-5] | C28H43N5O15 |
| 706.4963 | 706.3254 | 0.1609 | 227.8 | 86.79 | 1 | M -H2O [1-5] | C28H47N7O14 |
| 707.4731 | 707.3094 | 0.1637 | 231.4 | 88.04 | 1 | M -NH3 [1-5] | C28H46N6O15 |

### 5.2.5 MS$^3$ of the monomeric pentapeptide Penta(Ser)

**A**

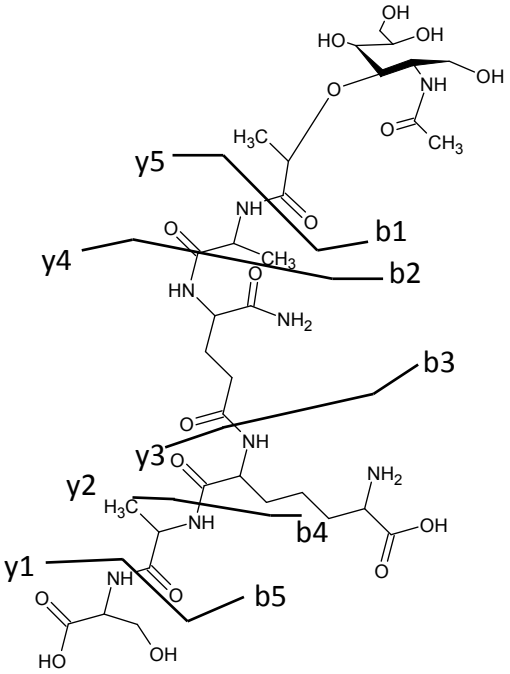


**B**

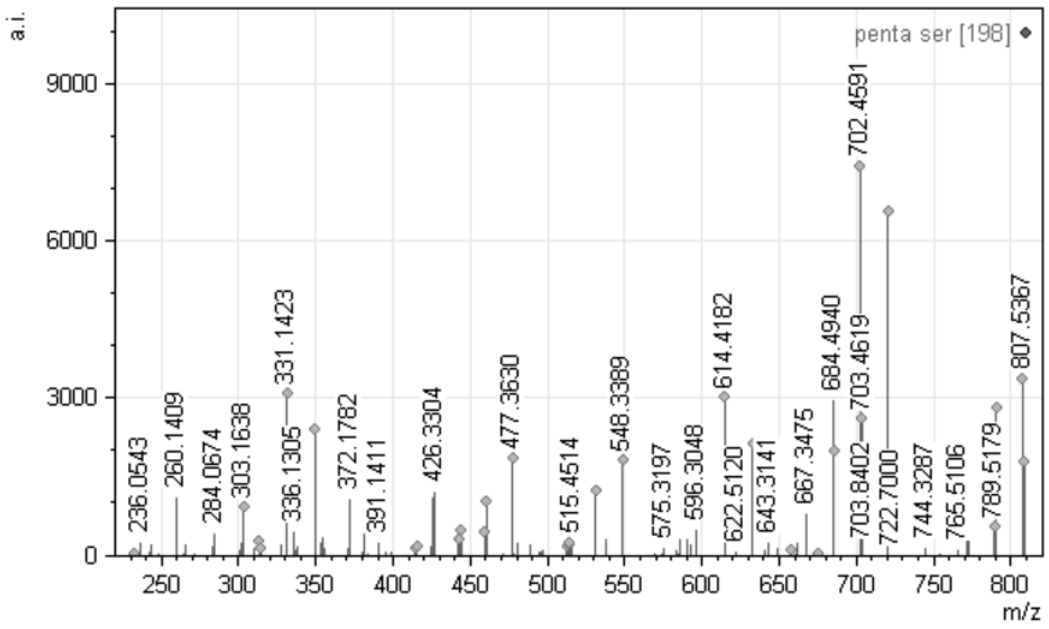


**Fig. 62. MS$^3$ of the pentapeptide Penta(Ser) at *m/z* 1028.5.** (A) Structure and fragmentation pattern of the reduced monosaccharide pentapeptide at *m/z* 825.4 (parental ion *m/z* 1028.5). (B) MS$^3$ spectrum (positive mode) annotated with mMass.

**Table 9. List of the matched fragments of the ion at *m/z* 825.4 annotated with mMass.**

M: molecular ion, b-ions: N-terminal fragments, y-ions: C-terminal fragments.

| Meas. m/z | Calc. m/z | δ (Da) | δ (ppm) | Rel. Int. (%) | z | Annotation | Formula |
|---|---|---|---|---|---|---|---|
| 232.0952 | 232.1179 | -0.0227 | -97.8 | 0.39 | 1 | im1 -H2O [1-1] | C10H17NO5 |
| 303.1638 | 303.1551 | 0.0088 | 28.9 | 12.39 | 1 | a2 -H2O [1-2] | C13H22N2O6 |
| 313.1120 | 313.1506 | -0.0386 | -123.3 | 3.84 | 1 | y3 -H2O -H2O [4-6] | C13H20N4O5 |
| 314.2393 | 314.1347 | 0.1047 | 333.2 | 1.81 | 1 | y3 -H2O -NH3 [4-6] | C13H19N3O6 |
| 314.2393 | 314.1234 | 0.1159 | 368.9 | 1.81 | 1 | b2 -H2O -NH3 [1-2] | C14H19NO7 |
| 331.1423 | 331.1612 | -0.0189 | -57.2 | 41.52 | 1 | y3 -H2O [4-6] | C13H22N4O6 |
| 331.1423 | 331.1500 | -0.0077 | -23.3 | 41.52 | 1 | b2 -H2O [1-2] | C14H22N2O7 |
| 349.1862 | 349.1718 | 0.0145 | 41.5 | 32.34 | 1 | y3 [4-6] | C13H24N4O7 |
| 349.1862 | 349.1605 | 0.0257 | 73.6 | 32.34 | 1 | b2 [1-2] | C14H24N2O8 |
| 414.2504 | 414.1871 | 0.0633 | 152.8 | 2.00 | 1 | a3 -H2O -NH3 [1-3] | C18H27N3O8 |
| 415.2387 | 415.1711 | 0.0676 | 162.9 | 2.41 | 1 | a3 -NH3 -NH3 [1-3] | C18H26N2O9 |
| 442.2691 | 442.1932 | 0.0958 | 216.7 | 4.25 | 1 | y4 -H2O -NH3 [3-6] | C18H27N5O8 |
| 442.2691 | 442.1820 | 0.1071 | 242.1 | 4.25 | 1 | b3 -H2O -NH3 [1-3] | C19H27N3O9 |
| 443.3707 | 443.1773 | 0.1934 | 436.5 | 6.69 | 1 | y4 -NH3 -NH3 [3-6] | C18H26N4O9 |
| 459.2503 | 459.2198 | 0.0305 | 66.4 | 5.84 | 1 | y4 -H2O [3-6] | C18H30N6O8 |
| 459.2503 | 459.2086 | 0.0417 | 90.9 | 5.84 | 1 | b3 -H2O [1-3] | C19H30N4O9 |
| 460.3437 | 460.2038 | 0.1399 | 304.0 | 13.71 | 1 | y4 -NH3 [3-6] | C18H29N5O9 |
| 460.3437 | 460.1926 | 0.1511 | 328.4 | 13.71 | 1 | b3 -NH3 [1-3] | C19H29N3O10 |
| 477.3630 | 477.2304 | 0.1327 | 278.0 | 24.75 | 1 | y4 [3-6] | C18H32N6O9 |
| 477.3630 | 477.2191 | 0.1439 | 301.6 | 24.75 | 1 | b3 [1-3] | C19H32N4O10 |
| 512.2429 | 512.2463 | -0.0035 | -6.8 | 2.16 | 1 | y5 -H2O -H2O [2-6] | C21H33N7O8 |
| 513.3195 | 513.2304 | 0.0892 | 173.7 | 2.63 | 1 | y5 -H2O -NH3 [2-6] | C21H32N6O9 |
| 514.2500 | 514.2144 | 0.0356 | 69.3 | 3.19 | 1 | y5 -NH3 -NH3 [2-6] | C21H31N5O10 |
| 531.3232 | 531.2409 | 0.0823 | 154.9 | 16.44 | 1 | y5 -NH3 [2-6] | C21H34N6O10 |
| 548.3389 | 548.2675 | 0.0715 | 130.3 | 24.36 | 1 | y5 [2-6] | C21H37N7O10 |
| 614.4182 | 614.2668 | 0.1514 | 246.5 | 40.63 | 1 | b4 -H2O -NH3 [1-4] | C26H39N5O12 |
| 632.4714 | 632.2774 | 0.1941 | 306.9 | 28.69 | 1 | b4 -NH3 [1-4] | C26H41N5O13 |
| 657.3824 | 657.3090 | 0.0734 | 111.6 | 1.24 | 1 | a5 -H2O -NH3 [1-5] | C28H44N6O12 |
| 675.3158 | 675.3196 | -0.0038 | -5.6 | 0.36 | 1 | a5 -NH3 [1-5] | C28H46N6O13 |
| 685.4539 | 685.3039 | 0.1499 | 218.8 | 26.59 | 1 | b5 -H2O -NH3 [1-5] | C29H44N6O13 |
| 702.4591 | 702.3305 | 0.1286 | 183.2 | 100.00 | 1 | b5 -H2O [1-5] | C29H47N7O13 |
| 703.4619 | 703.3145 | 0.1474 | 209.5 | 34.93 | 1 | b5 -NH3 [1-5] | C29H46N6O14 |
| 720.4768 | 720.3410 | 0.1358 | 188.5 | 88.24 | 1 | b5 [1-5] | C29H49N7O14 |
| 789.5179 | 789.3625 | 0.1555 | 196.9 | 7.34 | 1 | M -H2O -H2O [1-6] | C32H52N8O15 |
| 790.5266 | 790.3465 | 0.1801 | 227.9 | 37.85 | 1 | M -H2O -NH3 [1-6] | C32H51N7O16 |
| 807.5367 | 807.3731 | 0.1637 | 202.7 | 45.40 | 1 | M -H2O [1-6] | C32H54N8O16 |
| 808.4567 | 808.3571 | 0.0997 | 123.3 | 24.05 | 1 | M -NH3 [1-6] | C32H53N7O17 |

### 5.2.6 MS$^3$ of the monomeric tetrapeptide Tetra(Ser)

**A**

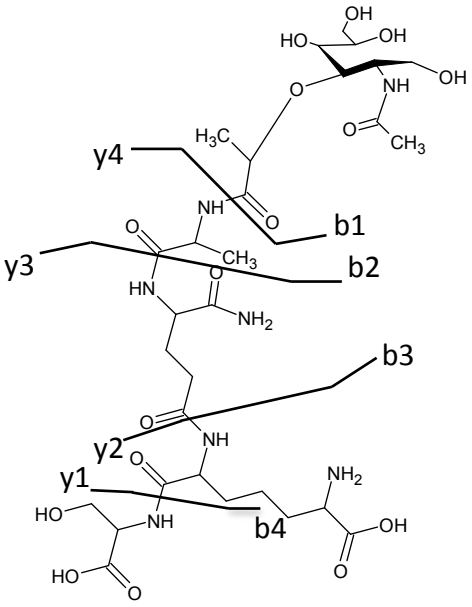


**B**

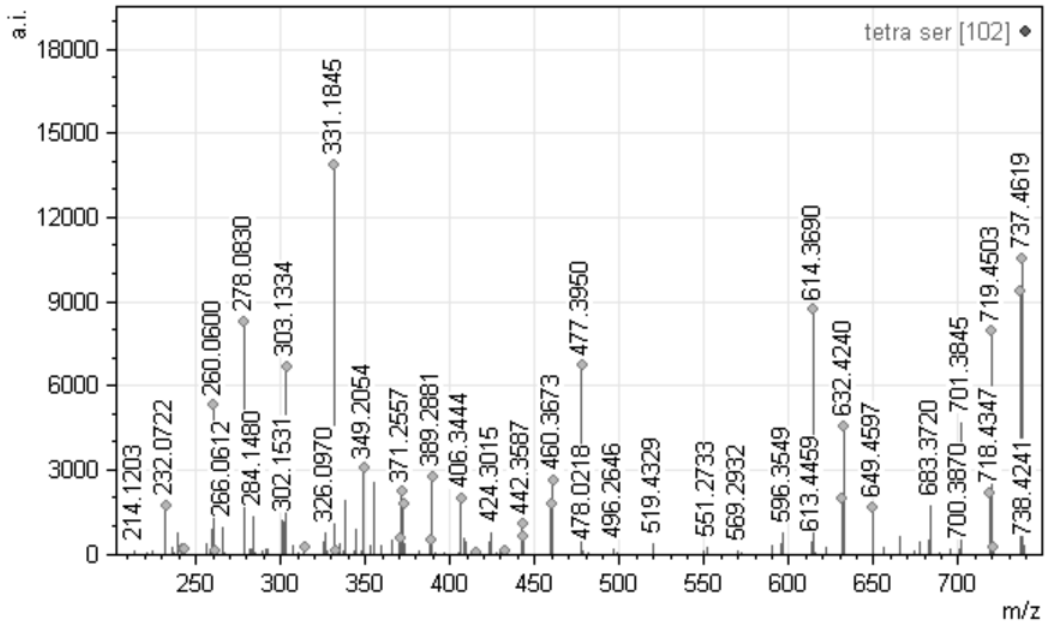


**Fig. 63. MS$^3$ of the tetrapeptide Tetra(Ser) at *m/z* 957.5.** (A) Structure and fragmentation pattern of the reduced monosaccharide tetrapeptide at *m/z* 754.7 (parental ion *m/z* 957.5). (B) MS$^3$ spectrum (positive mode) annotated with mMass.

**Table 10. List of the matched fragments of the ion at *m/z* 754.7 annotated with mMass.** M: molecular ion, b-ions: N-terminal fragments, y-ions: C-terminal fragments.

| Meas. m/z | Calc. m/z | δ (Da) | δ (ppm) | Rel. Int. (%) | z | Annotation | Formula |
|---|---|---|---|---|---|---|---|
| 232.0722 | 232.1179 | -0.0458 | -197.3 | 12.56 | 1 | im1 -H2O [1-1] | C10H17NO5 |
| 242.1126 | 242.1135 | -0.0009 | -3.9 | 1.30 | 1 | y2 -H2O -H2O [4-5] | C10H15N3O4 |
| 243.0761 | 243.0975 | -0.0215 | -88.4 | 1.42 | 1 | y2 -H2O -NH3 [4-5] | C10H14N2O5 |
| 260.0600 | 260.1241 | -0.0641 | -246.3 | 38.25 | 1 | y2 -H2O [4-5] | C10H17N3O5 |
| 261.0432 | 261.1081 | -0.0650 | -248.8 | 0.74 | 1 | y2 -NH3 [4-5] | C10H16N2O6 |
| 278.0830 | 278.1347 | -0.0517 | -185.7 | 59.75 | 1 | y2 [4-5] | C10H19N3O6 |
| 303.1334 | 303.1551 | -0.0216 | -71.4 | 48.09 | 1 | a2 -H2O [1-2] | C13H22N2O6 |
| 314.1123 | 314.1234 | -0.0111 | -35.3 | 1.65 | 1 | b2 -H2O -NH3 [1-2] | C14H19NO7 |
| 331.1845 | 331.1500 | 0.0345 | 104.3 | 100.00 | 1 | b2 -H2O [1-2] | C14H22N2O7 |
| 332.2401 | 332.1340 | 0.1061 | 319.6 | 1.13 | 1 | b2 -NH3 [1-2] | C14H21NO8 |
| 349.2054 | 349.1605 | 0.0448 | 128.4 | 22.08 | 1 | b2 [1-2] | C14H24N2O8 |
| 370.1547 | 370.1721 | -0.0174 | -47.0 | 4.21 | 1 | y3 -H2O -H2O [3-5] | C15H23N5O6 |
| 371.2557 | 371.1561 | 0.0996 | 268.3 | 16.13 | 1 | y3 -H2O -NH3 [3-5] | C15H22N4O7 |
| 372.2485 | 372.1401 | 0.1084 | 291.2 | 13.15 | 1 | y3 -NH3 -NH3 [3-5] | C15H21N3O8 |
| 388.2782 | 388.1827 | 0.0955 | 246.0 | 3.70 | 1 | y3 -H2O [3-5] | C15H25N5O7 |
| 389.2881 | 389.1667 | 0.1214 | 312.0 | 19.97 | 1 | y3 -NH3 [3-5] | C15H24N4O8 |
| 406.3444 | 406.1932 | 0.1511 | 372.0 | 14.47 | 1 | y3 [3-5] | C15H27N5O8 |
| 415.2381 | 415.1711 | 0.0670 | 161.4 | 0.36 | 1 | a3 -NH3 -NH3 [1-3] | C18H26N2O9 |
| 432.2631 | 432.1977 | 0.0654 | 151.3 | 0.92 | 1 | a3 -NH3 [1-3] | C18H29N3O9 |
| 442.3587 | 442.1932 | 0.1655 | 374.2 | 7.84 | 1 | y4 -H2O -NH3 [2-5] | C18H27N5O8 |
| 442.3587 | 442.1820 | 0.1767 | 399.6 | 7.84 | 1 | b3 -H2O -NH3 [1-3] | C19H27N3O9 |
| 443.2068 | 443.1773 | 0.0295 | 66.6 | 4.76 | 1 | y4 -NH3 -NH3 [2-5] | C18H26N4O9 |
| 443.2068 | 443.1660 | 0.0408 | 92.0 | 4.76 | 1 | b3 -NH3 -NH3 [1-3] | C19H26N2O10 |
| 459.3057 | 459.2198 | 0.0859 | 187.0 | 12.76 | 1 | y4 -H2O [2-5] | C18H30N6O8 |
| 459.3057 | 459.2086 | 0.0971 | 211.5 | 12.76 | 1 | b3 -H2O [1-3] | C19H30N4O9 |
| 460.3673 | 460.2038 | 0.1635 | 355.2 | 18.97 | 1 | y4 -NH3 [2-5] | C18H29N5O9 |
| 460.3673 | 460.1926 | 0.1747 | 379.6 | 18.97 | 1 | b3 -NH3 [1-3] | C19H29N3O10 |
| 477.3950 | 477.2304 | 0.1646 | 345.0 | 48.46 | 1 | y4 [2-5] | C18H32N6O9 |
| 477.3950 | 477.2191 | 0.1759 | 368.5 | 48.46 | 1 | b3 [1-3] | C19H32N4O10 |
| 614.3690 | 614.2668 | 0.1022 | 166.4 | 62.65 | 1 | b4 -H2O -NH3 [1-4] | C26H39N5O12 |
| 631.3611 | 631.2933 | 0.0678 | 107.4 | 14.16 | 1 | b4 -H2O [1-4] | C26H42N6O12 |
| 632.4240 | 632.2774 | 0.1466 | 231.8 | 32.92 | 1 | b4 -NH3 [1-4] | C26H41N5O13 |
| 649.4597 | 649.3039 | 0.1557 | 239.9 | 12.13 | 1 | b4 [1-4] | C26H44N6O13 |
| 718.4347 | 718.3254 | 0.1093 | 152.2 | 15.80 | 1 | M -H2O -H2O [1-5] | C29H47N7O14 |
| 719.4503 | 719.3094 | 0.1409 | 195.8 | 57.11 | 1 | M -H2O -NH3 [1-5] | C29H46N6O15 |
| 720.4484 | 720.2934 | 0.1550 | 215.1 | 1.87 | 1 | M -NH3 -NH3 [1-5] | C29H45N5O16 |
| 736.4606 | 736.3359 | 0.1246 | 169.3 | 67.26 | 1 | M -H2O [1-5] | C29H49N7O15 |
| 737.4619 | 737.3200 | 0.1420 | 192.5 | 75.88 | 1 | M -NH3 [1-5] | C29H48N6O16 |

## 5.3 MS$^2$ of *Microbispora* sp. 107891 UDP-linked PG precursors

### 5.3.1 MS$^2$ of UDP-MurNAc-tetrapeptide(Ala)

**A**

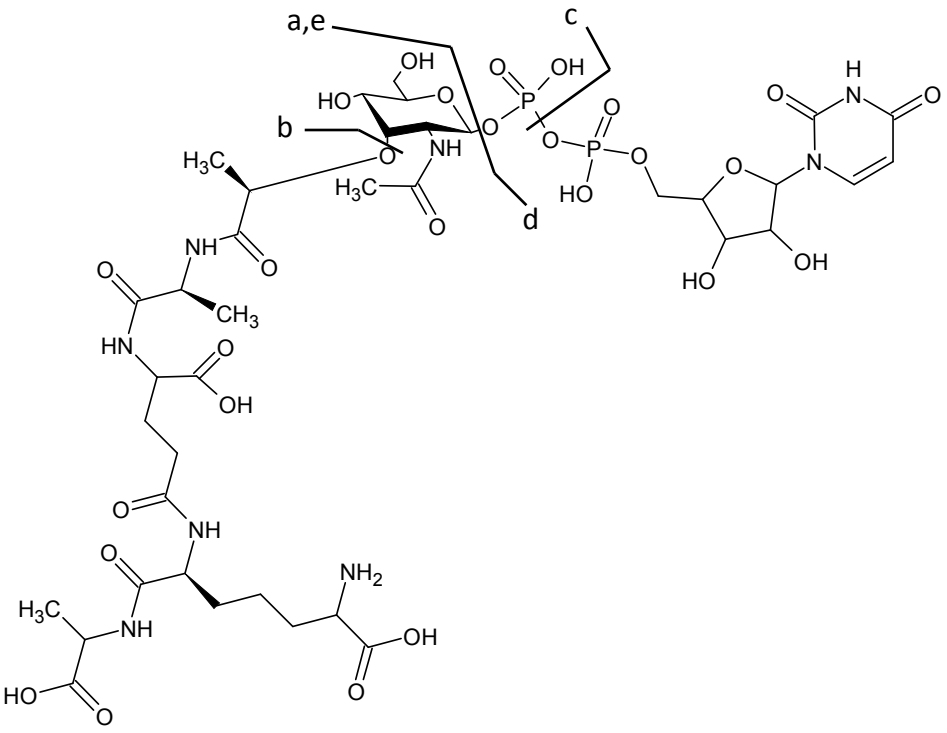

**B**

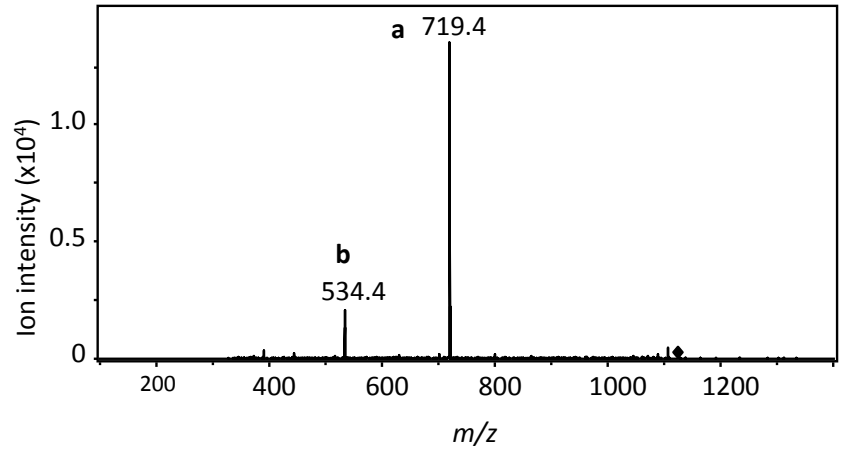


**C**

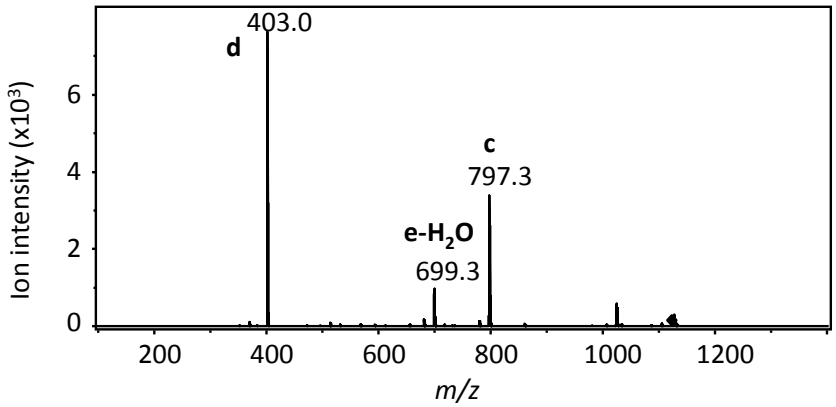


**Fig. 64. $MS^2$ of UDP-MurNAc-tetrapeptide(Ala).** (A) Structure and fragmentation pattern of UDP-MurNAc-tetrapeptide(Ala) (1122 Da). (B) $MS^2$ spectrum in the positive mode. (C) $MS^2$ spectrum in the negative mode.

**Table 11. Fragments of UDP-MurNAc tetrapeptide(Ala)**

| **Fragment*** | **UDP-MurNAc tetrapeptide(Ala)** | |
|---|---|---|
| | **Observed (*m/z*)** | **Calculated (*m/z*)** |
| a | 719.4 | 720.31 |
| b | 534.4 | 533.22 |
| c | 797.3 | 798.69 |
| d | 403.0 | 402.99** |
| e-$H_2O$ | 699.3 | 700.31 |

***** a, b: positive ions; c,d,e: negative ions

** negative charge probably on the oxygen of the phosphate group

Difference of 1 Da between the values of the observed a, b, c, e-$H_2O$ ions and the calculated ones.

### 5.3.2 $MS^2$ of UDP-MurNAc-pentapeptide(Ala)

**A**

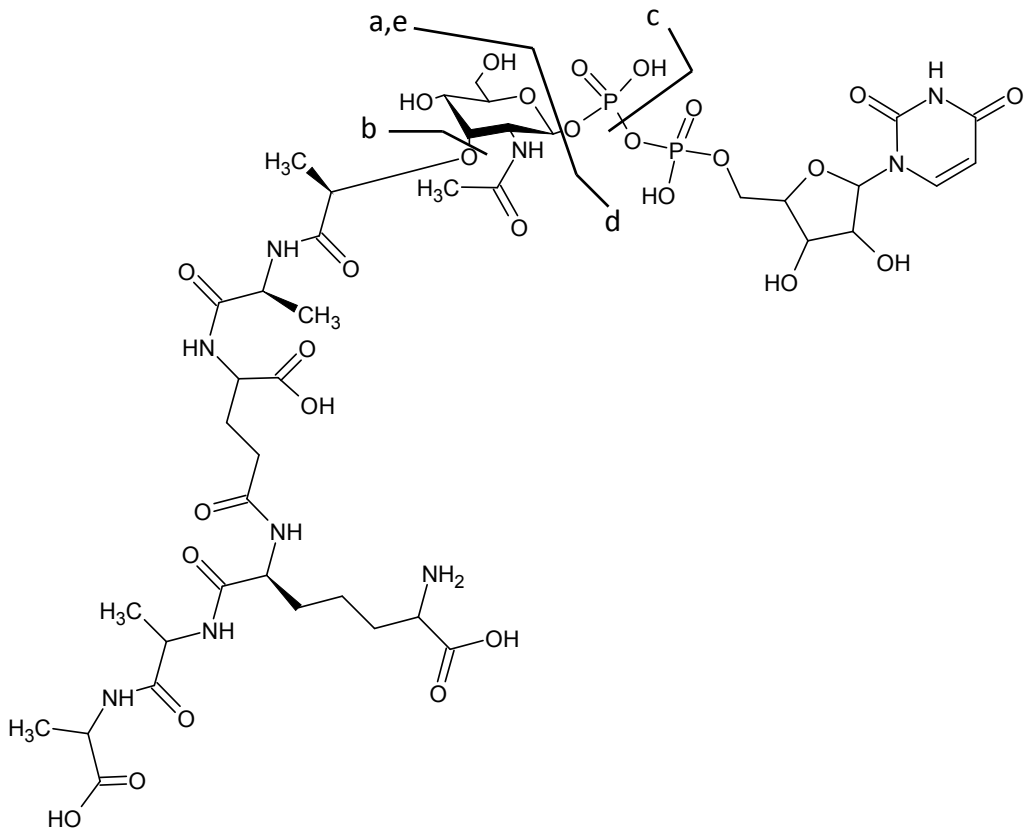

**B**

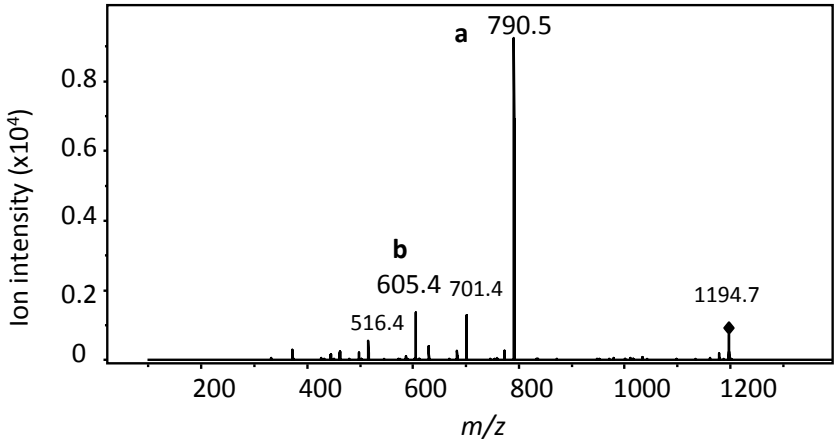


**C**

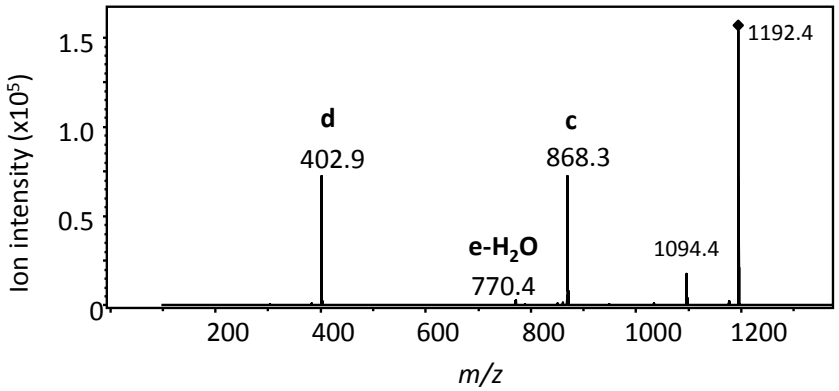


**Fig. 65. $MS^2$ of UDP-MurNAc-pentapeptide(Ala).** (A) Structure and fragmentation pattern of UDP-MurNAc-pentapeptide(Ala) (1193 Da). (B) $MS^2$ spectrum in the positive mode. (C) $MS^2$ spectrum in the negative mode.

**Table 12. Fragments of UDP-MurNAc pentapeptide(Ala)**

| **Fragment*** | **UDP-MurNAc-pentapeptide(Ala)** | |
|---|---|---|
| | **Observed (*m/z*)** | **Calculated (*m/z*)** |
| a | 790.5 | 791.35 |
| b | 605.4 | 604.27 |
| c | 868.3 | 869.33 |
| d | 402.9 | 402.99** |
| e-$H_2O$ | 770.4 | 771.35 |

***** a, b: positive ions; c,d,e: negative ions

** negative charge probably on the oxygen of the phosphate group

Difference of 1 Da between the values of the observed a, b, c, e-$H_2O$ ions and the calculated ones.

### 5.3.3 $MS^2$ of UDP-MurNAc-pentapeptide(Gly)

**A**

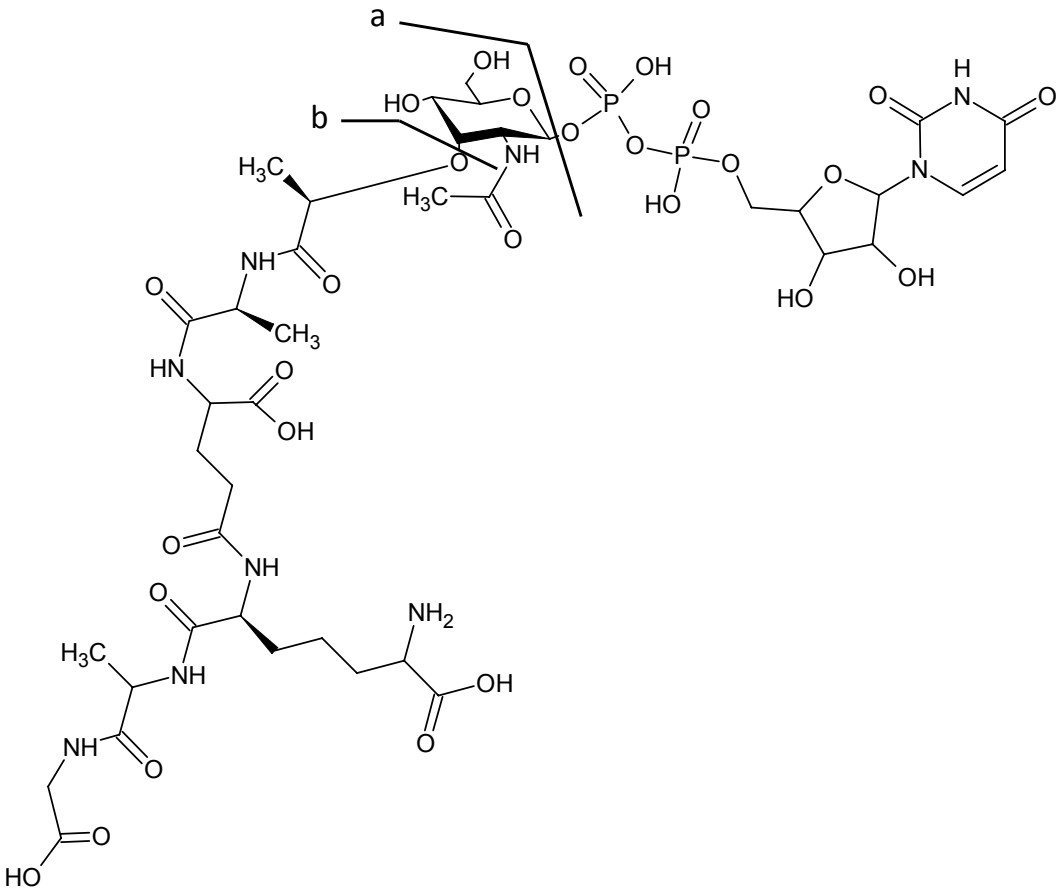


**B**

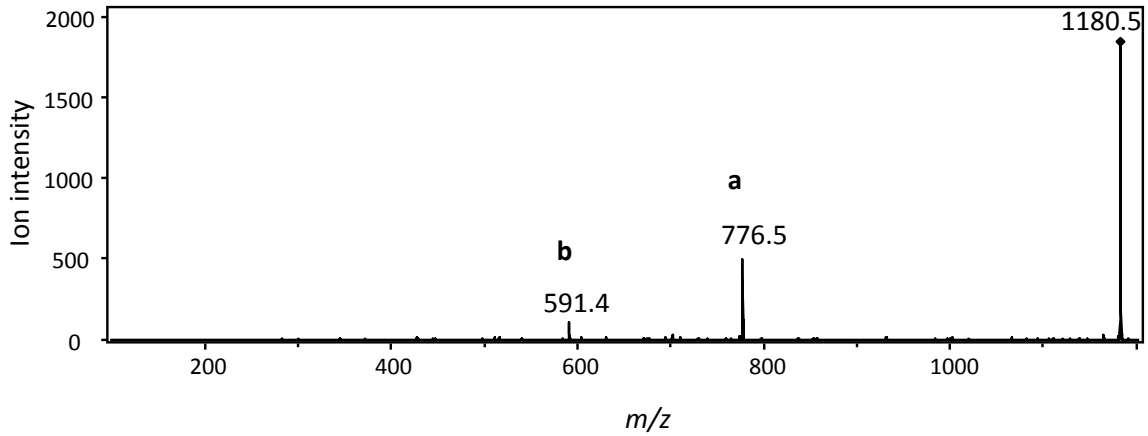


**Fig. 66. $MS^2$ of UDP-MurNAc-pentapeptide(Gly).** (A) Structure and fragmentation pattern of UDP-MurNAc-pentapeptide(Gly) (1179 Da). (B) $MS^2$ spectrum in the positive mode.

**Table 13. Fragments of UDP-MurNAc pentapeptide(Gly)**

| Fragment | UDP-MurNAc pentapeptide(Gly) | |
|---|---|---|
| | **Observed (*m/z*)** | **Calculated (*m/z*)** |
| **a** | 776.5 | 777.77 |
| **b** | 591.4 | 590.57 |

Difference of 1 Da between the values of the observed a, b ions and the calculated ones.

### 5.3.4 $MS^2$ of UDP-MurNAc-pentapeptide(Ser)

**A**

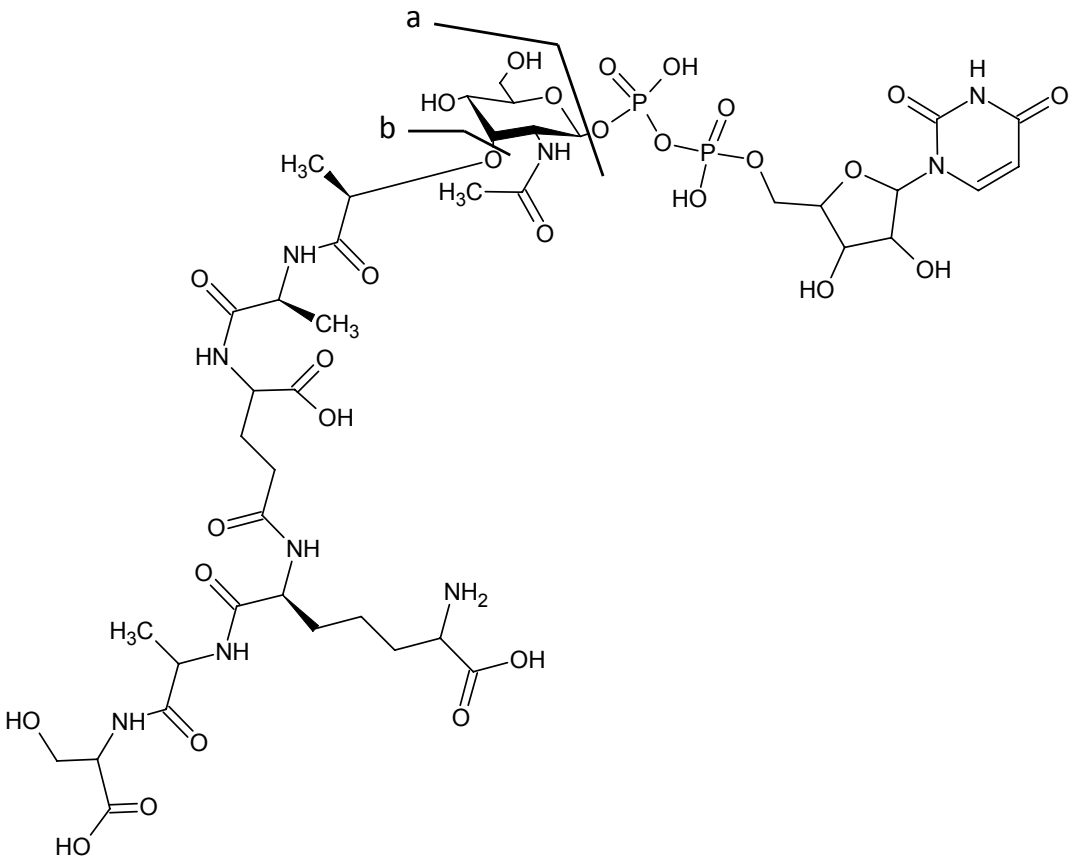

**B**

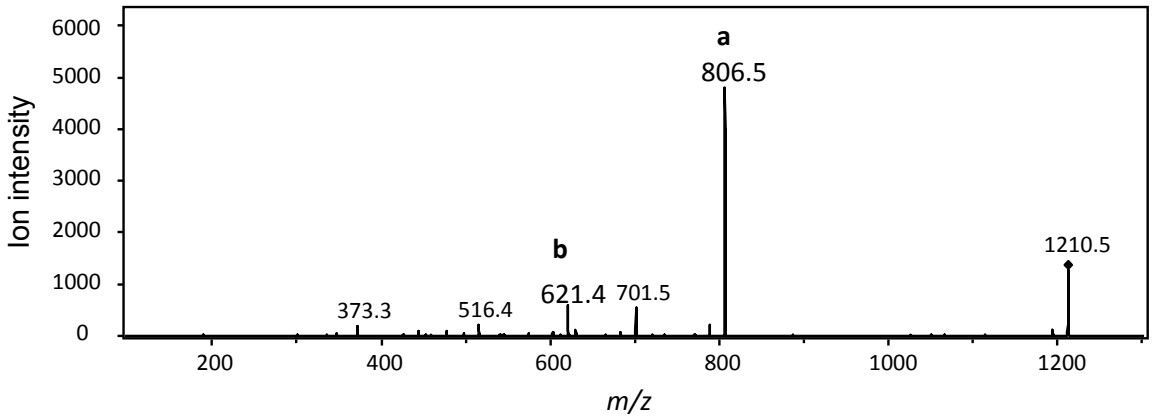


**Fig. 67. $MS^2$ of UDP-MurNAc-pentapeptide(Ser).** (A) Structure and fragmentation pattern of UDP-MurNAc-pentapeptide(Ser) (1209 Da). (B) $MS^2$ spectrum in the positive mode.

**Table 14. Fragments of UDP-MurNAc pentapeptide(Ser)**

| **Fragment** | **UDP-MurNAc pentapeptide(Ser)** | |
|---|---|---|
| | **Observed (*m/z*)** | **Calculated (*m/z*)** |
| **a** | 806.5 | 807.79 |
| **b** | 621.4 | 620.60 |

Difference of 1 Da between the values of the observed a, b ions and the calculated ones.

# 6. REFERENCES

Alkhatib, Z., Abts, A., Mavaro, A., Schmitt, L., Smits, S.H. (2012) Lantibiotics: how do producers become self-protected? *J Biotechnol* **159**: 145-154.

Alkhatib, Z., Lagedroste, M., Zaschke, J., Wagner, M., Abts, A., Fey, I., *et al.* (2014) The C-terminus of nisin is important for the ABC transporter NisFEG to confer immunity in *Lactococcus lactis*. *Microbiologyopen* **3**: 752-763.

Allgaier, H., Jung, G., Werner, U., Schneider, U., Zähner, H. (1985) Elucidation of the structure of epidermin, a ribosomally synthesized, tetracyclic heterodetic polypeptide antibiotic. *Angew Chem Int Ed Engl* **24**: 1051-1053.

Altena, K., Guder, A., Cramer, C., Bierbaum, G. (2000) Biosynthesis of the lantibiotic mersacidin: organization of a type B lantibiotic gene cluster. *Appl Environ Microbiol* **66**: 2565-2571.

Arnison, P.G. *et al*. (2013) Ribosomally synthesized and post-translationally modified peptide natural products: overview and recommendations for a universal nomenclature. *Nat Prod Rep* **30**: 108-160.

Arthur, M., Molinas, F., Depardieu, F., Courvalin, P. (1993) Characterization of Tn*1546*, a Tn*3*-related transposon conferring glycopeptide resistance by synthesis of depsipeptide peptidoglycan precursors in *Enterococcus faecium* BM4147. *J Bacteriol* **175**: 117-127.

Bagyan, I., Noback, M., Bron, S., Paidhungat, M., Setlow, P. (1998) Characterization of yhcN, a new forespore-specific gene of *Bacillus subtilis*. *Gene* **212**: 179-188.

Baltimore D. (1970) RNA-dependent DNA polymerase in virions of RNA tumor viruses. *Nature* **226**: 1209-1211.

Barreteau, H., Kovac, A., Boniface, A., Sova, M., Gobec, S., Blanot, D. (2008) Cytoplasmic steps of peptidoglycan biosynthesis. *FEMS Microbiol Rev* **32**: 168-207.

Bauer, R., and Dicks, L.M. (2005) Mode of action of lipid II-targeting lantibiotics. *Int J Food Microbiol* **101**: 201-216.

Benedict, R.G., Dvonch, W., Shotwell, O.L., Pridham, T.G., Lindenfelser, L.A. (1952) Cinnamycin, an antibiotic from *Streptomyces cinnamoneus* nov. sp. *Antibiot Chemother* **2**: 591-594.

Bera, A., Herbert, S., Jakob, A., Vollmer, W., Götz, F. (2005) Why are pathogenic staphylococci so lysozyme resistant? The peptidoglycan O-acetyltransferase OatA is the major determinant for lysozyme resistance of *Staphylococcus aureus*. *Mol Microbiol* **55**: 778-787.

Bernard, E., Rolain, T., Courtin, P., Hols, P., Chapot-Chartier, M.P. (2011) Identification of the amidotransferase AsnB1 as being responsible for meso-diaminopimelic acid amidation in *Lactobacillus plantarum* peptidoglycan. *J Bacteriol* **193**: 6323-6330.

Bertsche, U., Breukink, E., Kast, T., Vollmer, W. (2005) *In vitro* murein peptidoglycan synthesis by dimers of the bifunctional transglycosylase-transpeptidase PBP1B from *Escherichia coli*. *J Biol Chem* **280**: 38096-38101.

Bibb, M.J., Janssen, G.R., Ward, J.M. (1985) Cloning and analysis of the promoter region of the erythromycin resistance gene (*ermE*) of *Streptomyces erythraeus*. *Gene* **38**: 215-226.

Bielnicki, J., Devedjiev, Y., Derewenda, U., Dauter, Z., Joachimiak, A., Derewenda, Z.S. (2006) *B. subtilis* ykuD protein at 2.0 A resolution: insights into the structure and function of a novel, ubiquitous family of bacterial enzymes. *Proteins* **62**: 144-151.

Binda, E., Marcone, G.L., Pollegioni, L., Marinelli F. (2012) Characterization of VanYn, a novel D,D-peptidase/D,D-carboxypeptidase involved in glycopeptide antibiotic resistance in *Nonomuraea* sp. ATCC 39727. *FEBS J* **279**: 3203-3213.

Blake, K.L., Randall, C.P., O'Neill, A.J. (2011) *In vitro* studies indicate a high resistance potential for the lantibiotic nisin in *Staphylococcus aureus* and define a genetic basis for nisin resistance. *Antimicrob Agents Chemother* **55**: 2362-2368.

Blumberg, P.M. (1974) Penicillin binding components of bacterial cells and their relationship to the mechanism of penicillin action. *Ann N Y Acad Sci* **235**: 310-325.

Boakes, S., Cortes, J., Appleyard, A.N., Rudd, B.A., Dawson, M.J. (2009) Organization of the genes encoding the biosynthesis of actagardine and engineering of a variant generation system. *Mol Microbiol* **72**: 1126-1136.

Boakes, S., Appleyard, A.N., Cortes, J., Dawson, M.J. (2010) Organization of the biosynthetic genes encoding deoxyactagardine B (DAB), a new lantibiotic produced by *Actinoplanes liguriae* NCIMB43162. *J Antibiot* **63**: 351-358.

Bonelli, R.R., Schneider, T., Sahl, H.G., Wiedemann, I. (2006) Insights into in vivo activities of lantibiotics from gallidermin and epidermin mode-of-action studies. *Antimicrob Agents Chemother* **50**: 1449-1457.

Born, P., Breukink, E., Vollmer, W. (2006) *In vitro* synthesis of cross-linked murein and its attachment to sacculi by PBP1A from *Escherichia coli*. *J Biol Chem* **281**: 26985-26993.

Böttiger, T., Schneider, T., Martinez, B., Sahl, H.G., Wiedemann, I. (2009) Influence of Ca(2+) ions on the activity of lantibiotics containing a mersacidin-like lipid II binding motif. *Appl Environ Microbiol* **75**: 4427-4434.

Bouhss, A., Trunkfield, A.E., Bugg, T.D., Mengin-Lecreulx, D. (2008) The biosynthesis of peptidoglycan lipid-linked intermediates. *FEMS Microbiol Rev* **32**: 208-233.

Bradford, M.M. (1976) A rapid and sensitive method for the quantitation of microgram quantities of protein utilizing the principle of protein-dye binding. *Anal Biochem* **72**: 248-254.

Breukink, E., Wiedemann, I., van Kraaij, C., Kuipers, O.P., Sahl, H.G., de Kruijff, B. (1999) Use of the cell wall precursor lipid II by a pore-forming peptide antibiotic. *Science* **286**: 2361-2364.

Breukink, E., and de Kruijff, B. (2006) Lipid II as a target for antibiotics. *Nat Rev Drug Discov* **5**: 321-332.

Brötz, H., Josten, M., Wiedemann, I., Schneider, U., Götz, F., Bierbaum, G., Sahl, H.G. (1998a) Role of lipid-bound peptidoglycan precursors in the formation of pores by nisin, epidermin and other lantibiotics. *Mol Microbiol* **30**: 317-327.

Brötz, H., Bierbaum, G., Leopold, K., Reynolds, P.E., Sahl, H.G. (1998b) The lantibiotic mersacidin inhibits peptidoglycan synthesis by targeting lipid II. *Antimicrob Agents Chemother* **42**: 154-160.

Brown, S., Santa Maria, J.P. Jr, Walker, S. (2013) Wall teichoic acids of gram-positive bacteria. *Annu Rev Microbiol* **67**: 313-336.

Bugg, T.D., Braddick, D., Dowson, C.G., Roper, D.I. (2011) Bacterial cell wall assembly: still an attractive antibacterial target. *Trends Biotechnol* **29**: 167-173.

Bullock, W.O., Fernandez, J.M., Short, J.M. (1987) XL1-Blue: a high-efficiency plasmid transforming *recA Escherichia coli* strain with beta galactosidase selection. *Biotechniques* **5**: 376-378.

Buttner, M.J., Fearnley, I.M., Bibb, M.J. (1987) The agarase gene (*dagA*) of *Streptomyces coelicolor* A3(2): nucleotide sequence and transcriptional analysis. *Mol Gen Genet* **209**: 101-109.

Cain, B.D., Norton, P.J., Eubanks, W., Nick, H.S., Allen, C.M. (1993) Amplification of the *bacA* gene confers bacitracin resistance to *Escherichia coli*. *J Bacteriol* **175**: 3784-3789.

Castiglione, F., Cavaletti, L., Losi, D., Lazzarini, A., Carrano, L., Feroggio, M. *et al.* (2007) A novel lantibiotic acting on bacterial cell wall synthesis produced by the uncommon actinomycete *Planomonospora* sp. *Biochemistry* **46**: 5884-5895.

Castiglione, F., Lazzarini, A., Carrano, L., Corti, E., Ciciliato, I., Gastaldo, L., *et al.* (2008) Determining the structure and mode of action of microbisporicin, a potent lantibiotic active against multiresistant pathogens. *Chem Biol* **15**: 22-31.

Cava, F., de Pedro, M.A., Lam, H., Davis, B.M., Waldor, M.K. (2011) Distinct pathways for modification of the bacterial cell wall by non-canonical D-amino acids. *EMBO J* **30**: 3442-3453.

Chatterjee, S., Chatterjee, S., Lad, S.J., Phansalkar, M.S, Rupp, R.H., Ganguli, B.N., *et al.* (1992) Mersacidin, a new antibiotic from *Bacillus*. Fermentation, isolation, purification and chemical characterization. *J Antibiot* **45**: 832-838.

Chen, X., Tong, X., Xie, Y., Wang, Y., Ma, J., Gao, D., *et al.* (2006) Over-expression and purification of isotopically labelled recombinant ligand-binding domain of orphan nuclear receptor human B1-binding factor/human liver receptor homologue 1 for NMR studies. *Protein Expr Purif* **45**: 99-106.

Chenna, R., Sugawara, H., Koike, T., Lopez, R., Gibson, T.J., Higgins, D.G., Thompson, J.D. (2003) Multiple sequence alignment with the Clustal series of programs. *Nucleic Acids Res* **31**: 3497-3500.

Chilton, C.H., Freeman, J., Baines, S.D., Crowther, G.S., Nicholson, S. and Wilcox, M.H. (2013) Evaluation of the effect of oritavancin on *Clostridium difficile* spore germination, outgrowth and recovery. *J Antimicrob Chemother* **68**: 2078-2082.

Choung, S.Y., Kobayashi, T., Takemoto, K., Ishitsuka, H., Inoue, K. (1988) Interaction of a cyclic peptide, Ro09-0198, with phosphatidylethanolamine in liposomal membranes. *Biochim Biophys Acta* **940**: 180-187.

Christ, N.A., Bochmann, S., Gottstein, D., Duchardt-Ferner, E., Hellmich, U.A., Düsterhus, S., *et al.* (2012) The first structure of a lantibiotic immunity protein, SpaI from *Bacillus subtilis*, reveals a novel fold. *J Biol Chem* **287**: 35286-35298.

Cohen, S.N., Chang, A.C., Hsu, L. (1972) Nonchromosomal antibiotic resistance in bacteria: genetic transformation of *Escherichia coli* by R-factor DNA. *Proc Natl Sci USA* **69**: 2110-2114.

Combes, P., Till, R., Bee, S., Smith, M.C. (2002) The streptomyces genome contains multiple pseudo-*attB* sites for the (phi)C31-encoded site-specific recombination system. *J Bacteriol* **184**: 5746-5752.

Cotter, P.D., Hill, C., Ross, R.P. (2005) Bacterial lantibiotics: a strategy to improve therapeutic potential. *Curr Protein Pept Sci* **6**: 61-75.

Cudic, P., Kranz, J.K., Behenna, D.C., Kruger, R.G., Tadesse, H., Wand, A.J., *et al.* (2002) Complexation of peptidoglycan intermediates by the lipoglycodepsipeptide antibiotic ramoplanin: a minimal structural requirements for intermolecular complexation and fibril formation. *Proc Natl Acad Sci* **99**: 7384-7389.

Delisa, M.P., Tullman, D., Georgiou, G. (2003) Folding quality control in the export of proteins by the bacterial twin-arginine translocation pathway. *Proc Natl Acad Sci* **100**: 6115-6120.

Deng, Y., Li, C.Z., Zhu, Y.G., Wang, P.X., Qi, Q.D., Fu, J.J., *et al.* (2014) ApnI, a transmembrane protein responsible for subtilomycin immunity, unveils a novel model for lantibiotic immunity. *Appl Environ Microbiol* **80**: 6303-6315.

Desmarais, S.M., De Pedro, M.A., Cava, F., Huang K.C. (2013) Peptidolgycan and its peaks: how chromatography analyses can reveal bacterial cell wall structure and assembly. *Mol Microbiol* **89**: 1-13.

Donadio, S., Sosio, M., Serina, S., Mercorillo, D. (12 February 2009) Genes and proteins for the biosynthesis of the lantibiotic 107891. PCT patent application WO 2009/019524 A1.

Dramsi, S., Magnet, S., Davison, S., Arthur, M. (2008) Covalent attachment of proteins to peptidoglycan. *FEMS Microbiol Rev* **32**: 307-320.

Draper, L.A., Ross, R.P., Hill, C., Cotter, P.D. (2008) Lantibiotic immunity. *Curr Protein Pept Sci* **9**: 39-49.

Dubois, J.Y., Kouwen, T.R., Schurich, A.K., Reis, C.R., Ensing, H.T., Trip, E.N. (2009) Immunity to the bacteriocin sublancin 168 is determined by the SunI (YolF) protein of *Bacillus subtilis*. *Antimicrob Agents Chemother* **53**: 651-661.

Dyson, H.J., and Wright, P.E. (2005) Elucidation of the protein folding landscape by NMR. *Methods Enzymol* **394**: 299-321.

Field, D., Hill, C., Cotter, P.D., Ross, R.P. (2010) The dawning of a 'Golden era' in lantibiotic bioengineering. *Mol Microbiol* **78**: 1077-1087.

Flärdh, K., Richards, D.M., Hempel, A.M., Howard, M., Buttner, J.M. (2012) Regulation of apical growth and hyphal branching in *Streptomyces*. *Curr Opin Microbiol* **15**: 737-743.

Ford, C.F., Suominen, I., Glatz, C.E. (1991) Fusion tails for the recovery and purification of recombinant proteins. *Protein Expr Purif* **2**: 95-107.

Foulston, L.C. (2010) Cloning and analysis of the microbisporicin lantibiotic gene cluster from *Microbispora corallina*. PhD thesis. University of East Anglia (England).

Foulston, L.C., and Bibb, M.J. (2010) Microbisporicin gene cluster reveals unusual features of lantibiotic biosynthesis in actinomycetes. *Proc Natl Acad Sci USA* **107**: 13461-13466.

Foulston, L.C., and Bibb, M.J. (2011) Feed-forward regulation of microbisporicin biosynthesis in *Microbispora corallina*. *J Bacteriol* **193**: 3064-3071.

Fredenhagen, A., Fendrich, G., Maerki, F., Maerki, W., Gruner, J., Raschdorf, F., Peter, H.H. (1990) Duramycins B and C, two new lanthionine containing antibiotics as inhibitors of phospholipase A2. Structural revision of duramycin and cinnamycin. *J Antibiot* **43**: 1403-1412.

Garrido, M.C., Herrero, M., Kolter, R., Moreno, F. (1988) The export of the DNA replication inhibitor Microcin B17 provides immunity for the host cell. *EMBO J* **7**: 1853-1862.

Gebhard, S. (2012) ABC transporters of antimicrobial peptides in Firmicutes bacteria – phylogeny, function and regulation. *Mol Microbiol* **86**: 1295-1317.

Gibson, D.G., Young L., Chuang, R.Y., Venter J.C., Hutchison C.A. 3rd, Smith, H.O. (2009) Enzymatic assembly of DNA molecules up to several hundred kilobases. *Nat Methods* **6**: 343-345.

Glauner, B., Höltje, J.V., Schwarz, U. (1988) The composition of the murein of *Escherischia coli*. *J Biol Chem* **263**: 10088-10095.

Goto, Y., Li, B., Claesen, J., Shi, Y., Bibb, M.J., van der Donk, W.A. (2010) Discovery of unique lanthionine synthases reveals new mechanistic and evolutionary insights. *PLos Biol* **8**: e1000339.

Gotoh, N., Murata, T., Ozaki, T., Kimura, T., Kondo, A., Nishino, T. (2003) Intrinsic resistance of *Escherichia coli* to mureidomycin A and C due to expression of the multidrug efflux system AcrAB-TolC: comparison with the efflux systems of mureidomycin-susceptible *Pseudomonas aeruginosa*. *J Infect Chemother* **9**: 101-103.

Gravesen, A., Jydegaard Axelsen, A.M., Mendes de Silva, J., Hansen, T.B., Knøchel, S. (2002) Frequency of bacteriocin resistance development and associated fitness costs in *Listeria monocytogenes*. *Appl Environ Microbiol* **68**: 756-764.

Greenfield, N.J. (2006) Using circular dichroism spectra to estimate protein secondary structure. *Nat Protoc* **1**: 2876-2890.

Gross, E., and Morell, J.L. (1971) The structure of nisin. *J Am Chem Soc* **93**: 4634-4635.
Hammes, W., Schleifer, K.H., Kandler, O. (1973) Mode of action of glycine on the biosynthesis of peptidoglycan. *J Bacteriol* 116: 1029-1053.

Gut, I.M., Blanke, S.R., van der Donk, W.A. (2011) Mechanism of inhibition of *Bacillus anthracis* spore outgrowth by the lantibiotic nisin. *ACS Chem Biol* **6**: 744-752.

Hammes, W., Schleifer, K.H., Kandler, O. (1973) Mode of action of glycine on the biosynthesis of peptidoglycan. *J Bacteriol* **116**: 1029-1053.

Hanaki, H., Kuwahara-Arai, K., Boyle-Vavra, S., Daum, R.S., Labischinski, H., Hiramatsu, K. (1998) Activated cell-wall synthesis is associated with vancomycin resistance in methicillin-resistant *Staphylococcus aureus* clinical strains Mu3 and Mu50. *J Antimicrob Chemother* **42**: 199-209.

Hasper, H.E., Kramer, N.E., Smith, J.L., Hillman, J.D., Zachariah, C., Kuipers, O.P., *et al.* (2006) An alternative bactericidal mechanism of action for lantibiotic peptides that target lipid II. *Science* **313**: 1636-1637.

Håvarstein, L.S., Diep, D.B., Nes, I.F. (1995) A family of bacteriocin ABC transporters carry out proteolytic processing of their substrates concomitant with export. *Mol Microbiol* **16**: 229-240.

Healy, V.L., Lessard, I.A., Roper, D.I., Knox, J.R., Walsh, C.T. (2000) Vancomycin resistance in enterococci: reprogramming of the D-Ala-D-Ala ligases in bacterial peptidoglycan biosynthesis. *Chem Biol* **7**: R109-119.

Heidrich, C., Pag, U., Josten, M., Metzger, J., Jack, R.W., Bierbaum, G., *et al.* (1998) Isolation, characterization and heterologous expression of the novel lantibiotic epicidin 280 and analysis of its biosynthetic gene cluster. *Appl Environ Microbiol* **64**: 3140-3146.

Heinrich, J., Hein, K., Wiegert, T. (2009) Two proteolytic modules are involved in regulated intramembrane proteolysis of *Bacillus subtilis* RsiW. *Mol Microbiol* **74**: 1412-1426.

Himmelhoch, S.R. (1971) Chromatography of proteins on ion-exchange adsorbents. *Meth Enzymol* **22**: 273-286.

Hinsley, A.P., Stanley, N.R., Palmer, T., Berks, B.C. (2001) A naturally occurring bacterial Tat signal peptide lacking one of the 'invariant' arginine residues of the consensus targeting motif. *FEBS Lett* **497**: 45-49.

Hirokawa, T., Boon-Chieng, S., Mitaku, S. (1998) SOSUI: classification and secondary structure prediction system for membrane proteins. *Bioinformatics* **14**: 378-379.

Ho, S.N., Hunt, H.D., Horton, R.M., Pullen, J.K., Pease L.R. (1989) Site-directed mutagenesis by overlap extension using the polymerase chain reaction. *Gene* **77**: 51-59.

Hoffmann, A., Schneider, T., Pag, U., Sahl, H.G. (2004) Localization and functional analysis of PepI, the immunity peptide of Pep5-producing *Staphylococcus epidermidis* strain 5. *Appl Environ Microbiol* **70**: 3263-3271.

Hong, H.J., Hutchings, M.I., Neu, J.M., Wright, G.D., Paget, M.S., Buttner, M.J. (2004) Characterization of an inducible vancomycin resistance system in *Streptomyces coelicolor* reveals a novel gene (*vanK*) required for drug resistance. *Mol Microbiol* **52**: 1107-1121.

Hong, H.J., Hutchings, M.I., Hill, L.M., Buttner, M.J. (2005) The role of the novel Fem protein VanK in vancomycin resistance in *Streptomyces coelicolor*. *J Biol Chem* **280**: 13055-13061.

Horcajo, P., de Pedro, M.A., Cava, F. (2012) Peptidoglycan plasticity in bacteria: stress-induced peptidoglycan editing by non-canonical D-amino acids. *Microb Drug Resist* **18**: 306-313.

Hörner, T., Zähner, H., Kellner, R., Jung, G. (1989) Fermentation and isolation of epidermin, a lanthionine containing polypeptide antibiotic from *Staphylococcus epidermidis*. *Appl Microbiol Biotechnol* **30**: 219-225.

Hsu, S.T., Breukink, E., Bierbaum, G., Sahl, H.G., De Kruijff, B., Kaptein, R., *et al.* (2003) NMR study of mersacidin and lipid II interaction in dodecylphosphocoline micelles. Conformational changes are a key to antimicrobial activity. *J Biol Chem* **278**: 13110-13117.

Hsu, S.T., Breukink, E., Tischenko, E., Lutters, M.A., De Kruijff, B., Kaptein, R., *et al.* (2004) The nisin-lipid II complex reveals a pyrophosphate cage that provides a blueprint for novel antibiotics. *Nat Struct Mol Biol* **11**: 963-967.

Hugonnet, J.E., Haddache, N., Veckerlé, C., Dubost, L., Marie, A., Shikura, N., *et al.* (2014) Peptidoglycan cross-linking in glycopeptide resistant actinomycetales. *Antimicrob Agents Chemother* **58**: 1749-1756.

Hutchings, M.I., Palmer, T., Harrington, D.J., Sutcliffe, I.C. (2009) Lipoprotein biogenesis in Gram-positive bacteria: knowing when to hold 'em, knowing when to fold 'em. *Trends Microbiol* **17**: 13-21.

Islam, M.R., Nagao, J., Zendo, T., Sonomoto, K. (2012) Antimicrobial mechanism of lantibiotics. *Biochem Soc Trans* **40**: 1528-1533.

Jabes, D., Brunati, C., Candiani, G., Riva, S., Romano, G., Donadio, S. (2011) Efficacy of the new lantibiotic NAI-107 in experimental infections induced by multidrug-resistant Gram-positive pathogens. *Antimicrob Agents Chemother* **55**: 1671-1676.

Johnson, J.W., Fisher, J.F., Mobashery, S. (2013) Bacterial cell-wall recycling. *Ann N Y Acad Sci* **1277**: 54-75.

Kaletta, C., Entian, K.D., Kellner, R., Jung, G., Reis, M., Sahl, H.G. (1989) Pep5, a new lantibiotic: structural gene isolation and prepeptide sequence. *Arch Microbiol* **152**: 16-19.

Karimova, G., Pidoux, J., Ullmann, A., Ladant, D. (1998) A bacterial two-hybrid system based on a reconstituted signal transduction pathway. *Proc Natl Acad Sci* **95**: 5752-5756.

Kellner, R., Jung, G., Hörner, T., Zähner, H., Schnell, N., Entian, K.D., Götz, F. (1988) Gallidermin: a new lanthionine-containing polypeptide antibiotic. *Eur J Biochem* **177**: 53-59.

Kieser, T., Bibb, M.J., Buttner, M.J., Chater, K.F., Hopwood, D.A. (2000) *Practical Streptomyces Genetics.* Norwich: The John Innes Foundation.

Kimura, K., and Bugg, T.D. (2003) Recent advances in antimicrobial nucleoside antibiotics targeting cell wall biosynthesis. *Nat Prod Rep* **20**: 252-273.

Kirby, K.S., Fox-Carter, E., Guest M. (1967) Isolation of deoxyribonucleic acid and ribosomal ribonucleic acid from bacteria. *Biochem J* **104**: 258-262.

Klein, C., Kaletta, C., Entian, K.D. (1993) Biosynthesis of the lantibiotic subtilin is regulated by a histidine kinase/response regulator system. *Appl Environ Microbiol* **59**: 296-303.

Klein, C., and Entian, K.D. (1994) Genes involved in self-protection against the lantibiotic subtilin produced by *Bacillus subtilis* ATCC 6633. *Appl Environ Microbiol* **60**: 2793-2801.

Knerr, P.J., and van der Donk, W.A. (2012) Discovery, biosynthesis and engineering of lantipeptides. *Annu Rev Biochem* **81**: 479-505.

Kodani, S., Hudson, M.E., Durrant, M.C., Buttner, M.J., Nodwell, J.R., Willey, J.M. (2004) The SapB morphogen is a lantibiotic-like peptide derived from the product of the developmental gene ramS in *Streptomyces coelicolor*. *Proc Natl Acad Sci* **101**: 11448-11453.

Kohlrausch, U., and Hoeltje, J.V. (1991) One-step purification procedure for UDP-N-acetylmuramyl-peptide murein precursors from *Bacillus cereus*. *FEMS Microbiol Lett* **62**: 253-257.

Kolodkin-Gal, I., Romero, D., Cao, S., Clardy, J., Kolter, R., Losick, R. (2010) D-amino acids trigger biofilm disassembly. *Science* **328**: 627-629.

Koponen, O., Takala, T.M., Saarela, U., Qiao, M., Saris, P.E. (2004) Distribution of the NisI immunity protein and enhancement of nisin activity by the lipid-free NisI. *FEMS Microbiol Lett* **231**: 85-90.

Kuipers, O.P., Beerthuyzen, M.M., Siezen, R.J., De Vos, W.M. (1993) Characterization of the nisin gene cluster *nisABTCIPR* of *Lactococcus lactis*. Requiremet of expression of the *nisA* and *nisI* genes for development of immunity. *Eur J Biochem* **216**: 281-291.

Kuipers, O.P., Beerthuyzen, M.M., de Ruyter, P.G., Luesink, E.J., de Vos, W.M. (1995) Autoregulation of nisin biosynthesis in *Lactococcus lactis* by signal transduction. *J Biol Chem* **270**: 27299-27304.

Kumar, P., Arora, K., Lloyd, J.R., Lee, I.Y., Nair, V., Fischer, E., *et al.* (2012) Meropenem inhibits D,D-carboxypeptidase activity in *Mycobacterium tubercolosis*. *Mol Microbiol* **86**: 367-381.

Lambert, M.P., and Neuhaus, F.C. (1972) Mechanism of D-cycloserine action: alanine racemase from *Escherichia coli* W. *J Bacteriol* **110**: 978-987.

Lammertyn, E., Van Mellaert, L., Schacht, S., Dillen, C., Sablon, E., Van Broekhoven, A., Anne, J. (1997) Evaluation of a novel subtilisin inhibitor gene and mutant derivatives for the expression and secretion of mouse tumor necrosis factor alpha by *Streptomyces lividans*. *Appl Environ Microbiol* **63**:1808-1813.

Lavollay, M., Arthur, M., Fourgeaud, M., Dubost, L., Marie, A., Veziris, N., *et al.* (2008) The peptidoglycan of stationary-phase *Mycobacterium tuberculosis* predominantly contains cross-links generated by L,D-transpeptidation. *J Bacteriol* **190**: 4360-4366.

Lee M.D. (22 April 2003) New antibiotics derived from the cultures of *Microbispora corallina* and the physicochemical characteristics of those compounds; has units of dehydrobutyrine, dehydroalanine, aminovinylcysteine and tryptophan, Patent application EP1646646 A1.

Leimkuhler, C., Chen, L., Barrett, D., Panzone, G., Sun, B., Falcone, B., *et al.* (2005) Differential inhibition of *Staphylococcus aureus* PBP2 by glycopeptide antibiotics. *J Am Chem Soc* **127**: 3250-3251.

Lepak, A.J., Marchillo, K., Craig, W.A., Andes, D.R. (2014) In vivo pharmacokinetics and pharmacodynamics of the lantibiotic, NAI-107, in the neutropenic murine thigh infection model. *Antimicrob Agents Chemother* **59**: 1258-1264.

Ling, L.L., Schneider, T., Peoples, A.J., Spoering, A.L., Engels, I., Conlon, B.P. *et al.* (2015) A new antibiotic kills pathogens without detectable resistance. *Nature* **517**: 455-459.

MacNeil, D.J., Gewain, K.M., Ruby, C.L., Dezeny, G., Gibbons, P.H., MacNeil, T. (1992) Analysis of *Streptomyces avermitilis* genes required for avermectin biosynthesis utilizing a novel integration vector. *Gene* **111**: 61-68.

Maffioli, S.I., Potenza, D., Vasile, F., De Matteo, M., Sosio, M., Marsiglia, B., *et al.* (2009) Structure revision of the lantibiotic 97518. *J Nat Prod* **72**: 605-607.

Maffioli, S.I., Iorio, M., Sosio, M., Monciardini, P., Gaspari, E., Donadio, S. (2014) Characterization of the congeners in the lantibiotic NAI-107 complex. *J Nat Prod* **77**: 79-84.

Maffioli, S.I., Monciardini, P., Catacchio, B., Mazzetti, C., Münch, D., Brunati, C., *et al.* (2015) Family of class I lantibiotics from Actinomycetes and improvement of their antibacterial activities. *ACS Chem Biol* **10**: 1034-1042.

Magnet, S., Dubost, L., Marie, A., Arthur, M., Gutmann, L. (2008) Identification of the L,D-transpeptidases for peptidoglycan cross-linking in *Escherichia coli*. *J Bacteriol* **190**: 4782-4785.

Mahapatra, S., Crick, D.C., Brennan, P.J. (2000) Comparison of the UDP-N-Acetylmuramate:L-alanine ligase enzymes from *Mycobacterium tuberculosis* and *Mycobacterium leprae*. *J Bacteriol* **182**: 6827-6830.

Mainardi, J.L., Fourgeaud, M., Hugonnet, J.E., Dubost, L., Brouard, J.P., Quazzani, J., *et al.* (2005) A novel peptidoglycan cross-linking enzyme for a beta-lactam-resistant transpeptidation pathway. *J Biol Chem* **280**: 38136-38152.

Mainardi, J.L., Villet, R., Bugg, T.D., Mayer, C., Arthur, M. (2008) Evolution of peptidoglycan biosynthesis under the selective pressure of antibiotics in Gram-positive bacteria. *FEMS Microbiol Rev* **32**: 386-408.

Maisnier-Patin, S., and Richard, J. (1996) Cell wall changes in nisin-resistant variants of *Listeria innocua* grown in the presence of high nisin concentrations. *FEMS Microbiol Lett* **140**: 29-35.

Makino, A., Baba, T., Fujimoto, K., Iwamoto, K., Yano, Y., Terada, N., *et al.* (2003) Cinnamycin (Ro 09-0198) promotes cell binding and toxicity by inducing transbilayer lipid movement. *J Biol Chem* **278**: 3204-3209.

Marcone, G.L., Foulston, L., Binda, E., Marinelli, F., Bibb, M., Beltrametti, F. (2010) Methods for the genetic manipulation of *Nonomurea* sp. ATCC 39727. *J Ind Microbiol Biotechnol* **37**: 1097-1103.

Mattick, A.T., Hirsch, A. (1947) Further observations on an inhibitory substance (nisin) from lactic streptococci. *Lancet* **2**: 5-8.

Mazodier, P., Petter, R., Thompson, C. (1989) Intergenic conjugation between *Escherichia coli* and *Streptomyces* species. *J Bacteriol* **171**: 3583-3585.

McAuliffe, O., Hill, C., Ross, R.P. (2000) Identification and overexpression of *ltnI*, a novel gene which confers immunity to the two-component system lantibiotic lacticin 3147. *Microbiology* **146**: 129-138.

McClerren, A.L., Cooper, L.E., Quan, C., Thomas, P.M., Kelleher, N.L., van der Donk, W.A. (2006) Discovery and *in vitro* biosynthesis of haloduracin, a two-component lantibiotic. *Proc Natl Acad Sci* **103**: 17243-17248.

Mendel M., and Higa A. (1970) Calcium-dependent bacteriophage DNA infection. *J Mol Biol* **53**: 159-162.

Menges, R., Muth, G., Wohlleben, W., Stegmann, E. (2007) The ABC transporter Tba of *Amycolatopsis balhimycina* is required for efficient export of the glycopeptide antibiotic balhimycin. *Appl Microbiol Biotechnol* **77**: 125-134.

Mohammadi, T., van Dam, V., Sijbrandi, R., Vernet, T., Zapun, A., Bouhss, A., *et al.* (2011) Identification of FtsW as a transporter of lipid-linked cell wall precursors across the membrane. *EMBO J* **30**: 1425-1432.

Müller, A., Münch, D., Schmidt, Y., Reder-Christ, K., Schiffer, G., Bendas, G., *et al.* (2012a) Lipodepsipeptide empedopeptin inhibits cell wall biosynthesis through $Ca^{2+}$-dependent complex formation with peptidoglycan precursors. *J Biol Chem* **287**: 20270-20280.

Müller, A., Ulm, H., Reder-Christ, K., Sahl, H.G., Schneider, T. (2012b) Interaction of type A lantibiotics with undecaprenol-bound cell envelope precursors. *Microb Drug Resist* **18**: 261-270.

Mullis, K., Faloona, F., Scharf, S., Saiki, R., Horn, G., Erlich, H. (1986) Specific enzymatic amplification of DNA *in vitro*: the polymerase chain reaction. *Cold Spring Harbor Symposia on Quantitative Biology* **51**: 263-273.

Münch, D., Roemer, T., Lee, S.H., Engeser, M., Sahl, H.G., Schneider, T. (2012) Identification and in vitro analysis of the GatD/MurT enzyme-complex catalyzing lipid II amidation in *Staphylococcus aureus*. *J Biol Chem* **289**: 12063-12076.

Münch, D., Müller, A., Schneider, T., Kohl, B., Wenzel, M., Bandow, J.E., *et al.* (2014) The lantibiotic NAI-107 binds to bactoprenol bound cell wall precursors and impairs membrane functions. *J Biol Chem* **289**: 12063-12076.

Myronovskyi, M., Welle, E., Fedorenko, V., Luzhetskyy, A. (2011) Beta-glucuronidase as a sensitive and versatile reporter in actinomycetes. *Appl Environ Microbiol* **77**: 5370-5583.

Neumüller, A.M., Konz, D., Marahiel, M.A. (2001) The two-component regulatory system BacRS is associated with bacitracin 'self-resistance' of *Bacillus licheniformis* ATCC 10716. *Eur J Biochem* **268**: 3180-3189.

Newman, D.J., and Cragg, G.M. (2007) Natural products as sources of new drugs over the last 25 years. *Nat Prod* **70**: 461-477.

Niedermeyer, T.H., and Strohalm, M. (2012) mMass as a software tool for the annotation of cyclic peptide tandem mass spectra. *PLos One* **7**: e44913.

Nielsen, J.B., and Lampen, O. (1982) Glyceride-cysteine lipoproteins and secretion by Gram-positive bacteria. *J Bacteriol* **152**: 315-322.

Nukajima, Y., Kitpreechavanich, V., Suzuki, K, Kudo, T. (1999) *Microbispora corallina* sp. nov., a new species of the genus *Microbispora* isolated from Thai soil. *Int J Syst Bacteriol* **49**: 1761-1767.

Okanishi, M., Suzuki, K., Umezawa, H. (1974) Formation and reversion of Streptomycete protoplasts: cultural condition and morphological study. *J Gen Microbiol* **80**: 389-400.

Okuda, K., Aso, Y., Nagao, J., Shioya, K., Kanemasa, Y., Nakayama, J., Sonomoto, K. (2005) Characterization of functional domains of lantibiotic-binding immunity protein, NukH, from *Staphylococcus warneri* ISK-1. *FEMS Microbiol Lett* **250**: 19-25.

Okuda, K., Aso, Y., Nakayama, J., Sonomoto, K. (2008) Cooperative transport between NukFEG and NukH in immunity against the lantibiotic nukacin ISK-1 produced by *Staphylococcus warneri* ISK-1. *J Bacteriol* **190**: 356-362.

Okuda, K., Yanagihara, S., Sugayama, T., Zendo, T., Nakayama, J., Sonomoto, K. (2010) Functional significance of the E loop, a novel motif conserved in the lantibiotic immunity ATP-binding cassette transport system. *J Bacteriol* **192**: 2801-2808.

Okuda, K., and Sonomoto, K. (2011) Structural and functional diversity of lantibiotic immunity proteins. *Curr Pharm Biotechnol* **12**: 1231-1239.

Oman, T.J., Lupoli, T.J., Wang, T.S., Kahne, D., Walker, S., van der Donk, W.A. (2011) Haloduracin α binds the peptidoglycan precursor lipid II with 2:1 stoichiometry. *J Am Chem Soc* **133**: 17544-17547.

Ortega, M.A., Hao, Y., Zhang, Q., Walker, M.C., van der Donk, W.A., Nair, S.K. (2014) Structure and mechanism of the tRNA-dependent lantibiotic dehydratase NisB. *Nature* **517**: 509-512.

Ostash, B., and Walker, S. (2010) Moenomycin family antibiotics: chemical synthesis, biosynthesis, and biological activity. *Nat Prod Rep* **27**: 1594-1617.

Otto, M., Peschel, A., Götz, F. (1998) Producer self-protection against the lantibiotic epidermin by the ABC transporter EpiFEG of *Staphylococcus epidermidis* Tü3298. *FEMS Microbiol Lett* **166**: 203-211.

Parenti, F., Pagani, H., Beretta, G. (1976) Gardimycin, a new antibiotic from *Actinoplanes*. Description of the producer strain and fermentation studies. *J Antibiot* **29**: 501-506.

Peschel, A., and Götz, F. (1996) Analysis of the *Staphylococcus epidermidis* genes *epiF*, *-E*, and *-G* involved in epidermin immunity. *J Bacteriol* **178**: 531-536.

Peschel, A., Otto, M., Jack, R.W., Kalbacher, H., Jung, G., Götz, F. (1999) Inactivation of the *dlt* operon in *Staphylococcus aureus* confers sensitivity to defensins, protegrins and other antimicrobial peptides. *J Biol Chem* **274**: 8405-8410.

Pinho, M.G., Kjos, M., Veening, J.W. (2013) How to get (a)round: mechanisms controlling growth and division of coccoid bacteria. *Nat Rev Microbiol* **11**: 601-614.

Podlesek, Z., Comino, A., Herzog-Velikonja, B., Zgur-Bertok, D., Komel, R., Grabnar, M. (1995) *Bacillus licheniformis* bacitracin-resistance ABC transporter: relationship to mammalian multidrug resistance. *Mol Microbiol* **16**: 969-976.

Qiao, M., Immonen, T., Koponen, O., Saris, P.E. (1995) The cellular localization and effect on nisin immunity of the NisI protein from *Lactococcus lactis* N8 expressed in *Escherichia coli* and *L. lactis*. *FEMS Microbiol Lett* **131**: 75-80.

Qiao, M., and Saris, P.E. (1996) Evidence for a role of NisT in transport of the lantibiotic produced by *Lactococcus lactis* N8. *FEMS Microbiol Lett* **144**: 89-93.

Ra, R., Beerthuyzen, M.M., de Vos, W.M., Saris, P.E., Kuipers, O.P. (1999) Effects of gene disruptions in the nisin gene cluster of *Lactococcus lactis* on nisin production and producer immunity. *Microbiology* **145**: 1227-1233.

Rees, D.C., Johnson, E., Lewinson, O. (2009) ABC transporters: the power to change. *Nat Rev Mol Cell Biol* **10**: 218-227.

Reisinger, P., Seidel, H., Tschesche, H., Hammes, W.P. (1980) The effect of nisin on murein synthesis. *Arch Microbiol* **127**: 187-193.

Reynolds, P.E. (1989) Structure, biochemistry and mechanism of action of glycopeptide antibiotics. *Eur J Clin Microbiol Infect Dis* **8**: 943-950.

Rice L.B. (2012) Mechanisms of resistance and clinical relevance of resistance to β-lactams, glycopeptides and fluoroquinolones. *Mayo Clin Proc* **87**: 198-208.

Rincé, A., Dufour, A., Uguen, P., Le Pennec, J-P., Haras, D. (1997) Characterisation of the lacticin 481 operon: the *Lactococcus lactis* genes *lctF, lctE,* and *lctG* encode a putative ABC transporter involved in bacteriocin immunity. *Appl Environ Microbiol* **63**: 4252-4260.

Roces C., Courtin P., Kulakauskas S., Rodriguez A., Chapot-Chartier M.P., Martinez B. (2012) Isolation of *Lactococcus lactis* mutants simultaneously resistant to the cell wall-active bacteriocin Lcn972, lysozyme, nisin and bacteriophage C2. *Appl Environ Microbiol* **78**: 4157-4163.

Rogers, L.A. (1928) The inhibiting effect of *Streptococcus lactis* on *Lactobacillus bulgaricus*. *J Bacteriol* **16**: 321-325.

Rohrer, S., Berger-Bächi, B. (2003) FemABX peptidyl transferases: a link between branched-chain cell wall peptide formation and beta-lactam resistance in gram-positive cocci. *Antimicrob Agents Chemother* **47**: 837-846.

Ruzin, A., Severin, A., Ritacco, F., Tabei, K., Singh, G., Bradford, P.A., *et al.* (2002) Further evidence that a cell wall precursor [$C_{55}$-MurNAc-(peptide)-GlcNAc] serves as an acceptor in a sorting reaction. *J Bacteriol* **184**: 2141-2147.

Ruzin, A., Singh, G., Severin, A., Yang, Y., Dushin, R.G., Sutherland, A.G., *et al.* (2004) Mechanism of action of the mannopeptimycins, a novel class of glycopeptide antibiotics active against vancomycin-resistant gram-positive bacteria. *Antimicrob Agents Chemother* **48**: 728-738.

Ryan, M.P., Rea, M.C., Hill, C., Ross, R.P. (1996) An application in cheddar cheese manufacture for a strain of *Lactococcus lactis* producing a novel broad-spectrum bacteriocin, lacticin 3147. *Appl Environment Microbiol* **62**: 612-619.

Sacco, E., Hugonnet, J.E., Josseaume, N, Cremniter, J., Dubost, L., Marie, A., *et al.* (2010) Activation of the L,D-transpeptidation peptidoglycan cross-linking pathway by a metallo-D-D-carboxypeptidase in *Enterococcus faecium*. *Mol Microbiol* **75**: 874-885.

Sahl, H.G., and Bierbaum, G. (1998) Lantibiotics: biosynthesis and biological activities of uniquely modified peptides from Gram-positive bacteria. *Annu Rev Microbiol* **52**: 41-79.

Saiki, R.K., Gelfand D.H., Stoffel S., Scharf S.J., Higuchi R., Horn G.T., *et al.* (1988) Primer-directed enzymatic amplification of DNA with a thermostable DNA polymerase. *Science* **239**: 487-491.

Sambrook, J., and Russel, D.W. (2001) *Molecular Cloning-A Laboratory Manual*. New York: Cold Spring Harbor Laboratory Press.

Sandegren, L., and Andersson, D.I. (2009) Bacterial gene amplification: implications for the evolution of antibiotic resistance. *Nat Rev Microbiol* **7**: 578-588.

Sato, M., Kirimura, K., Kino, K. (2005) D-amino acid dipeptide production utilizing D-alanine-D-alanine ligases with novel substrate specificity. *J Biosci Bioeng* **99**: 623-628.

Sauvage, E., Kerff, F., Terrak, M., Ayala, J.A., Charlier, P. (2008) The penicillin-binding proteins: structure and role in peptidoglycan biosynthesis. *FEMS Microbiol Rev* **32**: 234-258.

Schäberle, T.F., Vollmer, W., Frasch, H.J., Hüttel, S., Kulik, A., Röttgen, M., *et al.* (2011) Self-resistance and cell wall composition in the glycopeptide producer *Amycolatopsis balhymicina*. *Antimicrob Agents Chemother* **55**: 4283-4289.

Schaerlaekens, K., Lammertyn, E., Geukens, N., De Keersmaeker, S., Anne, J., Van Mellaert, L. (2004) Comparison of the Sec and Tat secretion pathways for heterologous protein production by *Streptomyces lividans*. *J Biotechnol* **112**: 279-288.

Schleifer, K.H., and Kandler, O. (1972) Peptidoglycan types of bacterial cell walls and their taxonomic implications. *Bacteriol Rev* **36**: 407-477.

Schmitt-John, T., and Engels, J.W. (1992) Promoter constructions for efficient secretion expression in *Streptomyces lividans*. *Appl Microbiol Biotechnol* **36**: 493-498.

Schneider, T., Gries, K., Josten, M., Wiedemann, I., Pelzer, S., Labischinski, H., Sahl, H.G. (2009) The lipopeptide antibiotic friulimicin B inhibits cell wall biosynthesis through complex formation with bactoprenol phosphate. *Antimicrob Agents Chemother* **53**: 1610-1618.

Schnell, N., Entian, K.D., Schneider U., Götz, F., Zähner, H., Kellner, R., Jung, G. (1988) Prepeptide sequence of epidermin, a ribosomally synthesized antibiotic with four sulphide-rings. *Nature* **333**: 276-278.

Schnell, N., Engelke, G., Augustin J., Rosenstein, R., Ungermann, V., Götz, F., Entian, K.D. (1992) Analysis of genes involved in the biosynthesis of lantibiotic epidermin. *Eur J Biochem* **204**: 57-68.

Sham, L.T., Butler, E.K., Lebar, M.D., Kahne, D., Bernhardt, T.G., Ruiz, N. (2014) Bacterial cell wall. MurJ is the flippase of lipid-linked precursors for peptidoglycan biogenesis. *Science* **345**: 220-222.

Sherwood, E.J., and Bibb, M.J. (2013) The antibiotic planosporicin coordinates its own production in the actinomycete *Planobispora alba*. *Proc Natl Acad Sci* **110**: E2500-E2509.

Sherwood, E.J., Hesketh, A.R., Bibb, M.J. (2013) Cloning and analysis of the planosporicin lantibiotic biosynthetic gene cluster of *Planomonospora alba*. *J Bacteriol* **195**: 2309-2321.

Shiina, T., Tanaka, K., Takahashi, H. (1991) Sequence of *hrdB*, an essential gene encoding sigma-like transcription factor of *Streptomyces coelicolor* A3(2): homology to principal sigma factors. *Gene* **107**: 145-148.

Siegers, K., and Entian, K.D. (1995) Genes involved in immunity to the lantibiotic nisin produced by *Lactococcus lactis* 6F3. *Appl Environ Microbiol* **61**: 1082-1089.

Siewert, G., and Strominger, J.L. (1967) Bacitracin: an inhibitor of the dephosphorylation of lipid pyrophosphate, an intermediate in the biosynthesis of the peptidoglycan of bacterial cell walls. *Proc Natl Acad Sci* **57**: 767-773.

Sigle, S., Ladwig, N., Wohlleben, W., Muth, G. (2015) Synthesis of the spore envelope in the developmental life cycle of *Streptomyces coelicolor. Int J Med Microbiol* **305**: 183-189.

Simon, R., Priefer, U., Pühler, A. (1983) A broad host range mobilisation system for *in vivo* genetic engineering: transposon mutagenesis in Gram-negative bacteria. *Bio/Technology* **1**: 784-791.

Simone, M., Monciardini, P., Gaspari, E., Donadio, S., Maffioli, S.I. (2013) Isolation and characterization of NAI-802, a new lantibiotic produced by two different *Actinoplanes* strains. *J Antibiot* **66**: 73-78.

Singh, M.P., Petersen, P.J., Weiss, W.J., Janso, J.E., Luckman, S.W., Lenoy, E.B., *et al.* (2003) Mannopeptimycins, new cyclic glycopeptide antibiotics produced by *Streptomyces hygroscopicus* LL-AC98: antibacterial and mechanistic activities. *Antimicrob Agents Chemother* **47**: 62-69.

Sinha Roy, R., Yang, P., Kodali, S., Xiong, Y., Kim, R.M., Griffin, P.R., *et al.* (2001) Direct interaction of a vancomycin derivative with bacterial enzymes involved in cell wall biosynthesis. *Chem Biol* **8**: 1095-1106.

Skarzynski, T., Mistry, A., Wonacott, A., Hutchinson, S.E., Kelly, V.A., Duncan, K. (1996) Structure of UDP-acetylglucosamine enolpyruvyl transferase, an enzyme essential for the synthesis of bacterial peptidoglycan, complexed with substrate UDP-N-acetylglucosamine and the drug fosfomycin. *Structure* **4**: 1465-1474.

Sosio, M., Gallo, G., Pozzi, R., Serina, S., Monciardini, P., Bera, A., *et al.* (2014) Draft genome sequence of the *Microbispora* sp. strain ATCC-PTA-5024, producing the lantibiotic NAI-107. *Genome Announc* **2**: e01198-13.

Stein, T., Heinzmann, S., Solovieva, I., Entian, K.D. (2003) Function of *Lactococcus lactis* nisin immunity genes *nisI* and *nisFEG* after coordinated expression in the surrogate host *Bacillus subtilis*. *J Biol Chem* **278**: 89-94.

Stein, T., Heinzmann, S., Düsterhus, S., Borchert, S., Entian, K.D. (2005) Expression and functional analysis of the subtilin immunity genes *spaIFEG* in the subtilin-sensitive host *Bacillus subtilis* MO1099. *J Bacteriol* **187**: 822-828.

Sutcliffe I.C., and Russell R.R. (1995) Lipoproteins in Gram-positive bacteria. *J Bacteriol* **177**: 1123-1128.

Takala, T.M., and Saris, P.E. (2006) C terminus of NisI provides specificity to nisin. *Microbiology* **152**: 3543-3549.

Temin, H.M., Mizutani S. (1970) RNA-dependent DNA polymerase in virions of Rous sarcoma virus. *Nature* **226**: 1211-1213.

Thompson, B.J., Widdick, D.A., Hicks, M.G., Chandra, G., Sutcliffe, I.C., Palmer, T., Hutchings, M.I. (2010) Investigating lipoprotein biogenesis and function in the model Gram-positive bacterium *Streptomyces coelicolor*. *Mol Microbiol* **77**: 943-957.

Tipper, D.J., and Strominger, J.L. (1965) Mechanism of action of penicillins: a proposal based on their structural similarity to acyl-D-alanyl-D-alanine. *Proc Natl Acad Sci* **54**: 1133-1141.

Typas, A., Banzhaf, M., Gross, C.A., Vollmer, W. (2011) From the regulation of peptidoglycan synthesis to bacterial growth and morphology. *Nat Rev Microbiol* **10**: 123-136.

Tzanis, A., Dalton, K.A., Hesketh, A., den Hengst, C.D., Buttner, M.J., Thibessard, A., Kelemen, G.H. (2014) A sporulation-specific, *sigF*-dependent protein, SspA, affects septum positioning in *Streptomyces coelicolor*. *Mol Microbiol* **91**: 363-380.

Uguen, P., Le Pennec, J.P., Dufour, A. (2000) Lantibiotic biosynthesis: interactions between prelacticin 481 and its putative modification enzyme, LctM. *J Bacteriol* **182**: 5262-5266.

Uguen, P., Hindré, T., Didelot, S., Marty, C., Haras, D., Le Pennec, J.P., *et al.* (2005) Maturation by LctT is required for biosynthesis of full-lenght lantibiotic lacticin 481. *Appl Environ Microbiol* **71**: 562-565.

Valente, F.M., Pereira, P.M., Venceslau, S.S., Regalla, M., Coelho, A.V., Pereira, I.A. (2007) The [NiFeSe] hydrogenase from *Desulfovibrio vulgaris* Hildenborough is a bacterial lipoprotein lacking a typical lipoprotein signal peptide. *FEBS Lett* **581**: 3341-3344.

Valsesia, G., Medaglia, G., Held, M., Minas, W., Panke, S. (2007) Circumventing the effect of product toxicity: development of a novel two-stage production process for the lantibiotic gallidermin. *Appl Environ Microbiol* **73**: 1635-1645.

van de Kamp, M., Horstink, L.M., van den Hooven, H.W., Konings, R.N., Hilbers, C.W., Frey, A., *et al.* (1995) Sequence analysis by NMR spectroscopy of the peptide lantibiotic epilancin K7 from *Staphylococcus epidermidis* K7. *Eur J Biochem* **227**: 757-771.

van der Meer, J.R., Polman, J., Beerthuyzen, M.M., Siezen, R.J., Kuipers, O.P., De Vos, W.M. (1993) Characterization of the *Lactococcus lactis* nisin A operon genes *nisP*, encoding a subtilisin-like serine protease involved in precursor processing, and *nisR*, encoding a regulatory protein involved in nisin biosynthesis. *J Bacteriol* **175**: 2578-2588.

van Heijenoort, Y., Derrien, M., van Heijenoort, J. (1978) Polymerization by transglycosylation in the biosynthesis of the peptidoglycan of *Escherichia coli* K12 and its inhibition by antibiotics. *FEBS Lett* **89**: 141-144.

van Heijenoort, Y., Gomez, M., Derrien, M., Ayala, J., van Heijenoort, J. (1992) Membrane intermediates in the peptidoglycan metabolism of *Escherichia coli*: possible roles of PBP1b and PBP3. *J Bacteriol* **174**: 3549-3557.

van Heijenoort, J. (2001) Recent advances in the formation of the bacterial peptidoglycan monomer unit. *Nat Prod Rep* **18**: 503-519.

Vollmer, W. (2008) Structural variation in the glycan strands of bacterial peptidoglycan. *FEMS Microbiol Rev* **32**: 287-306.

Vollmer, W., Blanot, D., de Pedro, M.A. (2008a) Peptidoglycan structure and architecture. *FEMS Microbiol Rev* **32**: 149-167.

Vollmer, W., Joris, B., Charlier, P., Foster, S. (2008b) Bacterial peptidoglycan (murein) hydrolases. *FEMS Microbiol Rev* **32**: 259-286.

Walker, S., Chen, L., Hu, Y., Rew, Y., Shin, D., Boger, D.L. (2005) Chemistry and biology of ramoplanin: a lipoglycodepsipeptide with potent antibiotic activity. *Chem Rev* **105**: 449-476.

Weidel, W., Frank, H., Martin, H.H. (1960) The rigid layer of the cell wall of *Escherichia coli* strain B. *J Gen Microbiol* **22**: 158-166.

Widdick, D.A., Dodd, H.M., Barraille, P., White, J., Stein, T.H., Chater, K.F., Gasson, M.J., Bibb, M.J. (2003) Cloning and engineering of the cinnamycin biosynthetic gene cluster from *Streptomyces cinnamoneus* DSM 40005. *Proc Natl Acad Sci* **100**: 4316-4321.

Wiedemann, I., Breukink, E., van Kraaij, C., Kuipers, O.P., Bierbaum, G., de Kruijff B., Sahl, H.G. (2001) Specific binding of nisin to the peptidoglycan precursor lipid II combines pore formation and inhibition of cell wall biosynthesis for potent antibiotic activity. *J Biol Chem* **276**: 1772-1779.

Wiedemann, I., Benz, R., Sahl, H.G. (2004) Lipid II-mediated pore formation by the peptide antibiotic nisin: a black lipid membrane study. *J Bacteriol* **186**: 3259-3261.

Wiedemann, I., Böttiger, T., Bonelli, R.R., Wiese, A., Hagge, S.O., Gutsmann, T., *et al.* (2006) The mode of action of the lantibiotic lacticin 3147: a complex mechanism involving specific interaction of two peptides and the cell wall precursor lipid II. *Mol Microbiol* **61**: 285-296.

Wietzerbin, J., Das, B.C., Petit, J.F., Lederer, E., Leyh-Bouille, M., Ghuysen, J.M. (1974) Occurrence of D-alanyl-(D)-mesodiaminopimelic acid and meso-diaminopimelyl-mesodiaminopimelic acid interpeptide linkages in the peptidoglycan of Mycobacteria. *Biochemistry* **13**: 3471-3476.

Willey, J.M., and van der Donk, W.A. (2007) Lantibiotics: peptides of diverse structure and function. *Annu Rev Microbiol* **61**: 477-501.

Wright, G.D, Molinas, C., Arthur, M., Courvalin, P., Walsh, C.T. (1992) Characterization of vanY, a DD-carboxypeptidase from vancomycin-resistant *Enterococcus faecium* BM4147. *Antimicrob Agents Chemother* **36**: 1514-1518.

Wright, G.D. (2007) The antibiotic resistome: the nexus of chemical and genetic diversity. *Nat Rev Microbiol* **5**: 175-186.

Wright, G.D. (2010) Antibiotic resistance in the environment: a link to the clinic? *Curr Opin Microbiol* **13**: 589-594.

Wurch T., Lestienne, F., Pauwels P.J. (1998) A modified overlap extension PCR method to create chimeric genes in the absence of restriction enzymes. *Biotech Techniques* **12**: 653-657.

Wyke, A.W., and Perkins, H.R. (1975) The specificity of enzymes adding amino acids in the synthesis of the peptidoglycan precursors of *Corynebacterium poinsettiae* and *Corynebacterium insidiosum*. *J Gen Microbiol* **88**: 159-168.

Yim, G., Thaker, M.N., Koteva, K., Wright, G. (2014) Glycopeptide antibiotic biosynthesis. *J Antibiot* **67**: 31-41.

Zimmermann, N., Metzger, J.W., Jung, G. (1995) The tetracyclic lantibiotic actagardine. 1H-NMR and 13C-NMR assignment and revised primary structure. *Eur J Biochem* **228**: 786-797.

**I would like to thank**

**Prof. Dr. Wolfang Wohlleben** for his guidance and helpful discussions

**Dr. Evi Stegmann** for her supervision and the freedom I had to conduct the research

**Prof. Dr. Heike Brötz-Oesterhelt** for the assessment of this work

**Günther** for his support, suggestions and for adopting me in the espresso group

**Thomas Härtner** for his support and his good mood in the lab

**Andreas** for HPLC and LC/MS analyses and to be always ready to explore the ability of the mass spectrometer to fragment molecules

**Mulu** for the HPLC analyses of peptidoglycan and the nice discussions on Friday afternoon

**Marius** for his support and his critical perspective

**Regina** for sharing the lab with me and for understanding my occasional bad mood

**Hans-Jörg** for introducing me in the department and his tips in the lab

**Paul** for his work during the intership and his passion for the project

**Edgardo** for helping me with my first cloning and for his latin style which helped me to feel like in Italy

**All the people in the 10th floor** for making the department a nice place to work

**The LAPTOP partners** for all the discussions and the nice atmosphere to our meetings

**Stefano e Margherita** for introducing me in the world of Actinomycetes and natural products and to support me in the choice to go abroad for the PhD

**The 10th floor in Heuberger Tor,** especially Henco, Sasha, Hanna, Stephan, Yuan, Frieder for the great time we spent together

**La mia famiglia** per il suo supporto anche nei momenti più duri e per tutte le volte in cui mi ha visitato a Tuebingen

**La rampina** per le sue accoglienze ad ogni mio ritorno